Copyright

by

Alex Tyler Katz

2016

The Thesis Committee for Alex Tyler Katz
Certifies that this is the approved version of the following thesis:

Performance of Precast, Prestressed Concrete I-Girders Employing 0.7-in. Diameter Prestressing Strands under Shear-Critical Loading Conditions

APPROVED BY
SUPERVISING COMMITTEE:

Oguzhan Bayrak, Supervisor

Trevor Hrynyk, Co-Supervisor

Performance of Precast, Prestressed Concrete I-Girders Employing 0.7-in. Diameter Prestressing Strands under Shear-Critical Loading Conditions

by

Alex Tyler Katz, B.S.

Thesis

Presented to the Faculty of the Graduate School of

The University of Texas at Austin

in Partial Fulfillment

of the Requirements

for the Degree of

Master of Science in Engineering

The University of Texas at Austin

August 2016

Dedication

To the family of Hyun su Kim

Acknowledgements

Welcome to my written shoutout to everyone who put up with me enough to make the following pages, and the one page that will soon hang on my wall, possible. I must start with Dr. Bayrak and Dr. Hrynyk who took a chance on me, and provided me with a unique opportunity to develop my skills outside the classroom and join a distinguished family of alumni. Next, I must thank the technical staff at FSEL for all the time (often without pay) and mentorship they gave to me and to this project. I suppose they only kept me around after I got a forklift stuck in the mud and I designed a concrete mix with zero slump because they didn't have a choice. So, thank you Mr. Braley, Mr. Fillip, and Mr. Stasney for allowing me in your structural engineering laboratory and for teaching me how to create (and to destroy). I would be remiss if I did not take the opportunity to acknowledge the contributions of the lab staff. Truman, Bacon, Joel, and Dr. Brown all played a significant role in this project through technical guidance, breakfast tacos, or one-liners. And Ms. Damvar, Ms. Mueller, and Ms. Clayton are in on this too. Thank you ladies, not only for managing our projects, but for keeping us well fed and for balancing out all the testosterone at the lab.

Now for the hard part. To my team who has experienced the misfortune of having to work with me firsthand. Jessica and Roya have been working with me the longest and deserve an award for that. I hope you have enjoyed working with me as I have enjoyed working with you, and that you will remember this journey fondly. If you're reading this, take a minute to remember the late nights tying rebar cages, cleaning forms, preparing for presentations, and studying for exams. Those experiences certainly helped me in my profession and in life. Thank you for your huge role in the last two years of my life.

Next, we have the reinforcements. Thank you, Dennis Kim, for joining our project with a truly cheerful spirit. Despite the overwhelming nature of our work and the often lopsided responsibilities you were assigned, you remained steadfast in your efforts and you were truly a blessing to work with. I write these acknowledgements with a heavy heart for the tragedy you have experienced, and I hope to see your cheerful spirit return to Ferguson Lab soon.

The project was lucky enough to have the help of a University of Texas undergraduate as well. Thank you, Ryan Boehm, for your help on this project. This thesis was mostly written under an acceptable amount of sleep thanks, in part, to your contributions. I am confident that our work will be in good hands with you and Dennis in charge.

I must also bring the spotlight to our humble leader. Hossein Yousefpour deserves more than a few lines in a master's thesis for his tireless dedication to this team. However, this is currently my biggest stage. Hossein was at different times, a mentor, a teacher, a motivator, an advocate, and a friend. His unhuman work ethic will largely go unnoticed. Yet, without it, none of the papers, experiments, or studies produced by this team would have been possible. I can remember multiple occasions when his quick thinking saved thousands of research dollars and hundreds of man hours. It has been an honor to work under you, sir. Thank you for teaching me, and for learning alongside me.

Finally, I have been told to appreciate the small things along the way. So, I'd like to thank the coffee bean, and everyone who cultivates it. I believe God had us graduate students in mind with that one. Also, for margaritas, because sometimes life calls for margaritas.

Soli Deo gloria

Abstract

Performance of Precast, Prestressed Concrete I-Girders Employing 0.7-in. Diameter Prestressing Strands under Shear-Critical Loading Conditions

Alex Tyler Katz, M.S.E.

The University of Texas at Austin, 2016

Supervisor: Oguzhan Bayrak

Co-Supervisor: Trevor Hrynyk

The majority of precast, pretensioned concrete elements are currently fabricated using 0.5- or 0.6-in. diameter prestressing strands. However, in recent years, potential benefits such as reduced fabrication costs and extended span capabilities have led to an interest in using larger-diameter 0.7-in. strands in the pretensioning industry. Such an increase in the diameter of strands might impact the shear strength of pretensioned girders due to the possibility of atypical failure modes that are not considered in current design provisions.

An experimental program was conducted to study the effects of using 0.7-in. prestressing strands on the performance of precast, prestressed concrete I-girders under shear-critical loading conditions. Four full-scale pretensioned Texas bulb-tee girders (Tx-girders) employing 0.7-in. strands were fabricated and tested at Ferguson Structural

Engineering Laboratory at the University of Texas at Austin. The mild steel reinforcement in the specimens was detailed according to standard drawings by the Texas Department of Transportation for girders employing 0.6-in. strands. The test program investigated the shear failure in girders with different concrete release strengths, overall member depths, shear span-to-depth ratios, and strand patterns.

Analysis of the results revealed clear signs of atypical shear failure mechanisms in all specimens. Considerable strand slip was recorded at both ends of the specimens prior to peak load. In three of the specimens, the shear failure resulted in prominent horizontal cracks at the interface between the web and the bottom flange. However, all specimens demonstrated significant diagonal cracking prior to failure. Yielding of the stirrups was also confirmed in all specimens, indicating a shear-tension failure. The capacities of all specimens were conservatively estimated using the general procedure in AASHTO LRFD Bridge Design Specifications and the detailed method in ACI 318-14. The findings of this study reveal no concerns regarding the performance of existing design provisions in predicting the shear strength of Tx-girders that employ 0.7-in. diameter prestressing strands.

Table of Contents

List of Tables

List of Figures

CHAPTER 1: INTRODUCTION

1.1 INTRODUCTION

The majority of precast, pretensioned elements are currently fabricated using 0.5-in. (12.7-mm) or 0.6-in. (15.2-mm) diameter prestressing strands. However, in recent years, potential benefits such as reduced fabrication costs and extended span capabilities have led to an interest in using larger-diameter 0.7-in. (17.8-mm) strands in pretensioning industry. Such an increase in the diameter of strands might have serviceability and strength implications that are not considered in current design provisions and detailing requirements.

One of the primary concerns associated with the use of 0.7-in. (17.8-mm) strands is the effects of employing these larger-diameter strands on the shear strength of precast girders, especially for the new pretensioned bulb-T sections in which the geometry of the cross section has been optimized to enhance the flexural capacity. These highly-efficient shapes possess larger bottom flanges to allow for a greater number of prestressing strands, but are constructed with relatively thin webs. Pretensioned bulb-T sections with 0.7-in. (17.8-mm) strands are prone to two atypical shear failure mechanisms: horizontal shear failure and anchorage-induced shear failure (Figure 1-1). These failure modes, which have been observed in previous studies on modern precast bulb-T sections such as those by Garber et al. (2016) and Ross et al. (2014), do not occur in the web. Therefore, it

would not be appropriate to calculate shear strength corresponding to these mechanisms using equations that are developed to predict traditional web-shear failures.

Nakamura (2013) developed a database of 1,696 shear tests on prestressed concrete members from 1954-2010, which was used to evaluate the accuracy and conservativeness of several available shear design codes. Analysis of the database showed that the MCFT-based design codes, such as the general procedure in AASHTO LRFD Bridge Design Specifications (2014), are the most effective in accurately predicting the shear strength with a reasonable level of conservatism. However, most of the unconservative cases in the database were those that exhibited signs of horizontal shear damage or anchorage zone distress.

(a)

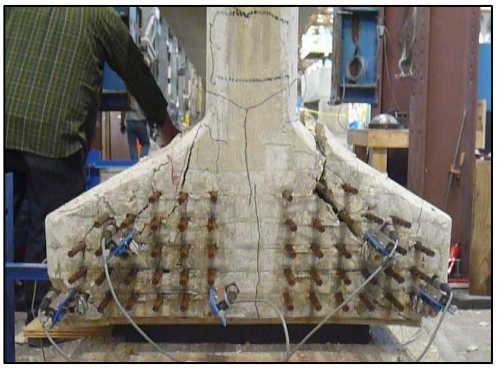

(b)

Figure 1-1: Examples of (a) horizontal shear failure (Hovel et al., 2012); and (b) anchorage-induced shear failure (Garber et al., 2016)

Horizontal shear failure is characterized by a breakdown of the web-flange interface, resulting in relative sliding of the web past the bottom flange. This failure mode occurs when the shear stress exceeds the capacity of the interface between the bottom

flange and the web. Although this failure mode has been previously observed in many experimental studies on pretensioned girders (Nakamura, Avendano, & Bayrak, 2013), it is not explicitly considered in the current design provisions. Hovell (2012) examined the mechanics of bending-induced horizontal shear stresses in I- and U-girders and developed a method for evaluating the horizontal shear performance of prestressed concrete beams. In this method, the horizontal shear crack is assumed to start at the point where a 45-degree shear crack originating from the applied load point intersects the web-flange interface. The capacity of the girder for resisting the horizontal shear failure in this method is also determined using the shear-friction theory.

Anchorage-induced shear failure is the result of strand slip or breakdown of bond between the strand and concrete. When a shear crack crosses the longitudinal steel, it is restrained from opening further by a restraining force from the reinforcement. As a result, an additional demand is introduced to the longitudinal reinforcement. Equation 1-1 is used in AASHTO LRFD Bridge Design Specifications (2014) to determine the total demand on the longitudinal reinforcement as a result of combined bending moment, axial force, and shear.

$$T = \frac{|M_u|}{\phi_f d_v} + 0.5\frac{N_u}{\phi_c} + \left(\left|\frac{V_u}{\phi_v} - V_p\right| - 0.5V_s\right)\cot\theta \qquad \text{Equation 1-1}$$

In Equation 1-1, T is the longitudinal force demand; M_u, N_u, and V_u are ultimate bending moment, axial force, and shear force at the section; ϕ_f, ϕ_c, and ϕ_v are resistance

factors; V_p is the vertical component of the effective prestressing force; V_s is shear resistance provided by the transverse reinforcement; and θ is the angle of inclination of diagonal compressive stresses.

In pretensioned concrete beams, the capacity of longitudinal steel in resisting this longitudinal demand is dependent on the distance from the end face of the girder. The strands transfer force to concrete through bond stresses that accumulate with distance from the end face of the girder. The length over which the strands reach the effective prestress level is referred to as the transfer length whereas development length is the length required to achieve the full strand force under external loads. Figure 1-2 shows available stresses in the strands depending on the location of critical section in the girder.

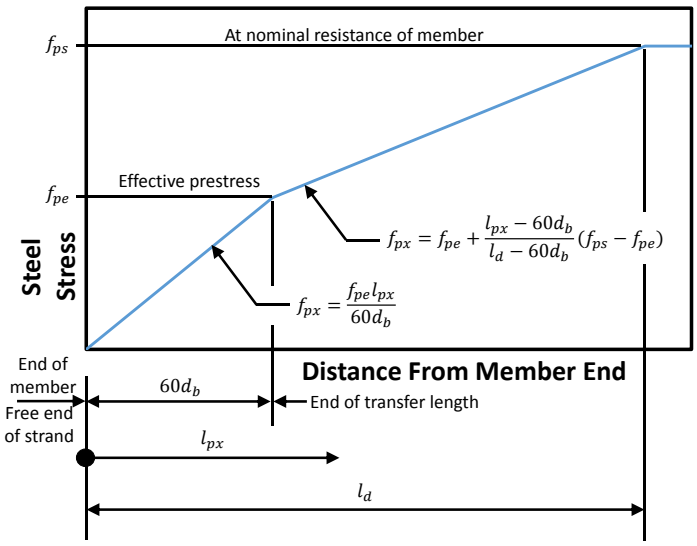

Figure 1-2: Idealized relationship between steel stress and distance from the free end of strand (Adapted from AASHTO (2014))

If the demand on longitudinal steel crossing the crack exceeds the available stress in the strands, the restraining force provided by the strand will not be sufficient to prevent further growth of the crack. As a result, progression of the diagonal shear crack crossing the longitudinal steel or total slippage and loss of bond in the strands will occur, leading to anchorage-induced shear failure. This failure mode is generally more likely at the inside edge of the bearing area of pretensioned girders, where the available capacity of the strands will be smaller because the bearing region is usually located within the transfer length.

Langefeld (2012) investigated the performance of Equation 1-1 and other provisions in AASHTO LRFD for estimating the anchorage performance in 72 shear tests from the database developed by Nakamura (2013). The results showed that AASHTO LRFD provisions yield conservative estimates for anchorage capacities but cannot be used to predict the occurrence of anchorage-induced shear failure. Many of the tests that were expected to fail in anchorage based on Equation 1-1 did not show signs of anchorage zone distress, which indicates the possibility of overly conservative estimates by the equation.

The introduction of 0.7-in. (17.8-mm) diameter prestressing strands will increase the likelihood of both aforementioned atypical shear failure modes. The general effect of larger strands on the factors influencing horizontal shear capacity is two-fold. First, larger strands allow for a more concentrated prestressing steel area (beneficial for flexural design), which can lead to the development of greater end-region stresses. These stresses

degrade the interface between the beam's web and bottom flange. Second, the use of larger-diameter strands makes it possible to provide a greater eccentricity of the prestressing force relative to the section's centroid. Therefore, to mobilize the flexural capacity of girders that employ larger-diameter strands, greater horizontal shear stresses need to develop on the weakened web-flange interface. Meanwhile, an increase in strand diameter results in a decrease in the ratio of perimeter, i.e. the surface area in contact with surrounding concrete, to cross-sectional area of the strand, which leads to a reduced bond strength available to help anchor the strands and an increased transfer length. As a result, girders that employ larger-diameter strands are more susceptible to anchorage-induced shear failure.

The atypical failure modes described above are highly dependent on the geometry of the pretensioned concrete element, reinforcement detailing, and interaction between stresses and damage due to shear force and those due to prestress transfer. Therefore, the mechanism of these failure modes can be evaluated only through full-scale shear tests.

The only cases of shear tests on full-scale I- or bulb-T girders employing 0.7-in. (17.8-mm) strands have been reported by Tadros and Morcous (2011). The specimens comprising the testing program consisted of three NU1100 girders, which contained 34 straight 0.7-in. (17.8-mm) diameter strands and were released at a concrete strength of 8 ksi (55 MPa). The girders were tested at a shear span that was 1.77 times the height of the specimen. Within the span that was tested in shear, 25 percent of the strands were debonded for lengths between 3.5 ft (1,067 mm) and 7 ft (2,134 mm). Occurrence of

strand slip before the peak load was noted. However, the ratio of measured failure load for the specimens to that calculated using the general procedure in AASHTO LRFD was reported between 1.16 and 1.24.

While the aforementioned study provides valuable information on the performance of bulb-T sections employing 0.7-in. (17.8-mm) strands under shear-critical loading, several aspects of the problem needs further investigation. First, the previously investigated NU1100 specimens were released at compressive strengths greater than that commonly used for the fabrication of pretensioned girders, and no cracking damage was reported within the specimen before the shear test. Therefore, the effects of damage within the end-region due to prestress transfer were not documented. The increased release strength might also be a contributing factor to a different bond strength and transfer length for the specimens, hence affecting the possibility of anchorage-induced shear failure. Second, the specimens contained specific details such as additional confinement reinforcement and debonded strands, which might affect the shear performance. Finally, while load-deflection and strand slip plots provide valuable insight into the behavior of the specimen, lack of instrumentation on transverse reinforcement prevented detailed information on the sequence of failure.

The primary focus of this thesis is on the effects of 0.7-in. (17.8-mm) diameter prestressing strands on the shear strength and failure mechanisms of Texas bulb-T girders (Tx-girders). To investigate this problem, a full-scale experimental program was developed, which consisted of shear tests on two Tx46 and two Tx70 girders. The

specimens employed 0.7-in. (17.8-mm) prestressing strands on a 2- by 2-in. (51-mm by 51-mm) grid spacing and were subjected to prestress transfer at release strengths between 5.2 ksi (36 MPa) and 8.3 ksi (57 MPa). The girders were extensively instrumented and monitored for cracking, strand slip, and end-region stresses at the time of prestress transfer and during shear testing. The results of the shear tests were used to evaluate the mechanisms of shear failure in pretensioned I-girders with 0.7-in. (17.8-mm) diameter strands and determine the suitability of shear design provisions within the current ACI 318-14 (2014) and AASHTO LRFD Bridge Design Specifications (2014) for prestressed beams utilizing 0.7-in. (17.8-mm) diameter strands.

The work presented in this thesis was performed in conjunction with an experimental investigation of the end-region behavior of pretensioned I-girders employing 0.7-in. (17.8-mm) strands, in which the behavior of the same full-scale specimens at the time of prestress transfer was investigated. Details of that study are reported in a separate publication by Salazar (2016). Moreover, the mechanics of prestress transfer and shear failure within the specimens comprising this test program were investigated in a computational study by Abyaneh (2016).

1.2 RESEARCH SIGNIFICANCE

The shear performance of pretensioned girders employing 0.7-in. (17.8-mm) strands may be negatively impacted due to the possibility of atypical failure modes. The full-scale experimental program presented in this thesis represents a major contribution to the knowledge of shear behavior of pretensioned girders with these larger-diameter

strands, in which the effects of shear-span-to-depth ratio, concrete release strength, strand layout, and damage due to prestress transfer are considered. Results from the extensively instrumented specimens in this study provide valuable insight into the failure mechanisms of girders with 0.7-in. (17.8-mm) strands, which is used to evaluate the efficacy of current design provisions.

1.3 THESIS ORGANIZATION

This thesis is divided into four chapters, including this introductory chapter. Chapter 2 provides a description of the experimental program, including information on specimen design and fabrication, test setup, and testing procedure. The results of the experimental program are presented and discussed in Chapter 3, and Chapter 4 includes the conclusions of the test program. Additional details of the test program are provided in four appendices, as follows:

- Appendix A includes the details of design and fabrication process and the photos of the test setup,
- Appendix B provides the information on the instrumentation used for the shear tests, including the calibration information,
- Appendix C provides detailed information on the results of the test program, including strains, strand slip measurements, and cracking patterns, and
- Appendix D includes detailed calculations for estimating the load-carrying capacity of the specimens using code provisions.

CHAPTER 2: EXPERIMENTAL PROGRAM

To investigate the shear performance of pretensioned I-girders employing 0.7-in. (17.8-mm) strands, four full-scale specimens were fabricated at Ferguson Structural Engineering Laboratory (FSEL) at the University of Texas at Austin. By fabricating the specimens in the laboratory environment, the research team was able to extensively instrument the specimens and monitor parameters of interest from the time the strands were stressed until the specimens were tested under shear-critical loading conditions. A brief overview of the design and fabrication process for the specimens is provided in this section. Details of the fabrication process and the observed behaviors of the specimens at the time of prestress transfer are reported by Salazar (2016) in a separate publication focused on the end-region serviceability of girders employing 0.7-in. (17.8-mm) strands.

2.1 SPECIMEN DESIGN

The specimens comprising the test program consisted of two Tx-46 and two Tx-70 girders that were 30 ft (9 m) long. The cross-sectional geometry and properties of these specimens are shown in Figure 2-1 and Table 2-1, respectively.

Table 2-1: Girder cross-sectional properties

Design properties	Tx46	Tx70
Height, in. (mm)	46 (1,168)	70 (1,778)
A_g, in.^{2} (mm^2)	761 (490,967)	966 (623,225)
y_b, in. (mm)	20.10 (511)	31.91 (811)
I_g, in.^{4} (mm^4)	198,089 (82.4x(10)^9)	628,747 (261.7x(10)^9)
Weight, plf (kN/m)	819 (11.95)	1,040 (15.18)

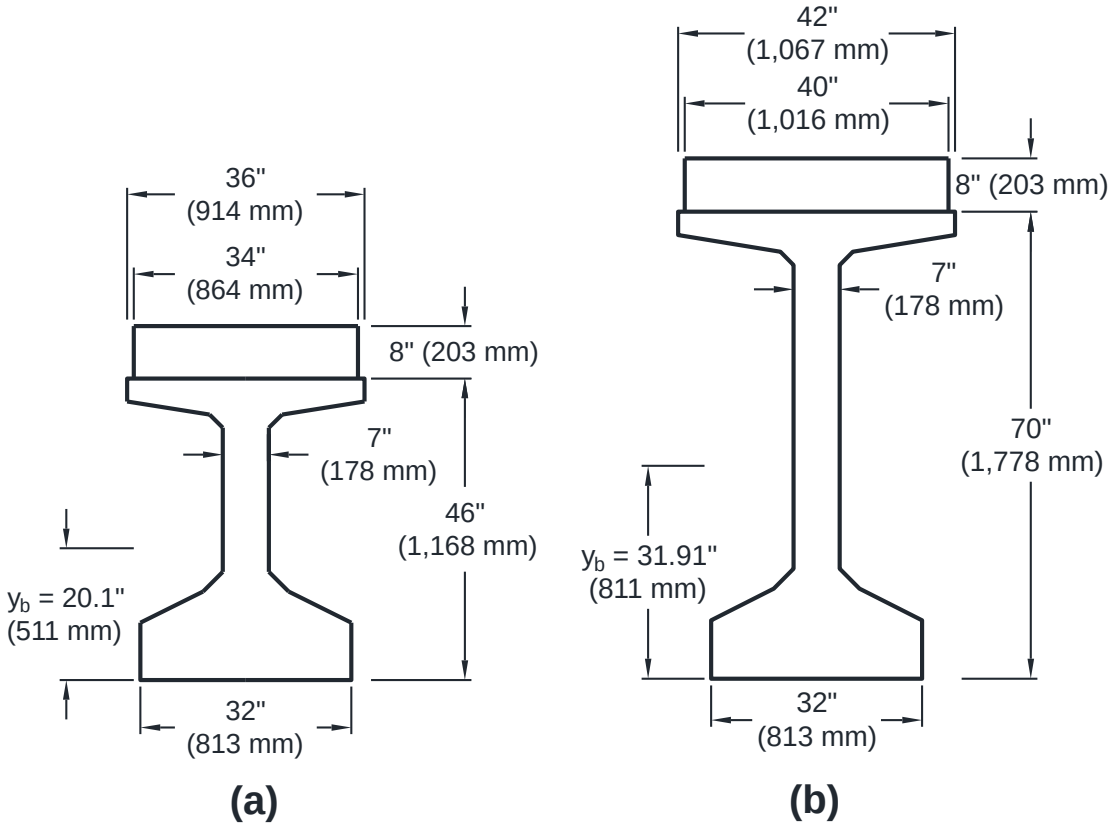

Figure 2-1: Standard dimension of (a) a Tx46 girder; (b) a Tx70 girder with CIP topping decks (Texas Department of Transportation (TxDOT), 2015)

The longitudinal steel in the bottom flanges of the specimens was comprised of straight, 0.7-in. (17.8-mm) diameter, strands that were located on a standard 2- by 2-in. (51- by 51-mm) grid. To control the stresses at the girder ends, four 0.7-in. (17.8-mm)

strands were also provided within the top flange, which were stressed to different levels among the four specimens. The mild-steel reinforcement used within the end-region of the specimens and that used for shear reinforcement were detailed according to standard drawings developed by the Texas Department of Transportation (2015). Details and spacing of the mild-steel reinforcement are shown in Figure 2-2 and Figure 2-3, respectively.

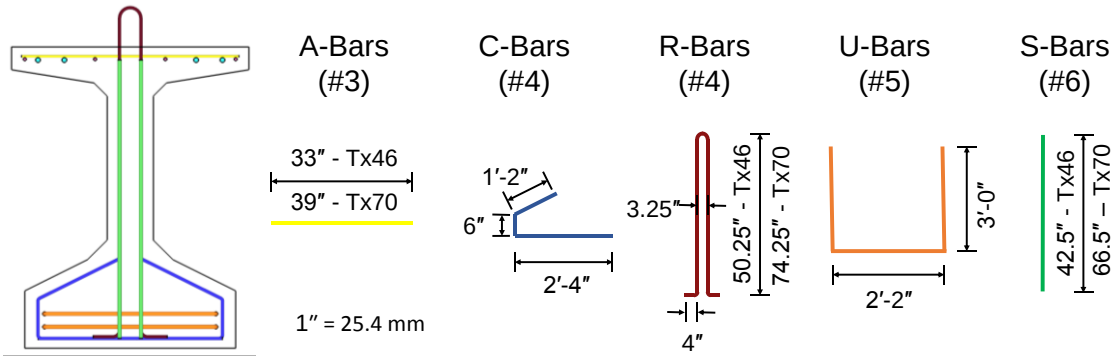

Figure 2-2: Standard end-region detailing for Tx-girders (Texas Department of Transportation (TxDOT), 2015)

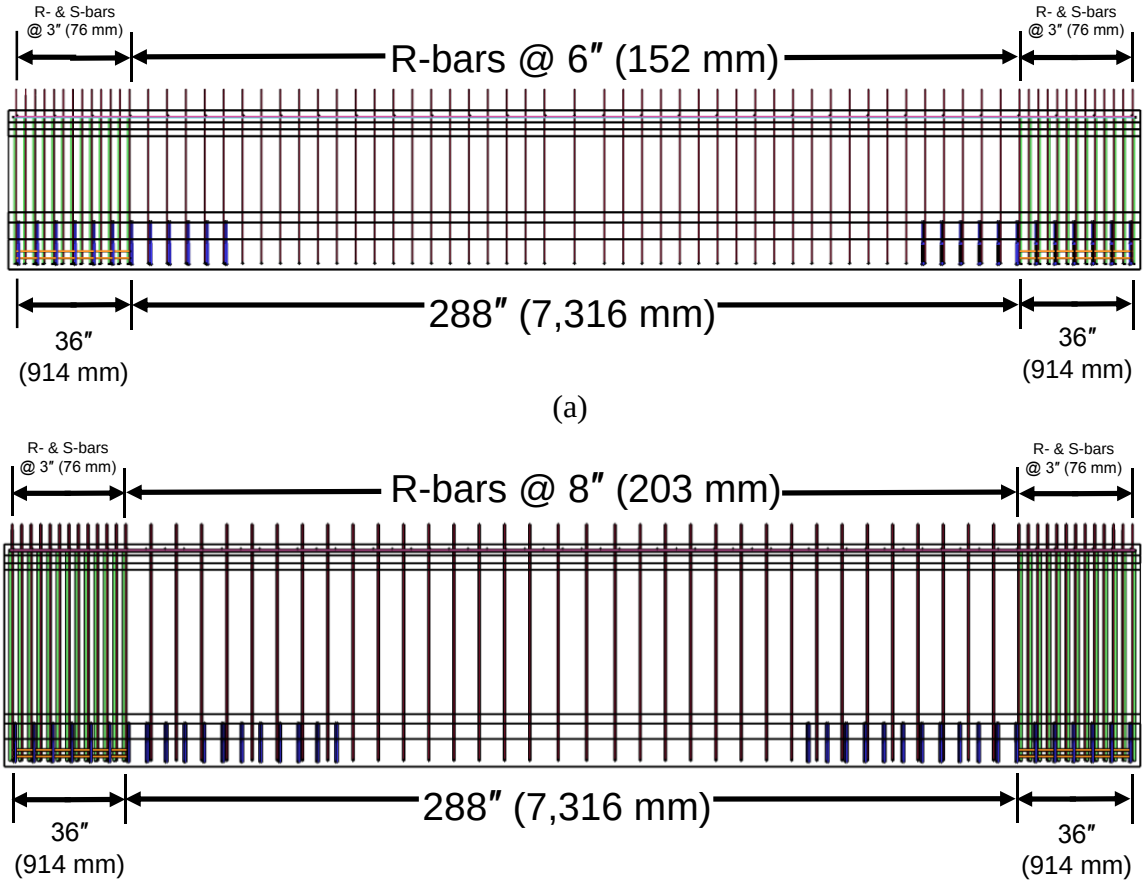

Figure 2-3: Shear and confinement reinforcement for (a) Tx46 specimens; and (b) Tx70 specimens

A summary of the main design parameters for the specimens is presented in Table 2-2. Along with the dimensional change from the Tx46 specimens to the Tx70 specimens, the strand patterns within the specimens were changed to explore different conditions with respect to end-region stresses. To generate the most critical conditions for end-region stresses, all specimens were designed to reach the maximum allowable stresses at prestress transfer according to the AASHTO LRFD Bridge Design Specifications (2014). Furthermore, these girder designs were specifically developed to

explore the effects of two extreme scenarios: maximum eccentricity of strands and maximum effective prestressing force.

Table 2-2: Specimen design details

Design properties	Tx46-I	Tx46-II	Tx70-I	Tx70-II
Strand pattern	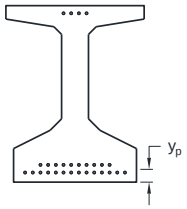	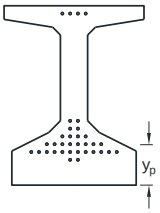	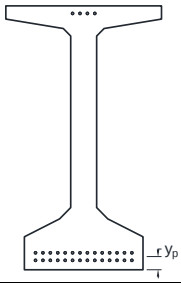	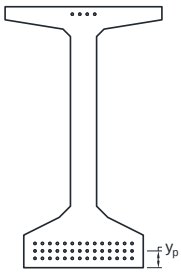
Design concrete release strength, ksi (MPa)	5.5 (37.9)	5.2 (35.9)	5.5 (37.9)	7.8 (53.8)
Number of bottom strands	24	30	28	42
Total area of bottom strands, $in.^2$ (mm^2)	7.056 (4,552)	8.82 (5,690)	8.232 (5,311)	12.348 (7,966)
y_p, in. (mm)	3.33 (85)	10.37 (263)	3.5 (89)	4.5 (114)
Jacking stress for top strands, ksi (MPa)	157.5 (1,086)	202.5 (1,396)	110.0 (758)	202.5 (1,396)
Jacking stress for bottom strands, ksi (MPa)	202.5 (1,396)	202.5 (1,396)	202.5 (1,396)	202.5 (1,396)

The design compressive release strength was varied between 5.2 ksi (37.9 MPa) and 7.8 ksi (53.8 MPa). Tx46-I was designed according to typical practice of filling each row from the bottom up for optimized flexural capacity. The resulting pattern generated the greatest spalling stresses possible at the time of prestress transfer for the Tx-girder

released at 5.5 ksi (37.9 MPa). The unconventional strand pattern in Tx46-II was chosen to maximize the number of strands and, therefore, the total prestressing force. Consequently, Tx46-II was subjected to the greatest bursting stresses possible in the Tx46 girder with the concrete release strength of 5.2 ksi (37.9 MPa). Specimens Tx70-I and Tx70-II were both designed according to the typical philosophy of maximizing moment capacity and were filled with the maximum number of strands that did not violate stress limits. However, another row of strands could be accommodated in Tx70-II because of a higher concrete release strength of 7.8 ksi (53.8 MPa) that was assumed in the girder design.

2.2 SPECIMEN FABRICATION

The specimens were fabricated at the prestressing facility at FSEL according to common industry practices. Strand stressing was conducted by extending a series of hydraulic rams, during which the forces in the rams were carefully controlled and the strand elongation was measured and verified against the applied load. The mild reinforcement cage was then tied around the stressed strands. A considerable number of strain gauges were installed on the strands and mild-steel reinforcement to monitor the strains at the time of prestress transfer and during the shear tests. Moreover, three vibrating wire strain gauges (VWGs) were embedded at the midspan of the specimens to monitor short- and long-term prestress losses.

Once the reinforcement and embedded instrumentation were installed, the side forms were assembled, and the concrete was cast. The material constituents of the concrete mixture used for each specimen is shown in

Table 2-3. The concrete for Tx46-I and Tx46-II was batched and mixed at FSEL. To simplify beam fabrication at FSEL, Tx70-I and Tx70-II were fabricated using the concrete that was batched and mixed by a nearby commercial precast component manufacturing plant and transported to FSEL. Compressive strength measurements from match-cured cylinders were used to determine the appropriate time to release the prestressing strands. The strands were released by gradual retraction of hydraulic rams, during which strains and camber were measured and recorded. The two end-regions of each specimen were extensively monitored for end-region stresses and cracking, details of which are reported by Salazar (2016). In this thesis, these two ends are referred to as the live end, i.e. the end that was closer to the moving hydraulic rams during fabrication, and the dead end, which was next to the fixed stressing plate in the prestressing facility.

Table 2-3: Concrete mixture proportions

Material		Details	Quantity				
			Specimen				Units
			Tx46-I	Tx46-II	Tx70-I	Tx70-II	
Cementitious materials		Type III cement	725 (430)	725 (430)	600 (356)	800.5 (475)	lb/yd^3 (kg/m^3)
		Type F fly ash	0	0	200 (119)	195.5 (116)	lb/yd^3 (kg/m^3)
Coarse aggregate		3/8" crushed limestone	1,951 (1,157)	1,956 (1,160)	1,400 (831)	1,345 (798)	lb/yd^3 (kg/m^3)
Fine aggregate		Concrete sand	1,072 (636)	1,082 (642)	1,400 (831)	1,117 (663)	lb/yd^3 (kg/m^3)
Water content		-	285 (169)	274 (163)	192 (114)	282 (167)	lb/yd^3 (kg/m^3)
w/cm ratio		-	0.39	0.38	0.24	0.28	-
Admixtures	High-range water reducer	Sika Viscocrete 2110	29 (1,122)	14.5 (561)	45 (1,741)	80.5 (3,114)	oz/yd^3 (mL/m^3)
	Retarder	Sika Plastiment	29 (1,122)	29 (1,122)	30 (1,160)	40 (1,547)	
	Air entraining agent	Sika Air	-	-	4 (155)	-	

Within three weeks after the release of prestressing force, a reinforced concrete slab that had a thickness of 8 in. (203 mm) and a width that was 2 in. (51 mm) less than that of the top flange was constructed on each specimen. The specific deck width was 34 in. (864 mm) for the Tx46 specimens and 40 in. (1,016 mm) for the Tx70 specimens. Once the concrete in the beam and the deck had cured sufficiently, the beams were moved to the test setup and loaded in a shear-critical loading configuration until failure. The girders had a minimum age of 28 days at the time of the shear test.

Relevant measured mechanical properties for concrete and reinforcement comprising each specimen are summarized in Table 2-4. The reported values are an

average from a minimum of three specimens for each material test. The concrete material and reinforcement properties reported in this section were used to calculate nominal shear capacities, as discussed in Chapter 3 and Appendix D.

Table 2-4: Summary of measured mechanical properties

Property		Test method	Tx46-I	Tx46-II	Tx70-I	Tx70-II
Girder concrete	Release strength, ksi (MPa)	ASTM C39	5.7 (39.6)	5.2 (35.9)	6.5 (44.9)	8.3 (57.2)
	Test day strength, ksi (MPa)		7.6 (52.4)	6.9 (47.7)	10.7 (73.9)	12.7 (87.6)
	Test day modulus of elasticity, ksi (MPa)	ASTM C469	4,910 (33,890)	5,420 (37,400)	6,100 (42,030)	6,020 (41,470)
	Test day splitting tensile strength, ksi (MPa)	ASTM C496	0.63 (4.34)	0.56 (3.86)	0.86 (5.93)	0.97 (6.69)
	Test day modulus of rupture, ksi (MPa)	ASTM C78	0.83 (5.72)	0.89 (6.14)	1.07 (7.38)	-
Slab concrete	Test day strength, ksi (MPa)	ASTM C39	10.71 (73.8)	7.93 (54.7)	7.94 (54.7)	9.17 (63.2)
	Test day modulus of elasticity, ksi (MPa)	ASTM C469	6,930 (47,750)	5,910 (34,560)	5,970 (41,130)	5,890 (40,620)
No. 4 bars	Yield strength, ksi (MPa)	ASTM A370	60.7 (419)		72.2 (498)	
	Ultimate strength, ksi (MPa)		99.3 (685)		111.6 (769)	
No. 6 bars	Yield strength, ksi (MPa)		74.0 (510)		67.7 (467)	
	Ultimate strength, ksi (MPa)		114.7 (791)		106.7 (736)	
Strands	Modulus of elasticity, ksi (MPa)	ASTM A1061	27,810 (192,000)			
	Yield strength, ksi (MPa)		232.0 (1,600)			
	Ultimate strength, ksi (MPa)		276.1 (1,904)			

2.3 TEST SETUP

Each specimen was loaded as a simply supported member until failure in a shear-critical loading configuration. Since the specimens had a relatively small length of 30 ft (9 m), only one shear test was performed on each specimen. Therefore, to evaluate the potential differences between the behavior of the live and dead ends and to ensure a consistent shear span-to-depth ratio regardless of the failed span, all specimens were subjected to a symmetric loading configuration in which both ends of the specimen were subjected to the same shear force.

2.3.1 Loading Configuration

Figure 2-4 shows the test configuration for the Tx46 specimens. As can be seen in this figure, each Tx46 specimen was subjected to two equal, symmetric concentrated loads that were applied using a steel spreader beam. Steel rollers were used to transfer the load from the spreader beam to the test specimen at desired locations. Using this setup, the shear span could be changed as needed by moving the location of the rollers along the spreader beam. A shear span-to-depth ratio of 3.0 was used for the Tx46 specimens to facilitate a shear failure while avoiding deep-beam behavior.

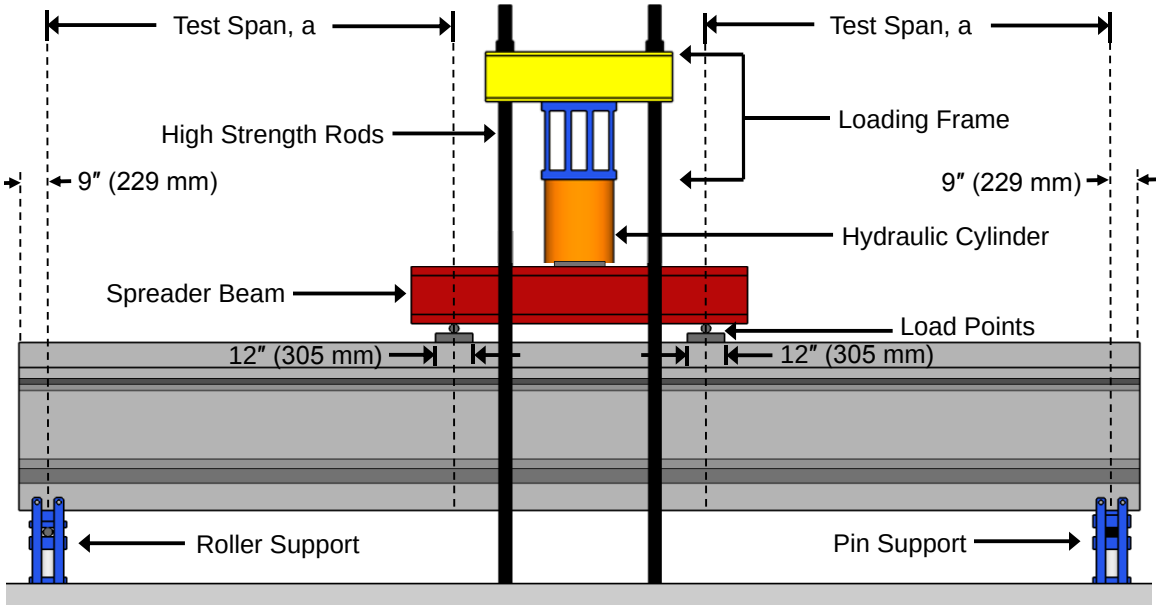

Figure 2-4: Shear test setup for the Tx46 specimens

The Tx70 specimens were subjected to a point load at the midspan to obtain the highest shear span possible (Figure 2-5). This configuration resulted in two shear spans with equal lengths, each with a span-to-depth ratio of approximately 2.3 for both specimens.

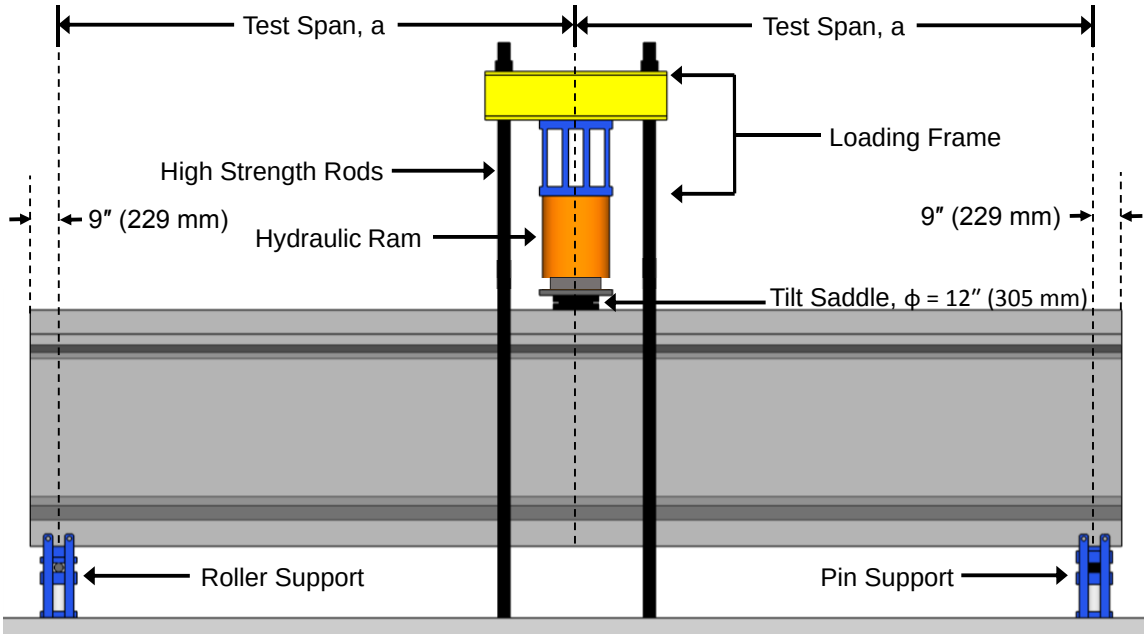

Figure 2-5: Shear test setup for the Tx70 specimens

The specimens were supported by a roller support fixture at one end and a pin support fixture at the other end. Both support fixtures were carefully designed and fabricated using machined steel components to provide precise boundary conditions (Figure 2-6). The roller support included a 3-in. (76-mm) diameter roller that permitted free rotation and translation while the pin support included a tilt-saddle that permitted only free rotation. Each support fixture also included two load cells to measure the support reactions during the structural test. The beams rested directly on steel bearings on top of support fixtures with accompanying ¼-in. (6-mm) thick neoprene pads to prevent stress concentrations due to potentially uneven bearing surfaces. High-strength gypsum cement was used as a leveling compound between the support fixtures and the testing floor and between the loading plates and the top surfaces of the specimens.

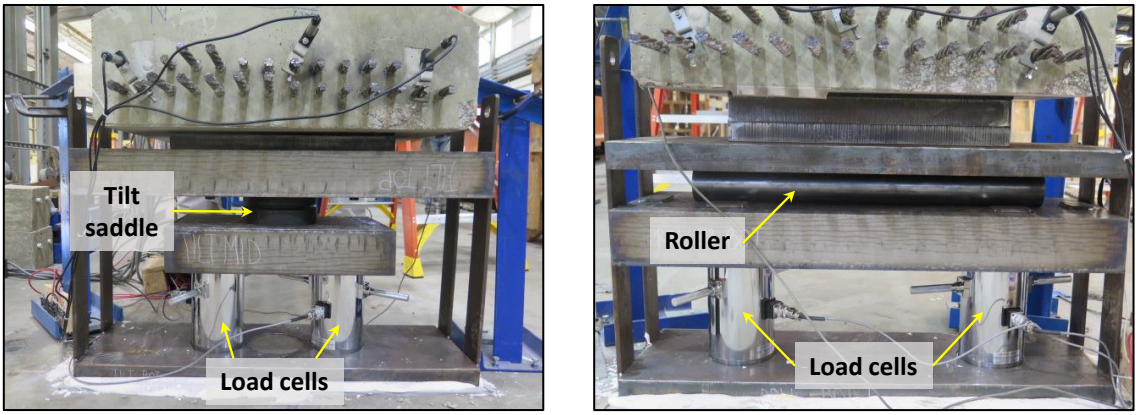

(a) (b)

Figure 2-6: (a) Pin support fixture; (b) Roller support fixture

Given the loading configurations presented above, the shear force and bending moment diagrams for the Tx46 and Tx70 specimens were as shown in Figure 2-7(a) and (b). In the Tx46 specimens, a constant moment region existed over the midspan regions. However, since the specimens were designed to fail in shear before showing any flexural distress, no changes in the shear performance of the specimens were expected due to this configuration. The diagrams in

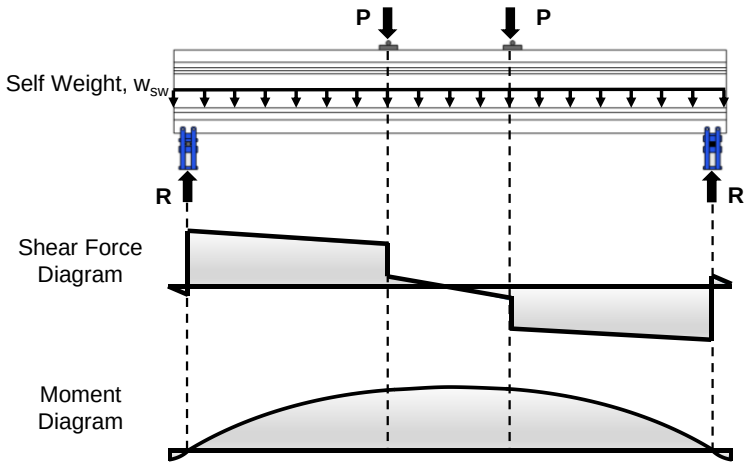

(a)

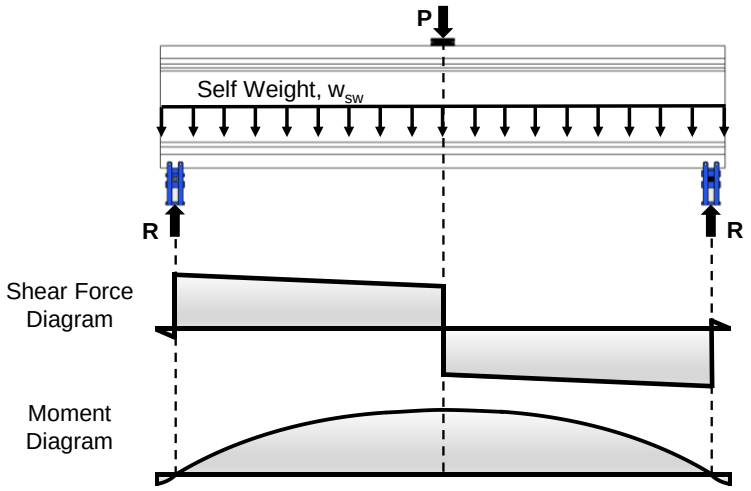

(b)

Figure 2-7 represent the bending moments and shear forces assuming small point loads with respect to the self-weight of the beam. At ultimate conditions, the large point loads dominate the shear and moment diagrams, and the effects of self-weight become negligible.

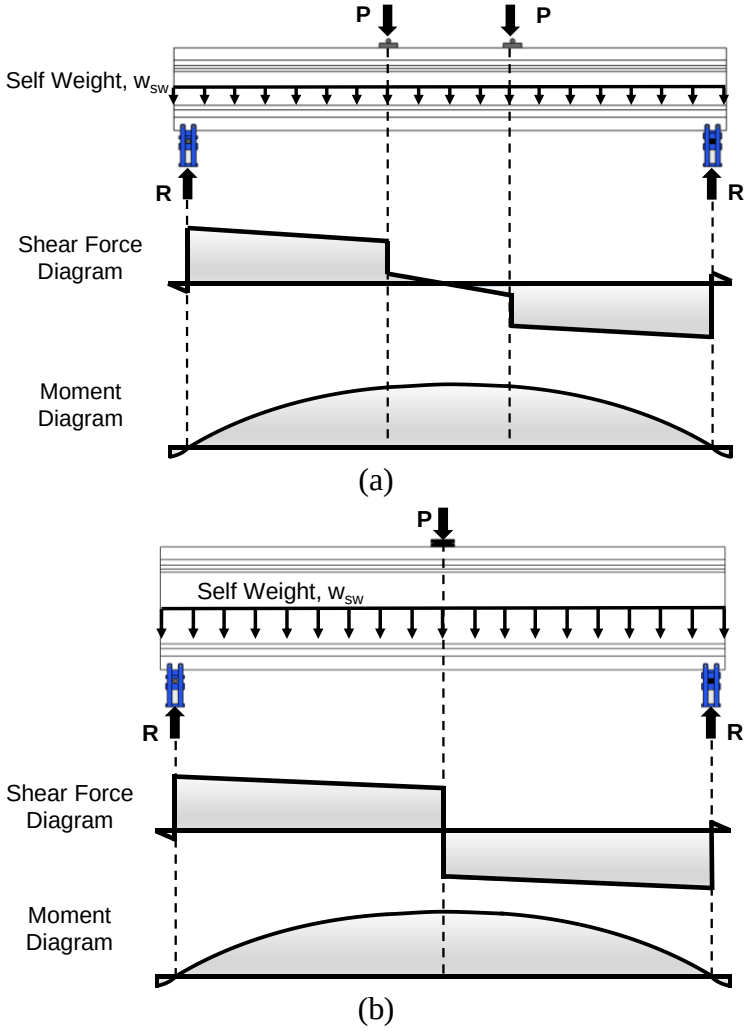

Figure 2-7: Shear force and bending moment diagrams for (a) Tx46 specimens; (b) Tx70 specimens

Load was applied to the specimens using a single hydraulic ram that was pressurized by means of a pneumatically controlled hydraulic pump. The hydraulic cylinder had a capacity of 2,000 kips (8,900 kN) and as shown in Figure 2-4 and Figure 2-5, reacted against a stiff loading frame that was connected to the strong floor by way of high-strength steel rods.

2.3.2 Instrumentation

Each specimen was extensively instrumented to monitor loads, displacements, strains, and strand slip throughout the structural test. The load for each test was monitored using four 500 kip (2,200 kN) load cells placed in the support fixtures. These load cells were also monitored during the initial placement of the specimens and the loading frame into the test setup for an accurate measurement of self-weight. Linear potentiometers (LPOTs) were placed on both sides of the beam at the supports and directly under the load points to measure the vertical displacements under the load points and at the supports (Figure 2-8 (a)). Stress development in the transverse reinforcement was monitored via strain gauges installed on the stirrups during specimen fabrication. For the Tx46 specimens, 15 stirrups were monitored on each end, which corresponded to a distance of 50.5 in. (1,280 mm) from the end face of the specimens. For the Tx70 specimens, 21 stirrups were monitored on each end for a distance of 86.5 in. (2,200 mm) from the end face. To reveal whether or not the specimen showed signs of anchorage zone distress, strand slip was measured at each end of the specimens. For Tx46 specimens, the strand slip was measured for three strands at each end using Linear Strain Conversion Transducers (LSCTs). For Tx70 specimens, these measurements were made using LPOTs on five strands at each end (Figure 2-8 (b)).

Each test span of Tx70-I and Tx70-II was also instrumented for concrete surface strains using the NDI Optotrak Certus optical tracking system (Figure 2-8 (c)). The markers for the optical tracking system were located on a 1- by 1-ft (305- by 305-mm)

grid, which covered the full depth of the web over a 7-ft (2.1-m) length. The coordinates of the markers were recorded at a frequency of 2 Hz during the structural test.

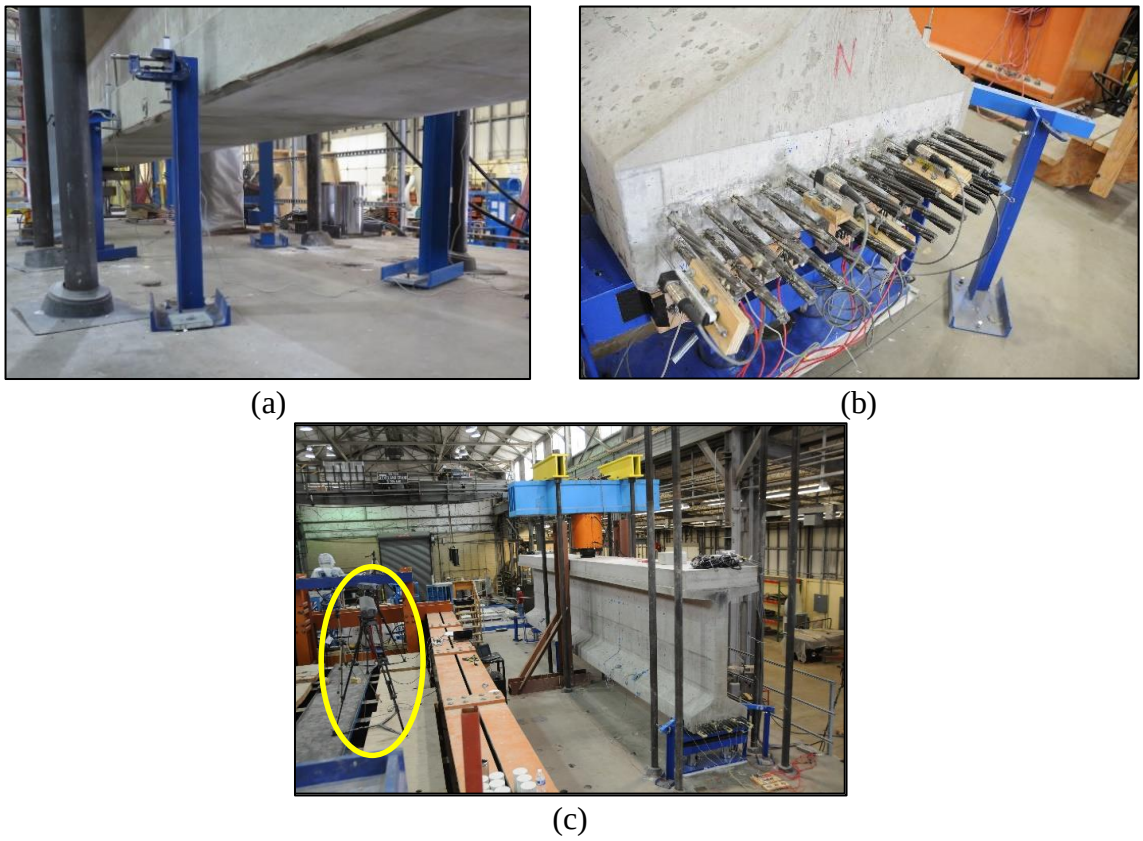

Figure 2-8: Shear test instrumentation: (a) LPOTs applied to the beam under load points for Tx46-I; (b) LPOTs mounted on strands for Tx70-I; (c) Optical tracking system for Tx70-I.

2.3.3 Testing Procedure

During each test, load was applied in a series of stages that were smaller than one-tenth of the nominal capacity of the specimen, as estimated using AASHTO LRFD Bridge Design Specifications (2014). Typical load stage increments of 50 kip (222 kN) and 100 kip (445 kN) were used for Tx46 and Tx70 specimens, respectively. Each increment of loading was applied in a continuous, quasi-static manner, at a rate of 500 lb

(2.22 kN) per second or less. After each load stage was reached, loading was paused, and the conditions of the specimen were visually inspected and recorded. Once the specimen sustained significant damage, visual inspection efforts were suspended, and the specimen was subsequently loaded to failure while simultaneously recording data and video.

CHAPTER 3: RESULTS AND DISCUSSION

This chapter includes details and observations from the test program and provides an analysis of the results obtained from the shear tests. During shear tests, the specimens were aligned in a north-south orientation, with the live end at north.

3.1 EFFECTS OF PRESTRESS TRANSFER ON THE SPECIMENS

Figure 3-1 shows the stresses that were recorded in the transverse reinforcement within the end regions of the specimens at the time of prestress transfer, as reported by Salazar (2016). It is visible from this figure that stresses up to 26 ksi (179 MPa) were detected in the stirrups. However, stresses exceeding 10 ksi (69 MPa) were observed in only the first four stirrups, which were located within the overhang region of the specimens or over the support. The stresses in the stirrups that were within the clear span of the specimens were generally limited to 10 ksi (69 MPa). These stresses were not expected to have a noticeable effect on the contribution of the stirrups to the load-carrying capacity, especially in the sections expected to be critical in resisting shear.

The transverse stresses within the girder end regions were expected to change due to time-dependent effects. However, the monitoring of such changes was not considered. Thus, the stresses reported in the stirrups in this chapter start from zero at the beginning of the shear test.

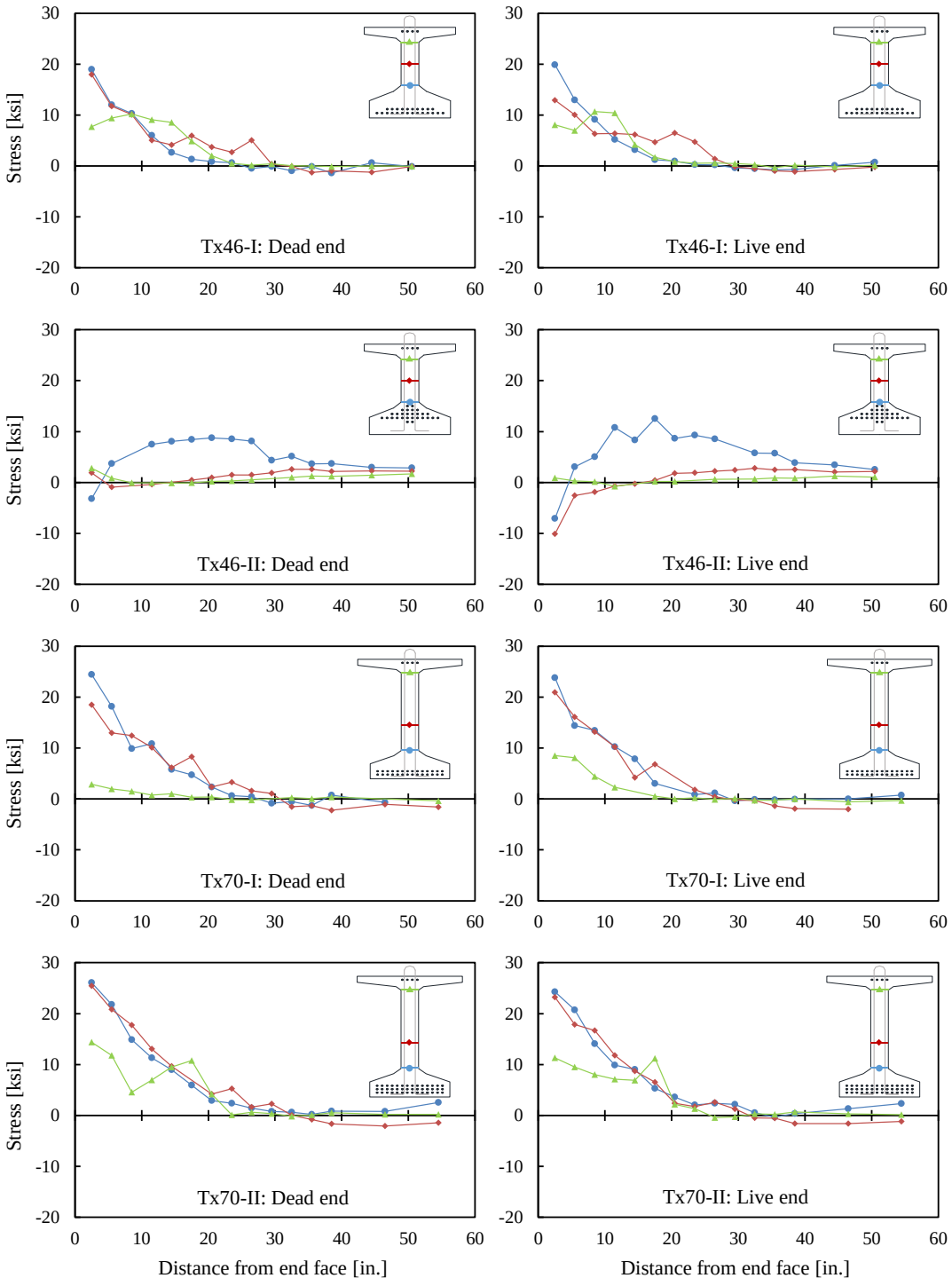

Figure 3-1: Stresses within the end-region reinforcement of the specimens (Salazar, 2016)

All four specimens had noticeable cracking within their end regions due to prestress transfer. Among all specimens, the maximum width of these cracks prior to start of the shear test was approximately 0.008 in. (0.20 mm). In the figures presented in the following sections of this chapter, these cracks are illustrated by blue lines. The extent of damage (i.e., the length and width of cracks) was slightly greater at the dead ends of the specimens than at their live ends. Detailed information regarding the end-region stresses and widths and patterns of the cracks observed prior to shear test is presented and discussed by Salazar (2016).

3.2 TX46-I RESULTS

Prior to the shear test on Tx46-I, noticeable cracking was observed at the web-flange interface near the beam ends due to prestress transfer. A continuous series of cracks along this interface was observed over approximate distances of 2 and 3 ft (610 and 910 mm) from the dead and live ends, respectively. The maximum crack width at the interface prior to the start of the shear test was approximately 0.006 in. (0.15 mm).

Figure 3-2 shows the plots of load-deflection and load-strand slip for Tx46-I. In this figure and similar figures in this chapter, the reaction force on the vertical axis consists of the effect of the applied load as well as self-weight of the specimen and the loading frame. Therefore, the reaction force is not zero at the beginning of the test. As mentioned in Chapter 2, LPOTs were used at each support and each load point on both sides of the specimen. The deflections shown in these figures are the average deflections

obtained from the two sides of the specimen after subtracting the rigid-body displacement of the specimen due to support deformations.

Initial load increments for this specimen resulted almost exclusively in the extension of existing cracks from the prestress transfer and the creation of new horizontal cracks at the flange-web interface. Major diagonal cracking occurred in the dead- and live-end spans at total reaction forces of 228 and 235 kips (1,014 and 1,045 kN), respectively. Diagonal cracking was accompanied by a noticeable reduction in the overall specimen stiffness. Slippage of the instrumented strands was first detected during the final loading stage at a reaction force of approximately 413 kips (1,840 kN) and coincided with a gradual and loss of stiffness. Stirrup yielding was first recorded at 455 kips (2,022 kN) of reaction force. However, since the instrumented stirrups were all located within a distance of 50.5 in. (1,280 mm) from the face of the support, it is likely that the first yielding in the stirrups may have occurred outside this region, under smaller load levels.

The start of noticeable strand slip coincided with a considerable change in the stiffness of the specimen. However, due to the limited number of strands that were instrumented, it is not clear whether strand slip or yielding in the non-instrumented stirrups was the major contributor to the loss of stiffness. After the confirmed stirrup yielding, the load-versus-slip plot shows significant slippage of both monitored strands on the bottom row without any increase in load, indicating bond failure.

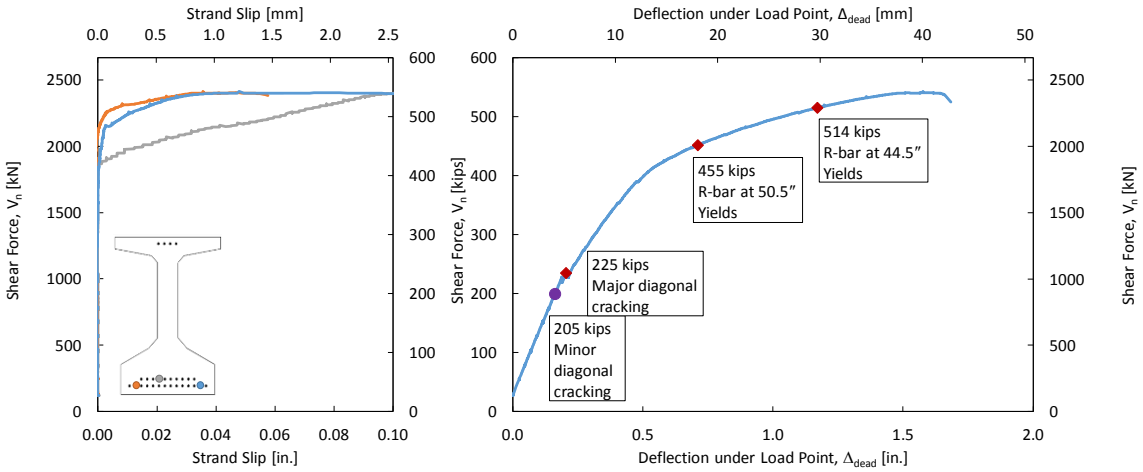

Figure 3-2: Plots of reaction force versus deflection and strand slip for the dead-end span of Tx46-I

The beam deflected an additional 0.91 in. (23 mm) after the first yielding was detected in the stirrups. The ultimate recorded shear force was 543 kips (2,413 kN) and failure occurred in the dead end span. At peak load, the deflection under the load point and the maximum strand slip were recorded as 1.58 in. (40 mm) and 0.108 in. (2.70 mm), respectively.

Figure 3-3 shows tensile stresses in the stirrups of Tx46-I at peak shear force. Yielding was detected in stirrups that were at distances of 14.5 in. (370 mm) and 17.5 in. (440 mm) from the end face of the member. Subsequent stirrups showed negligible stresses until a distance of 35.5 in. (900 mm) from the end face, where yielding was observed in the stirrups once again.

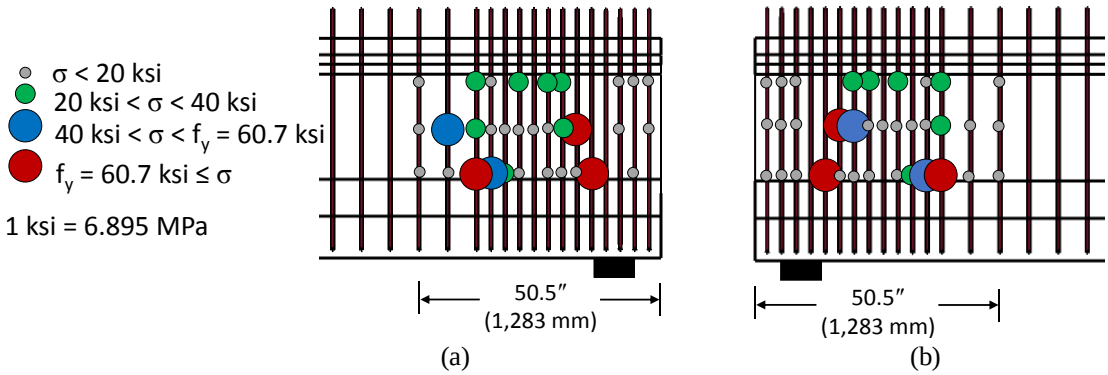

Figure 3-3: Stirrup stresses at peak load in Tx46-I: (a) dead end; and (b) live end

The cracking patterns observed immediately prior to failure of the specimen are presented in Figure 3-4. The primary features were long diagonal cracks extending from the load application point to the supports. The inclination angles of the diagonal cracks in the web with the horizontal direction ranged approximately between 32 and 36 degrees. No sign of flexural distress (e.g. flexural cracking or crushing of the compression block) was observed in the specimen. There was a greater extent of cracking along the horizontal interface between the web and the bottom flange on the west side of the dead end span.

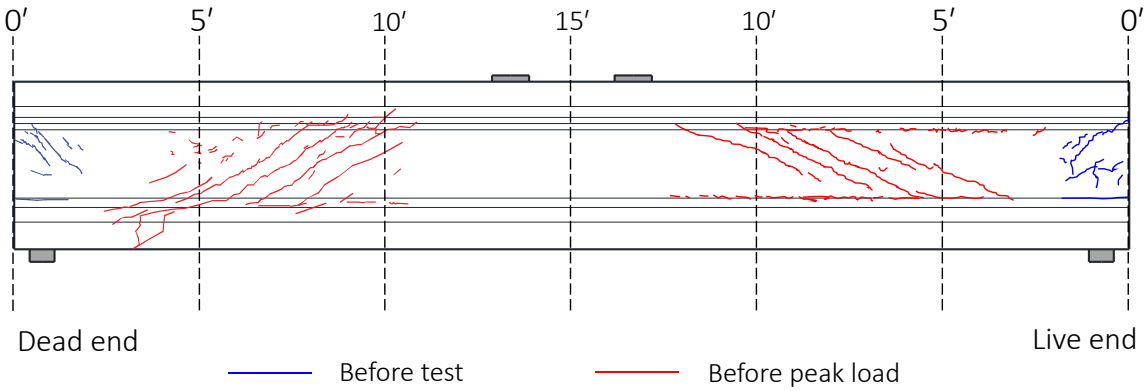

One web shear crack grew to reach the ultimate tensile fiber of the beam at a distance of approximately 2.5 ft (760 mm) from the face of the support.

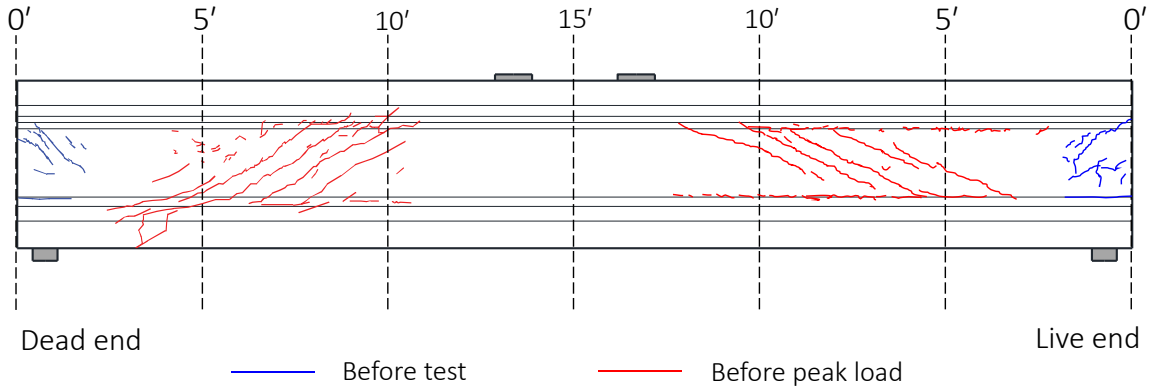

Figure 3-4: Cracking pattern immediately prior to failure on the east face of Tx46-I

Failure of Tx46-I was accompanied by substantial cracking and spalling of concrete. One side of the specimen showed a distinct horizontal crack at the web-flange interface, which extended from the end face of the beam over a distance of approximately 10 ft (3 m). At the end face, the web slid past the bottom flange by approximately 1 in. (25 mm) (Figure 3-7). Large cracks between the strands, typical of bond failure, also formed in the end region. A large longitudinal crack was also observed on the bottom side of the specimen (Figure 3-6). This crack originated at a distance of approximately 4 ft (1,220 mm) from the dead-end face of the beam where a shear crack projected through the beam's bottom flange, and extended along the beam to midspan. Moreover, large areas of cover concrete spalled off the bottom flange on both sides of the dead-end span, exposing the confining end-region reinforcement (Figure 3-6 and Figure 3-7).

Cover concrete in the bottom region of the web also spalled off in the vicinity of the support.

(a) (b)

Figure 3-5: Post-failure conditions of Tx46-I: (a) isometric view of the failed end; and (b) displacement of web relative to bottom flange at end face

Figure 3-6: East and bottom sides of Tx46-I after failure

Figure 3-7: West side of Tx46-I after failure

3.3 TX46-II RESULTS

Tx46-II was designed to represent critical conditions with respect to end-region bursting stresses. As a result, prior to the shear test, both dead and live ends of the specimen demonstrated an almost continuous horizontal crack at the web-flange interface, which extended from the end face to an approximate distance of 4 ft (1.2 m). The maximum crack width observed prior to the shear test was 0.004 in. (0.10 mm), which was at multiple locations along the flange-web interface.

The load-deflection and load-strand slip plots for Tx46-II are shown in Figure 3-8. Throughout the test, the load-deflection plot shows a gradual loss of stiffness. First diagonal cracks were noted almost simultaneously in both test spans at a reaction force of approximately 154 kips (685 kN), which grew in length, width, and number until failure of the specimen. However, the development of new diagonal cracks did not correspond to a sudden change in the stiffness of the specimen.

As can be seen in the inset to Figure 3-8, the strand pattern in Tx46-II allowed for greater separation among strands monitored for strand slip. The two strands located at a distance of 12.5 in. (320 mm) from the bottom of the beam began to slip almost simultaneously at a reaction force of approximately 174 kips (774 kN). The strand located at 8.5 in. (220 mm) from the bottom of the beam did not show any slippage until a reaction force of 322 kips (1,432 kips). The first confirmed yielding in the stirrups occurred toward the end of the test, at a shear load level of 430 kips (1,913 kN). The load-versus-slip plot for this specimen also shows considerable softening at the final

stages of the test, suggesting a breakdown of bond. The final softening of the specimen appears to be due to a combination of yielding in the stirrups and loss of anchorage for the strands.

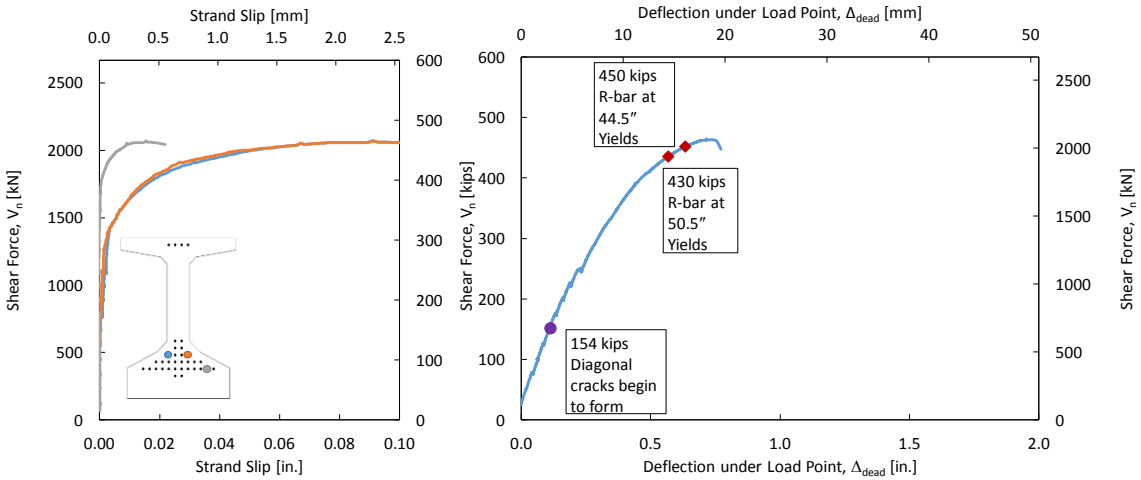

Figure 3-8: Plots of reaction force versus deflection and strand slip for the dead-end span of Tx46-II

The peak reaction force was recorded as 465 kips (2,067 kN), after which the specimen failed in the test span next to the dead end. The deflection recorded under the load point at peak load was 0.76 in. (19.3 mm) whereas the maximum observed strand slip at peak load was 0.108 in (2.75 mm).

Stirrup stresses in Tx46-II at peak load are shown in Figure 3-9. Very small stresses were measured within the first 29.5 in. (750 mm) from the support. However, in regions farther from the support, considerable tensile stresses developed in the stirrups. At the dead-end span of the specimen, where failure occurred, yielding was detected in

two instrumented stirrups that were located at 44.5 in. (1,130 mm) and 50.5 in. (1,280 mm) from the end face.

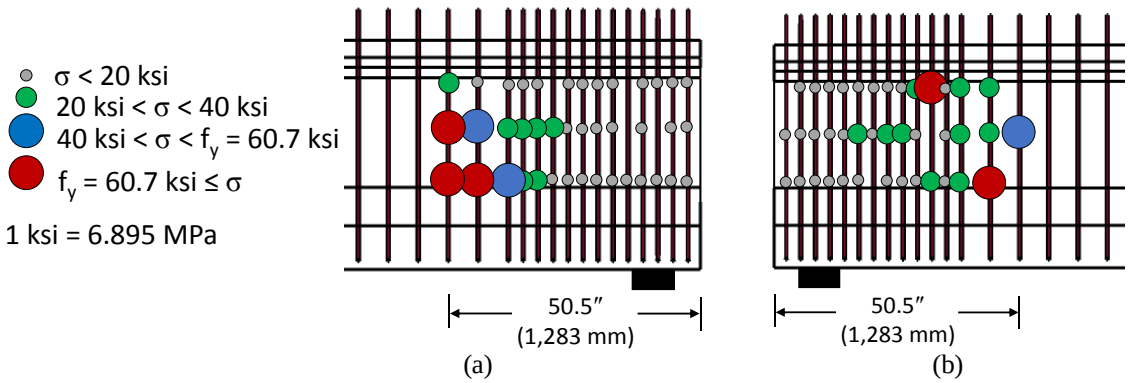

Figure 3-9: Stirrup stresses at peak load in Tx46-II: (a) dead end; and (b) live end

The cracking observed in Tx46-II immediately prior to failure is shown in Figure 3-10. Due to the circumstances surrounding the test, a map of the cracking immediately prior to peak load on the west side of the live end span was not recorded. Considerable diagonal cracking occurred in the web, over a region that extended from the face of the support to a distance of approximately 2 ft (610 mm) from the load point. The angle between diagonal cracks in the web and the horizontal direction ranged between 27 degrees in the regions farther from supports and 53 degrees near the supports. Some cracks also formed over the supports and extended to the end face of the specimen. No signs of flexural damage were observed throughout the test.

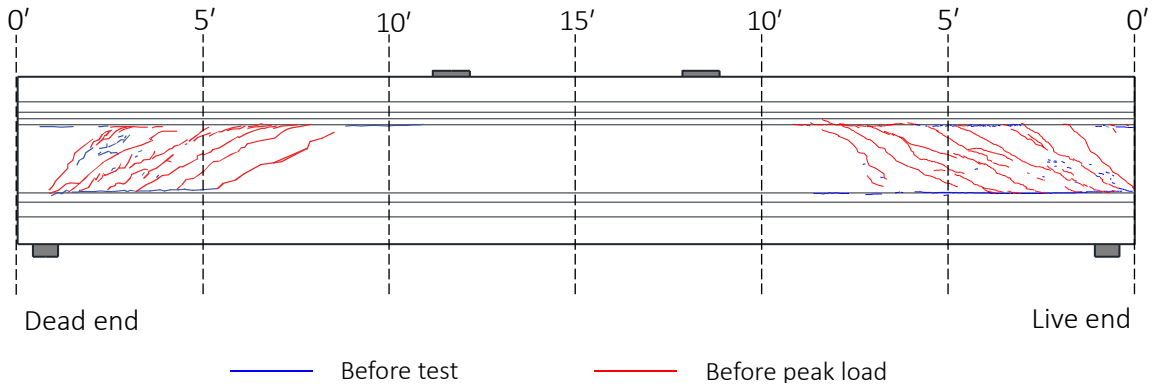

Figure 3-10: Cracking pattern immediately prior to failure on the east face of Tx46-II

Failure of the specimen was accompanied by a short duration of sustained noise, likely caused by concrete cracking or bond failure. Large cracks propagated vertically in columns of strands at the end face (Figure 3-11). No spalling of cover concrete was observed in the bottom flange. However, noticeable spalling was observed over a region of the girder that was 2.5 ft (760 mm) long and 1.5 ft (460 mm) tall (Figure 3-13). This region, which started above the support at the web-flange interface, revealed that the diagonal cracks penetrated a greater depth into the web than the horizontal crack at the web-flange interface. A continuous horizontal crack along the web-flange interface was observed on one side of the specimen after failure (Figure 3-12).

(a) (b)

Figure 3-11: Post-failure conditions of Tx46-II: (a) end-face, and (b) displacement of web relative to bottom flange at end face

Figure 3-12: Southwest side of Tx46-II after failure

Figure 3-13: Southeast side of Tx46-II after failure

3.4 TX70-I RESULTS

Tx70-I was designed to examine the effects of using 0.7-in. (17.8-mm) strands in a deeper beam with maximized moment capacity. Spalling cracks dominated the damage observed at release. End-region cracks in the web propagated longitudinally and diagonally from the ends of the beam to a distance of approximately 3 ft (910 mm). Horizontal cracking was observed at the interface between web and bottom flange within a distance of approximately 1 ft (300 mm) from each end of the specimen.

Figure 3-15 shows the load-deflection and load-strand slip plots for Tx70-I. During the early stages of the shear test, most of the damage was limited to the extension of the end-region cracks formed during prestress transfer. Small, discontinuous cracks were observed at the bottom flange-web and top flange-web interfaces early in the test. At a reaction force of approximately 104 kips (462 kN), cracks were observed on each end face of the member slightly below the flange-web interface (Figure 3-14). These cracks extended through the thickness of the member. At approximately 205 kips (911 kN) of reaction force, a vertical crack was formed on the specimen's live-end face, extending from the bottom of the member to one of the strands in the bottom row.

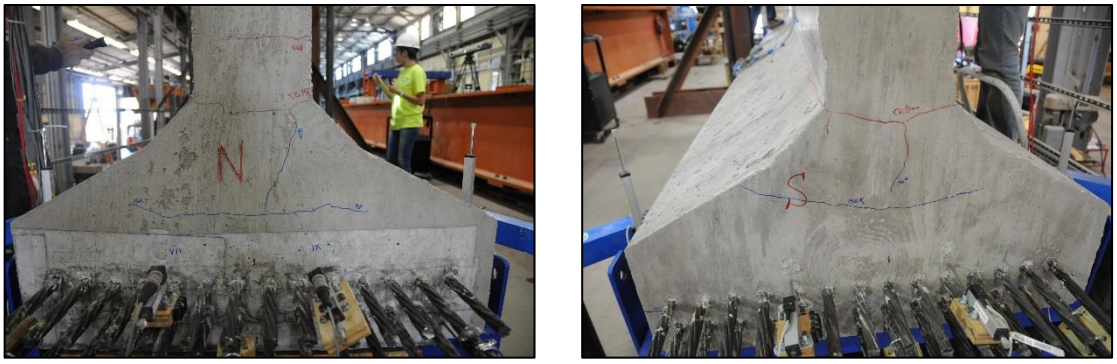

(a) (b)

Figure 3-14: End-face cracking in the early stages of shear test on Tx70-I

Multiple diagonal cracks formed simultaneously in both test spans at a reaction force of 304 kips (1,351 kN), leading to a noticeable change in the stiffness of the member. Strand slip was initiated at a reaction force of approximately 410 kips (1,824 kN), but noticeable slip was not measured in the strands until 500 kips (2,224 kN). The first yielding in the stirrups was detected later, at a reaction force of approximately 573 kips (2,549 kN), and considerable yielding was detected in the stirrups before failure. Yielding of each stirrup is denoted in Figure 3-15 by a red diamond. The increase in the number of yielded stirrups also corresponds to a considerable reduction in the member stiffness. This softening happened concurrently with significant increase in the measured slip from all strands, indicating likely bond failure.

The maximum recorded shear force was 750 kips (3,333 kN). The beam deflected 0.85 in. (22 mm) under the load point before failing at the dead-end span. The maximum recorded strand slip at peak load was 0.075 in. (1.91 mm).

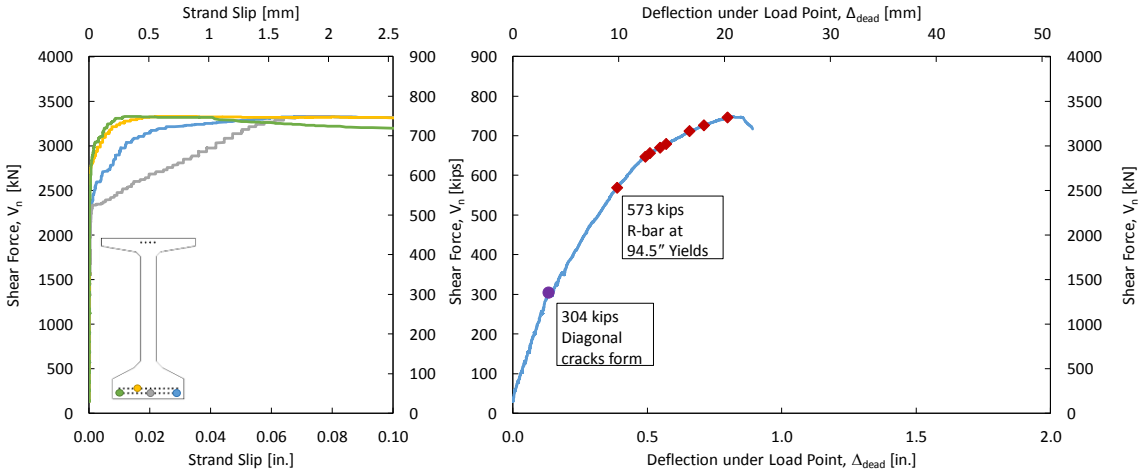

Figure 3-15: Plots of reaction force versus deflection and strand slip for the dead-end span of Tx70-I

Figure 3-16 shows the stresses in stirrups at peak load. The stresses were found to be very small in stirrups that were within 26.5 in. (670 mm) from the end face of the specimen. However, yielding was observed in almost all of the stirrups outside the heavily reinforced end-region of the girder.

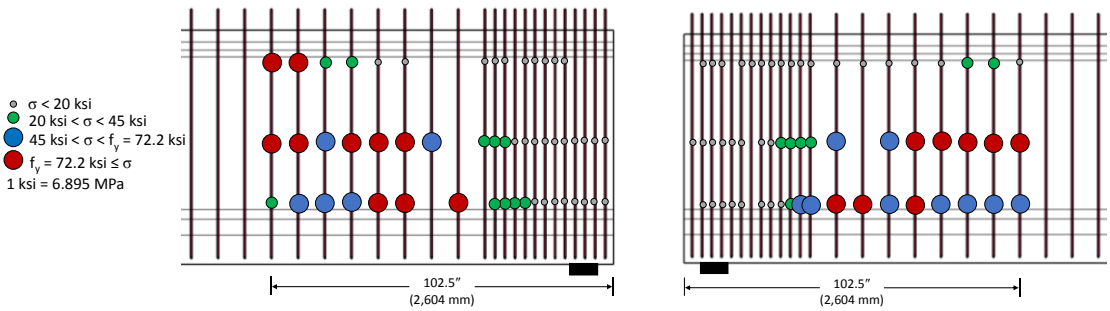

Figure 3-16: Stirrup stresses at peak load in Tx70-I: (a) dead end; and (b) live end

Figure 3-17 shows the extent of cracking in the specimen immediately prior to failure. Diagonal cracks formed between the load point and the supports over a length of approximately 9 ft (2,740 mm). The inclination angles of the diagonal cracks in the web

were all approximately near 19 degrees. No continuous horizontal cracking was observed near supports on either the bottom flange-web interface or the top flange-web interface. No signs of flexural damage were observed prior to failure.

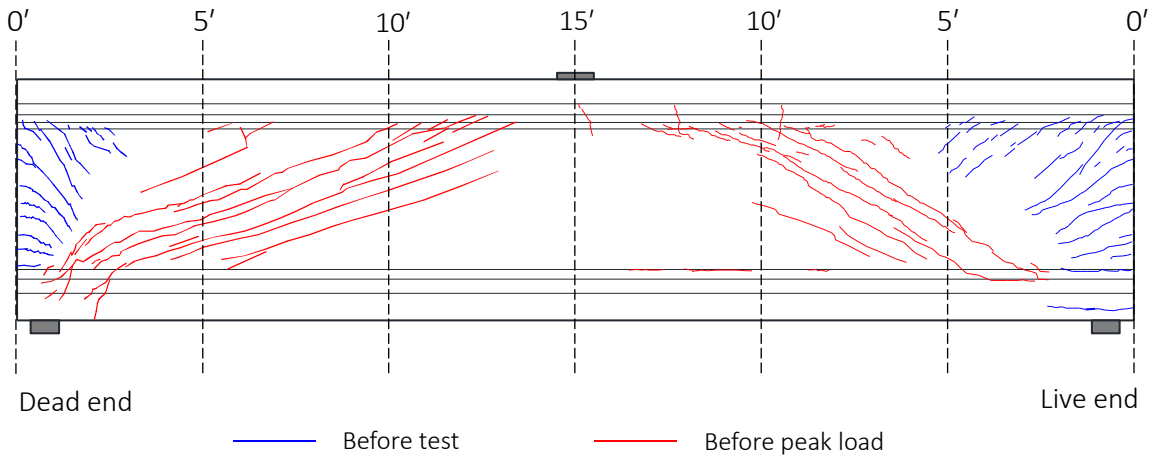

Figure 3-17: Cracking pattern immediately prior to failure on the east face of Tx70-I

The large amount of energy released at failure caused significant damage to the specimen. Notably, there was significant cracking through both rows of the strands at the end face of the member (Figure 3-18), reflecting a bond failure. At the elevation of the bottom row of the strands, a longitudinal crack was also observed on one side of the specimen, which extended over a distance of approximately 4 ft (1,220 mm) from the support (Figure 3-19). Sections of cover concrete at the dead end face spalled off. Spalling of the side cover was also observed in the bottom flange in a region that extended between 4 ft (1,220 mm) and 10 ft (3,050 mm) from the end face of the girder. No clear signs of horizontal shear damage were observed after failure. The bottom face of

the specimen experienced extensive damage at a distance of approximately 3 ft (910 mm) from the end face, resulting in the spalling of bottom cover concrete.

(a) (b)

Figure 3-18: Post-failure conditions of Tx70-I: (a) end-face, and (b) damage to the bottom face of the girder in the vicinity of the support

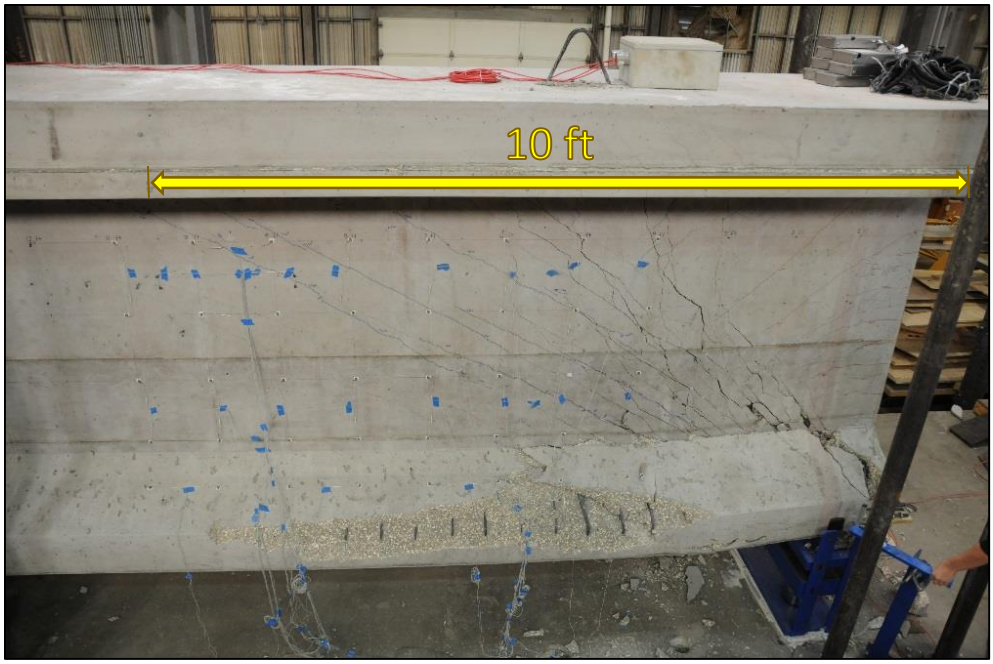

Figure 3-19: Southwest side of Tx70-I after failure

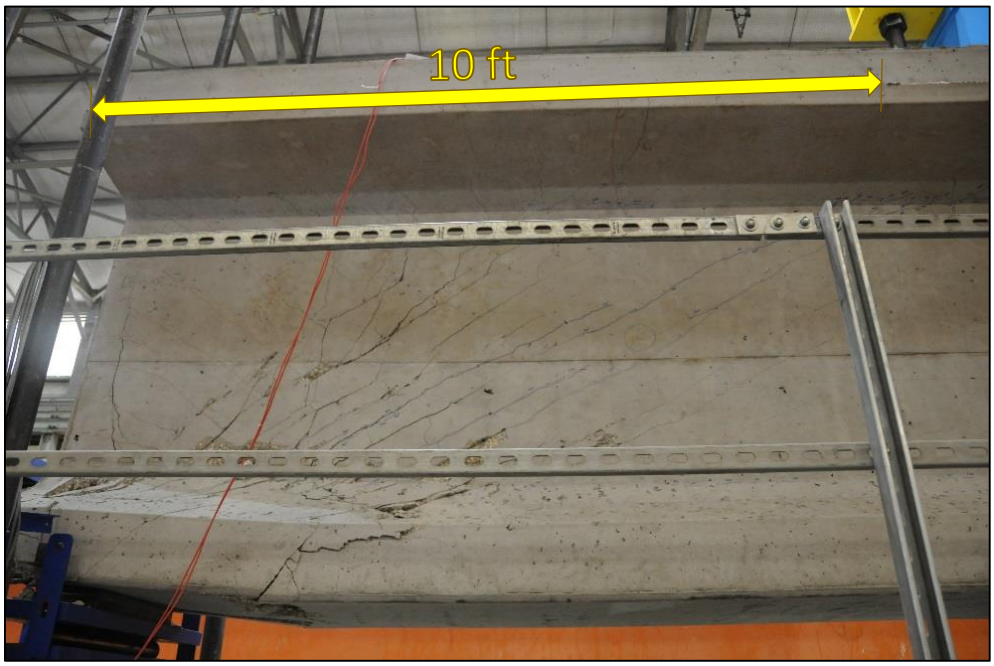

Figure 3-20: Southeast side of Tx70-I after failure

3.5 TX70-II RESULTS

Tx70-II was designed with a similar philosophy to that for Tx70-I. However, this specimen was able to accommodate 14 more 0.7-in. (17.8-mm) strands due to its higher release strength of 8.3 ksi (57 MPa). Prior to the start of the shear test, spalling cracks were observed that extended over a distance of approximately 6 ft (1,830 mm) from each end of the specimen. Horizontal cracks were also observed at the web-bottom flange interface that extended from each end face to a longitudinal distance of approximately 2 ft (610 mm). Several cracks were observed passing through the thickness of the specimen, both in the web and the bottom flange at each end face. A maximum crack width of 0.007 in. (0.18 mm) was recorded near the dead end of the specimen.

Initial loading steps on Tx70-II mostly resulted in small, discontinuous cracks at the bottom flange-web interface at various locations. Early in the test, horizontal cracks also formed in the top half of the web, which began near the load point and extended towards the supports. With the increase in load, these cracks extended to an approximate length of 6.5 ft (2 m) in each span until the development of diagonal web cracking halted their growth.

The load-deflection and load-strand slip plots for Tx70-II are provided in Figure 3-21. Minor diagonal cracking was first observed in both test spans at a reaction force of 333 kips (1,481 kN). At a reaction force of 383 kips (1,704 kN), major diagonal cracking developed, which coincided with a drop in load and a noticeable loss in the overall stiffness. Subsequent loading resulted in a growth in the number, length, and

width of diagonal cracks. However, the secondary stiffness remained mostly constant until the late stages of the test. One of the strands in the top row started to slip at a reaction force of 492 kips (2,189 kN). Stirrup yielding (signified by the red diamonds on the load-deflection plot) was recorded later in the test, beginning at a reaction force of 687 kips (3,056 kN). All instrumented strands experienced major slip towards the end of the test. It appears that the combined effect of strand slip and stirrup yielding resulted in a loss of overall stiffness prior to failure.

The ultimate reaction force was recorded as 837 kips (3,720 kN), after which the specimen failed in the live-end span. At peak load, the deflection under the load point was 0.66 in. (16.8 mm) whereas the maximum strand slip was recorded as 0.119 in. (3.0 mm).

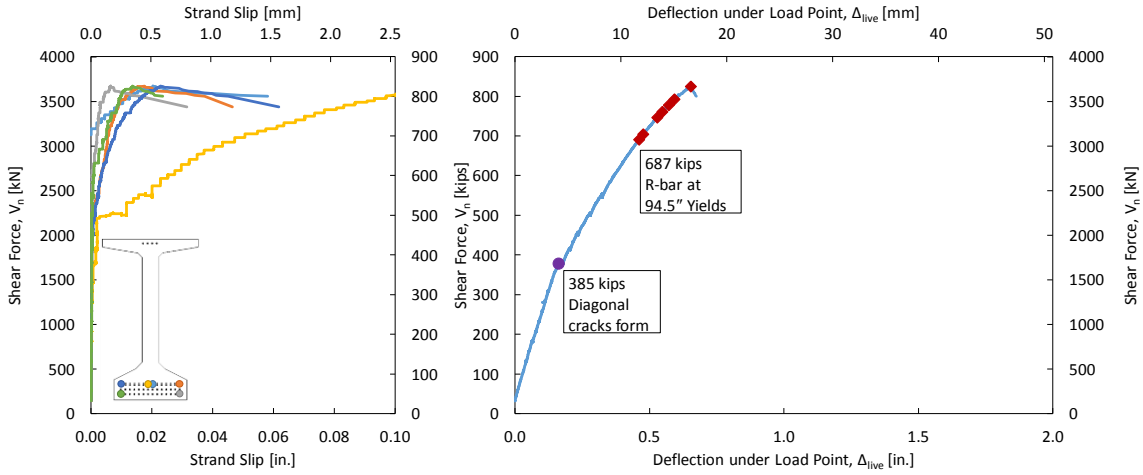

Figure 3-21: Plots of reaction force versus deflection and strand slip for the live-end span of Tx70-II

Figure 3-22 displays the tensile stresses in the stirrups in Tx70-II. The stresses were very small within the first 26.5 in. (670 mm) from each end face. In the live-end span, which eventually failed in shear, yielding was observed in almost all bars outside the tightly spaced end-region reinforcement until the last instrumented stirrup at 102.5 in. (2,600 mm). Similar observations were made from the dead-end span.

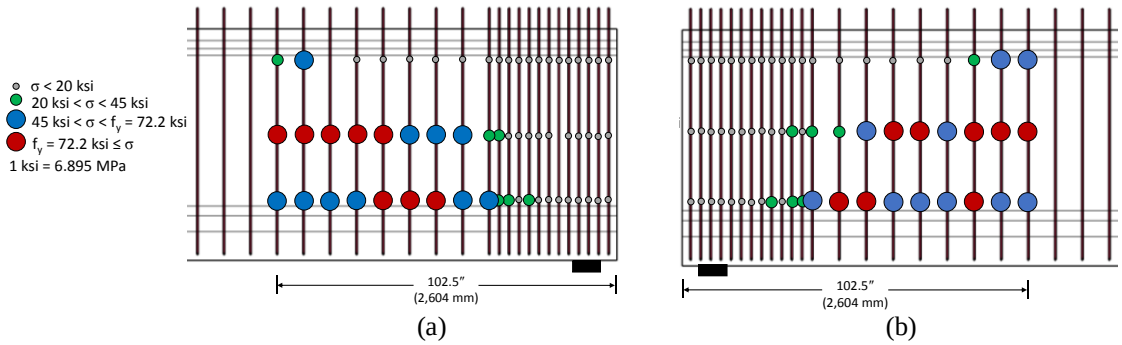

Figure 3-22: Stirrup stresses at peak load in Tx70-II: (a) dead end; and (b) live end

Figure 3-23 shows the extent of cracking observed in the specimen immediately prior to failure. Both spans displayed a large field of tightly spaced diagonal cracks, which covered almost the entire web between the loading point and the supports. The inclination angles of the diagonal crack in the web were all approximately near 32 degrees. In addition to the horizontal cracks at the top half of the web, which were previously noted, notable horizontal cracks were also visible at the interfaces between the web and top and bottom flanges prior to failure. No signs of flexural damage, such as flexural cracking or crushing of the compressive concrete under the loading point, was observed prior to failure.

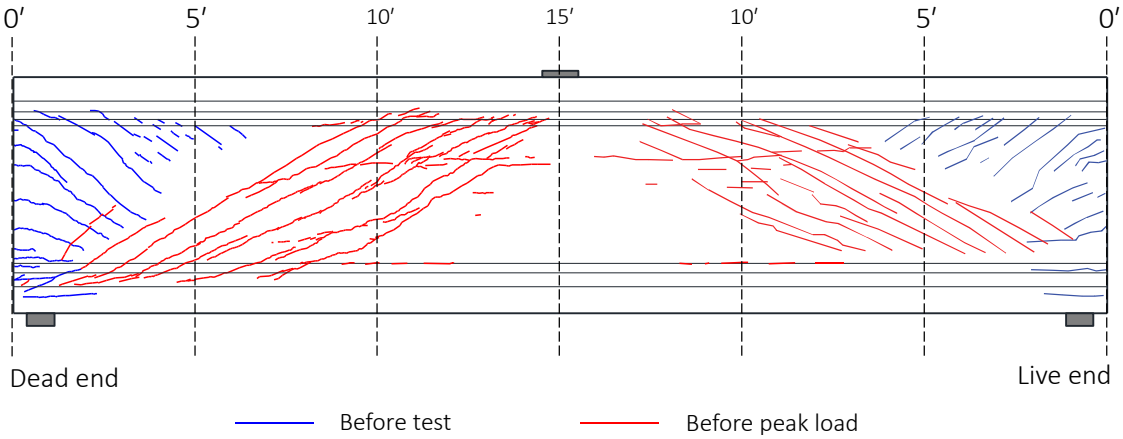

Figure 3-23: Cracking pattern immediately prior to failure on the east face of Tx70-II

Within the test series, the failure of Tx70-II occurred with the least warning, i.e. exhibiting the smallest softening in stiffness. The failure occurred slowly in approximately three seconds, accompanied by loud, hollow sounds. Significant cracking was observed between the strands at the end face of the failed span, typical of bond failure (Figure 3-24 (a)). Moreover, the end face of the specimen revealed noticeable vertical cracks that extended from the bottom flange through the entire depth of the web (Figure 3-24 (b)). The diagonal cracks joined in a large continuous horizontal crack through the interface between the bottom flange and the web. Moreover, similar to the Tx46 specimens, the end face of Tx70-II showed a movement of the web relative to the bottom flange, which was measured as 1 in. (25 mm). Large portions of cover concrete over the confining reinforcement had spalled off the bottom flanges on both sides of the beam after failure (Figure 3-25 and Figure 3-26). As visible in Figure 3-27, longitudinal cracking along the strands and transverse cracking was observed on the bottom face of the beam near the support.

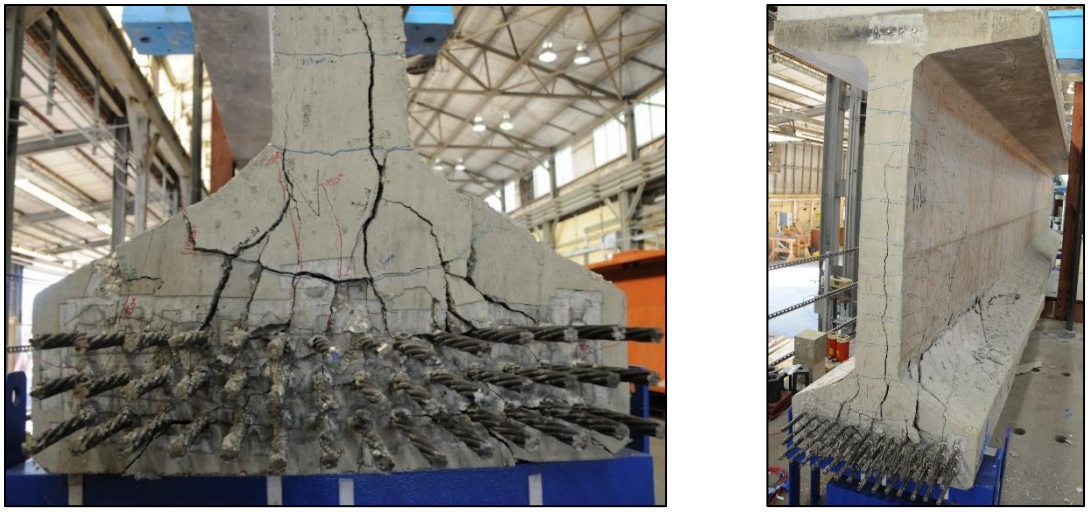

(a) (b)

Figure 3-24: Post-failure conditions of Tx70-II at the end face: (a) details of the bottom flange cracking, and (b) vertical cracking in the web

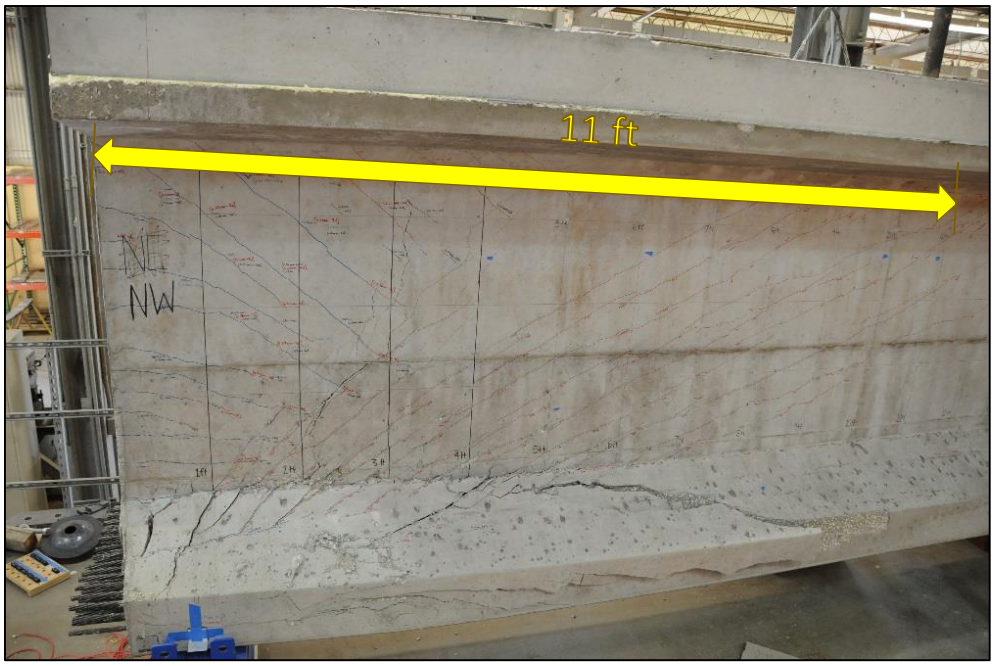

Figure 3-25: Northwest side of Tx70-II after failure

Figure 3-26: Northeast side and bottom of Tx70-II after failure

Figure 3-27: Bottom side of Tx70-II after failure

3.6 DISCUSSION OF TESTS RESULTS

The results presented above demonstrate evidence of atypical shear failure mechanisms in all four specimens. All specimens showed clear signs of anchorage-zone distress. A strand slip exceeding 0.01 in. (0.3 mm), which has been used by some researchers (Tadros & Morcous, 2011) as an indicator of bond failure, was observed in at least one strand in each specimen prior to the first detected yielding in the stirrups. At peak load, the maximum measured strand slip in all specimens was greater than 0.075 in. (1.9 mm). The final stages of load-versus-slip plots for all specimens were primarily horizontal, which reveals no resistance against strand slip. The specimens also experienced considerable cracking in the vicinity of the supports. Moreover, the end faces of the failed span in each specimen showed patterns of cracking between strand rows and columns, indicating bond failure.

The observed damage in Tx46-I and Tx70-II was very similar to observations reported by Garber et al. (2016) for a Tx46 specimen containing 0.5-in. (12.7-mm) diameter strands, failure of which was categorized as anchorage-induced shear failure. However, the magnitude of strand slip measured in all of the specimens comprising the current test program far exceeded the maximum slip numbers reported by Garber et al. (2016).

Significant horizontal cracks along the web-flange interface were also prominent features in Tx46-I, Tx46-II, and Tx70-II after failure. In these three specimens, failure resulted in distinctive sliding of the web past the bottom flange. Moreover, in Tx46-I and

Tx70-II, occurrence and growth of horizontal cracks were observed well before the development of diagonal cracking in the web. These features are indicative of horizontal shear distress in the specimens.

On the other hand, in all four specimens in the current test program, significant diagonal cracking occurred, and yielding of the stirrups was confirmed. In the Tx70 specimens, which were more extensively instrumented in the shear span, widespread yielding of the stirrups was observed outside the closely spaced end-region reinforcement. In the Tx46 specimens, yielding was confirmed in at least a few stirrups in each test span, although it is believed that several non-instrumented stirrups likely yielded prior to the first detected yielding.

Table 3-1 shows a summary of the capacity estimates from several design procedures as well as the peak shear forces measured during the structural tests. Nominal capacities of the specimens in the test program were calculated according to the general procedure in AASHTO LRFD (2014) and the detailed method in ACI 318-14 (2014). These estimates are shown in the table as $V_{\mathrm{AASHTO-MCFT}}$ and V_{ACI}, respectively. Furthermore, the shear force resulting in anchorage-zone failure, $V_{\mathrm{Anchorage}}$ was obtained by rearranging Equation 1-1 as Equation 3-1 (Garber et al., 2016). The final capacity estimate from AASHTO LRFD (2014) specifications, V_{AASHTO}, is the lesser of $V_{\mathrm{AASHTO-MCFT}}$ and $V_{\mathrm{Anchorage}}$.

$$V_{\text{Anchorage}} = \frac{V_u}{\phi_v} = \left(A_{ps}f_{ps} + A_s f_y - \frac{|M_u|}{\phi_f d_v} + 0.5\frac{N_u}{\phi_c}\right)\tan(\theta) + V_p + 0.5V_s \qquad \text{Equation 3-1}$$

In Equation 3-1, f_{ps} is the available stress in the strands, which changes depending on the distance from the end face of the specimen as illustrated in Figure 1-2. Therefore, the shear corresponding to anchorage failure was calculated at several sections along each specimen, and the minimum value was reported as $V_{\text{Anchorage}}$. The transfer and development lengths used for this calculation were taken as $60d_b$ and the l_d estimated from Equation 5.11.4.2-1 in AASHTO LRFD, respectively. It is important to note that in this test program, the strands in all specimens had sufficient development length to reach their yield strength at the location of the load point.

Table 3-1 also contains the shear force corresponding to the computed flexural failure of the specimens, $V_{Flexure}$. Since the specimens were carefully designed to fail in shear rather than flexure, $V_{Flexure}$ was noticeably greater than the maximum shear force recorded for each specimen. Further, the shear capacity associated with horizontal shear failure, V_{HS}, was also predicted using the method proposed by Hovell et al. (2012) and is presented in Table 3-1. The estimated development length and the effective prestress at the midspan of the specimen after losses, as obtained from VWG measurements, are presented in this table. The full extent of shear-related calculations performed for the specimens are provided in Appendix D. Note that the critical section used in the design calculations was procedure-dependent. For consistency, all reported shear forces in

Table 3-1 are calculated at the centroid of the supports and therefore represent the reaction forces corresponding to failure. For the purpose of this thesis, all resistance factors were taken equal to 1.0.

Table 3-1: Summary of experimental and nominal capacities

Parameter	Tx46-I	Tx46-II	Tx70-I	Tx70-II
f_{pe}, ksi (MPa)	157 (1,085)	167 (1,150)	164 (1,130)	157 (1,080)
l_d, in. (cm)	142.3 (361)	135.2 (344)	137.5 (349)	142.9 (363)
V_{Flexure}, kips (kN)	613 (2,727)	705 (3,136)	929 (4,132)	1,350 (6,005)
$V_{\text{AASHTO-MCFT}}$, kips (kN)	463 (2,060)	426 (1,895)	683 (3,038)	743 (3,305)
$V_{\text{Anchorage}}$, kips (kN)	451 (2,006)	522 (2,322)	581 (2,584)	772 (3,434)
V_{AASHTO}, kips (kN)	**451 (2,006)**	**426 (1,895)**	**581 (2,584)**	**743 (3,305)**
V_{ACI}, kips (kN)	**375 (1,668)**	**395 (1,757)**	**586 (2,607)**	**651 (2,896)**
V_{HS}, kips (kN)	452 (2,011)	392 (1,745)	631 (2,807)	623 (2,771)
V_{Test}, kips (kN)	543 (2,416)	465 (2,068)	749 (3,332)	835 (3,714)

As can be seen in Table 3-1, despite the atypical failure modes observed in the test program, the AASHTO LRFD (2014) and ACI 318 (2014) provisions provided conservative estimates for the load-carrying capacity of all specimens. The horizontal shear capacities predicted by Hovell et al.'s method were also conservative. According to this method, the load-carrying capacity of Tx46-II and Tx70-II were estimated to be less than that predicted from AASHTO LRFD provisions due to horizontal shear failure.

The ratio of measured capacity of the specimens to nominal capacities predicted by code equations is shown in Figure 3-28. As can be seen in this figure, the estimated capacities from the ACI detailed method (2014) were generally more conservative than the results of the general procedure in AASHTO LRFD (2014) when anchorage requirements were not considered. However, predictions from general method in AASHTO LRFD (2014) were consistently more accurate. This observation matched the general results from previous studies on beams employing 0.6-in. (15.2-mm) and 0.5-in. (12.7-mm) strands (Nakamura, Avendano, & Bayrak, 2013). Figure 3-28 also shows that the capacity of all specimens exceeded $V_{\mathrm{AASHTO-MCFT}}$ and therefore, neglecting the $V_{\mathrm{Anchorage}}$ limit resulted in capacity estimates that were closer to experimental results. Although all specimens showed clear signs of anchorage-zone distress, $V_{\mathrm{Anchorage}}$ was the governing parameter for the load-carrying capacity of only Tx46-I and Tx70-I. Therefore, using $V_{\mathrm{Anchorage}}$ from Equation 3-1 does not appear to be a reliable indicator of the failure mode in the specimens. This observation is potentially due to the assumptions used in estimating f_{ps}, which are based on the simplified bilinear approximation of strand stresses shown in Figure 1-2.

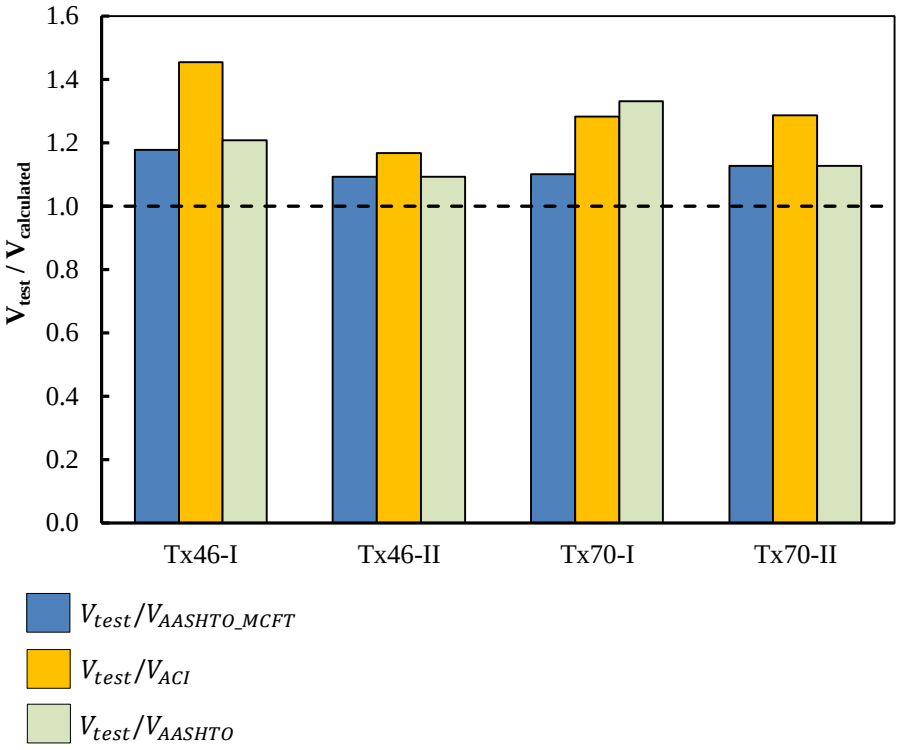

Figure 3-28: Ratios of measured to calculated shear capacities

The conservativeness of design codes in estimating the shear capacity of the specimens in this test program may be explained by the traditional shear failure mechanisms that were also observed. In all four specimens, yielding of the stirrups was confirmed prior to peak load. In the Tx70 specimens, which were more extensively instrumented, softening of the load-deflection response of the specimens was much better correlated with the detected yielding in the stirrups than with the observed strand slip. In summary, the presence of anchorage-zone distress did not prevent the specimens from developing the tension-controlled shear failures inherently assumed in the formulation of the shear design provisions employed.

Occurrence of atypical shear failure mechanisms may be alarming to design engineers, as atypical failure mechanisms are not accounted for explicitly in existing shear design provisions. However, these atypical failure modes are not exclusive to prestressed I-girders employing 0.7-in. (17.8-mm) strands. Previous tests on Tx-girders reported by Garber et al. (2016) and Hovell (2012) demonstrated that atypical shear mechanisms were possible in the same family of girders employing 0.5-in. (12.7-mm) and 0.6-in. (15.2-mm) diameter prestressing strands.

Comparing the results of shear tests in this test program with the data points in the database developed by Nakamura et al. (2013) sheds light on the impacts of using 0.7-in. (17.8-mm) strands on the performance of ACI 318 (2014) and AASHTO LRFD (2014) provisions. Figure 3-29 shows such a comparison as a function of the shear span-to-depth ratios of the specimens. For consistency with other points in the database, the $V_{\text{test}}/V_{\text{calc}}$ ratios in the figure are calculated at a distance equal to effective depth of the member from the face of the supports. Moreover, the longitudinal requirement, i.e. $V_{\text{Anchorage}}$, is not considered in the plot reflecting AASHTO LRFD. As can be seen in this figure, the girders investigated in this test program demonstrated $V_{\text{test}}/V_{\text{calc}}$ ratios that were conservative but generally less conservative than the majority of data points representing traditional shear failures, especially when AASHTO LRFD provisions are considered.

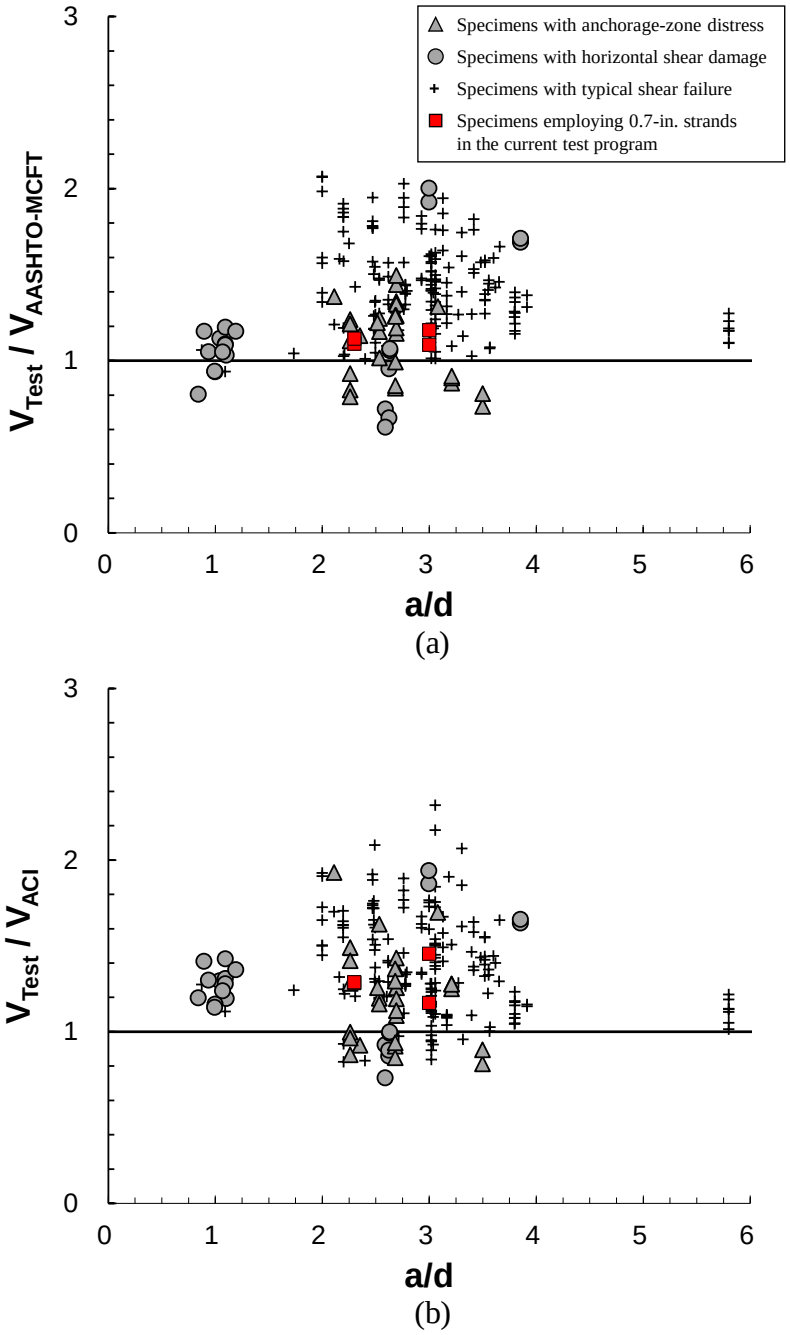

Figure 3-29: Comparison of 0.7-in. strand shear tests with the UTPCSDB (Nakamura, Avendano, & Bayrak, 2013) for (a) AASHTO LRFD general procedure (2014) and (b) ACI 318-14 detailed method (2014)

The Tx46 and Tx70 specimens investigated in this test program had relatively large shear reinforcement ratios of 1.0 percent and 0.7 percent, respectively. However, all specimens achieved yielding in the stirrups before the peak load. It is evident that stirrup yielding will occur earlier in Tx-girders with smaller shear reinforcement ratios. Therefore, no concerns are currently identified regarding the conservativeness of AASHTO LRFD 2014 or ACI 318-14 provisions in estimating the shear capacity of Tx-girders employing 0.7-in. (17.8-mm) strands.

The results, however, show a clear need for further research into the longitudinal demand on the strands due to combined effect of shear forces and bending moments and the capacity of 0.7-in. (17.8-mm) strands in resisting that demand. The current procedure, which is based on existing equations for transfer and development lengths and the assumption of bilinear changes in available strand capacity along the girder, does not appear to be a reliable indicator of the performance of girders with 0.7-in. (17.8-mm) strands with regard to anchorage.

CHAPTER 4: SUMMARY AND CONCLUSIONS

As part of a comprehensive research program on the behavior of precast, prestressed girders employing 0.7-in. (17.8-mm) diameter prestressing strands, four full-scale Tx-girders were fabricated in a controlled environment at Ferguson Structural Engineering Laboratory and tested in shear-critical loading conditions. An array of variables affecting the shear behavior was used for designing the specimens, which included different strand patterns, concrete release strengths, member depths, and shear-span-to depth ratios. The specimens were reinforced according to the standard detailing for Tx-girders used by the Texas Department of Transportation (2015).

The specimens were designed to fail in shear and were subjected to symmetric loading configurations, in which equal loads were applied to two test spans adjacent to the live and dead ends of the specimens. The first two specimens were Tx46 girders loaded in a four-point loading configuration that resulted in a span-to-depth ratio of 3.0. The other two specimens were Tx70 girders loaded in three-point loading with a span-to-depth ratio of 2.3. All of the specimens were extensively instrumented and carefully monitored at the times of prestress transfer and structural testing. The monitored parameters included loads and deflections, strains in the stirrups, cracking patterns, and slippage of the prestressing strands at the end face of the girders.

The end-region behavior of the specimens at the time of prestress transfer is reported in detail by Salazar (2016). All specimens demonstrated cracking within their

end-regions as a result of prestress transfer. The maximum crack width prior to shear test was recorded as 0.008 in. (0.20 mm). Prestress transfer also resulted in stresses in the transverse steel within the end region of the specimens. However, the effect of these stresses on the remaining capacity of stirrups within the main span of the girders is believed to be relatively insignificant.

Failures of the specimens under shear critical loading revealed features that were not typical. Pronounced strand slip was measured in each test span of all specimens prior to peak load. Moreover, in three specimens, continuous horizontal cracking was observed at the flange-web interface over the majority of the failed spans. Prominent sliding of the web past the bottom flange was observed in the end faces of these three specimens after failure. Alongside these atypical characteristics, extensive diagonal cracking was observed, and yielding of the stirrups was confirmed in each test span prior to peak load.

To evaluate the adequacy of existing shear design provisions when applied to prestressed I-girders employing 0.7-in. (17.8-mm) strands, the nominal shear capacity of the specimens was calculated according to the general procedure of the AASHTO LRFD Bridge Design Specifications (2014) and the detailed one-way shear design method provided in ACI-318 (2014). The level of conservativism of the existing code provisions was then evaluated by determining the ratio of the measured-to-calculated shear capacities. It was found that the existing code provisions provided conservative estimates of nominal shear capacity for all four specimens. The ACI detailed method (2014) yielded generally more conservative strength estimates than the MCFT-based provisions

of the AASHTO LRFD general procedure (2014) and further, the capacities determined on the basis of AASHTO LRFD were found to be more accurate.

The ratios of measured-to-calculated shear capacities for the specimens were also compared with strength ratios developed for an existing database of shear tests on prestressed concrete members developed by Nakamura et al. (2013). It was found that the specimens comprising the current test program represented generally less conservative estimates than the majority of specimens in the database, which demonstrated typical shear failures.

The longitudinal demand requirements in AASHTO LRFD provisions were not found to be a reliable indicator of anchorage-zone distress in the specimens. Those provisions failed to predict the anchorage-zone distress in two of the specimens. In the other two specimens, the measured capacity was closer to that estimated from the general procedure while ignoring the longitudinal demand requirements.

The results of the test program clearly show that the use of 0.7-in. (17.8 mm) prestressing strands increases the likelihood of atypical shear failure mechanisms in pretensioned girders. However, the presence of these mechanisms did not prohibit the yielding of stirrups, which governs the capacity of girders in calculations reflecting traditional failure mechanisms. As a result, no concerns were identified regarding the conservativeness of the AASHTO LRFD general procedure (2014) and the ACI detailed method (2014) for Tx-girders employing 0.7-in. (17.8-mm) strands.

Due to the wide array of variables known to affect the shear behavior of prestressed girders, additional full-scale tests are necessary before generalizing the conclusions presented above to a wider variety of cross sections, span-to-depth ratios, and reinforcement detailings. The performance of the longitudinal demand equation in AASHTO LRFD specifications was deemed unsatisfactory in predicting the possibility of anchorage-zone distress or the load associated with anchorage-induced shear failure. Therefore, further research seems essential on the assumptions used in this procedure, including transfer and development lengths and bilinear changes in the capacity of strands with increase in distance from end face of the girder.

Valuable insight into the behavior of pretensioned girders employing larger-diameter strands might also be obtained from computational studies on the mechanics of shear failure in such elements using verified finite element models. The results presented in this study provide valuable validation data for such models. Abyaneh (2016) used the results of this test program, and several other studies, to investigate phenomena controlling the behavior of pretensioned girders employing larger-diameter strands and gain insight into influences associated with modifying end-region reinforcement details.

APPENDICES

Appendix A: Specimen Design and Fabrication

Appendix A provides details of the specimen design and fabrication as follows. Additional materials can be found in Salazar (2016).

- *Reinforcement details for CIP topping decks:* Figure A-1
- *Tx46-I shear test setup:* Figure A-2
- *Tx46-II shear test setup:* Figure A-3
- *Tx70-I shear test setup:* Figure A-4
- *Vision system installation on Tx70-I:* Figure A-5
- *Tx70-II shear test setup:* Figure A-6
- *Tx70-II shear test setup:* Figure A-7
- *Data acquisition system setup for Tx70-II:* Figure A-8

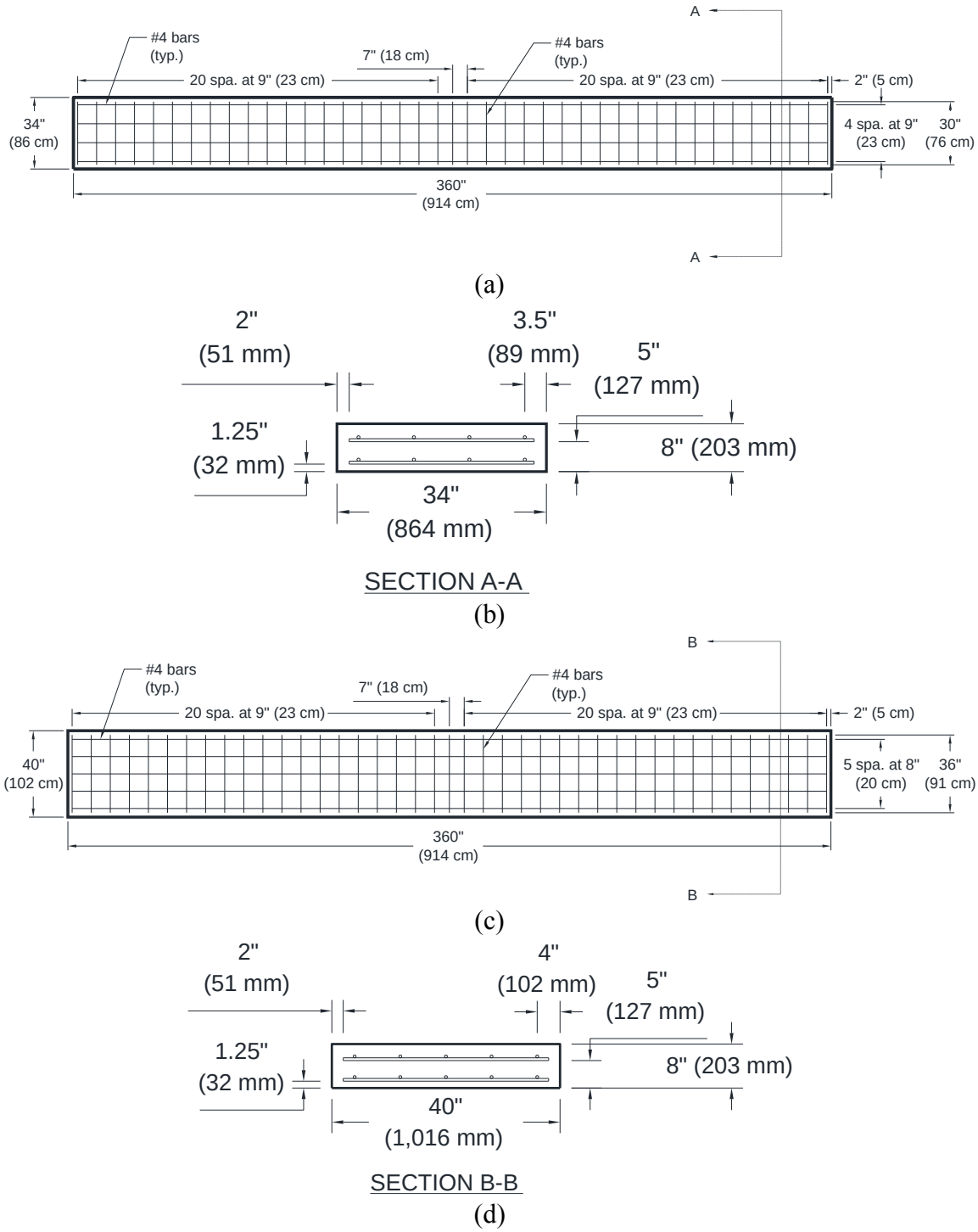

Figure A-1: Reinforcement details for CIP topping decks for (a) and (b) Tx46 specimens; and (c) and (d) Tx70 specimens

Figure A-2: Shear test setup for Tx46-I as seen from the west

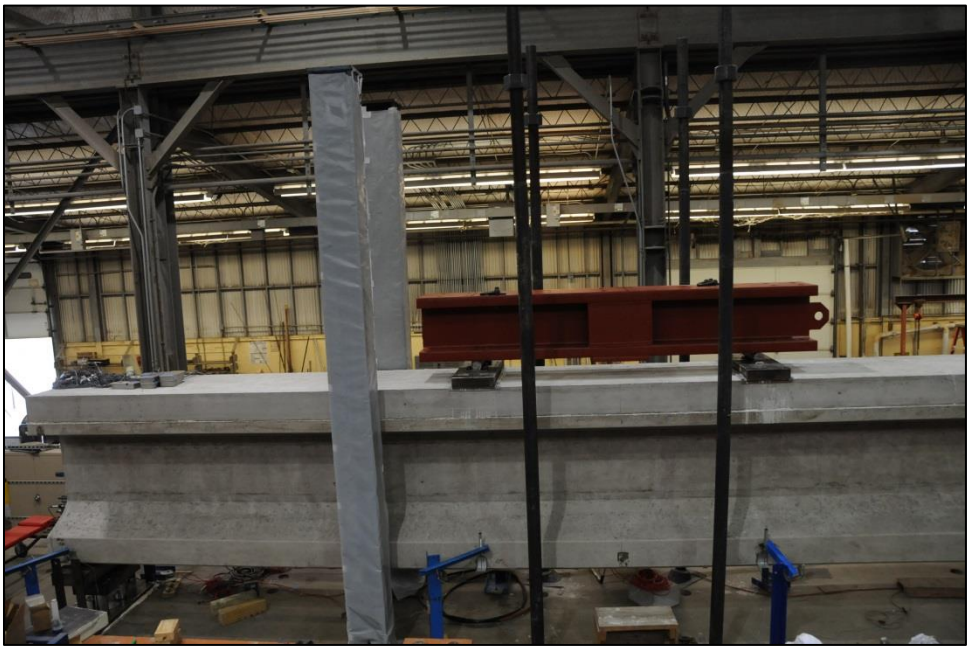

Figure A-3: Shear test setup for Tx46-II before the load frame was placed

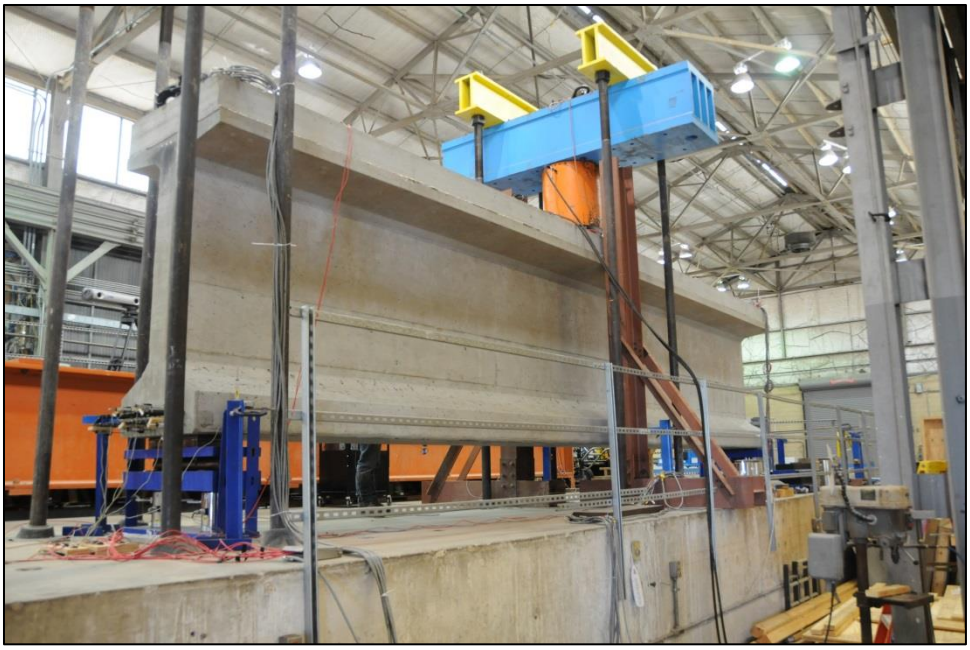

Figure A-4: Shear test setup for Tx70-I seen from the east

Figure A-5: Installing the vision system markers on the west face of Tx70-I prior to the shear test

Figure A-6: Shear test setup for Tx70-II seen from the west

Figure A-7: Shear test setup for Tx70-II seen from the east

Figure A-8: Data acquisition systems used during the shear test of Tx70-II

APPENDIX B: TEST SETUP AND INSTRUMENTATION DETAILS

Appendix B contains details of the experimental setup design and the as-built locations of the instruments, supports, and loading devices.

B.1 EXPERIMENTAL SETUP DESIGN

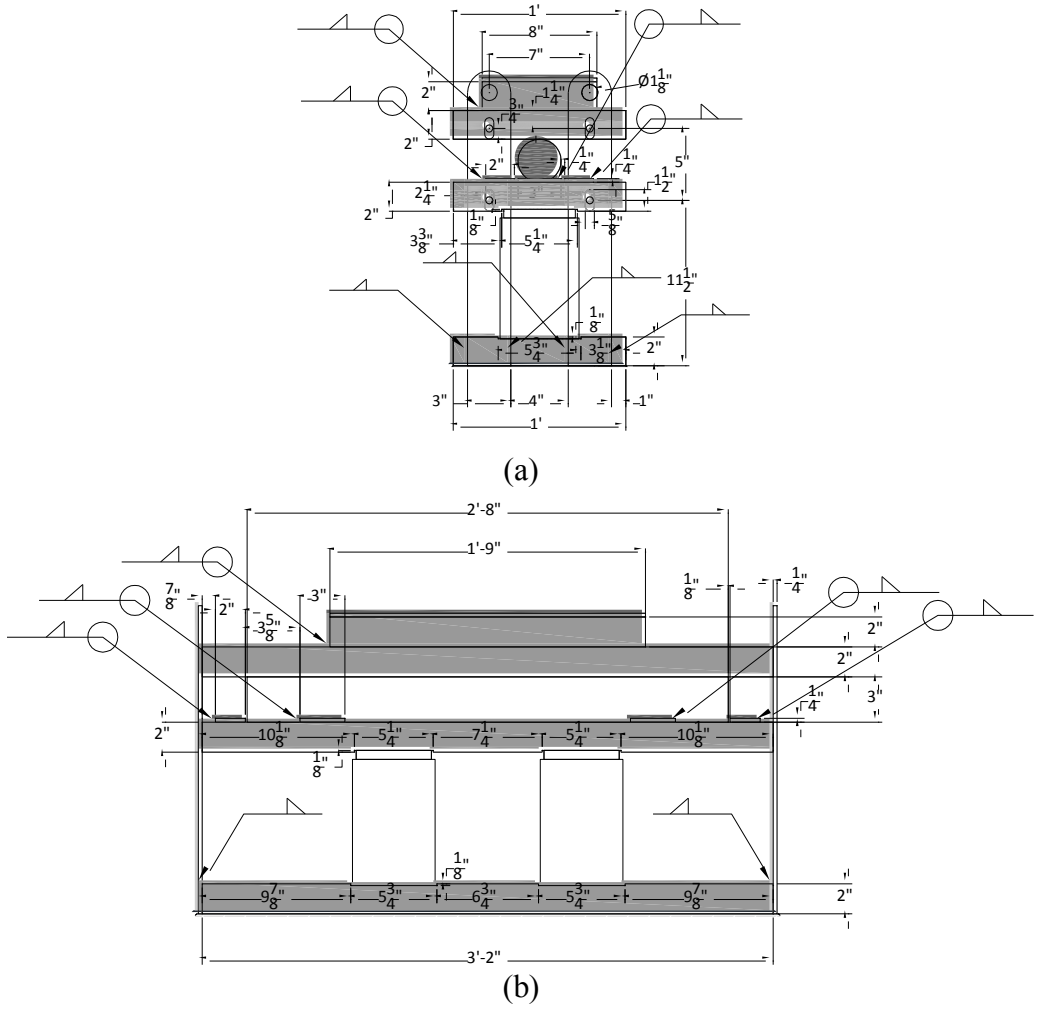

Figure B-1: Roller support structure (a) side profile, and (b) front profile

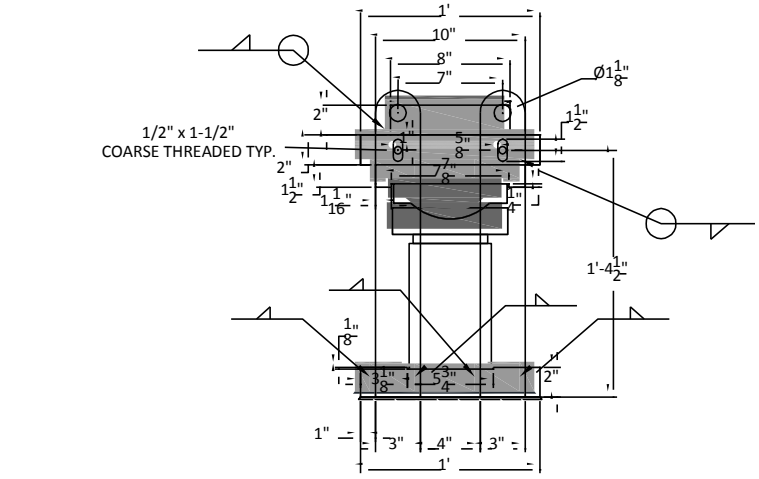

(a)

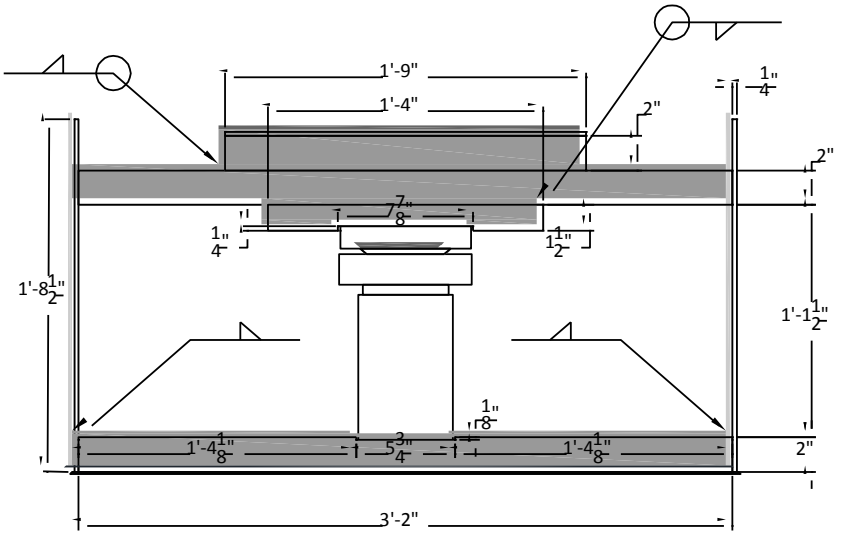

(b)

Figure B-2: Pin support structure (a) side profile, and (b) front profile

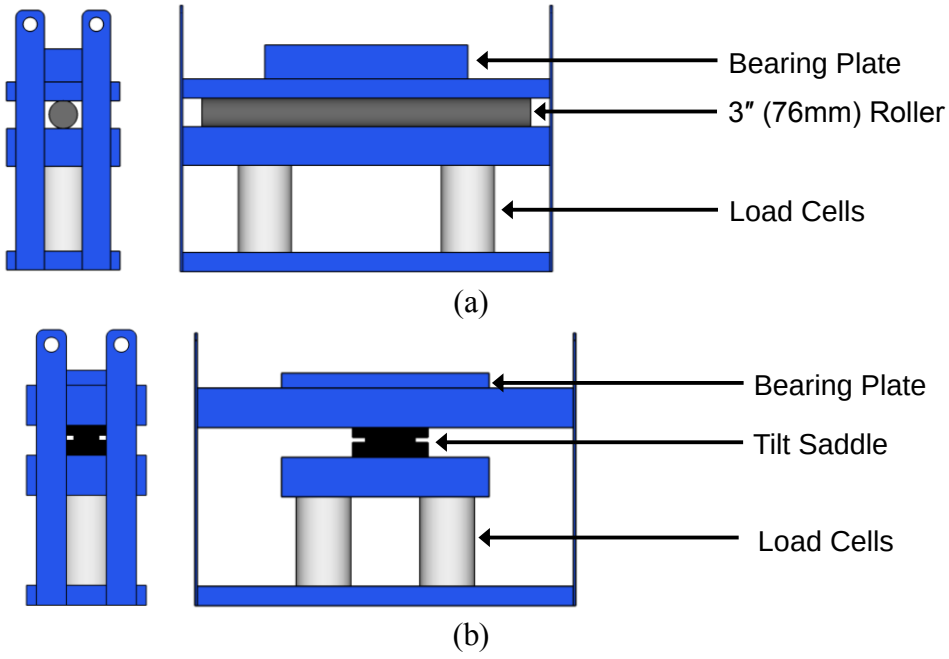

Figure B-3: Labelled diagrams of (a) roller support structure and (b) pin support structure

Figure B-4: Roller support structure installed in shear test setup for Tx70-II

Figure B-5: Pin support structure installed in shear test setup for Tx70-II

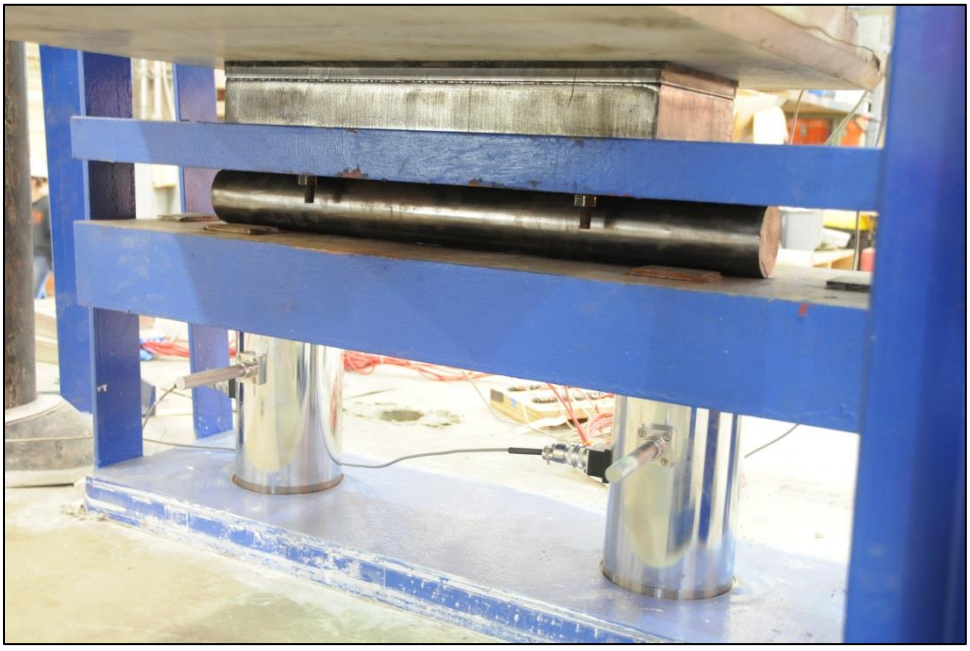

Figure B-6: Roller support structure prior to the Tx70-II shear test

Figure B-7: Pin support structure prior to the Tx70-II shear test

B.2 AS-BUILT LOCATIONS OF THE INSTRUMENTS, SUPPORTS, AND LOADING DEVICES

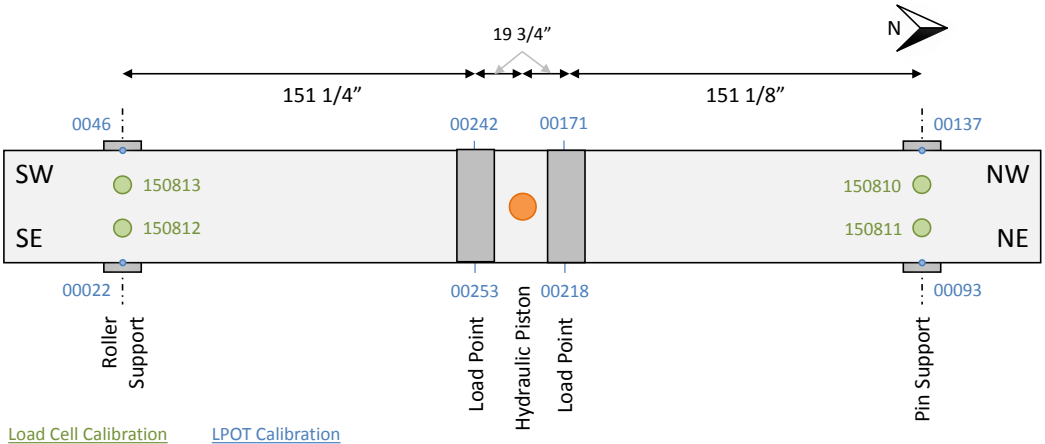

Load Cell Calibration (from in-house calibration test)
SW: 2.3231
SE: 2.3446
NW: 2.3357
NE: 2.3345
Note: SE calibration value from manufacturer

LPOT Calibration
SW –End: -2.0377
SE – End: 2.0455
SW – Mid: 4.0090
SE – Mid: 4.0110
NW – Mid: 4.0105
NE – Mid: 4.0089
NW – End: 2.0437
NW – Mid: -2.0380

LSCT Calibration

Label ID	LSCT Serial #	Calibration
A	15131	6.9175
B	15043	6.8762
C	15133	6.9214
G	15134	7.0222
H	15135	6.9259
I	15132	6.9568

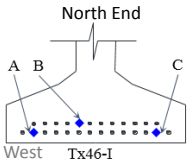

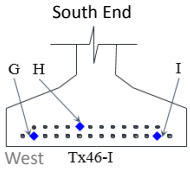

Figure B-8: As-built instrumentation layout and calibration factors for Tx46-I shear test

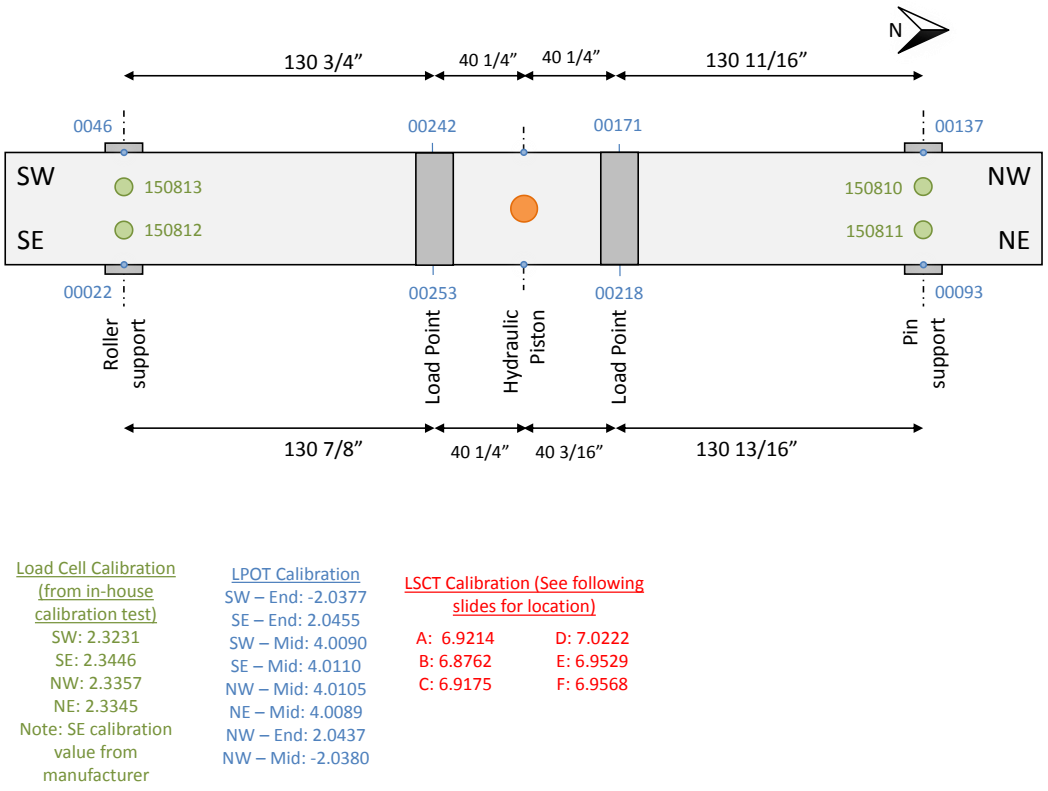

Figure B-9: As-built instrumentation layout and calibration factors for Tx46-II shear test

	NORTH													
Row	EAST							WEST						
8							R8C1	R8C1						
7							R7C1	R7C1						
6						B 15043	R6C1	R6C1	C 15131					
5				R5C4	R5C3	R5C2	R5C1	R5C1	R5C2	R5C3	R5C4			
4		R4C6	A 15133	R4C4	R4C3	R4C2	R4C1	R4C1	R4C2	R4C3	R4C4	R4C5	R4C6	
3							R3C1	R3C1						
2														
1														
Column	7	6	5	4	3	2	1	1	2	3	4	5	6	7

Figure B-10: As-built LSCT layout on live end strands of Tx46-II

	SOUTH													
Row	WEST							EAST						
8							R8C1	R8C1						
7							R7C1	R7C1						
6						D 15134	R6C1	R6C1	E 15135					
5				R5C4	R5C3	R5C2	R5C1	R5C1	R5C2	R5C3	R5C4			
4		R4C6	R4C5	R4C4	R4C3	R4C2	R4C1	R4C1	R4C2	R4C3	R4C4	F 15132	R4C6	
3							R3C1	R3C1						
2														
1														
Column	7	6	5	4	3	2	1	1	2	3	4	5	6	7

Figure B-11: As-built LSCT layout on dead end strands of Tx46-II

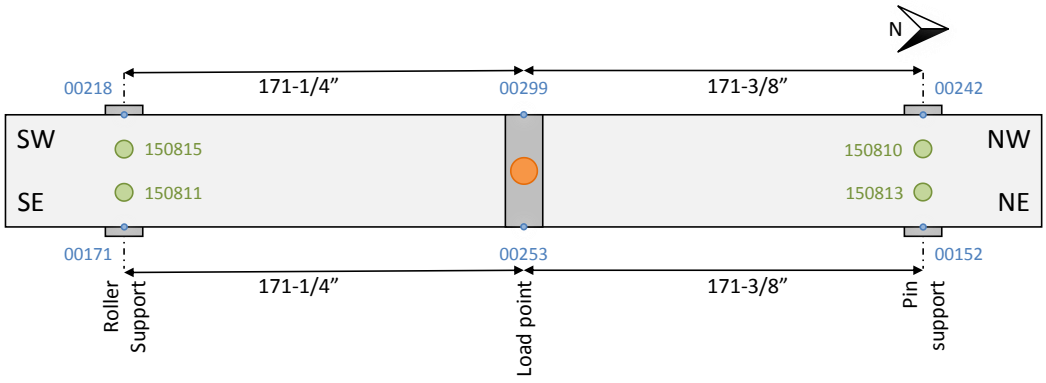

Load Cell Calibration (from in-house calibration tests)
SW: 2.3469
SE: 2.3345
NW: 2.3357
NE: 2.3231

Deflection LPOT Calibration
SW: 4.0089
SE: 4.0105
NW: 4.0090
NE: 4.0347
MID W: 4.0094
MID E: 4.0110

Strand Slip LPOT Calibration (See following figures for location)

A: -2.0406	F: 2.0437
B: -2.0393	G: 2.0430
C: -2.0377	H: 2.0451
D: -2.0354	I: 2.0611
E: -2.0415	J: 2.0455

Figure B-12: As-built instrumentation layout and calibration factors of Tx70-I shear test

	NORTH													
Row	EAST							WEST						
8														
7														
6														
5														
4														
3														
2	R2C7	R2C6	R2C5	R2C4	B 68	R2C2	R2C1	R2C1	R2C2	D 66	R2C4	R2C5	R2C6	R2C7
1	A 137	R1C6	R1C5	R1C4	R1C3	R1C2	R1C1	C 46	R1C2	R1C3	R1C4	R1C5	R1C6	E 85
Col	7	6	5	4	3	2	1	1	2	3	4	5	6	7

Figure B-13: As-built LPOT layout on live end strands of Tx70-I during shear test

	SOUTH													
Row	WEST							EAST						
8														
7														
6														
5														
4														
3														
2	R2C7	R2C6	R2C5	R2C4	G 182	R2C2	R2C1	R2C1	R2C2	I 38	R2C4	R2C5	R2C6	R2C7
1	F 137	R1C6	R1C5	R1C4	R1C3	R1C2	R1C1	H 23	R1C2	R1C3	R1C4	R1C5	R1C6	J 22
Col	7	6	5	4	3	2	1	1	2	3	4	5	6	7

Figure B-14: As-built LPOT layout on dead end strands of Tx70-I during shear test

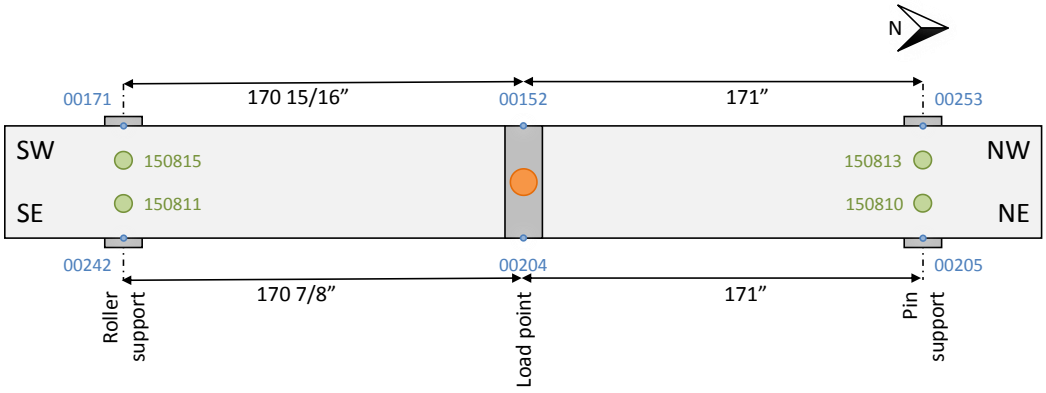

Load Cell Calibration (from in-house calibration tests)
SW: 2.3469
SE: 2.3345
NW: 2.3231
NE: 2.3357

Deflection LPOT Calibration
SW: 4.0105
SE: 4.0090
NW: 4.0110
NE: 4.0120
MIDW: 4.0347
MIDE: 4.0109

Strand Slip LPOT Calibration

Label ID	Serial Number; Calibration	Label ID	Serial Number; Calibration
A	00022 2.0455	G	00086 -2.0425
B	00094 2.0354	H	00137 2.0437
C	00258 4.0099	I	00085 -2.0415
D	00046 -2.0377	J	00182 2.0430
E	00299 4.0094	K	00024 -2.0383
F	00066 -2.0355	L	00068 -2.0393

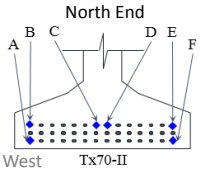

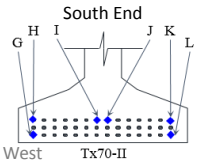

Figure B-15: As-built instrumentation layout and calibration factors for Tx70-II shear test

Appendix C: Experimental Results

Appendix C provides experimental results that were not included in Chapter 3.

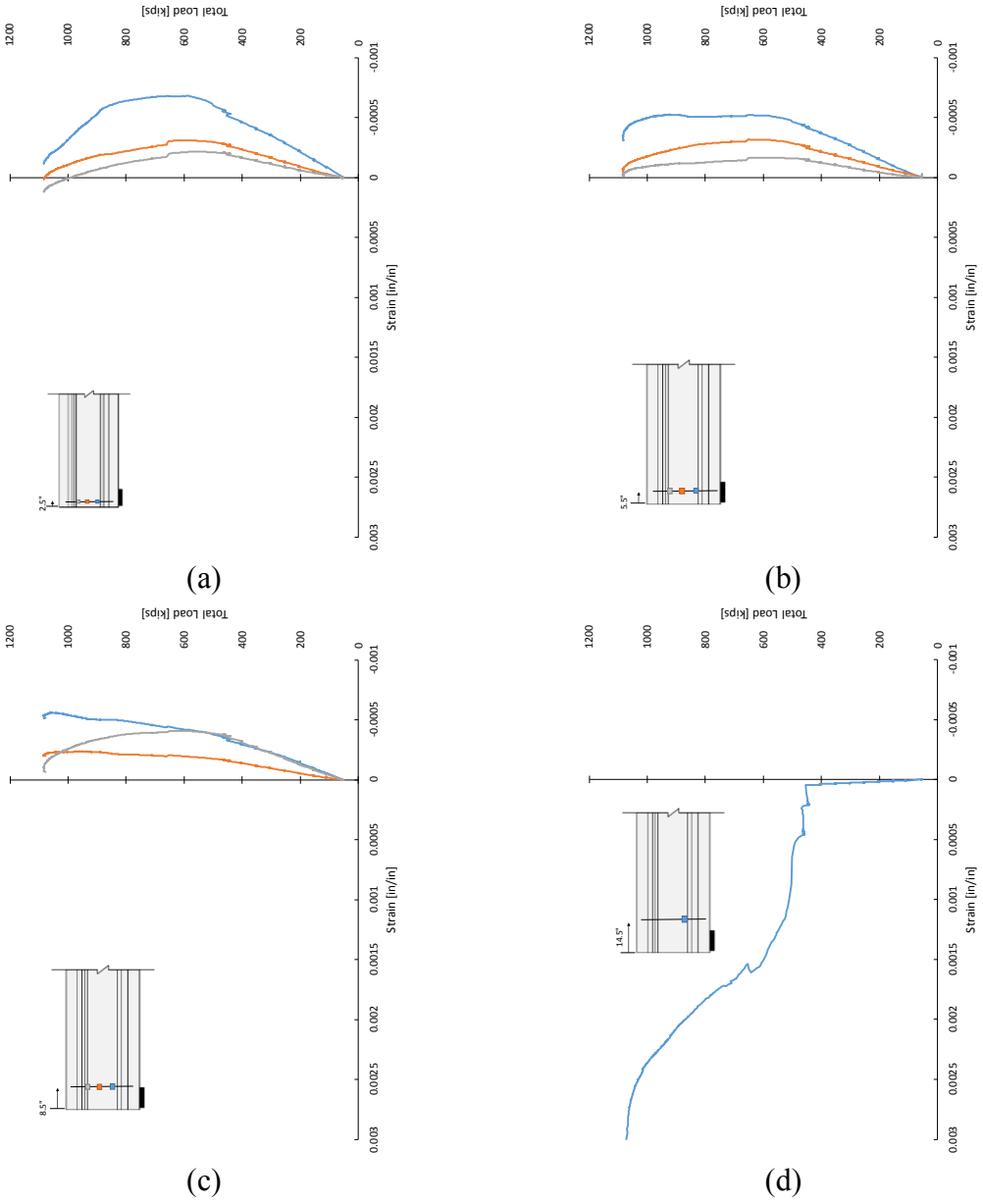

Figure C-1: Total load vs. strain plots from strain gauges on stirrups (a) 2.5 in., (b) 5.5 in., (c) 8.5 in., and (d) 14.5 in. from the live end face of Tx46-I

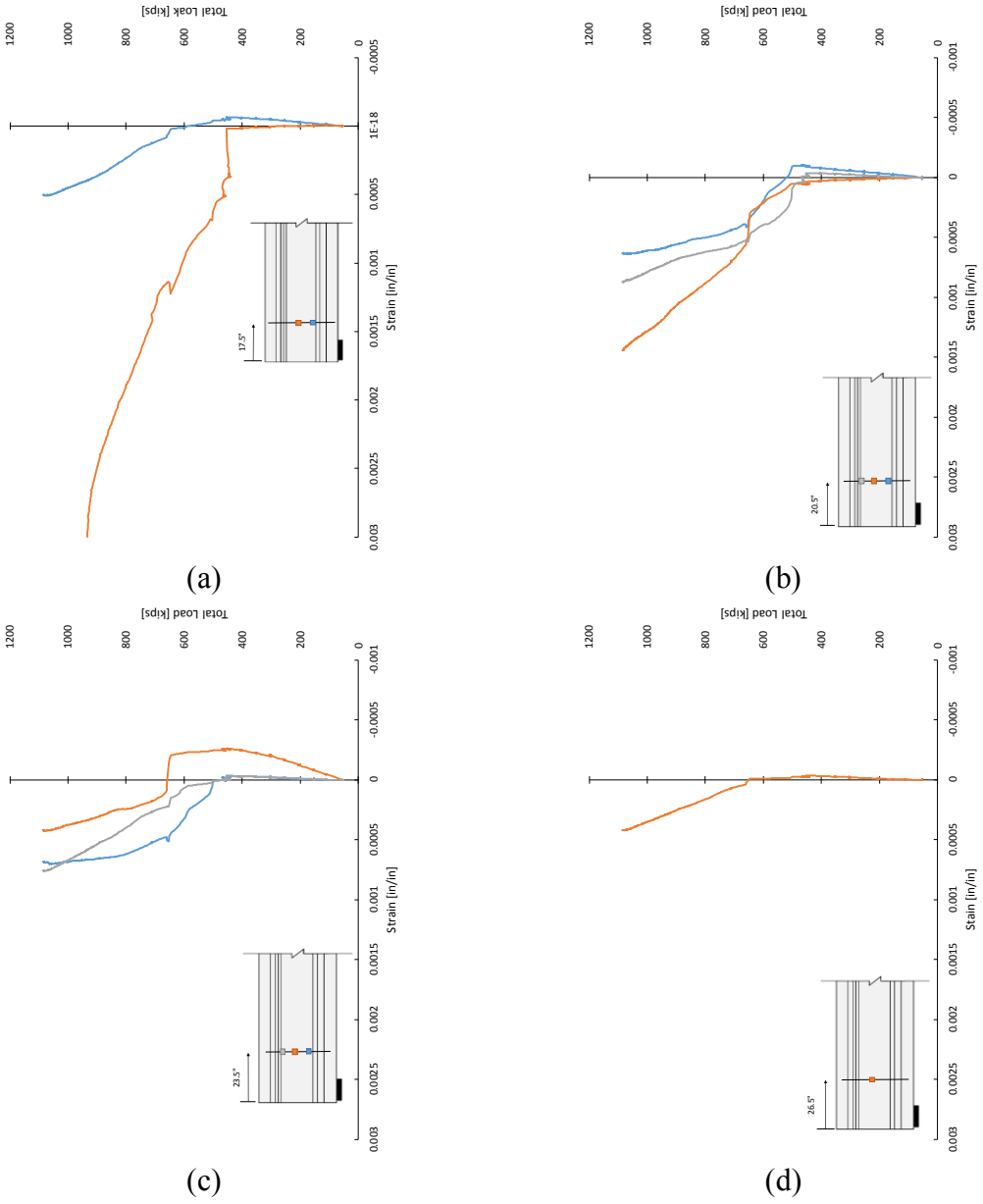

Figure C-2: Total load vs. strain plots from strain gauges on stirrups (a) 17.5 in., (b) 20.5 in., (c) 23.5 in., and (d) 26.5 in. from the live end face of Tx46-I

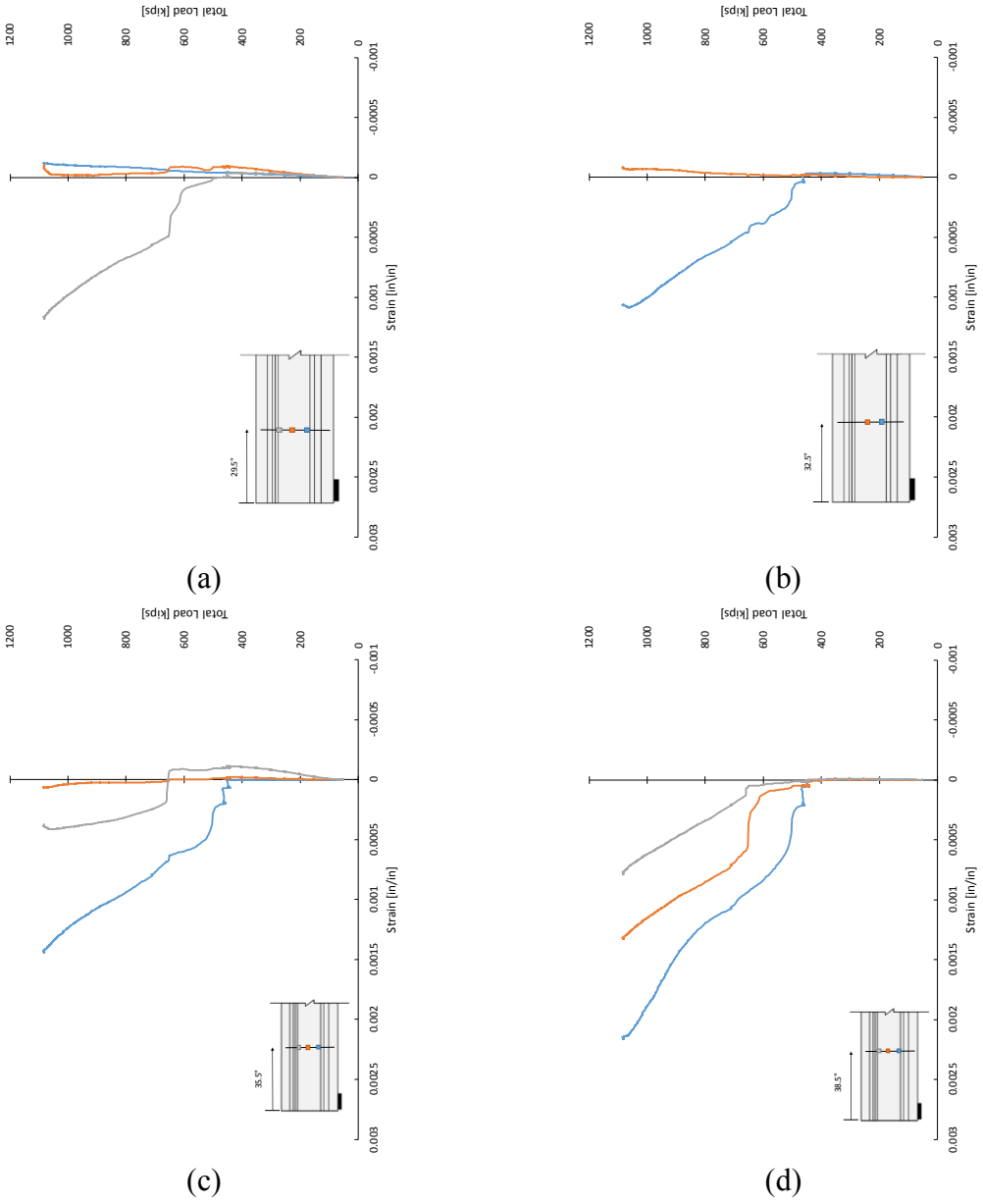

Figure C-3: Total load vs. strain plots from strain gauges on stirrups (a) 29.5 in., (b) 32.5 in., (c) 35.5 in., and (d) 38.5 in. from the live end face of Tx46-I

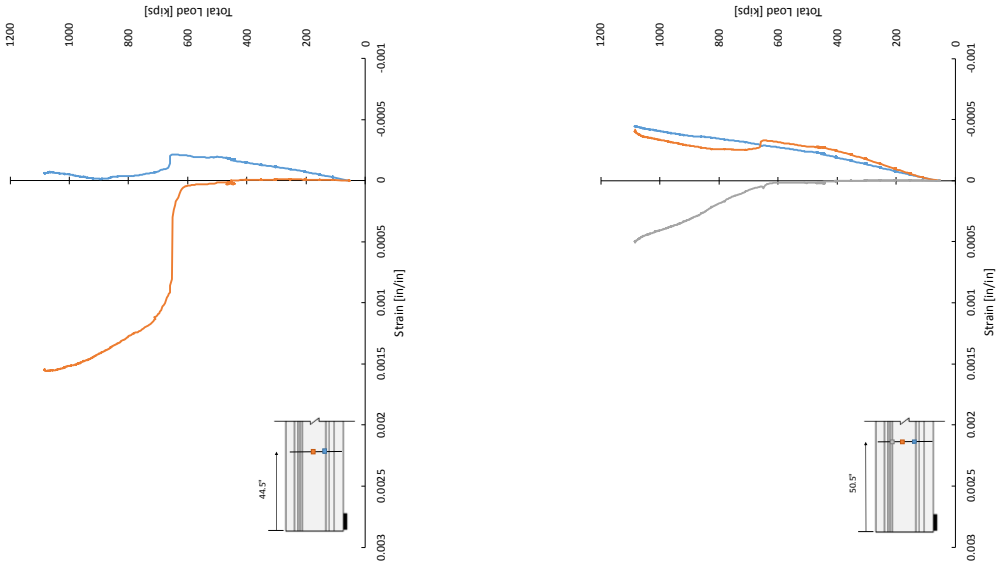

(a) (b)

Figure C-4: Total load vs. strain plots from strain gauges on stirrups (a) 44.5 in. and (b) 50.5 in. from the live end face of Tx46-I

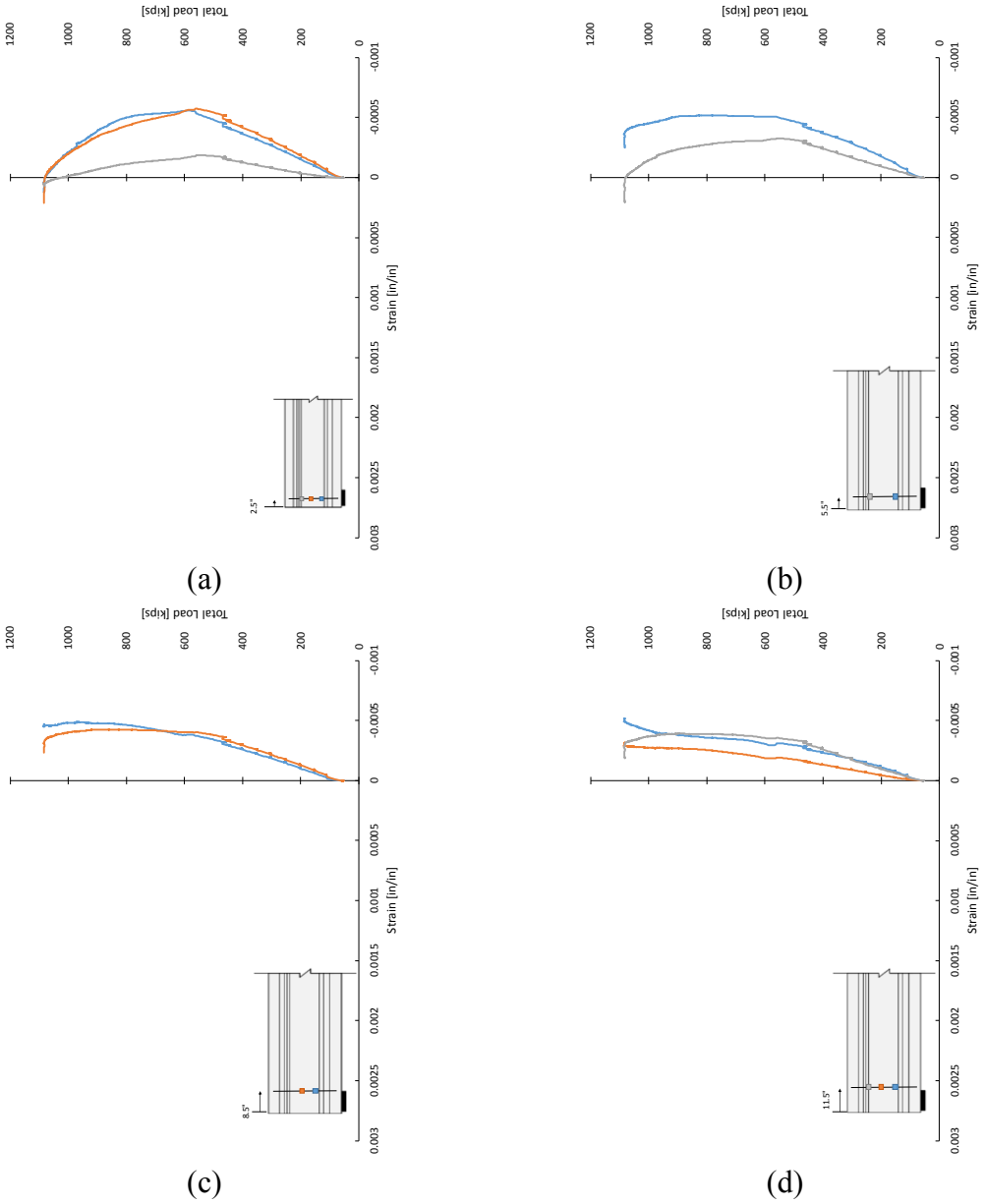

Figure C-5: Total load vs. strain plots from strain gauges on stirrups (a) 2.5 in., (b) 5.5 in., (c) 8.5 in., and (d) 11.5 in. from the dead end face of Tx46-I

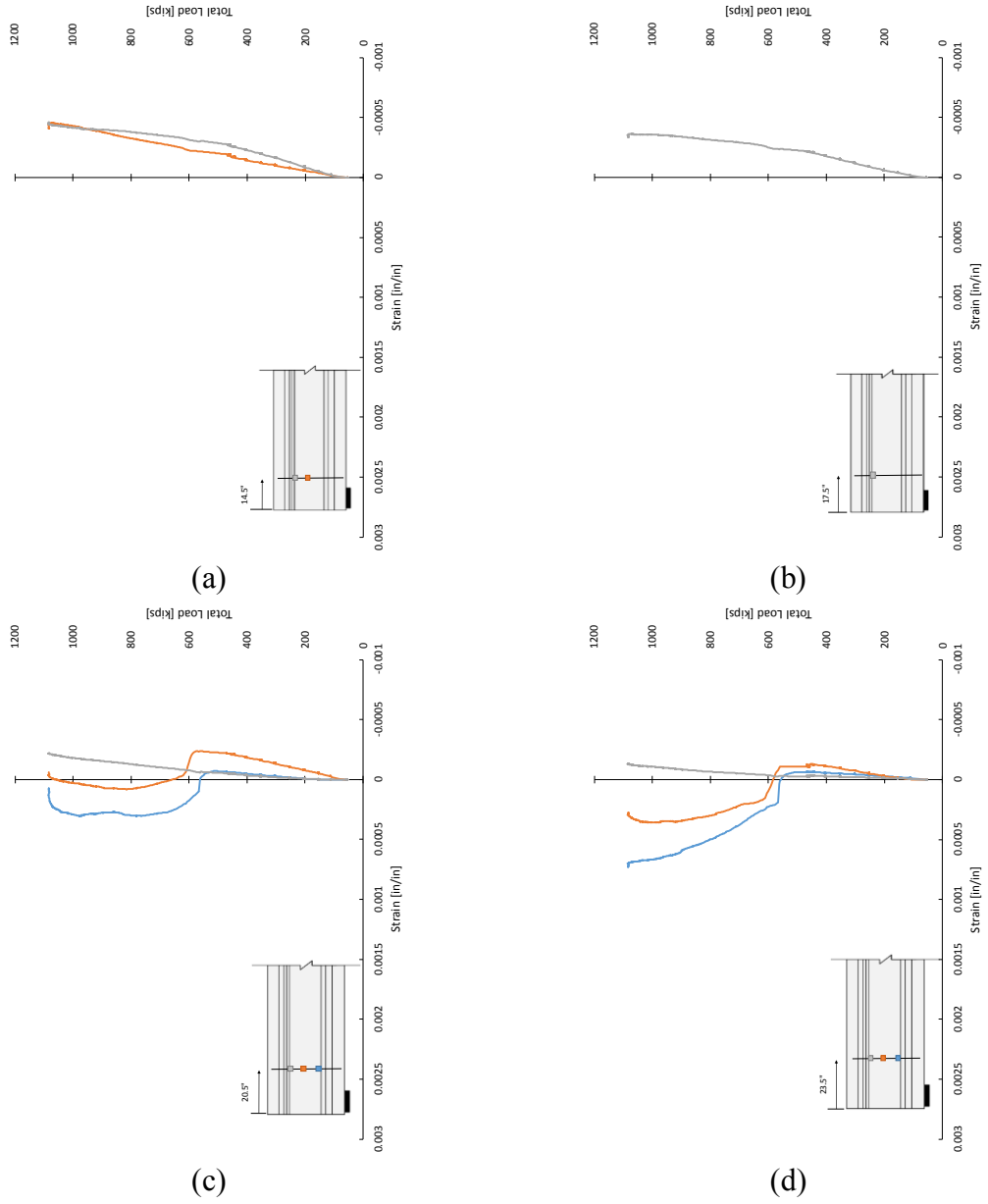

Figure C-6: Total load vs. strain plots from strain gauges on stirrups (a) 14.5 in., (b) 17.5 in., (c) 20.5 in., and (d) 23.5 in. from the dead end face of Tx46-I

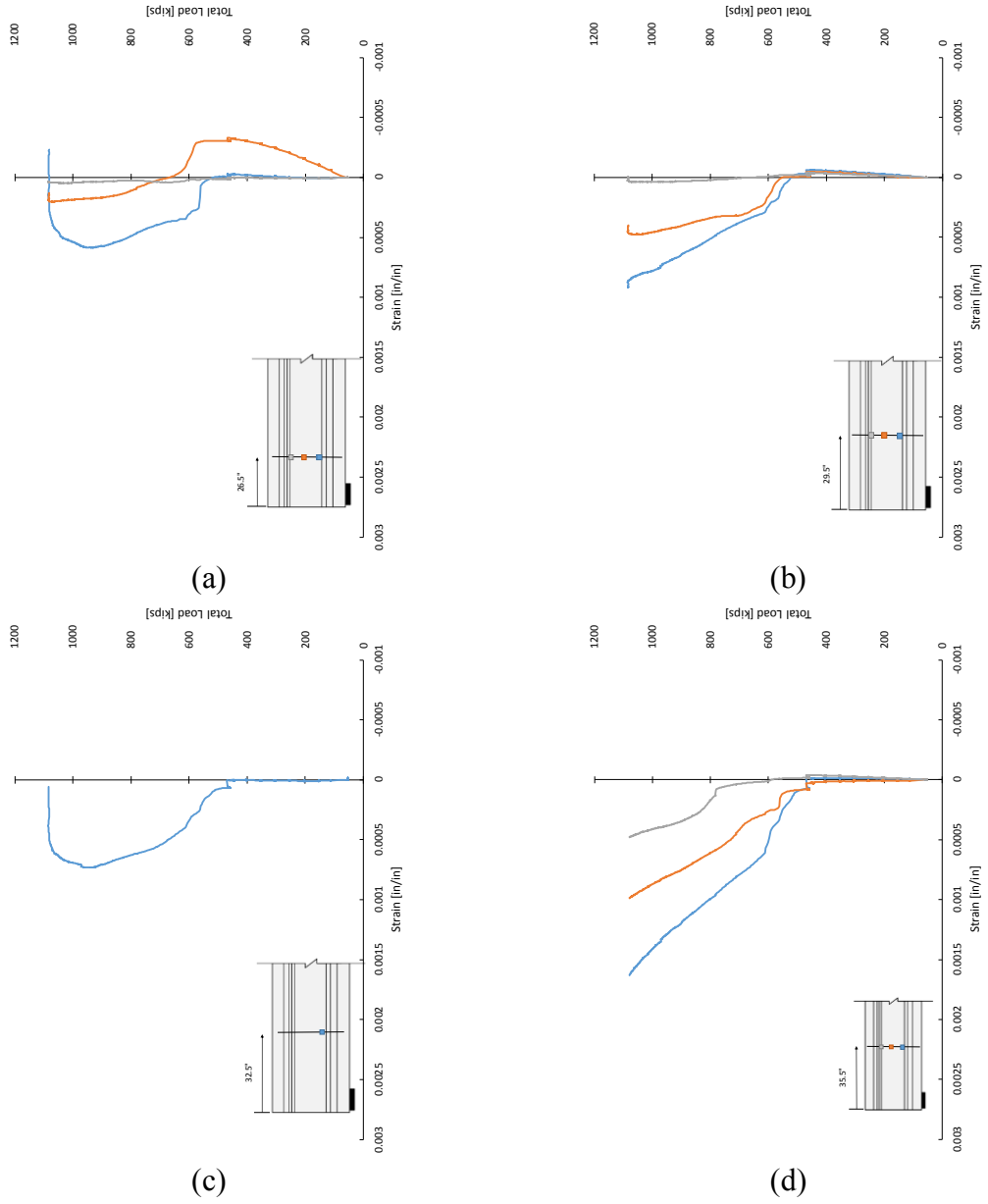

Figure C-7: Total load vs. strain plots from strain gauges on stirrups (a) 26.5 in., (b) 29.5 in., (c) 32.5 in., and (d) 35.5 in. from the dead end face of Tx46-I

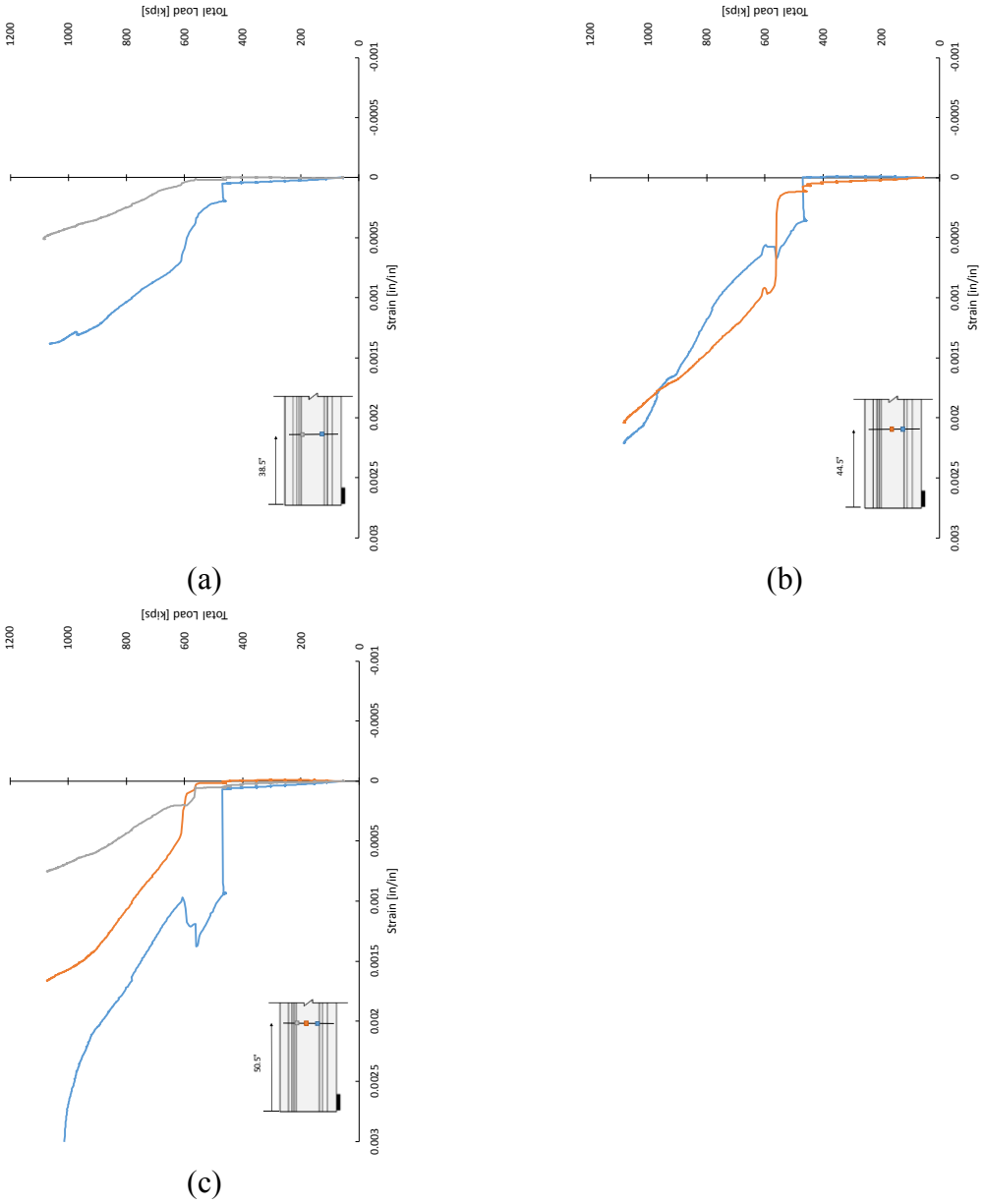

Figure C-8: Total load vs. strain plots from strain gauges on stirrups (a) 38.5 in., (b) 44.5 in., and (c) 50.5 in. from the dead end face of Tx46-I

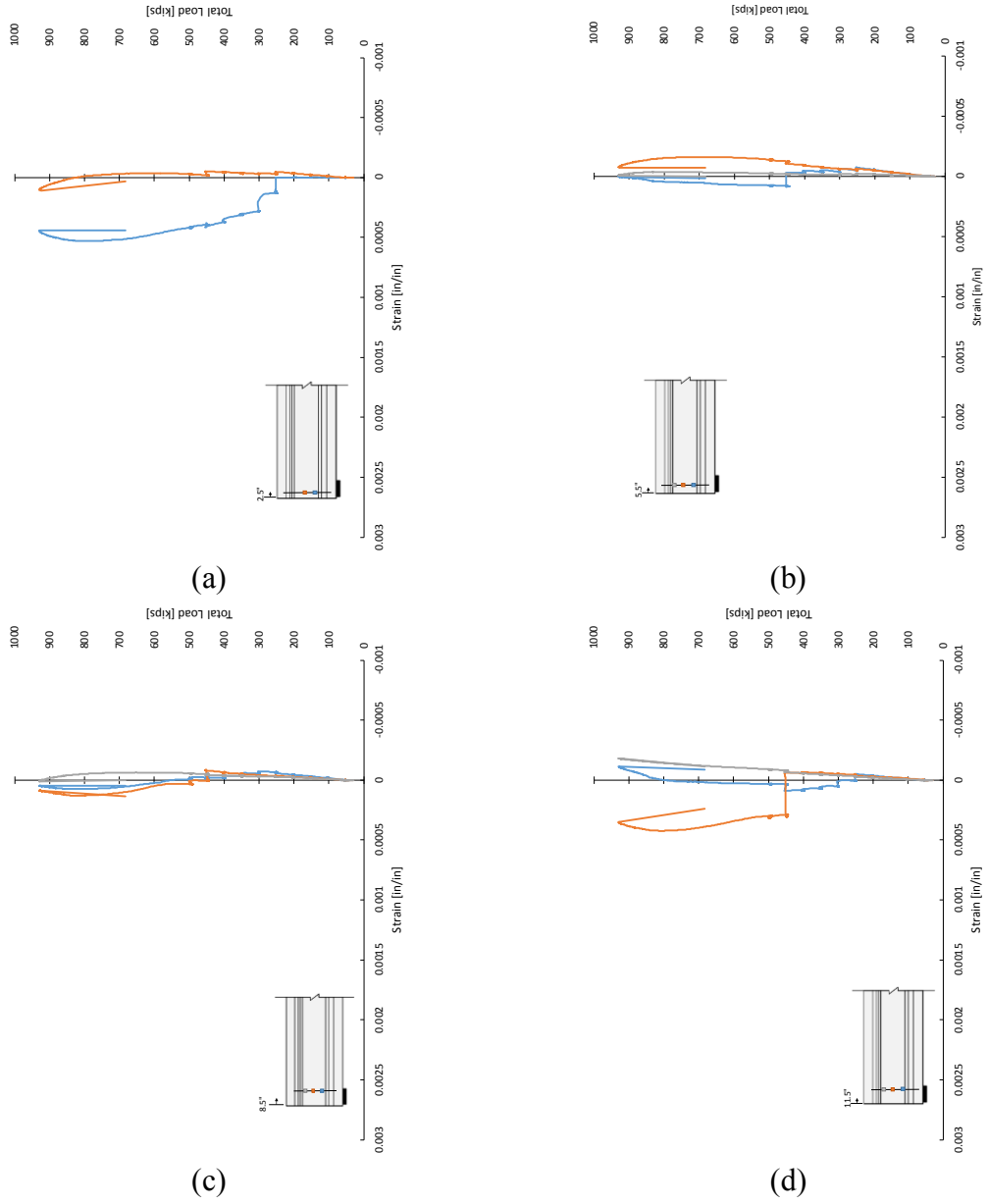

Figure C-9: Total load vs. strain plots from strain gauges on stirrups (a) 2.5 in., (b) 5.5 in., (c) 8.5 in., and (d) 11.5 in. from the live end face of Tx46-II

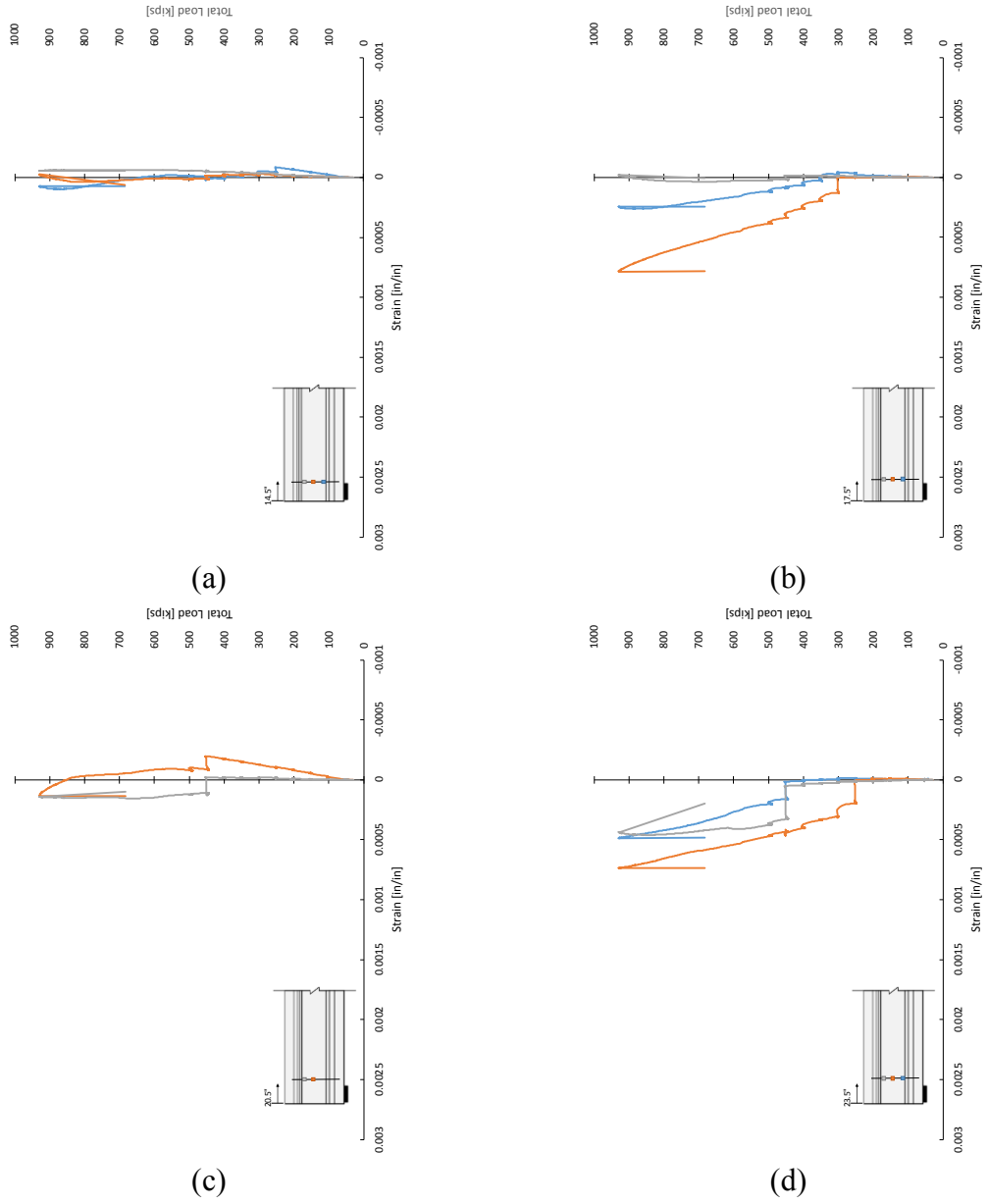

Figure C-10: Total load vs. strain plots from strain gauges on stirrups (a) 14.5 in., (b) 17.5 in., (c) 20.5 in., and (d) 23.5 in. from the live end face of Tx46-II

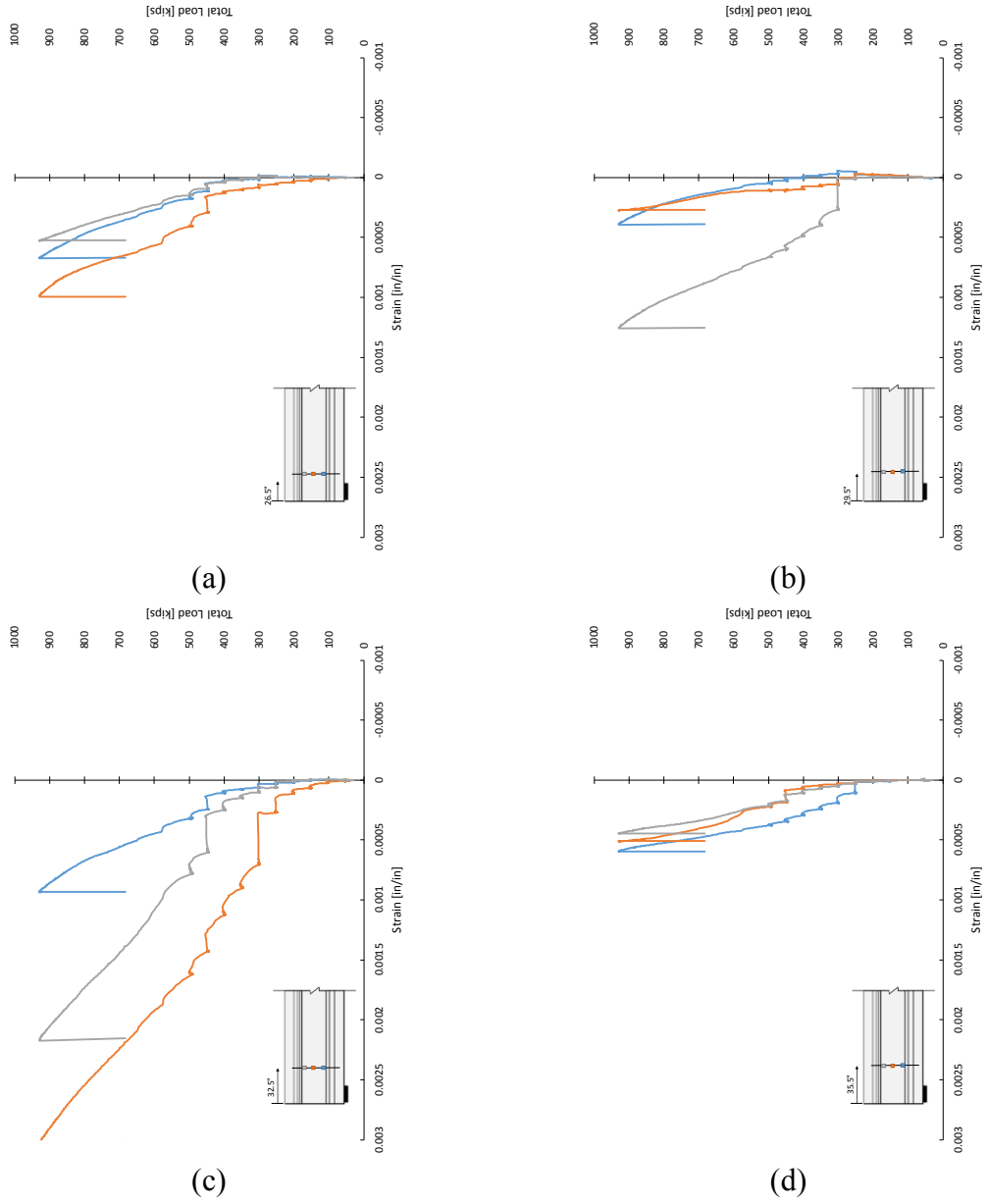

Figure C-11: Total load vs. strain plots from strain gauges on stirrups (a) 26.5 in., (b) 29.5 in., (c) 32.5 in., and (d) 35.5 in. from the live end face of Tx46-II

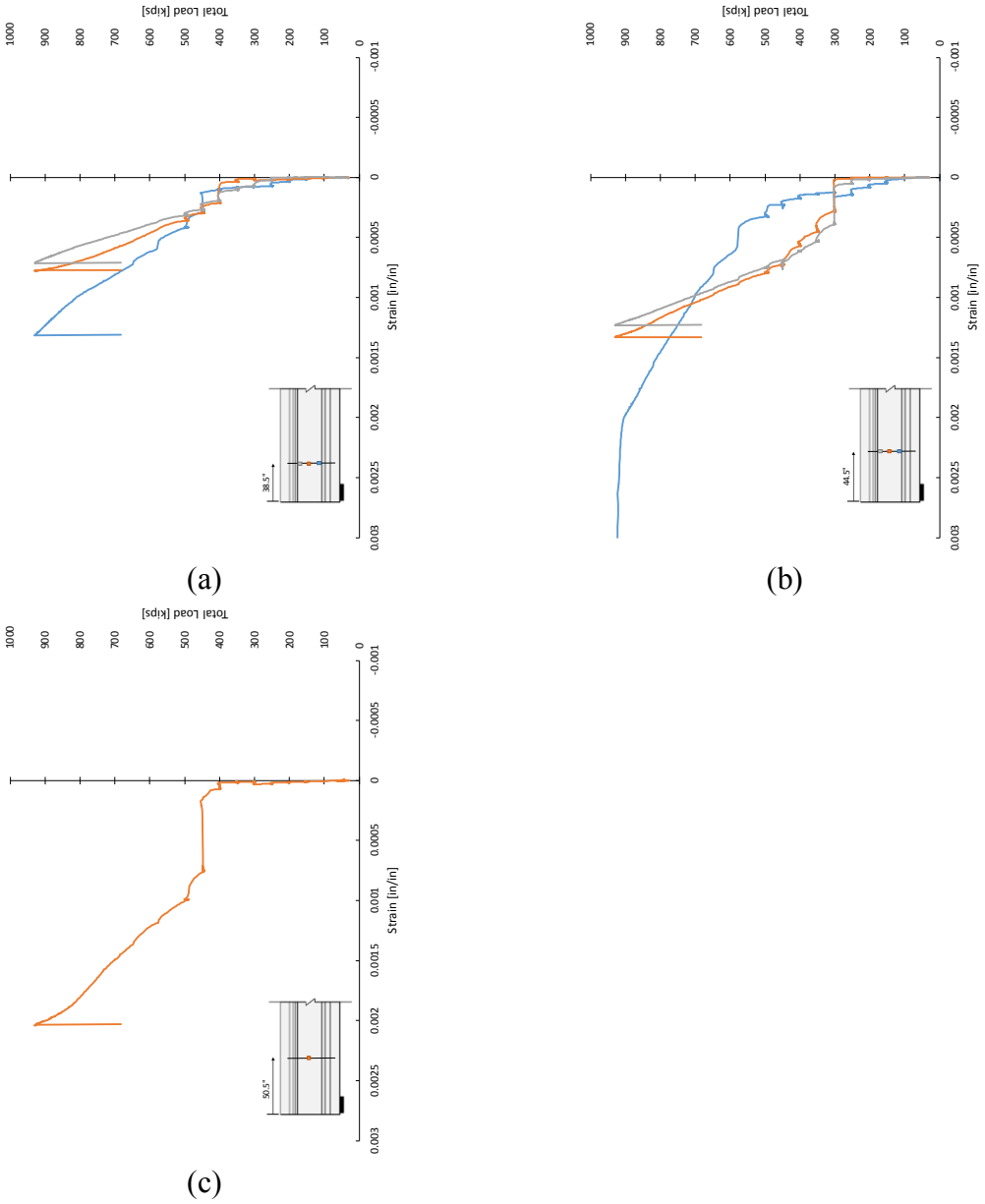

Figure C-12: Total load vs. strain plots from strain gauges on stirrups (a) 38.5 in., (b) 44.5 in., and (c) 50.5 in. from the live end face of Tx46-II

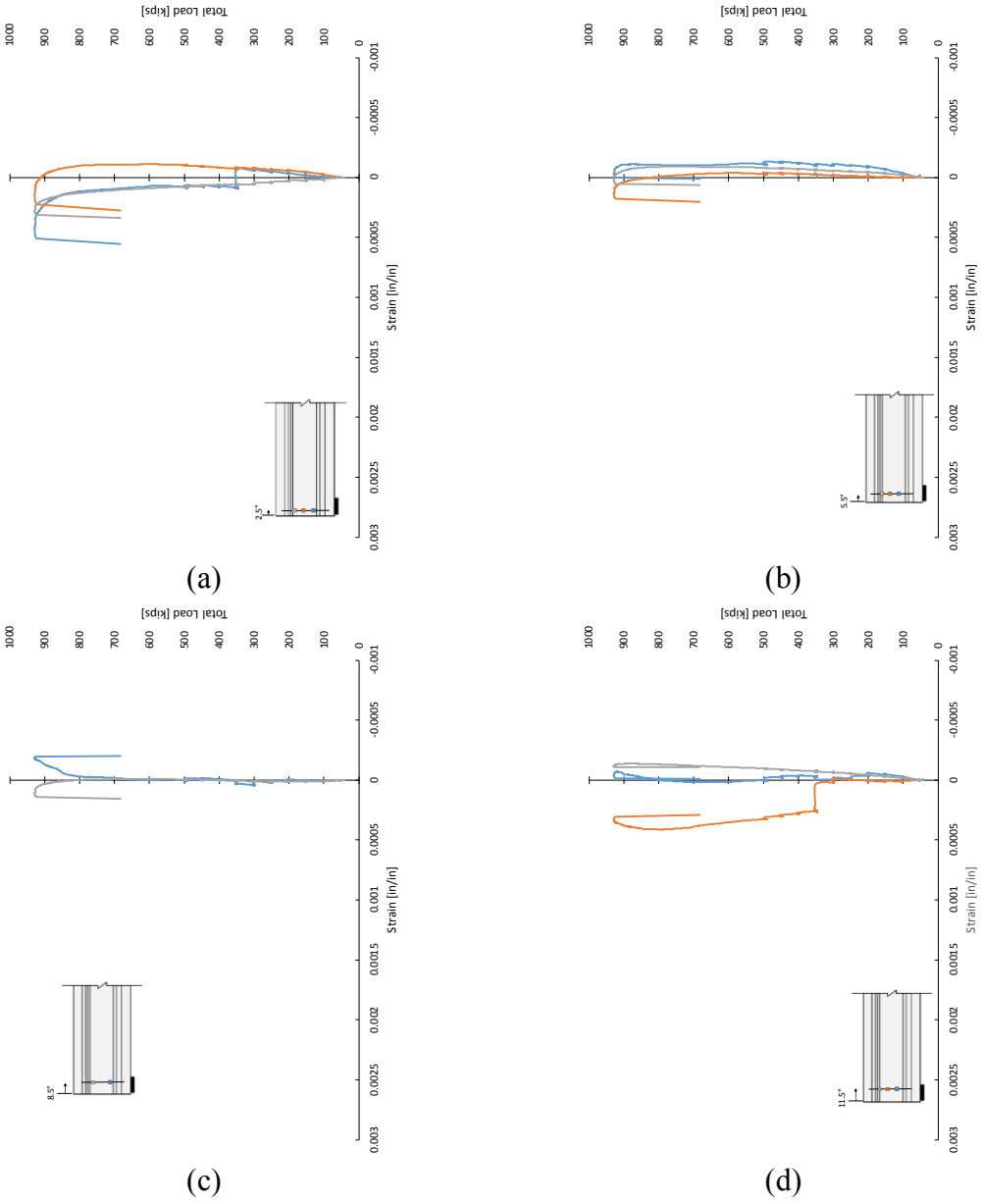

Figure C-13: Total load vs. strain plots from strain gauges on stirrups (a) 2.5 in., (b) 5.5 in., (c) 8.5 in., and (d) 11.5 in. from the dead end face of Tx46-II

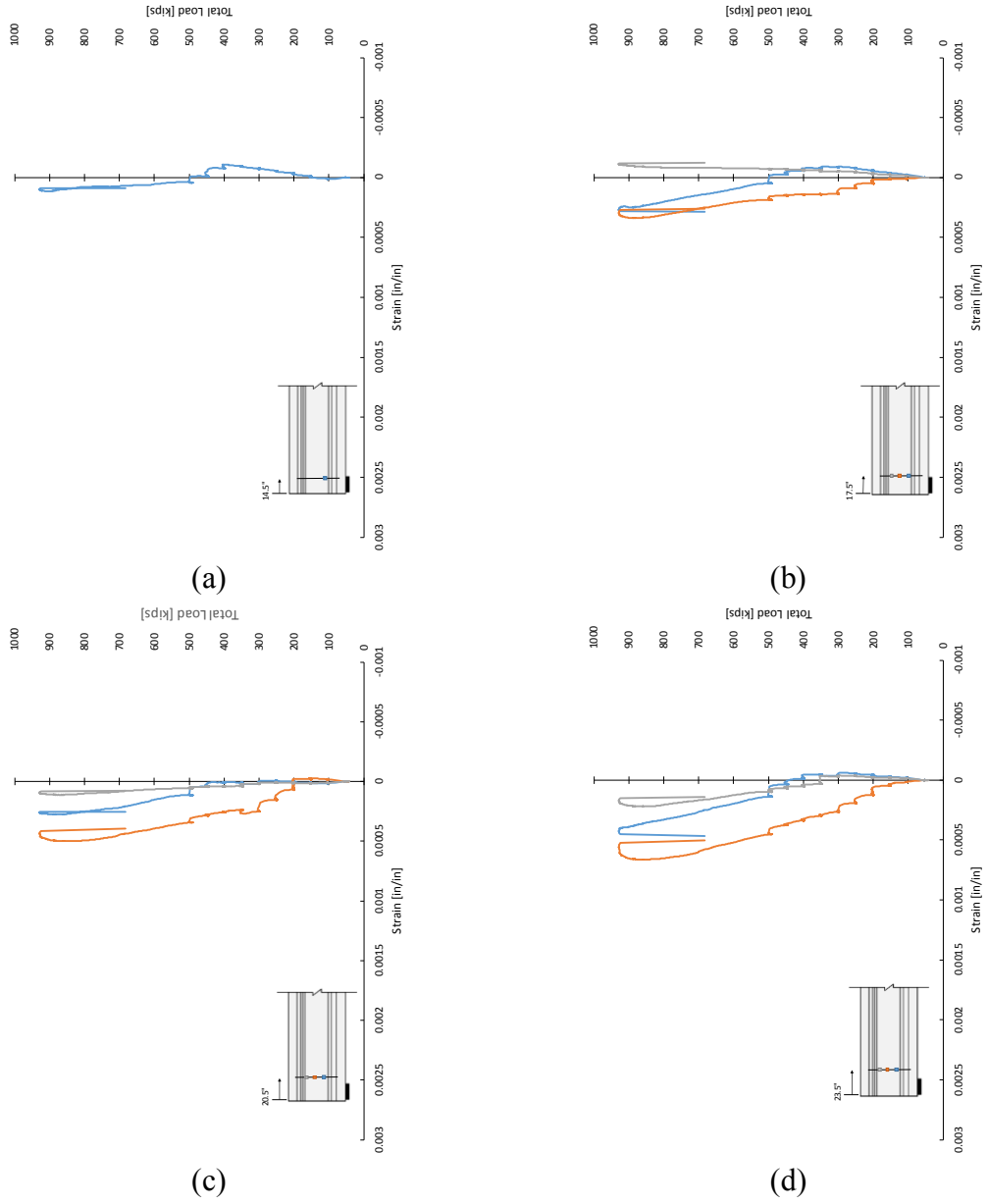

Figure C-14: Total load vs. strain plots from strain gauges on stirrups (a) 14.5 in., (b) 17.5 in., (c) 20.5 in., and (d) 23.5 in. from the dead end face of Tx46-II

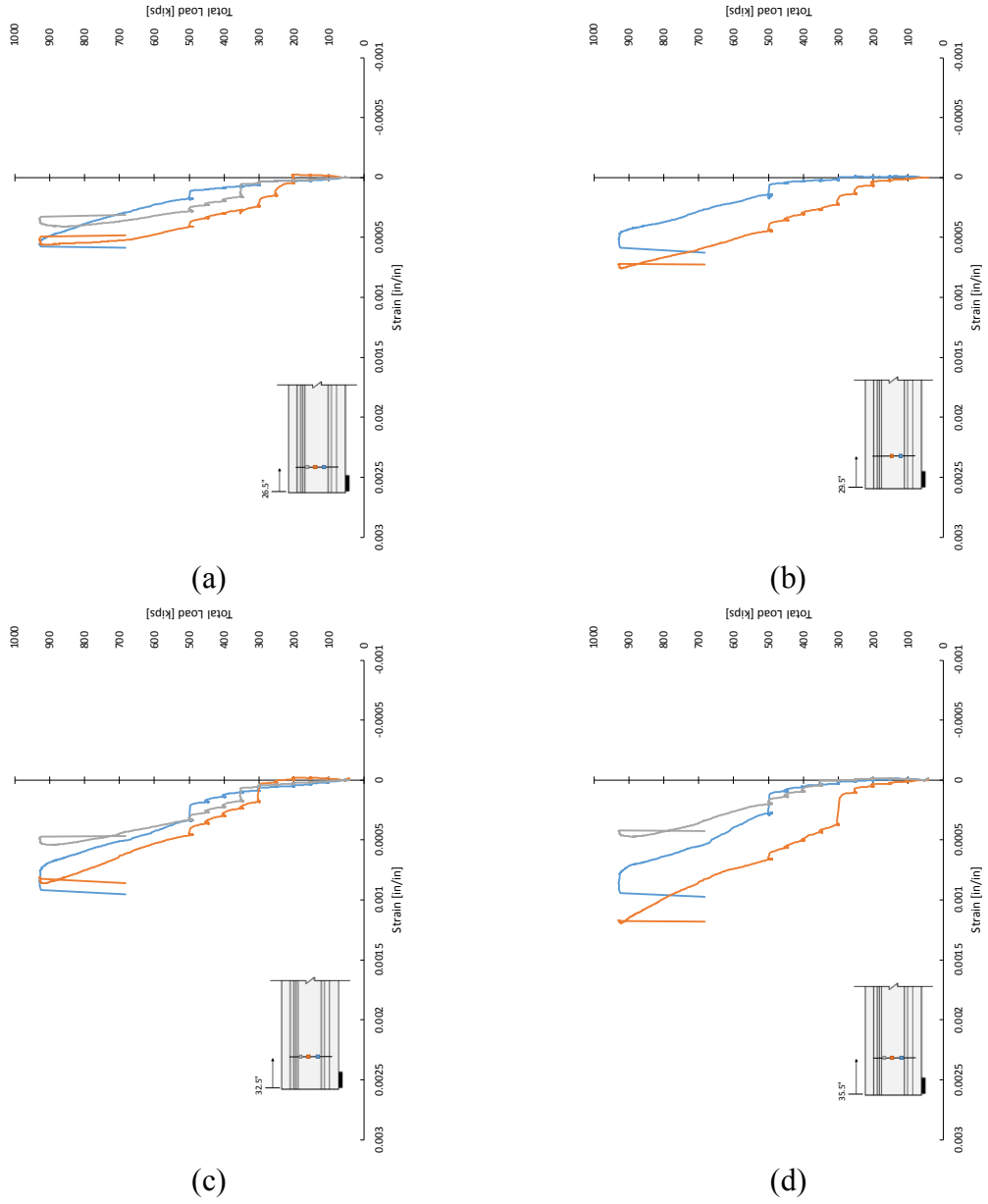

Figure C-15: Total load vs. strain plots from strain gauges on stirrups (a) 26.5 in., (b) 29.5 in., (c) 32.5 in., and (d) 35.5 in. from the dead end face of Tx46-II

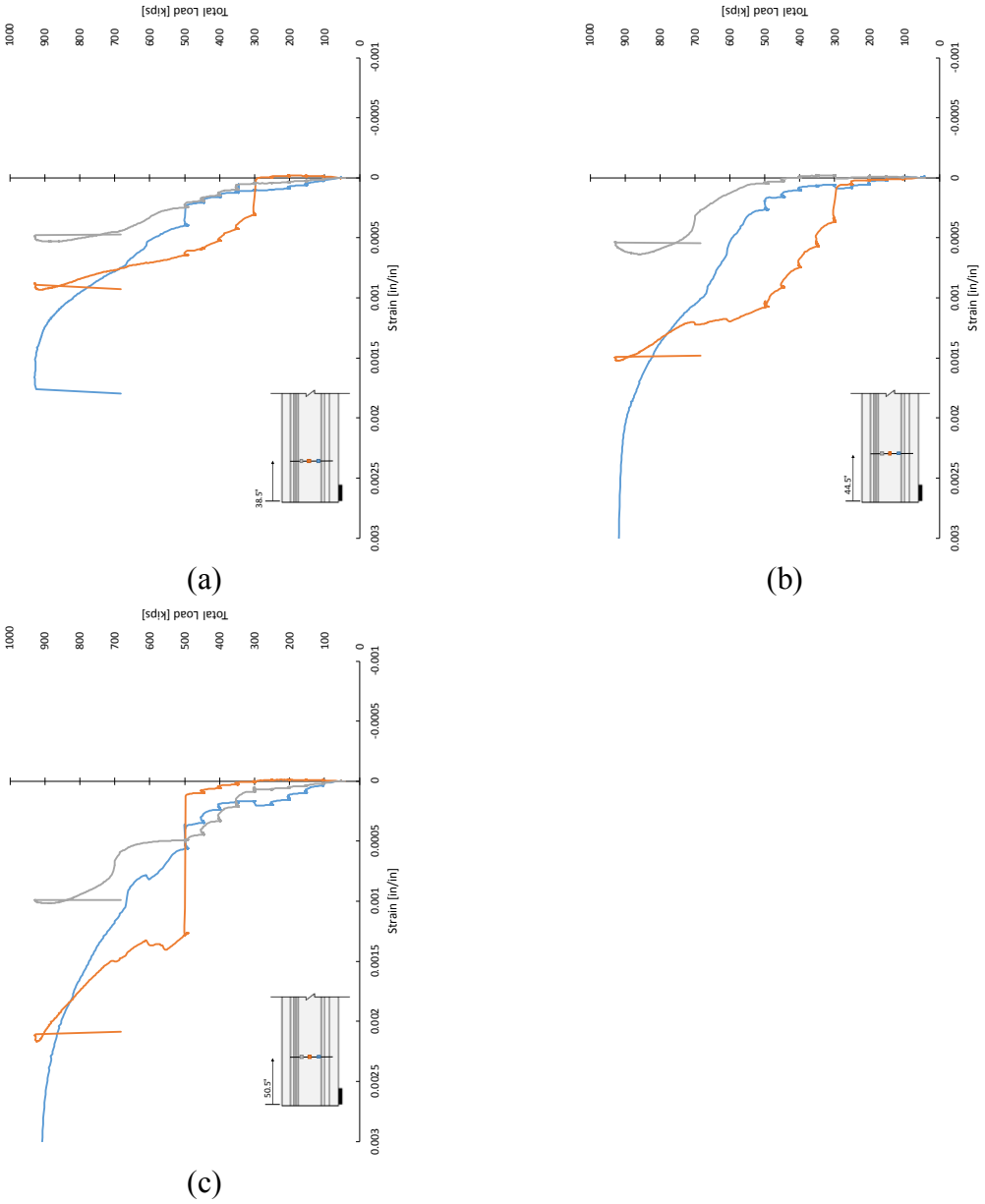

Figure C-16: Total load vs. strain plots from strain gauges on stirrups (a) 38.5 in., (b) 44.5 in., and (c) 50.5 in. from the dead end face of Tx46-II

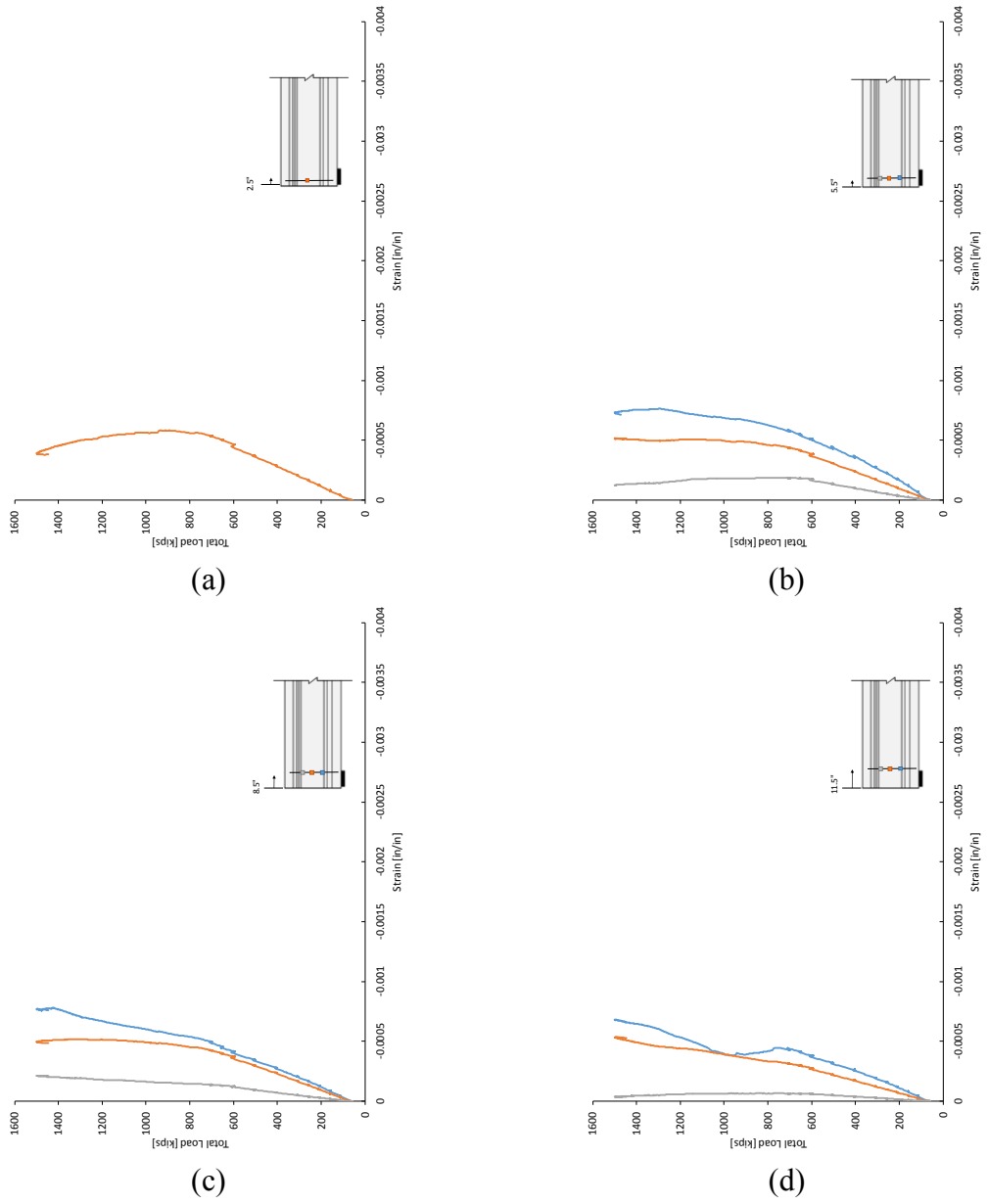

Figure C-17: Total load vs. strain plots from strain gauges on stirrups (a) 2.5 in., (b) 5.5 in., (c) 8.5 in., and (d) 11.5 in. from the live end face of Tx70-I

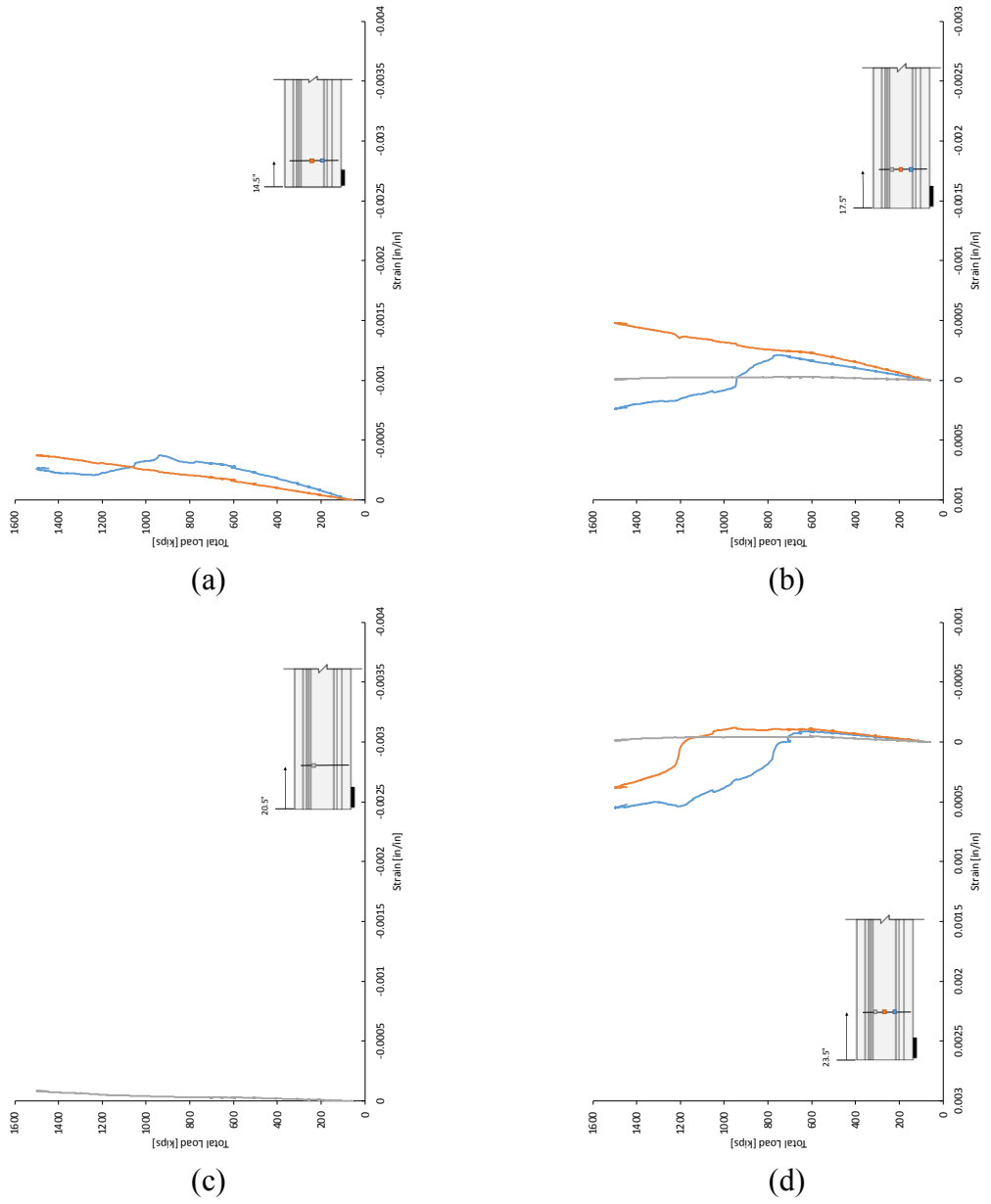

Figure C-18: Total load vs. strain plots from strain gauges on stirrups (a) 14.5 in., (b) 17.5 in., (c) 20.5 in., and (d) 23.5 in. from the live end face of Tx70-I

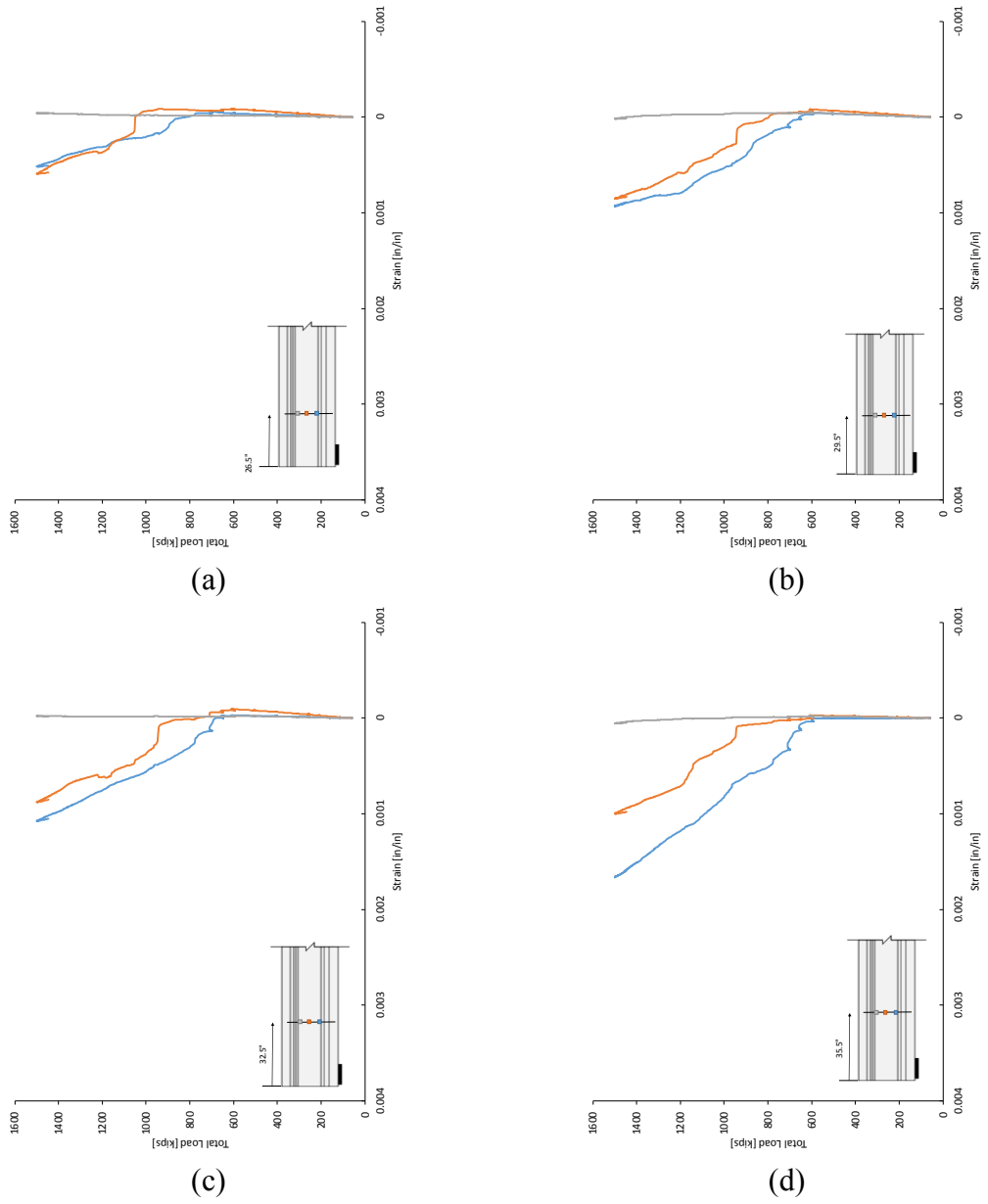

Figure C-19: Total load vs. strain plots from strain gauges on stirrups (a) 26.5 in., (b) 29.5 in., (c) 32.5 in., and (d) 35.5 in. from the live end face of Tx70-I

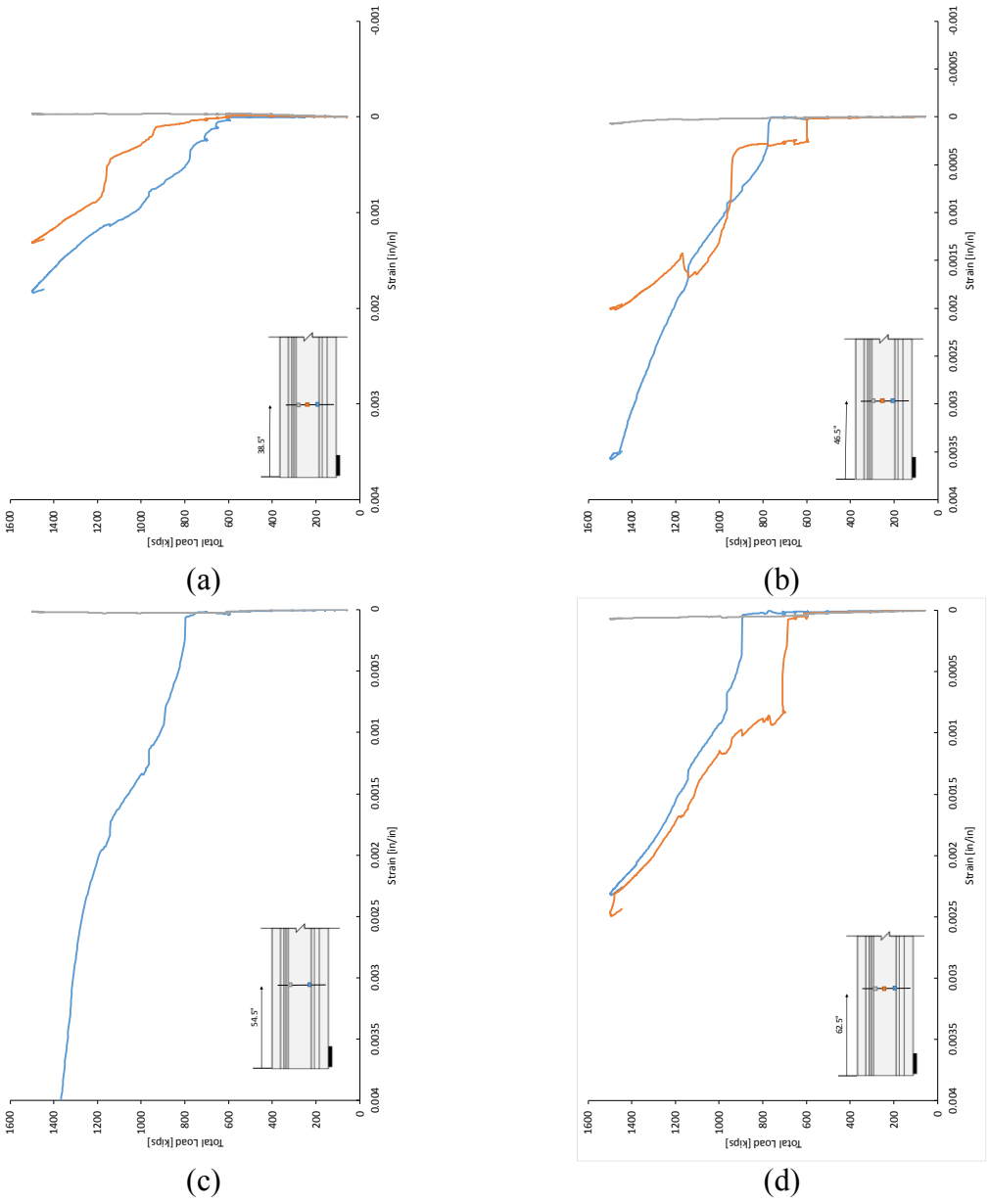

Figure C-20: Total load vs. strain plots from strain gauges on stirrups (a) 38.5 in., (b) 46.5 in., (c) 54.5 in., and (d) 62.5 in. from the live end face of Tx70-I

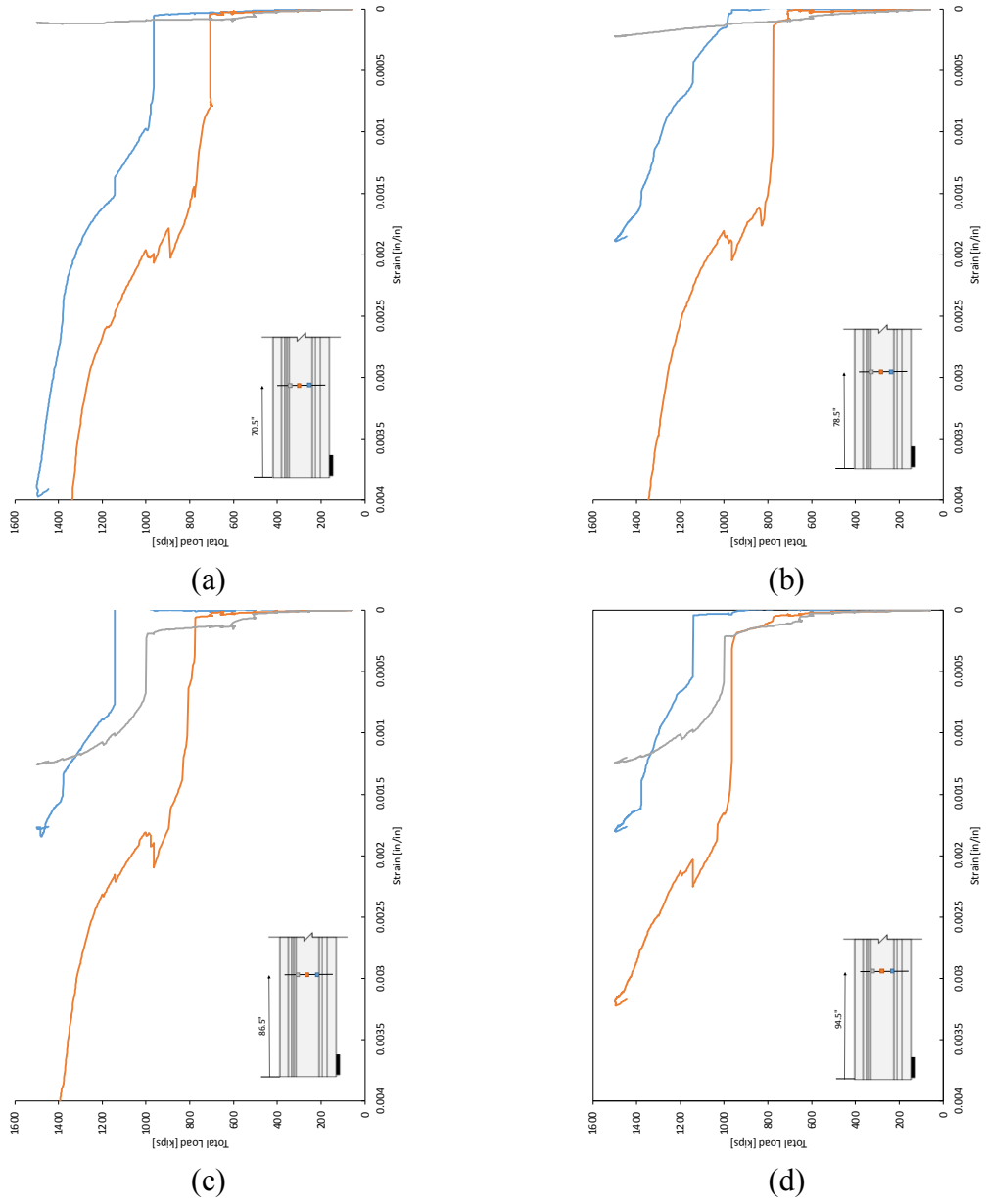

Figure C-21: Total load vs. strain plots from strain gauges on stirrups (a) 70.5 in., (b) 78.5 in., (c) 86.5 in., and (d) 94.5 in. from the live end face of Tx70-I

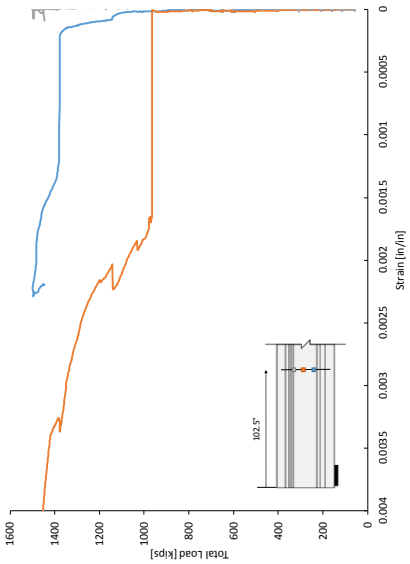

Figure C-22: Total load vs. strain plots from strain gauges on stirrups 102.5 in. from the live end face of Tx70-I

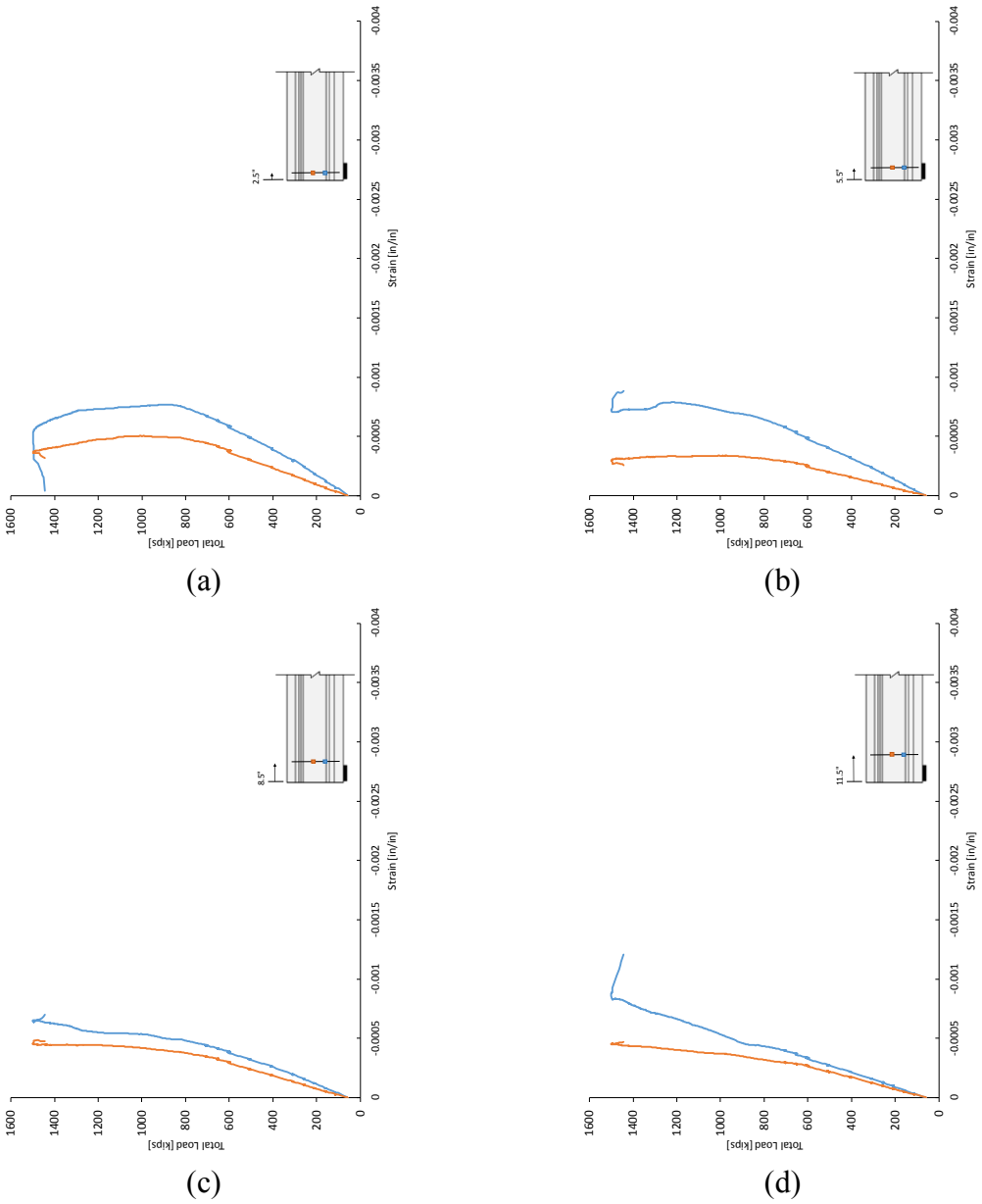

Figure C-23: Total load vs. strain plots from strain gauges on stirrups (a) 2.5 in., (b) 5.5 in., (c) 8.5 in., and (d) 11.5 in. from the dead end face of Tx70-I

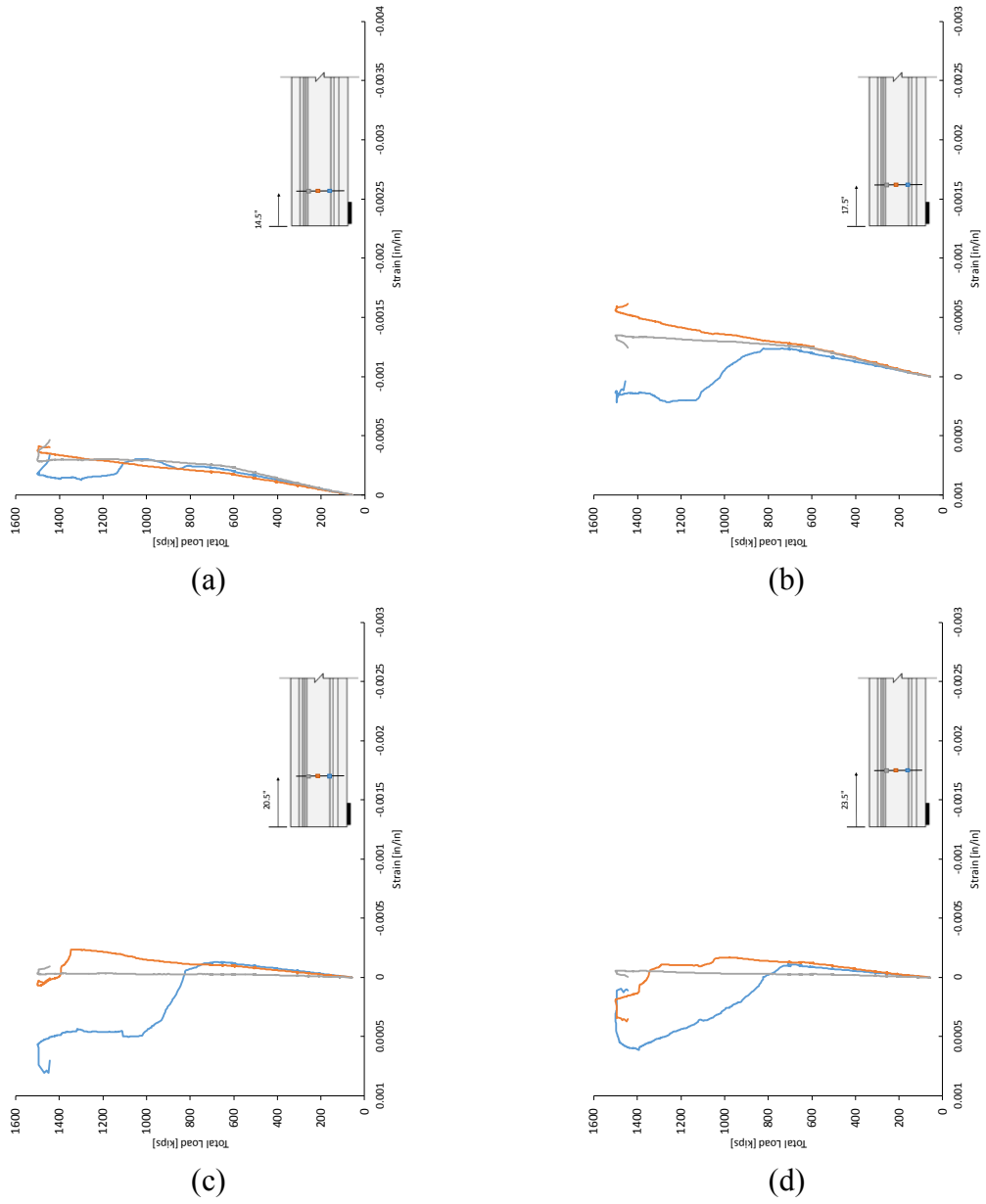

Figure C-24: Total load vs. strain plots from strain gauges on stirrups (a) 14.5 in., (b) 17.5 in., (c) 20.5 in., and (d) 23.5 in. from the dead end face of Tx70-I

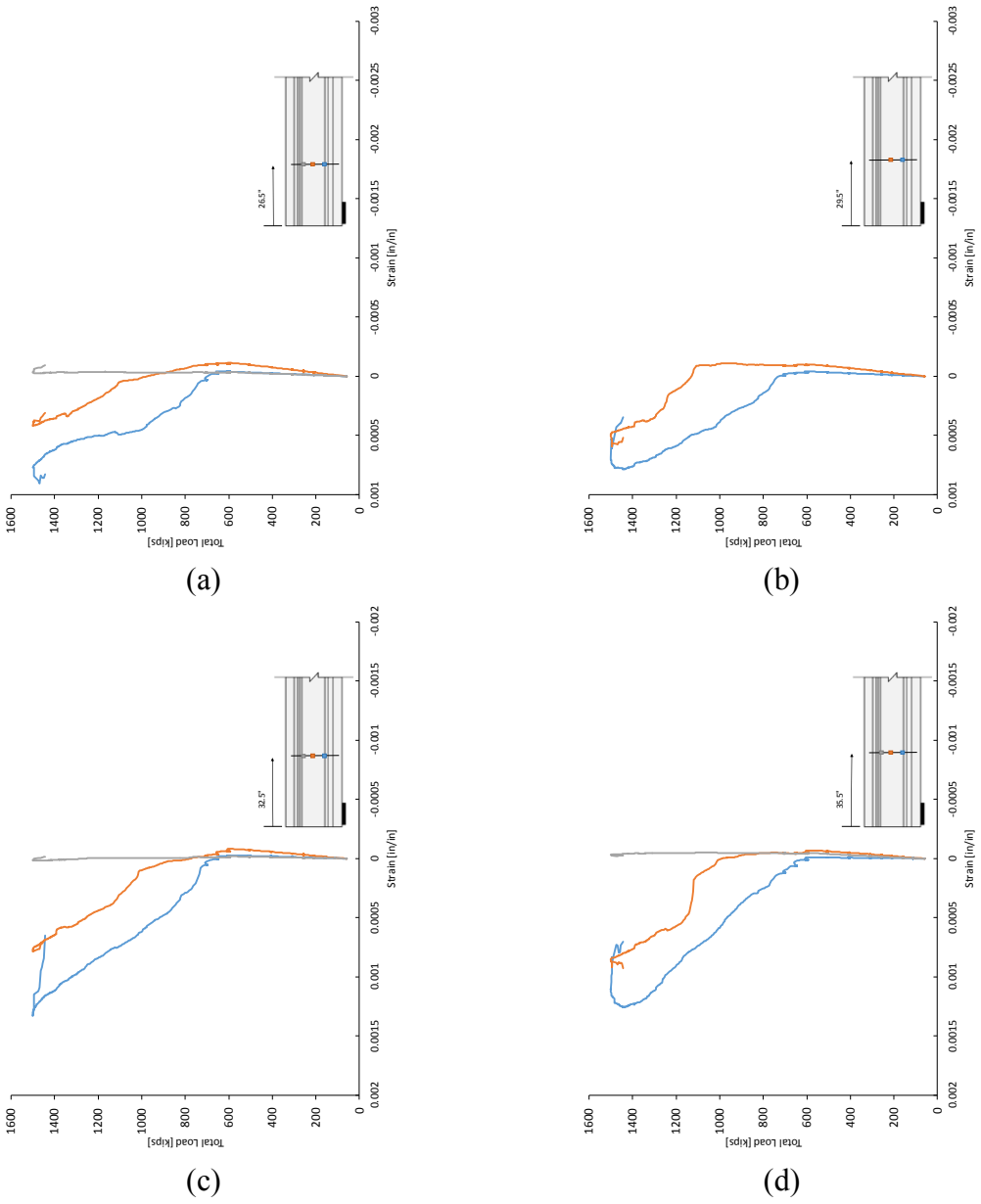

Figure C-25: Total load vs. strain plots from strain gauges on stirrups (a) 26.5 in., (b) 29.5 in., (c) 32.5 in., and (d) 35.5 in. from the dead end face of Tx70-I

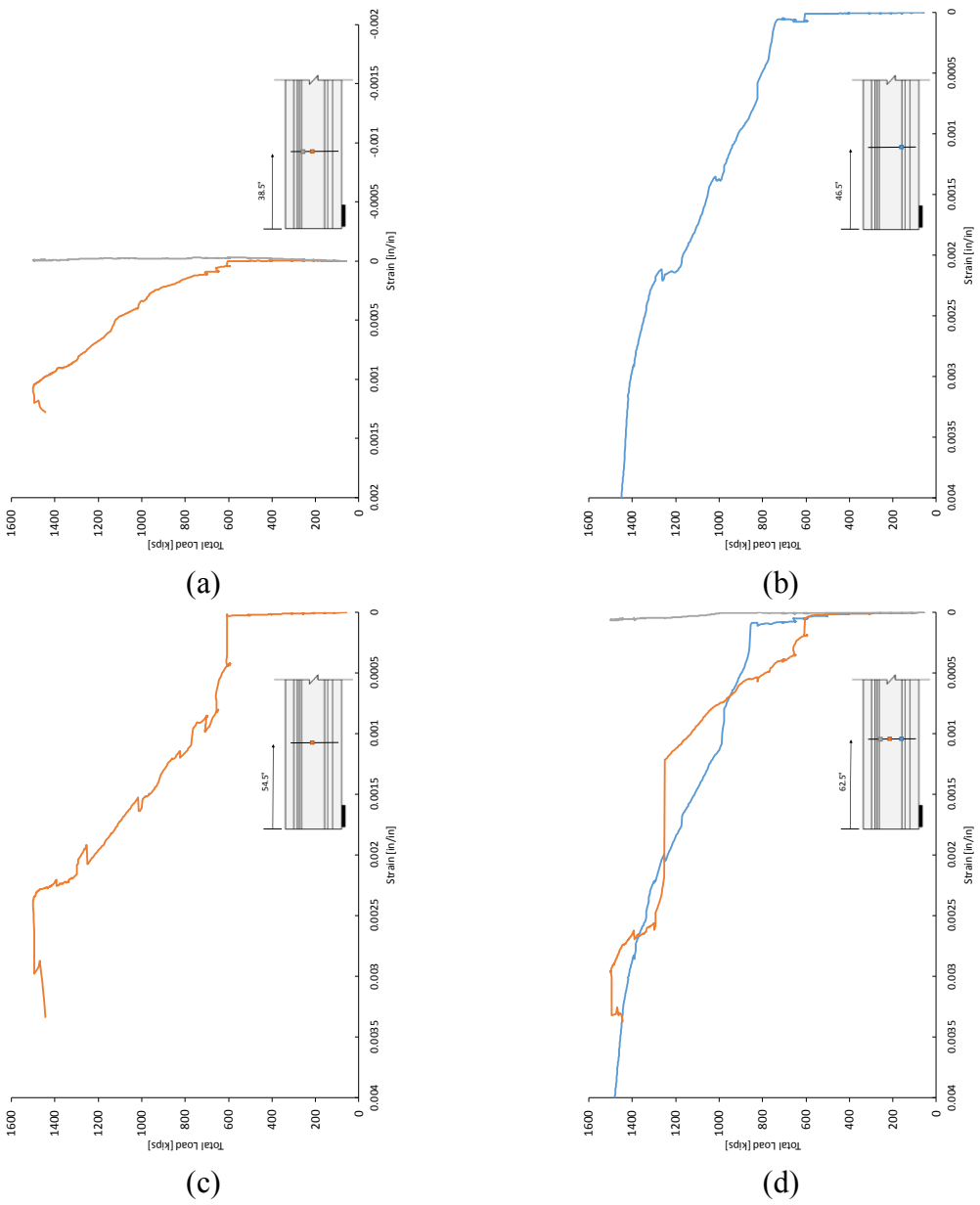

Figure C-26: Total load vs. strain plots from strain gauges on stirrups (a) 38.5 in., (b) 46.5 in., (c) 54.5 in., and (d) 62.5 in. from the dead end face of Tx70-I

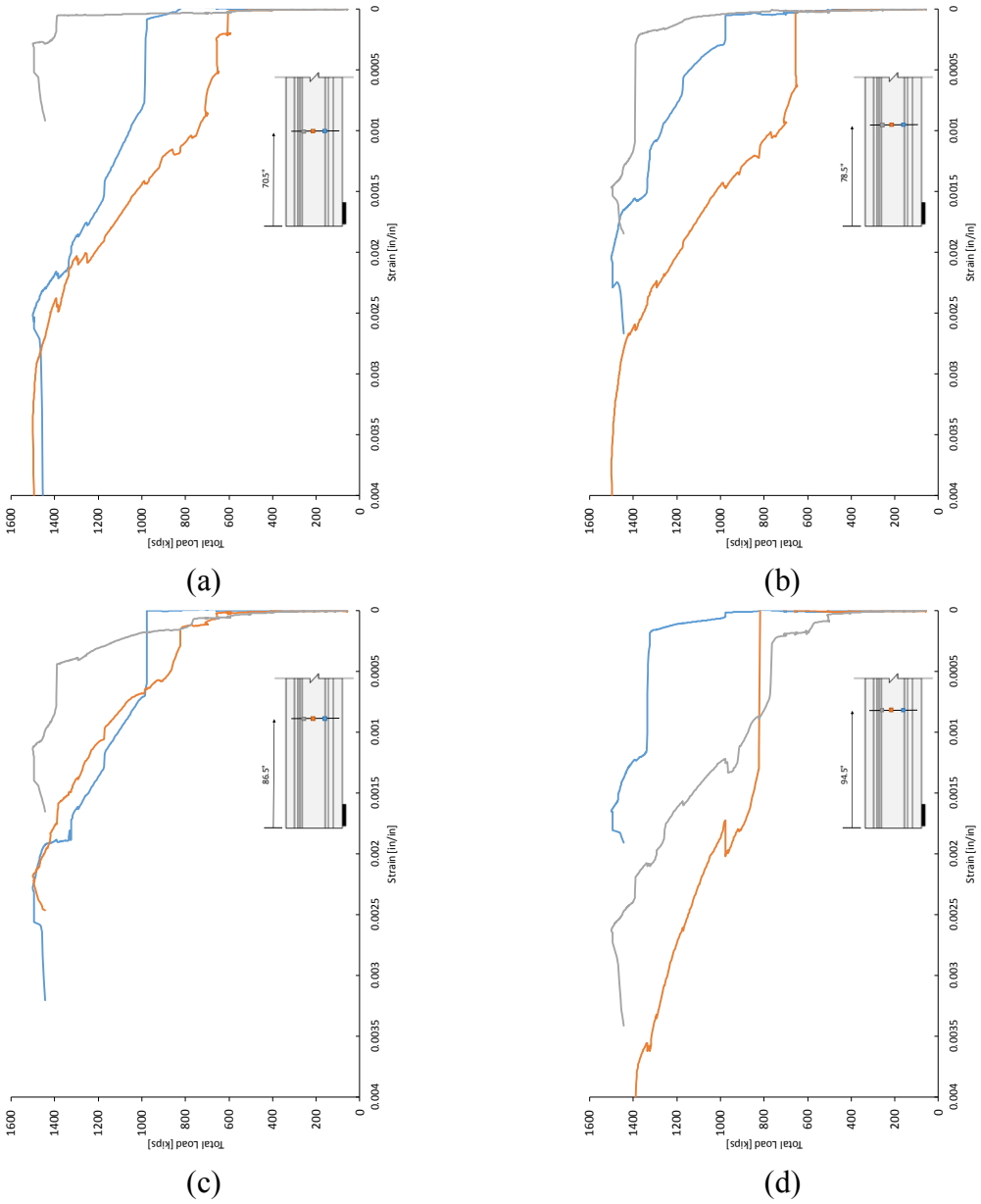

Figure C-27: Total load vs. strain plots from strain gauges on stirrups (a) 70.5 in., (b) 78.5 in., (c) 86.5 in., and (d) 94.5 in. from the dead end face of Tx70-I

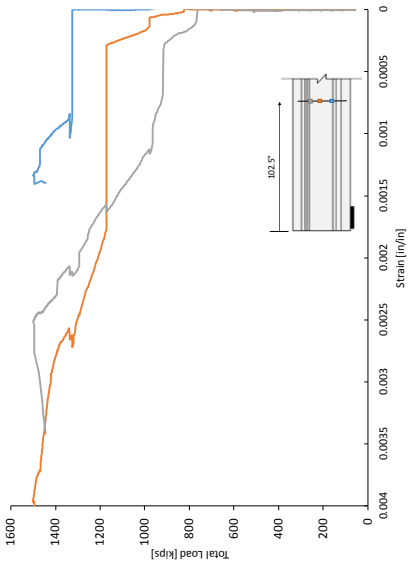

Figure C-28: Total load vs. strain plots from strain gauges on stirrups 102.5 in. from the dead end face of Tx70-I

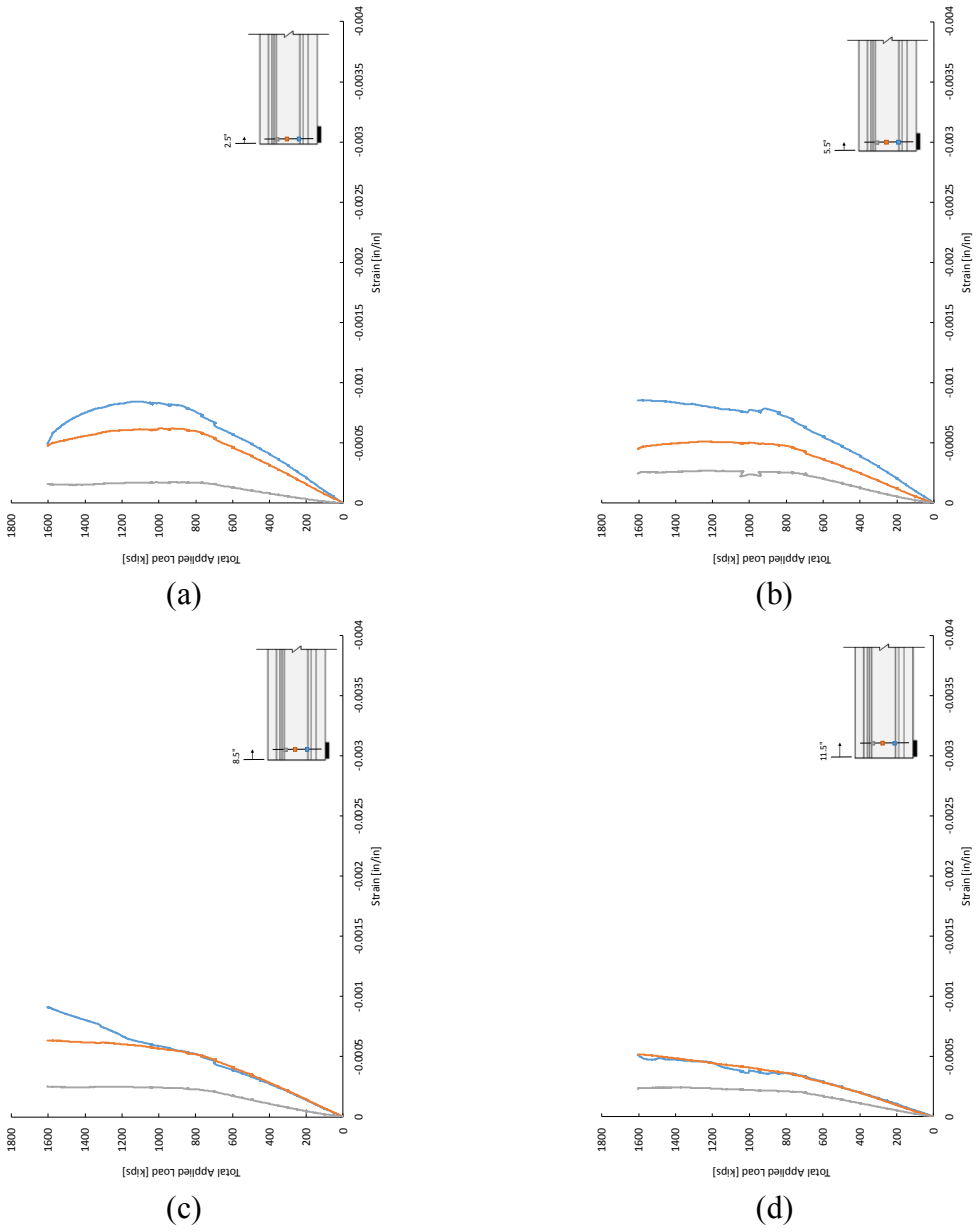

Figure C-29: Total applied load vs. strain plots from strain gauges on stirrups (a) 2.5 in., (b) 5.5 in., (c) 8.5 in., and (d) 11.5 in. from the live end face of Tx70-II

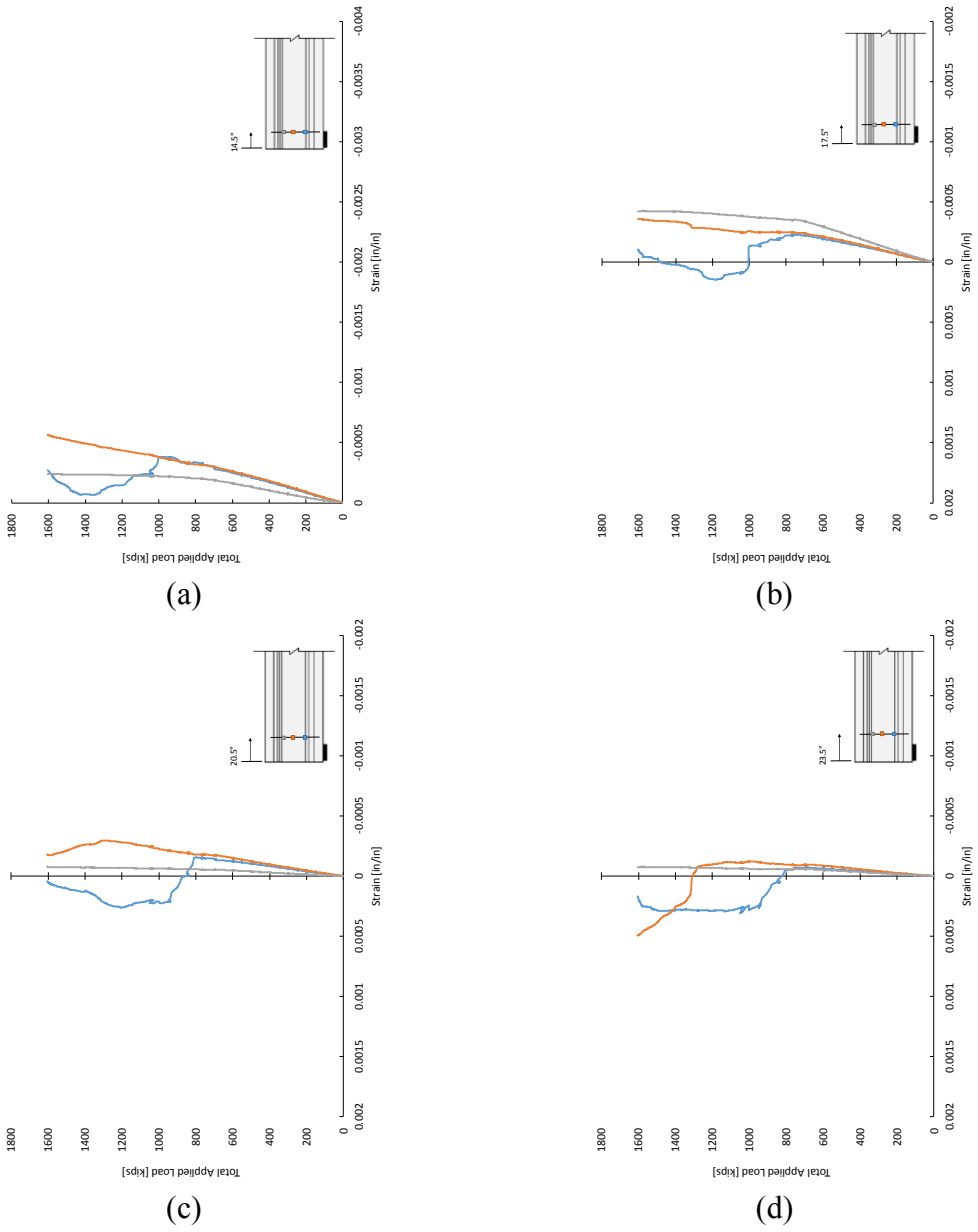

Figure C-30: Total applied load vs. strain plots from strain gauges on stirrups (a) 14.5 in., (b) 17.5 in., (c) 20.5 in., and (d) 23.5 in. from the live end face of Tx70-II

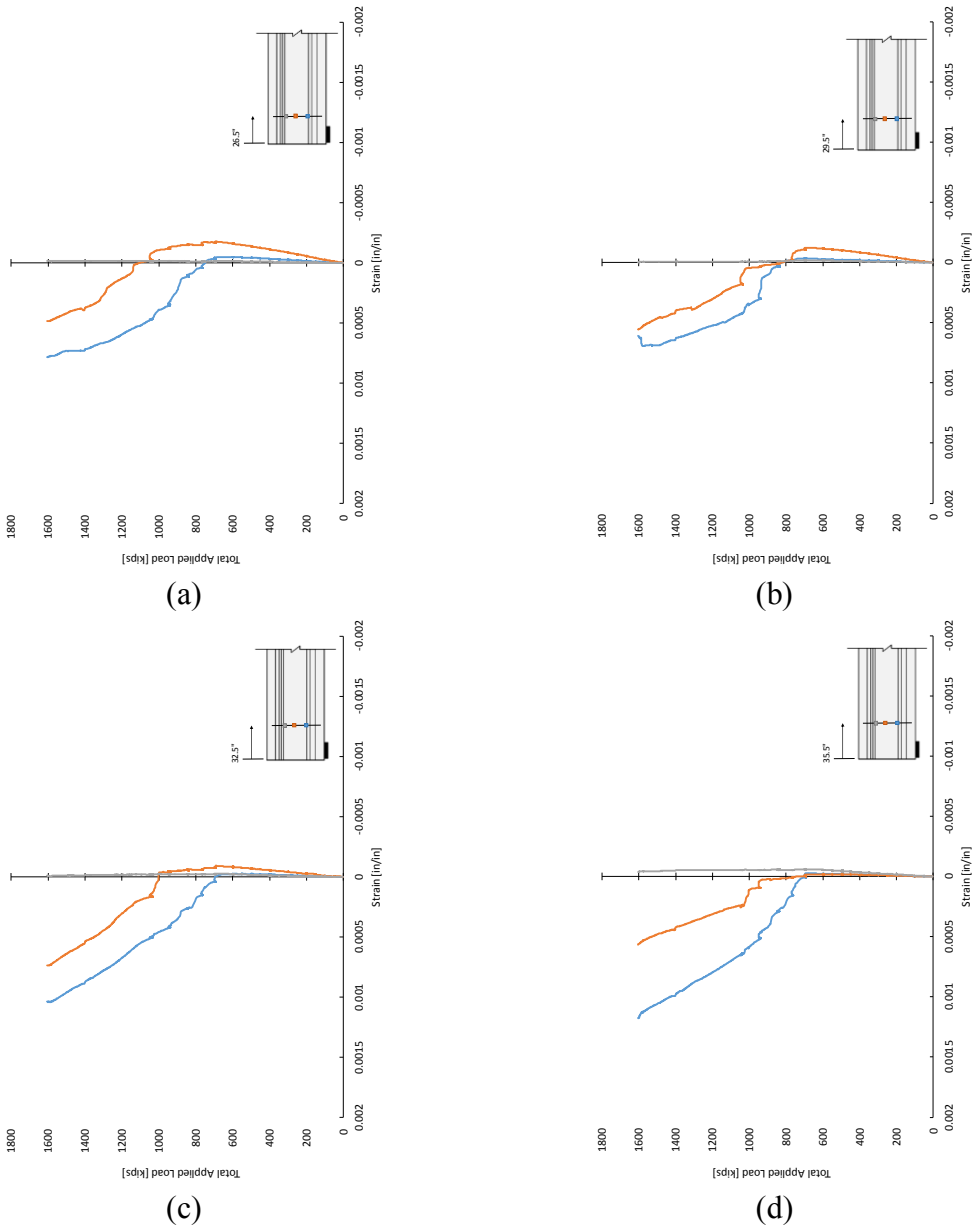

Figure C-31: Total applied load vs. strain plots from strain gauges on stirrups (a) 26.5 in., (b) 29.5 in., (c) 32.5 in., and (d) 35.5 in. from the live end face of Tx70-II

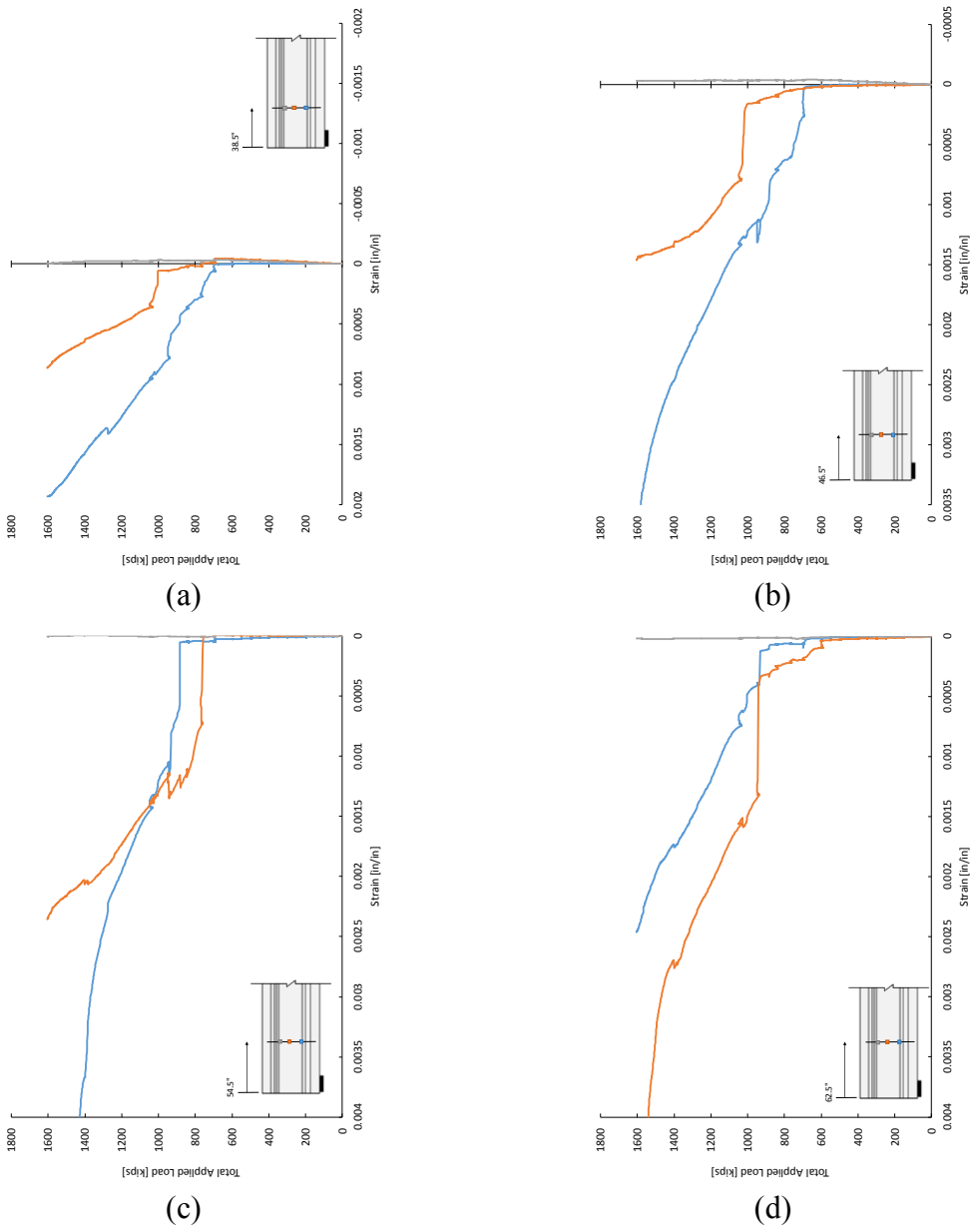

Figure C-32: Total applied load vs. strain plots from strain gauges on stirrups (a) 38.5 in., (b) 46.5 in., (c) 54.5 in., and (d) 62.5 in. from the live end face of Tx70-II

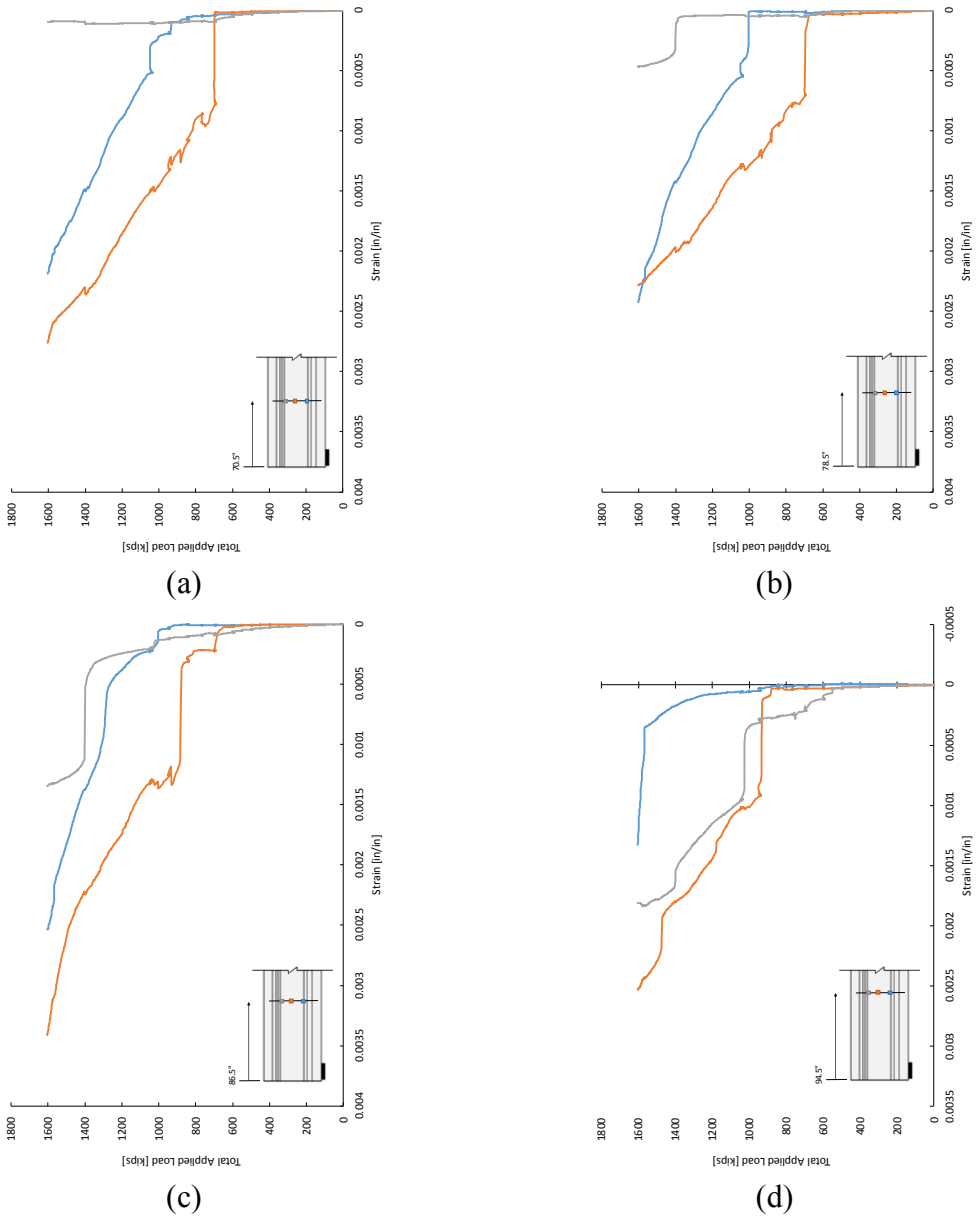

Figure C-33: Total applied load vs. strain plots from strain gauges on stirrups (a) 70.5 in., (b) 78.5 in., (c) 86.5 in., and (d) 94.5 in. from the live end face of Tx70-II

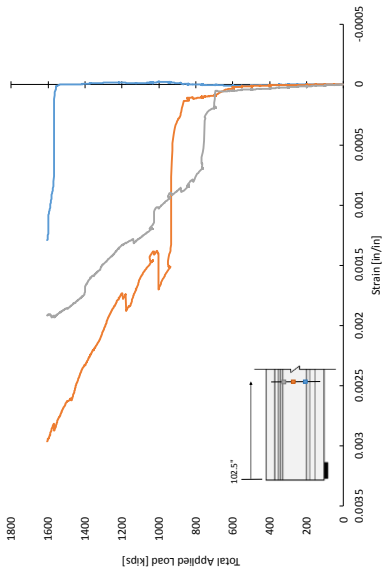

Figure C-34: Total applied load vs. strain plots from strain gauges on stirrups 102.5 in. from the live end face of Tx70-II

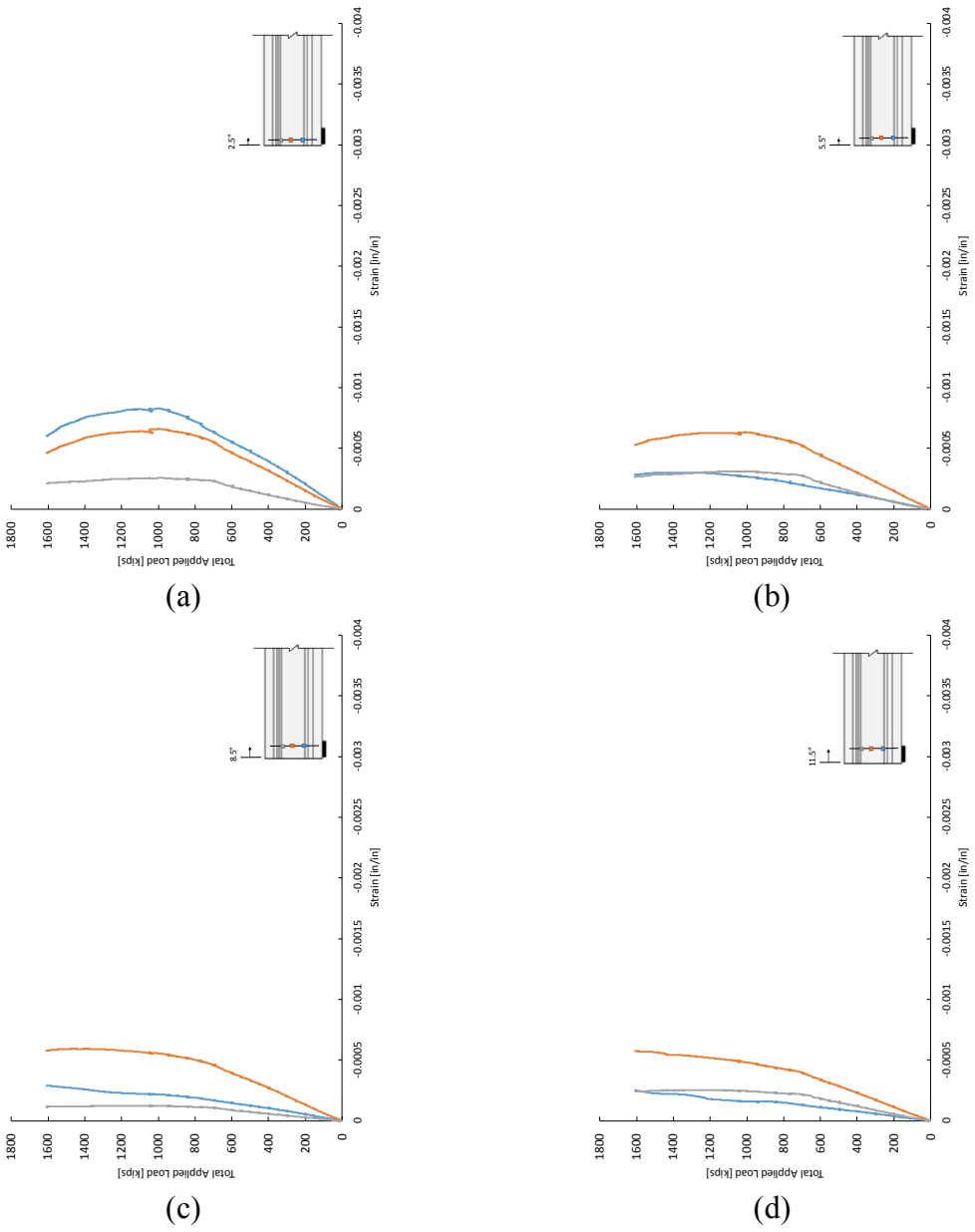

Figure C-35: Total applied load vs. strain plots from strain gauges on stirrups (a) 2.5 in., (b) 5.5 in., (c) 8.5 in., and (d) 11.5 in. from the dead end face of Tx70-II

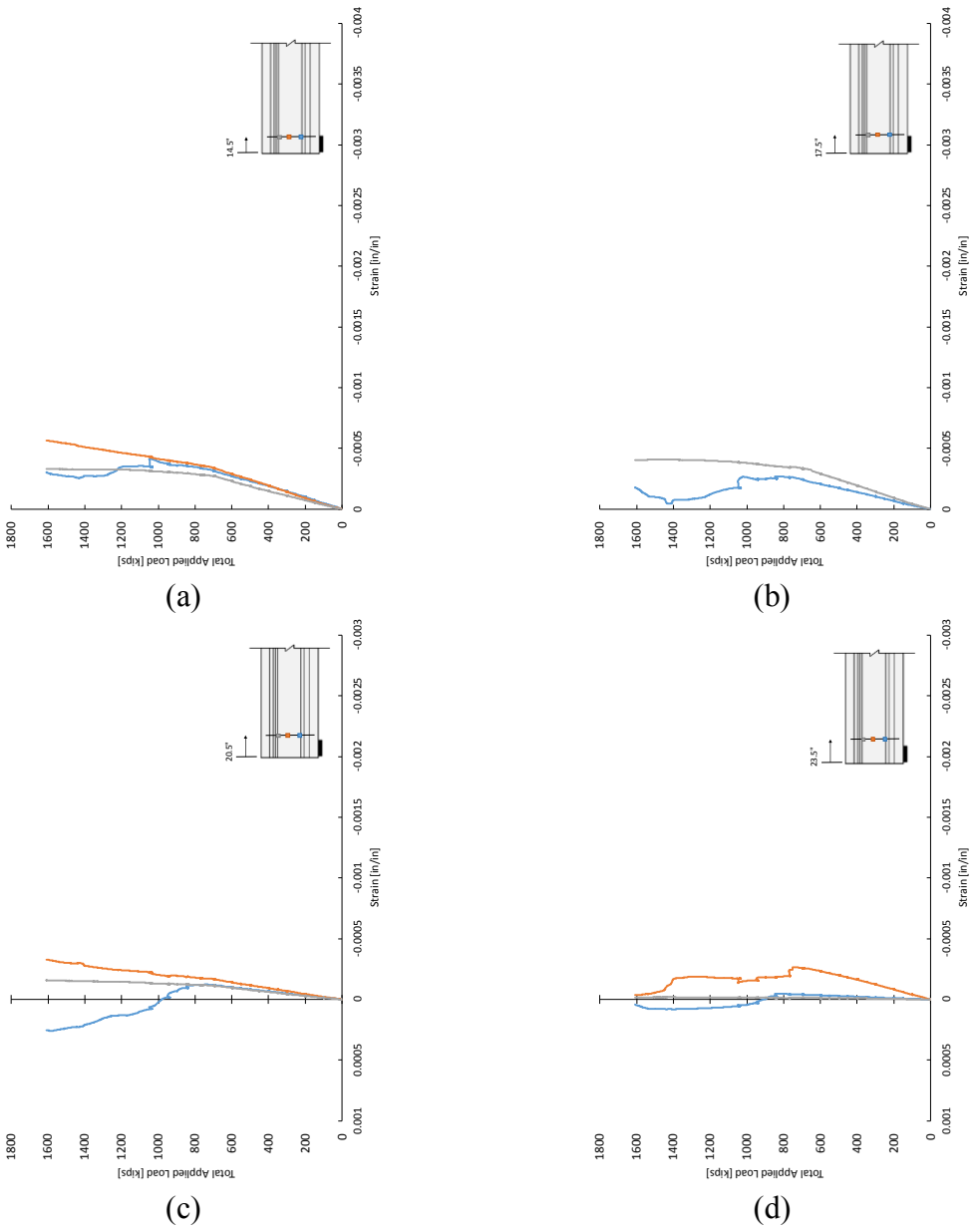

Figure C-36: Total applied load vs. strain plots from strain gauges on stirrups (a) 14.5 in., (b) 17.5 in., (c) 20.5 in., and (d) 23.5 in. from the dead end face of Tx70-II

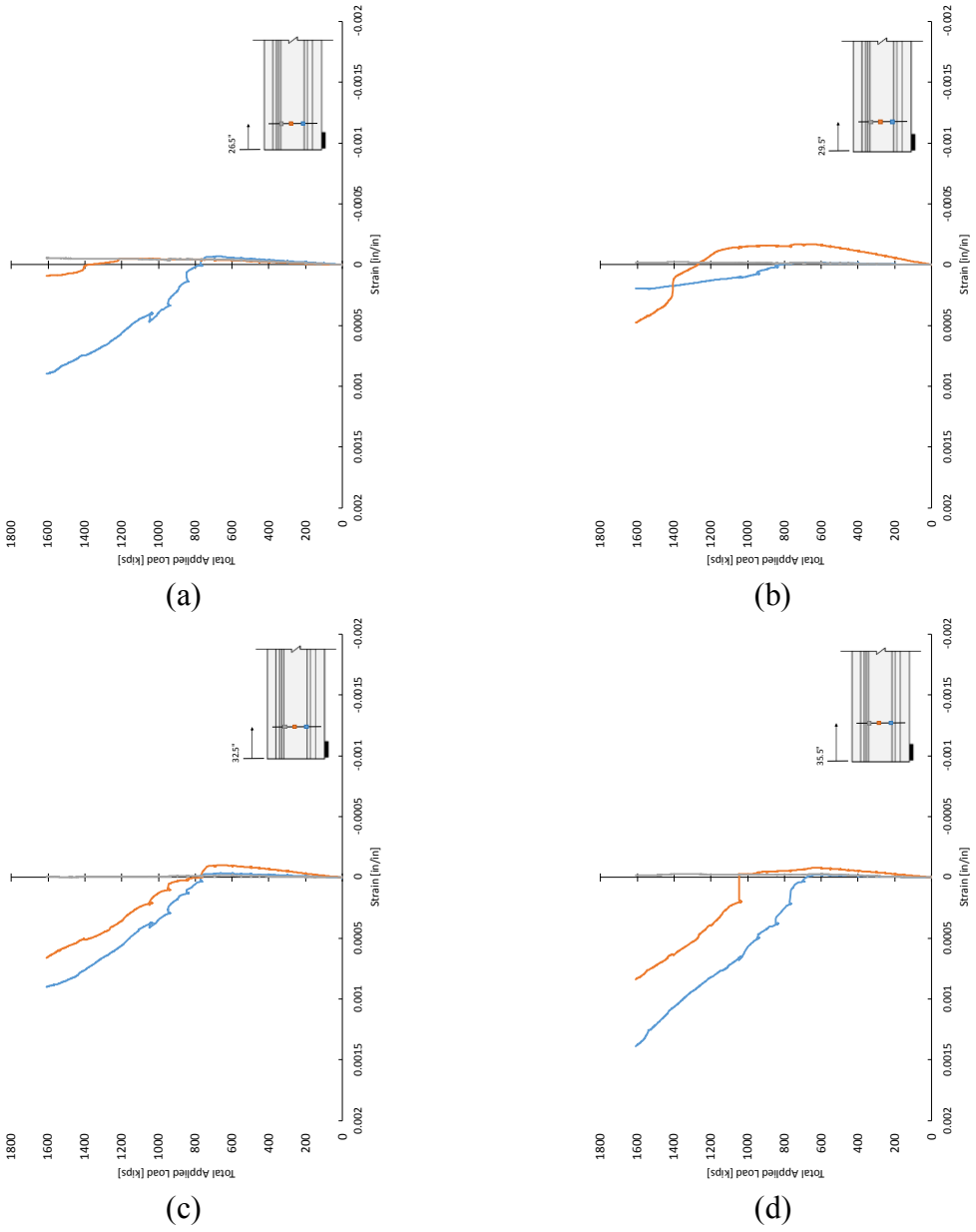

Figure C-37: Total applied load vs. strain plots from strain gauges on stirrups (a) 26.5 in., (b) 29.5 in., (c) 32.5 in., and (d) 35.5 in. from the dead end face of Tx70-II

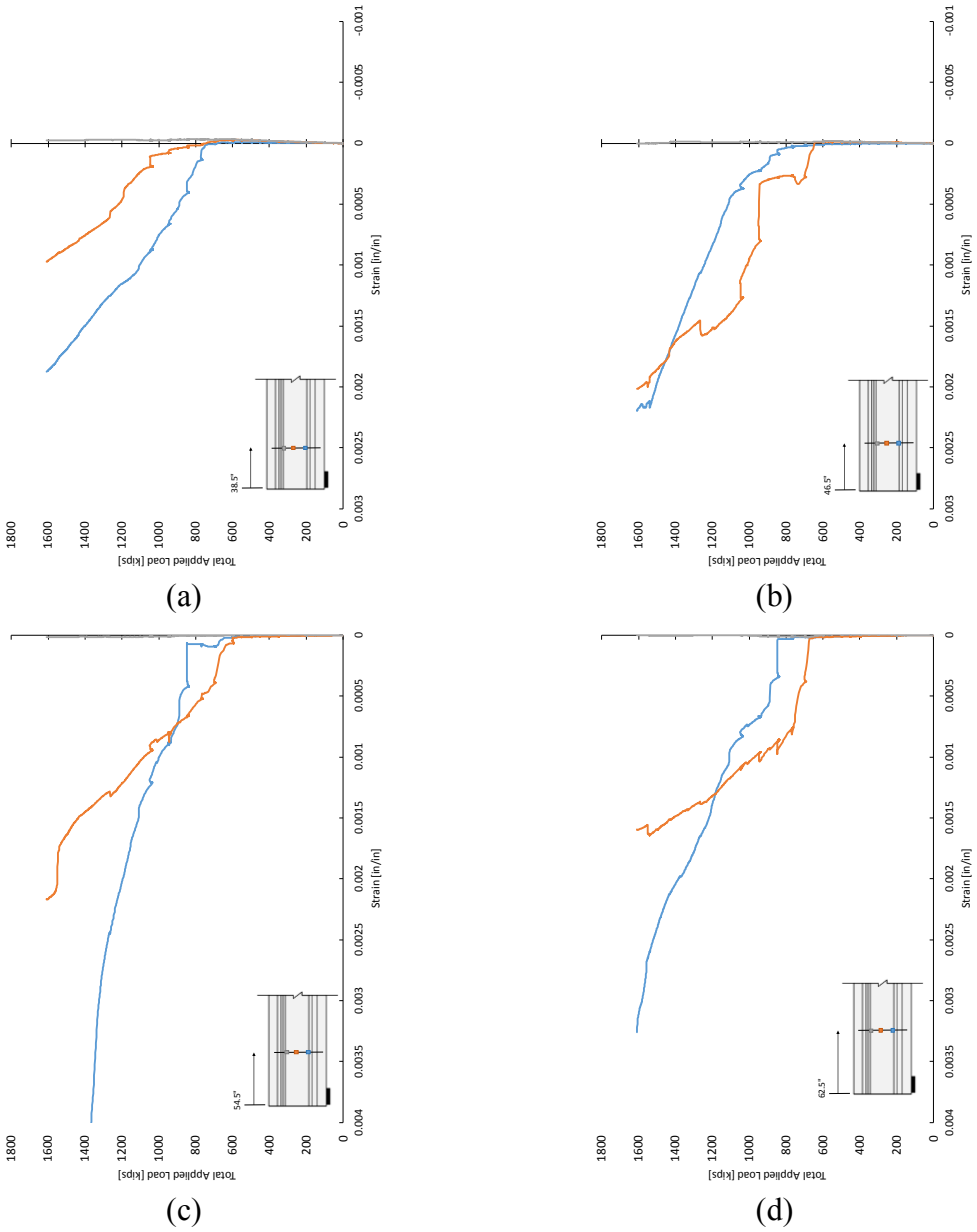

Figure C-38: Total applied load vs. strain plots from strain gauges on stirrups (a) 38.5 in., (b) 46.5 in., (c) 54.5 in., and (d) 62.5 in. from the dead end face of Tx70-II

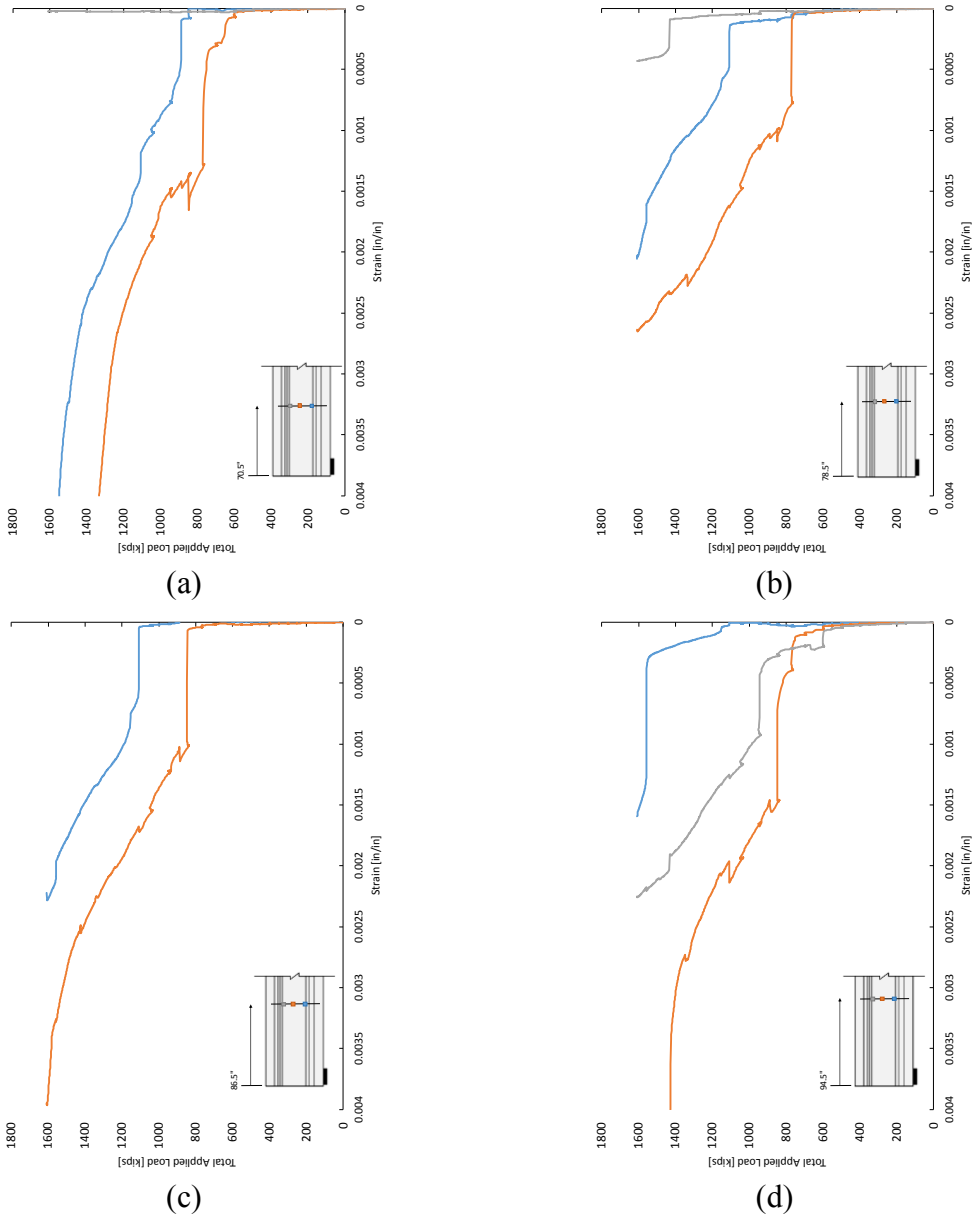

Figure C-39: Total applied load vs. strain plots from strain gauges on stirrups (a) 70.5 in., (b) 78.5 in., (c) 86.5 in., and (d) 94.5 in. from the dead end face of Tx70-II

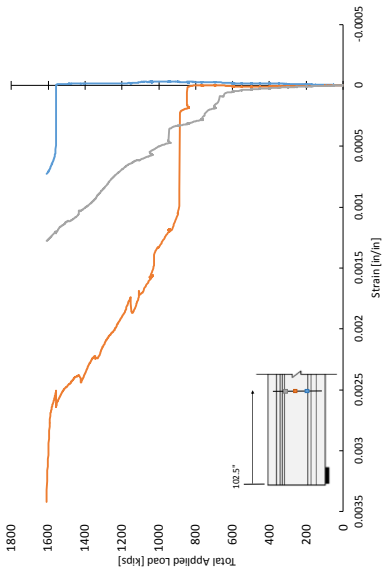

Figure C-40: Total applied load vs. strain plots from strain gauges on stirrups 102.5 in. from the dead end face of Tx70-II

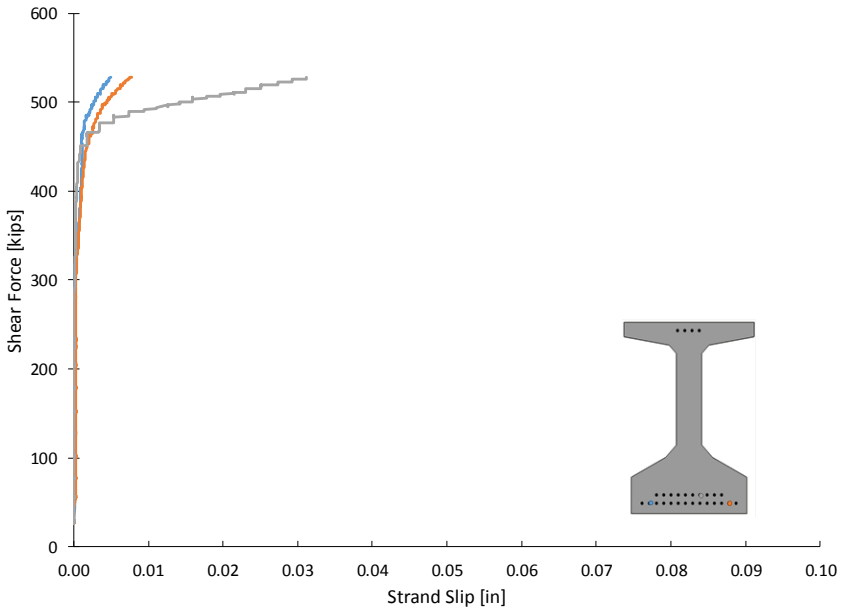

(a)

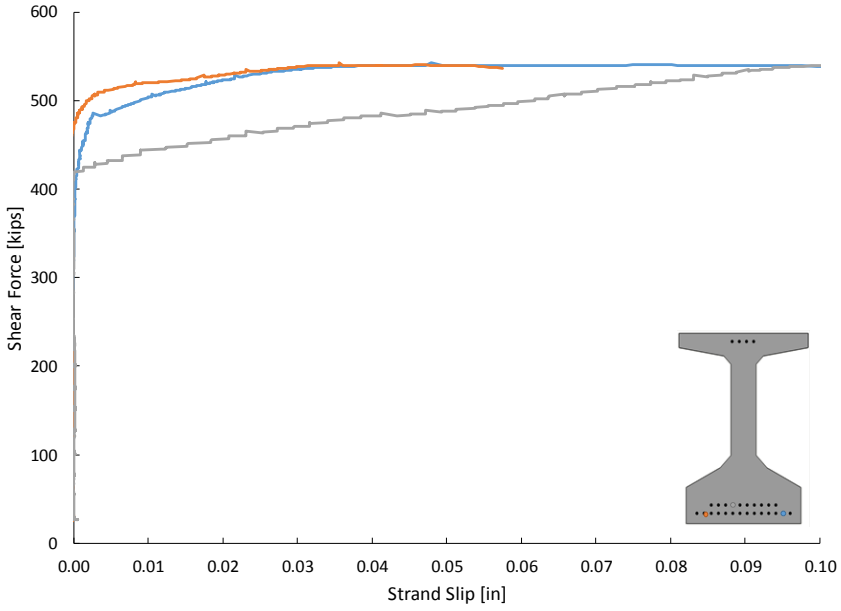

(b)

Figure C-41: Shear force vs. strand slip in Tx46-I (a) live end, and (b) dead end

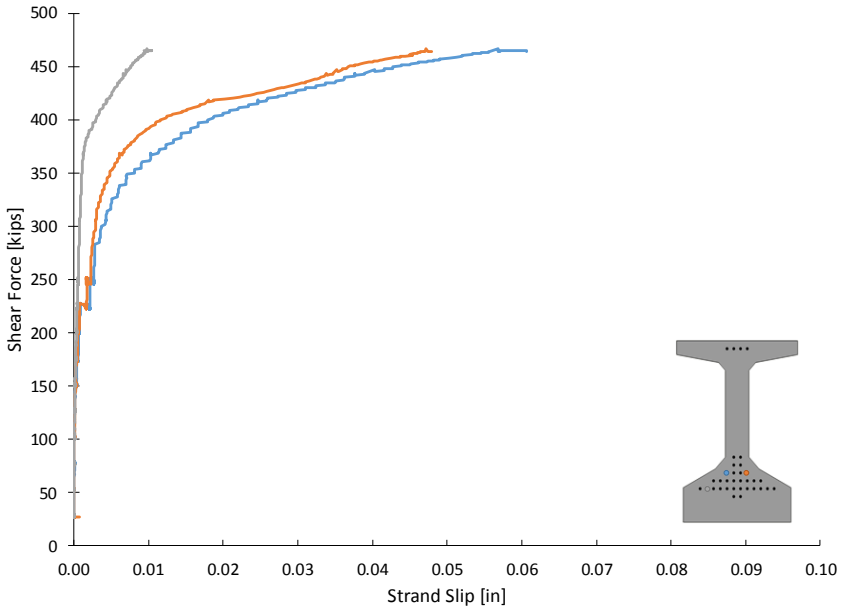

(a)

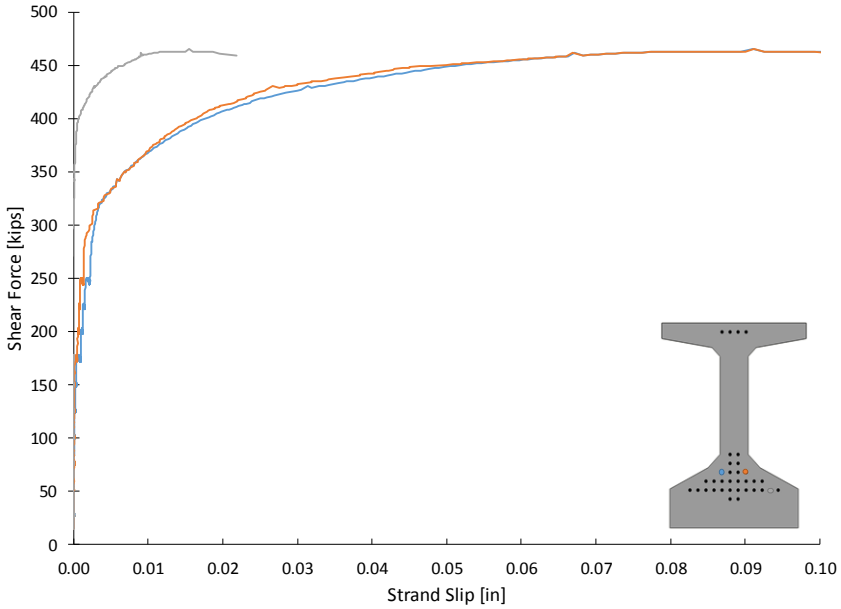

(b)

Figure C-42: Shear force vs. strand slip in Tx46-II (a) live end, and (b) dead end

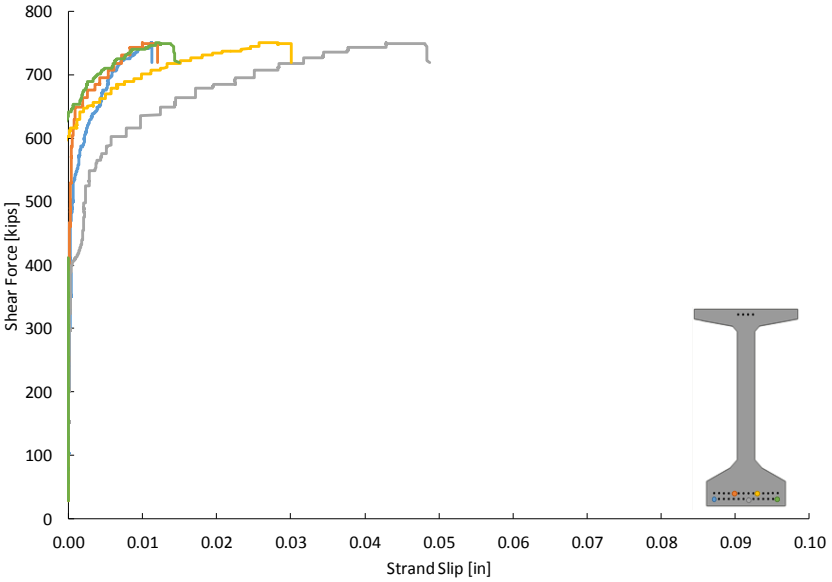

(a)

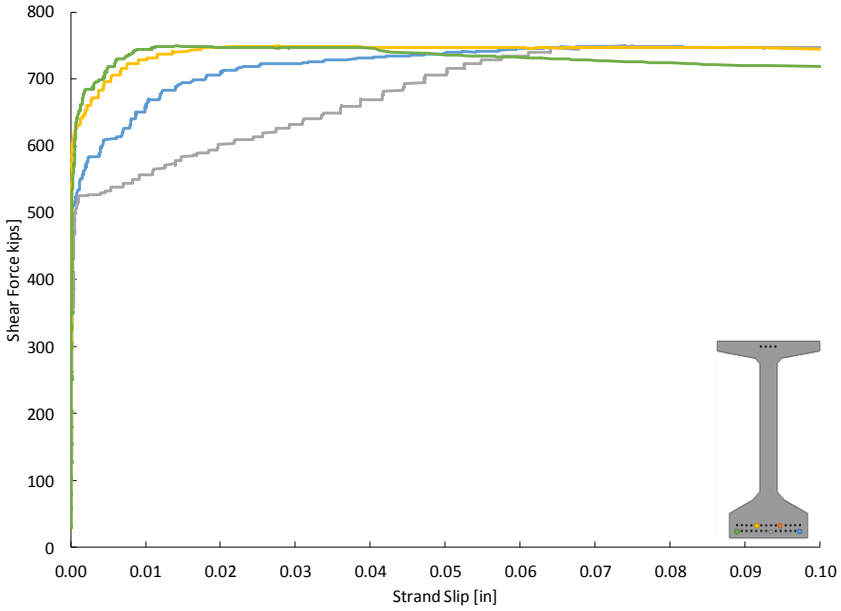

(b)

Figure C-43: Shear force vs. strand slip in Tx70-I (a) live end, and (b) dead end

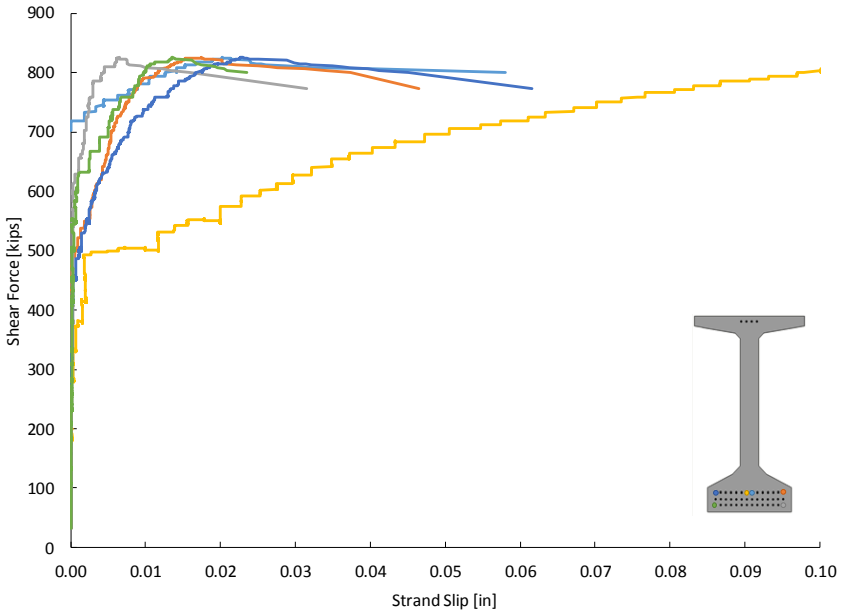

(a)

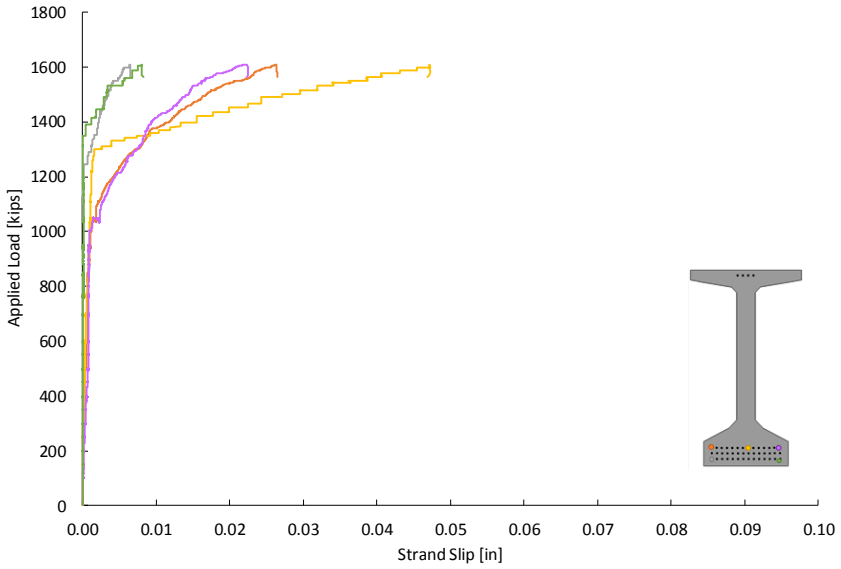

(b)

Figure C-44: Shear force vs. strand slip in Tx70-II (a) live end, and (b) applied load vs. strand slip in Tx70-II dead end

Table C-1: Selected concrete surface strain data for the live end span of Tx70-I from the Optotrak vision system

Distance From End										
	Face	6 ft	7 ft	8 ft	9 ft	10 ft	11 ft	12 ft		
Strain at R = 5 kips	Bot	-4.34E-05	3.02E-06	2.52E-05	1.37E-05	2.24E-05	1.50E-05	1.36E-05		
	Mid	6.53E-05	2.13E-05	-4.01E-06	2.07E-05	-5.24E-05	1.00E-06	1.01E-05		
	Top	1.56E-06	8.07E-06	-1.52E-05	1.55E-05	-2.89E-05	1.42E-05	1.02E-05		
Strain Before Cracking	Bot	-1.30E-04	2.89E-05	7.85E-05	4.11E-05	6.66E-05	9.39E-05	-1.16E-05		
	Mid	5.27E-05	4.99E-05	-8.17E-05	7.42E-05	-2.26E-06	4.21E-05	7.16E-05		
	Top	-8.25E-05	-6.59E-05	9.57E-05	-6.60E-05	-9.97E-05	1.71E-05	3.25E-05		
Strain at Peak	Bot	1.97E-04	1.49E-03	2.03E-03	2.37E-03	2.33E-03	3.11E-03	4.26E-03		
	Mid	1.65E-03	2.53E-03	3.71E-03	4.18E-03	2.52E-03	3.68E-03	2.02E-03		
	Top	3.68E-03	3.82E-03	2.41E-03	2.17E-03	3.65E-03	1.77E-03	9.27E-04		

Table C-2: Selected concrete surface strain data for the dead end span of Tx70-I from the Optotrak vision system

Distance from end face		5 ft	6 ft	7 ft	8 ft	9 ft	10 ft	11 ft	12 ft
Strain at R = 5 kips	Bot	1.54E-05	1.19E-05	1.33E-06	3.05E-06	-6.34E-06	3.90E-06	6.37E-06	4.18E-05
	Mid	7.57E-06	2.89E-06	2.26E-05	-1.84E-06	8.56E-06	1.55E-05	1.31E-05	-5.12E-06
	Top	8.53E-06	1.67E-05	1.18E-06	1.46E-05	4.02E-07	1.83E-06	6.60E-06	6.58E-06
Strain Before Cracking	Bot	-7.29E-05	2.17E-05	-7.15E-05	-4.85E-06	7.96E-05	-5.82E-05	9.66E-05	2.07E-04
	Mid	5.64E-05	-1.82E-05	9.28E-05	-5.73E-06	-5.87E-05	1.29E-04	6.97E-06	-6.44E-05
	Top	-1.09E-05	6.41E-05	4.30E-06	-6.90E-06	-2.95E-05	-1.72E-05	5.65E-05	1.25E-05
Strain at Peak	Bot	6.82E-04	2.00E-03	1.05E-03	3.57E-03	2.34E-03	3.37E-03	3.55E-03	3.00E-03
	Mid	1.24E-03	1.70E-03	3.49E-03	2.33E-03	3.91E-03	2.31E-03	2.63E-03	1.28E-03
	Top	2.70E-03	3.15E-03	3.14E-03	2.91E-03	2.09E-03	1.78E-03	2.53E-04	9.06E-05

Table C-3: Selected concrete surface strain data for the live end span of Tx70-II from the Optotrak vision system

Distance From End Face		4 ft	5 ft	6 ft	7 ft	8 ft	9 ft	10 ft	11 ft
At R = 5 kips	Bot	-1.16E-04	-2.34E-04	-1.76E-04	1.50E-05	-7.93E-05	2.72E-05	1.25E-05	-1.15E-04
	Mid	5.89E-05	2.00E-05	1.72E-05	-1.12E-05	5.44E-05	-6.29E-05	-9.48E-05	-1.49E-05
	Top	-1.40E-04	-6.24E-05	-2.65E-05	3.68E-05	-4.35E-05	-6.26E-05	-3.66E-05	-5.71E-05
Just before diagonal cracking	Bot	-7.18E-05	-7.27E-06	-8.99E-05	6.44E-05	6.07E-05	2.45E-05	4.62E-05	1.08E-05
	Mid	3.72E-05	-3.87E-06	8.25E-05	3.72E-05	9.48E-05	-4.06E-05	-1.34E-04	-1.84E-05
	Top	-8.03E-06	3.53E-05	2.09E-05	7.30E-05	2.13E-05	1.13E-04	2.05E-04	-2.73E-05
At peak load	Bot	3.56E-03	4.61E-03	4.15E-03	2.83E-03	3.70E-03	1.06E-03	5.96E-04	4.98E-04
	Mid	8.59E-04	1.93E-03	2.54E-03	3.39E-03	3.51E-03	3.39E-03	2.26E-03	6.38E-04
	Top	3.37E-04	3.11E-04	2.22E-03	1.91E-03	1.93E-03	3.05E-03	3.44E-03	2.25E-03

Table C-4: Selected concrete surface strain data for the dead end span of Tx70-II from the Optotrak vision system

Distance From End Face		4 ft	5 ft	6 ft	7 ft	8 ft	9 ft	10 ft	11 ft
Strain at R = 5 kips	Bot	-1.14E-05	-2.81E-05	-1.91E-05	-2.75E-05	-5.56E-05	-4.46E-05	-2.45E-05	-3.31E-05
	Mid	-5.42E-05	-4.42E-05	-3.64E-05	-2.83E-05	-3.12E-05	-2.49E-05	-3.38E-05	-4.73E-05
	Top	-2.29E-05	-2.82E-05	-3.52E-05	-4.60E-05	-3.78E-05	-3.72E-05	-4.55E-05	-4.83E-05
Strain Before Cracking	Bot	5.88E-05	1.02E-04	-3.68E-05	-3.90E-06	-5.73E-05	2.14E-05	7.02E-05	9.48E-05
	Mid	5.77E-05	3.28E-05	1.12E-04	5.48E-05	1.24E-04	8.74E-05	-1.17E-05	-1.24E-04
	Top	-3.72E-05	-2.65E-05	9.18E-06	1.22E-05	1.20E-04	1.86E-04	1.22E-04	3.05E-05
Strain at peak	Bot	3.06E-03	3.35E-03	4.62E-03	4.13E-03	2.17E-03	1.96E-03	1.01E-03	1.65E-04
	Mid	1.01E-03	1.76E-03	1.70E-03	2.83E-03	5.16E-03	2.47E-03	1.57E-03	8.69E-04
	Top	7.74E-06	4.50E-04	1.25E-03	1.60E-03	1.91E-03	4.99E-03	4.28E-03	2.18E-03

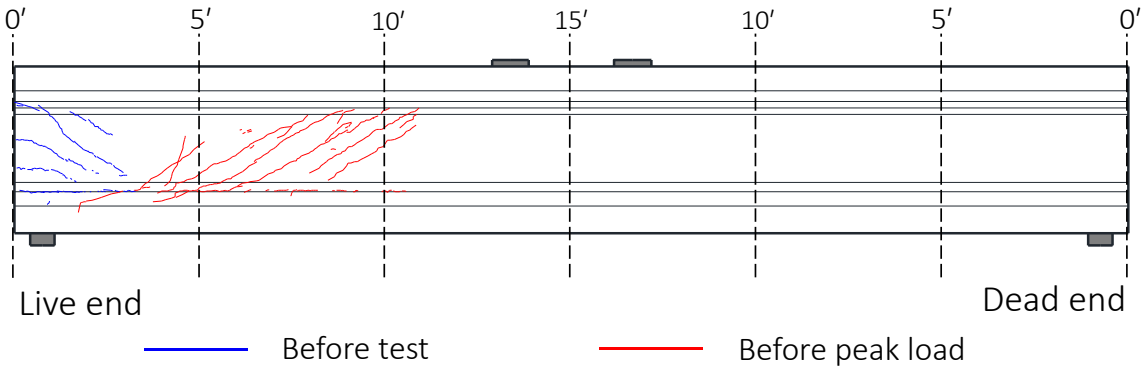

Figure C-45: Cracking pattern immediately prior to failure on northwest side of Tx46-I

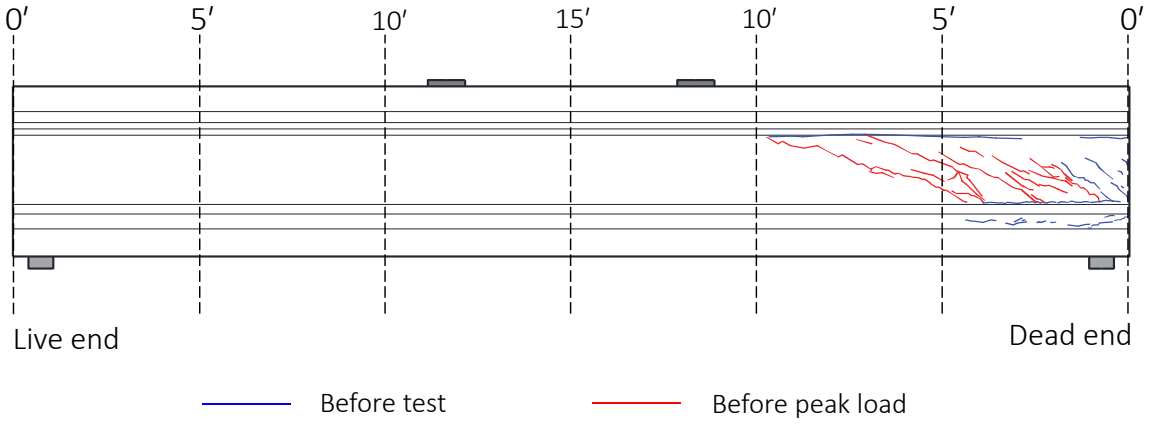

Figure C-46: Cracking pattern immediately prior to failure on southwest side of Tx46-II

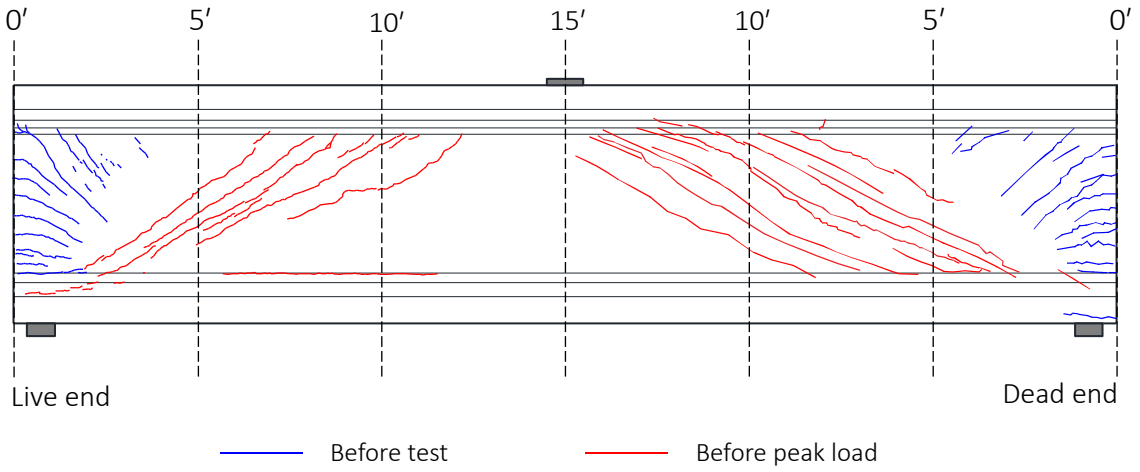

Figure C-47: Cracking pattern immediately prior to failure on west side of Tx70-I

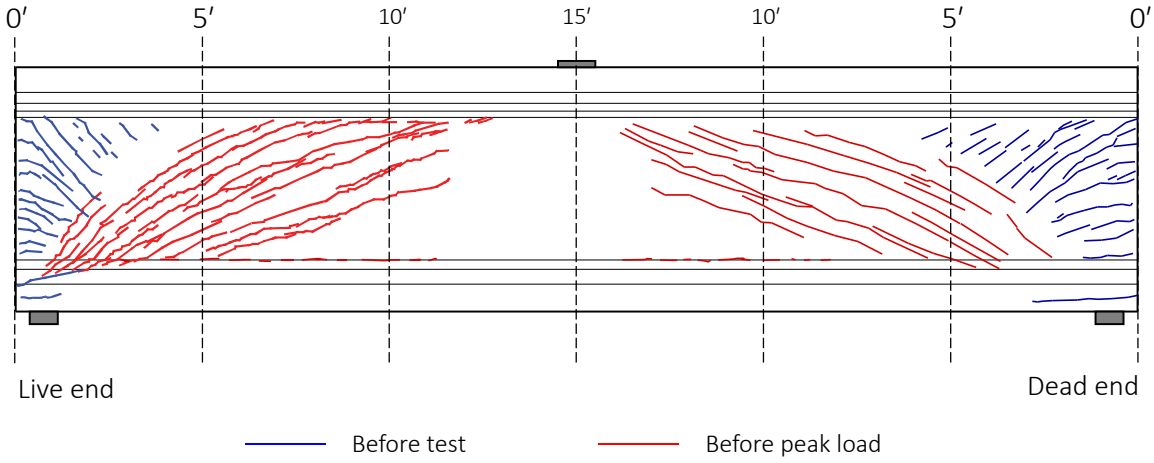

Figure C-48: Cracking pattern immediately prior to failure on west side of Tx70-II

Appendix D: Analysis Details

Appendix D contains a reproduced version of the calculations originally produced in MATHCAD to calculate the specimen shear capacities.

Figure D-1: Tx46-I Nominal Shear Capacity

Per AASHTO 5.8.4.3

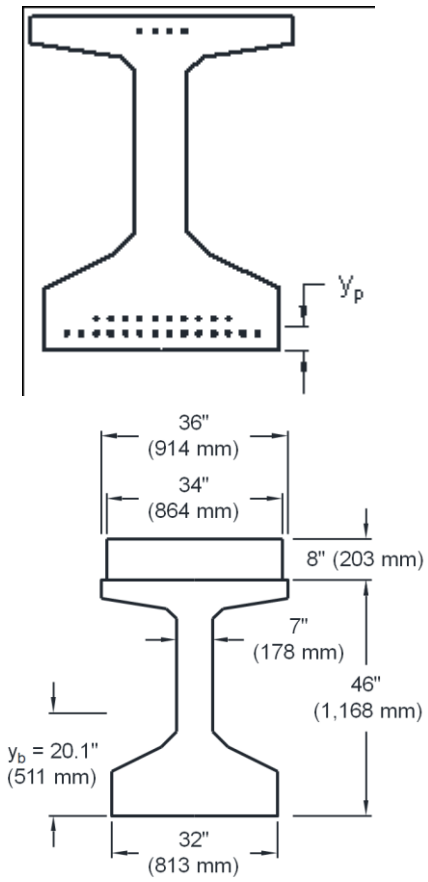

Input Parameters:

Specimen Geometry:

Beam Geometry:

$h_{beam} := 46in$

$b_f := 36in$

$b_w := 7in$

$y_b := 20.1in$

$A_g := 761in^2$

$L := 30ft$

Deck Geometry:

$t_{deck} := 8in$

$b_{deck} := 34in$

$h_{deck} := 8in$

Specimen Self Weight:

$SW := 34.830965kip$

$w_{sw} := \frac{SW}{L} = 0.09675\frac{kip}{in}$

Measured Material Properties:

Beam Concrete:

$f'_c := 7.6ksi$

$E_c := 4915ksi$

Deck Concrete:

$f'_{cdeck} := 10.71ksi$

$E_{cdeck} := 6926ksi$

Transformed Specimen Geometry:

$h_{tot} := h_{beam} + h_{deck} = 54 \cdot in$

Area of concrete on the flexural tension side of the member:

$$A_{ct} := 16.5in \cdot 32in - (4.75in \cdot 9.5in) - (2 \cdot 3in \cdot 9.5in) - 9in^2 + \left(\frac{h_{tot}}{2} - 16.5in\right) \cdot 7in = 490.$$

Compression Rebar:

$f_{ypbars} := 71.8ksi$

$f_{ytbars} := 60.7ksi$

$A_{tbar} := 0.2in^2$

$A_{pbar} := 0.44in^2$

Tension Rebar:

$A_s := 0in^2$

$E_s := 29000ksi$

Prestressing Strands:

$f_{pu} := 270ksi$

$f_{py} := 0.9 \cdot f_{pu} = 243 \cdot ksi$

$f_{pobot} := 202.5ksi$

$E_p := 29000ksi$

$A_{strand} := 0.294in^2$

$N_{botstrands} := 24$

$N_{topstrands} := 4$

$A_{pbot} := A_{strand} \cdot N_{botstrands} = 7.056in^2$

$A_{ptop} := A_{strand} \cdot N_{topstrands} = 1.176in^2$

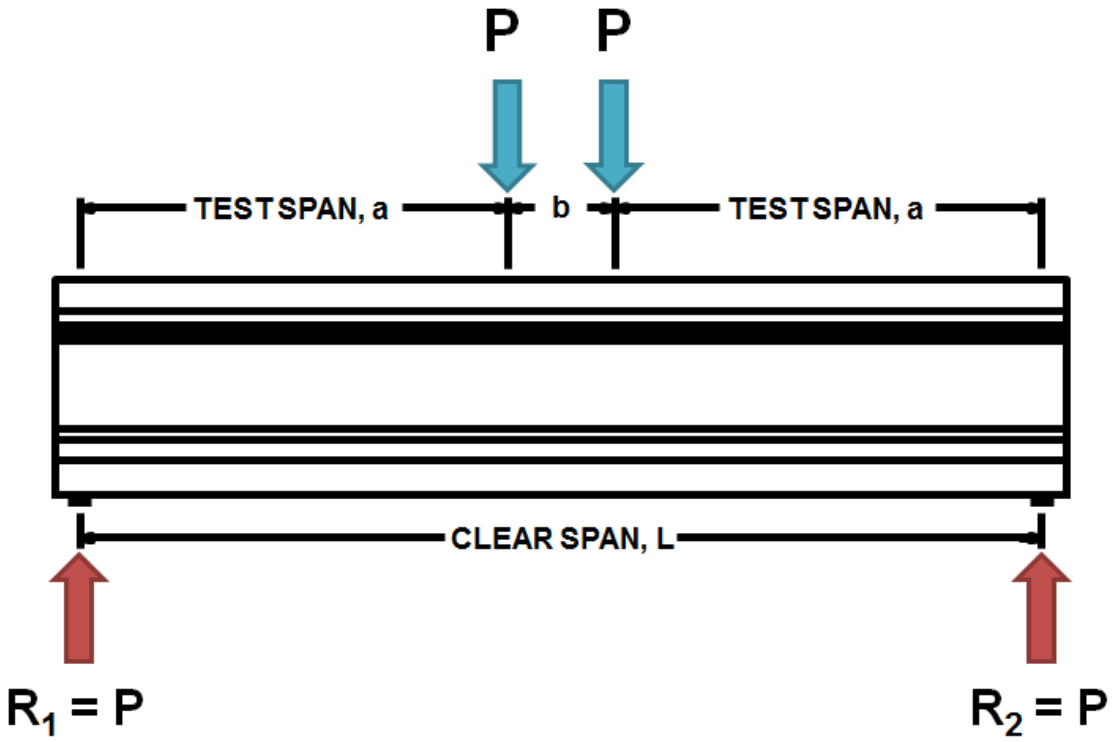

Shear Test Setup:

$L_{span} := 342in$

$a := 151.125in$ <- Measured as built

$P_{trial} := 515kip$ <- Initial guess for subsequent calcs

$d_v := 45.603in$ <- Calculated by layered sectional analysis

$L_{bearing} := 8in$

$L_{loadplate} := 12in$

$x_{crit} := a - \frac{L_{loadplate}}{2} - d_v = 99.522in$ <- Location of critical section for shear taken from left support

Solve for Nominal Shear Capacity:

Given <- Solve block for P_trial

Shear at critical section due to applied loads:

$$V_{crit}(P_{trial}) := P_{trial}$$

Shear at critical section due to self- weight:

$$V_{sw} := \left(\frac{w_{sw} \cdot L_{span}}{2}\right) - w_{sw} \cdot x_{crit} = 6.916\,kip$$

Total shear at critical section:

$$V_u(P_{trial}) := V_{crit}(P_{trial}) + V_{sw}$$

Shear due to vertical component of prestressing force:

$$V_p := 0ksi$$

Moment at critical section due to applied loads:

$$M_{crit}(P_{trial}) := P_{trial} \cdot x_{crit}$$

Moment at critical section due to self- weight:

$$M_{sw} := \frac{w_{sw} \cdot L_{span}}{2} \cdot x_{crit} - \frac{w_{sw} \cdot x_{crit}^{2}}{2} = 1167.413\,kip \cdot in$$

Total moment at critical section:

$$M_{u1}(P_{trial}) := \left|M_{crit}(P_{trial}) + M_{sw}\right|$$

Apply limit to Mu:

$$M_u(P_{trial}) := \begin{cases} M_{u1}(P_{trial}) & \text{if } M_{u1}(P_{trial}) \geq \left|V_u(P_{trial}) - V_p\right| \cdot d_v \\ \left(\left|V_u(P_{trial}) - V_p\right| \cdot d_v\right) & \text{otherwise} \end{cases}$$

Longitudinal Strain:

$$N_u := 0kip$$

$$\varepsilon_{s1}(P_{trial}) := \frac{\left(\frac{\left|M_u(P_{trial})\right|}{d_v} + 0.5N_u + \left|V_u(P_{trial}) - V_p\right| - A_{pbot} \cdot f_{pobot}\right)}{\left(E_s \cdot A_s + E_p \cdot A_{pbot}\right)}$$

$$\varepsilon_{salt}(P_{trial}) := \frac{\left(\frac{\left|M_u(P_{trial})\right|}{d_v} + 0.5N_u + \left|V_u(P_{trial}) - V_p\right| - A_{pbot} \cdot f_{pobot}\right)}{\left(E_s \cdot A_s + E_p \cdot A_{pbot} + E_c \cdot A_{ct}\right)}$$

Apply limits to ε_s:

$$\varepsilon_{s2}(P_{trial}) := \begin{cases} \varepsilon_{s1}(P_{trial}) & \text{if } \varepsilon_{s1}(P_{trial}) \geq 0 \\ \varepsilon_{salt}(P_{trial}) & \text{otherwise} \end{cases}$$

$$\varepsilon_s(P_{trial}) := \begin{cases} -0.0004 \text{ if } \varepsilon_{s2}(P_{trial}) \leq -0.0004 \\ \varepsilon_{s2}(P_{trial}) & \text{if } -0.0004 \leq \varepsilon_{s2}(P_{trial}) \leq 0.00(\\ 0.006 \text{ otherwise} \end{cases}$$

Check for min shear reinforcement:

$$s_v(x_{crit}) := \begin{cases} 3in & \text{if } x_{crit} \leq 36in \\ 6in & \text{otherwise} \end{cases}$$

$$\rho_v := \frac{2A_{tbar} \cdot 100}{s_v(x_{crit}) \cdot b_w} = 0.952 \qquad \rho_{vmin} := 0.0316 \frac{100\sqrt{\left(\frac{f'_c}{ksi}\right)}}{\frac{f_{ytbars}}{ksi}} = 0.144$$

Therefore, minimum shear reinforcement exists, and the size effect is not included

$$\beta(P_{trial}) := \frac{4.8}{(1 + 750 \cdot \varepsilon_s(P_{trial}))} \qquad \beta(P_{trial}) = 2.541$$

$$\theta(P_{trial}) := 29 + 3500\varepsilon_s(P_{trial}) \qquad \theta(P_{trial}) = 33.149$$

Concrete contribution to shear capacity:

$$V_c(P_{trial}) := 0.0316\beta(P_{trial}) \cdot \sqrt{\frac{f'_c}{ksi}} \cdot b_w \cdot d_v \cdot ksi \qquad V_c(P_{trial}) = 70.658 kip$$

Reinforcement contribution to shear capacity:

$$V_s(P_{trial}) := \frac{2 \cdot A_{tbar} \cdot f_{ytbars} \cdot d_v \cdot \left(\cot\left(\theta(P_{trial}) \cdot \frac{\pi}{180}\right)\right)}{s_v(x_{crit})} \qquad V_s(P_{trial}) = 282.552 kip$$

Nominal shear capacity:

$$V_{n1}(P_{trial}) := V_c(P_{trial}) + V_s(P_{trial}) + V_p$$

Apply limit to nominal shear capacity:

$$V_{n2} := 0.25 \cdot f'_c \cdot b_w \cdot d_v = 606.52 kip$$

*Values not converged

$$V_n(P_{trial}) := \begin{cases} V_{n1}(P_{trial}) & \text{if } V_{n1}(P_{trial}) < V_{n2} \\ V_{n2} & \text{otherwise} \end{cases} \qquad V_n(P_{trial}) = 353.209 kip$$

$V_a(P_{trial}) := P_{trial} + V_{sw}$

$V_n(P_{trial}) = V_a(P_{trial})$

$P_{trial} := \text{Minerr}(P_{trial})$ <- Solve for P_trial

$P_{trial} = 445.275\,\text{kip}$ $\text{ERR} = 2.328 \times 10^{-10}$

$\boxed{V_n(P_{trial}) = 452.191\,\text{kip}}$ <- Converged Vn

Figure D-2: Tx46-II Nominal Shear Capacity

Per AASHTO 5.8.4.3

Input Parameters:

Specimen Geometry:

Beam Geometry:

$h_{beam} := 46in$

$b_f := 36in$

$b_w := 7in$

$y_b := 20.1in$

$A_g := 761in^2$

$L := 30ft$

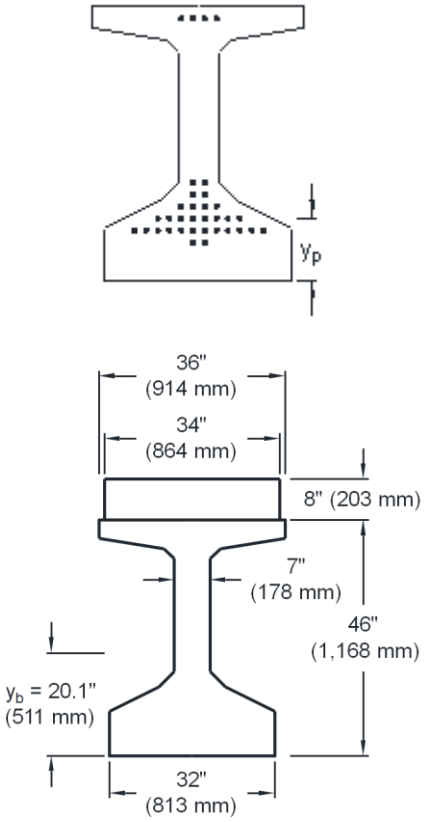

Deck Geometry:

$t_{deck} := 8in$

$b_{deck} := 34in$

$h_{deck} := 8in$

Specimen Self Weight:

$SW := 34.542853kip$ <- Measured

$w_{sw} := \frac{SW}{L} = 0.09595\frac{kip}{in}$

Measured Material Properties:

Beam Concrete:

$f'_c := 6.92ksi$

$E_c := 5424ksi$

Deck Concrete:

$f'_{cdeck} := 7.93ksi$

$E_{cdeck} := 5013ksi$

Transformed Specimen Geometry:

$h_{tot} := h_{beam} + h_{deck} = 54 \cdot in$

Area of concrete on the flexural tension side of the member:

$$A_{ct} := 16.5in \cdot 32in - (4.75in \cdot 9.5in) - (2 \cdot 3in \cdot 9.5in) - 9in^2 + \left(\frac{h_{tot}}{2} - 16.5in \right) \cdot 7in = 490.375in^2$$

Compression Rebar:

$f_{ypbars} := 71.8ksi$

$f_{ytbars} := 60.7ksi$

$A_{tbar} := 0.2in^2$

$A_{pbar} := 0.44in^2$

Tension Rebar:

$A_s := 0in^2$

$E_s := 29000ksi$

Prestressing Strands:

$f_{pu} := 270ksi$

$f_{py} := 0.9 \cdot f_{pu} = 243 \cdot ksi$

$f_{pobot} := 202.5ksi$

$E_p := 29000ksi$

$A_{strand} := 0.294in^2$

$N_{botstrands} := 30$

$N_{topstrands} := 4$

$A_{pbot} := A_{strand} \cdot N_{botstrands} = 8.82in^2$

$A_{ptop} := A_{strand} \cdot N_{topstrands} = 1.176in^2$

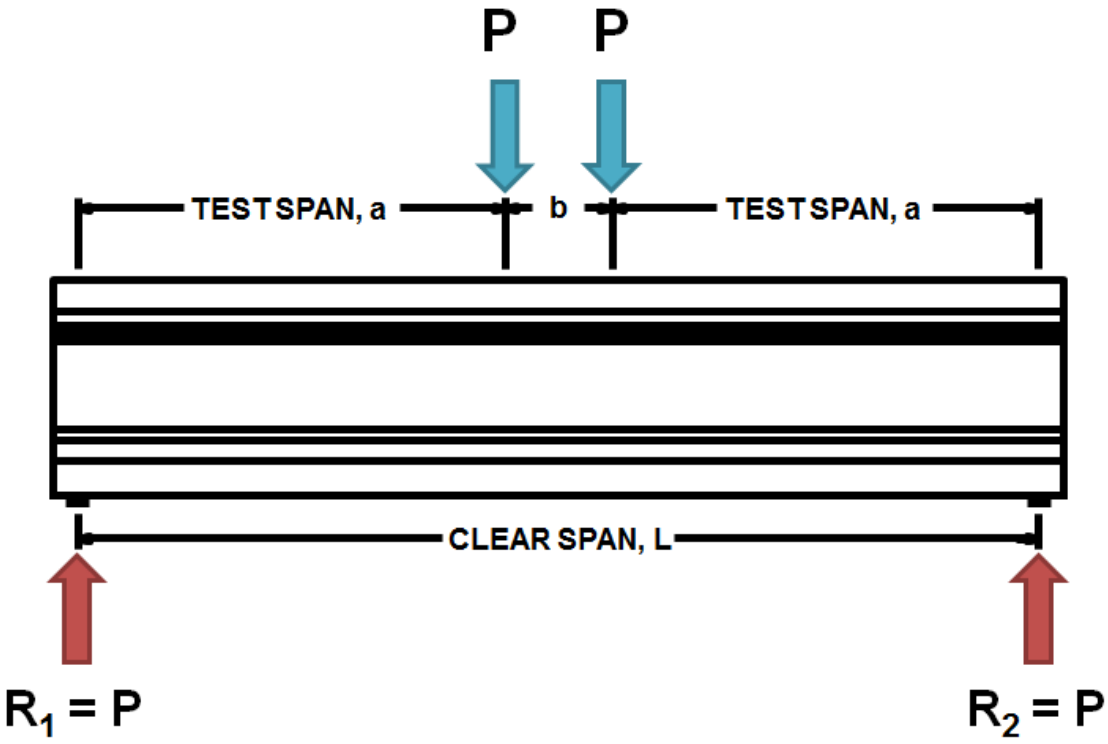

Shear Test Setup:

$L_{span} := 342in$

$a := 130.8in$ <- Measured as built

$P_{trial} := 450kip$ <- Initial guess for subsequent calcs

$d_v := 39.267in$ <- Calculated according to AASHTO 5.7.3.1

$L_{bearing} := 8in$

$L_{loadplate} := 12in$

$x_{crit} := a - \frac{L_{loadplate}}{2} - d_v = 85.533in$ <- Location of critical section for shear taken from left support

Solve for Nominal Shear Capacity:

Given <- Solve block for P_trial

Shear at critical section due to applied loads:

$V_{crit}(P_{trial}) := P_{trial}$

Shear at critical section due to self- weight:

$V_{sw} := \left(\frac{w_{sw} \cdot L_{span}}{2}\right) - w_{sw} \cdot x_{crit} = 8.201\,kip$

Total shear at critical section:

$V_u(P_{trial}) := V_{crit}(P_{trial}) + V_{sw}$

Shear due to vertical component of prestressing force:

$V_p := 0ksi$

Moment at critical section due to applied loads:

$M_{crit}(P_{trial}) := P_{trial} \cdot x_{crit}$

Moment at critical section due to self -weight:

$M_{sw} := \frac{w_{sw} \cdot L_{span}}{2} \cdot x_{crit} - \frac{w_{sw} \cdot x_{crit}^2}{2} = 1.052 \times 10^3 \cdot kip \cdot in$

Total moment at critical section:

$M_{u1}(P_{trial}) := \left|M_{crit}(P_{trial}) + M_{sw}\right|$

Apply limit to Mu:

$$M_u(P_{trial}) := \begin{cases} M_{u1}(P_{trial}) & \text{if } M_{u1}(P_{trial}) \geq \left|V_u(P_{trial}) - V_p\right| \cdot d_v \\ \left(\left|V_u(P_{trial}) - V_p\right| \cdot d_v\right) & \text{otherwise} \end{cases}$$

Longitudinal Strain:

$N_u := 0kip$

$$\varepsilon_{s1}(P_{trial}) := \frac{\left(\frac{\left|M_u(P_{trial})\right|}{d_v} + 0.5N_u + \left|V_u(P_{trial}) - V_p\right| - A_{pbot} \cdot f_{pobot}\right)}{\left(E_s \cdot A_s + E_p \cdot A_{pbot}\right)}$$

$$\varepsilon_{salt}(P_{trial}) := \frac{\left(\frac{\left|M_u(P_{trial})\right|}{d_v} + 0.5N_u + \left|V_u(P_{trial}) - V_p\right| - A_{pbot} \cdot f_{pobot}\right)}{\left(E_s \cdot A_s + E_p \cdot A_{pbot} + E_c \cdot A_{ct}\right)}$$

Apply limits to ε _s:

$$\varepsilon_{s2}(P_{trial}) := \begin{cases} \varepsilon_{s1}(P_{trial}) & \text{if } \varepsilon_{s1}(P_{trial}) \geq 0 \\ \varepsilon_{salt}(P_{trial}) & \text{otherwise} \end{cases}$$

$$\varepsilon_s(P_{trial}) := \begin{cases} -0.0004 \text{ if } \varepsilon_{s2}(P_{trial}) \leq -0.0004 \\ \varepsilon_{s2}(P_{trial}) \text{ if } -0.0004 \leq \varepsilon_{s2}(P_{trial}) \leq 0.00(\\ 0.006 \text{ otherwise} \end{cases}$$

Check for min shear reinforcement:

$$s_v(x_{crit}) := \begin{cases} 3in & \text{if } x_{crit} \leq 36in \\ 6in & \text{otherwise} \end{cases}$$

$$\rho_v := \frac{2A_{tbar} \cdot 100}{s_v(x_{crit}) \cdot b_w} = 0.952 \qquad \rho_{vmin} := 0.0316 \frac{100\sqrt{\left(\frac{f'_c}{ksi}\right)}}{\frac{f_{ytbars}}{ksi}} = 0.137$$

Therefore, minimum shear reinforcement exists, and the size effect is not included

$$\beta(P_{trial}) := \frac{4.8}{\left(1 + 750 \cdot \varepsilon_s(P_{trial})\right)} \qquad \beta(P_{trial}) = 5.232$$

$$\theta(P_{trial}) := 29 + 3500\varepsilon_s(P_{trial}) \qquad \theta(P_{trial}) = 28.615$$

Concrete contribution to shear capacity:

$$V_c(P_{trial}) := 0.0316\beta(P_{trial}) \cdot \sqrt{\frac{f'_c}{ksi}} \cdot b_w \cdot d_v \cdot ksi \qquad V_c(P_{trial}) = 119.541kip$$

Reinforcement contribution to shear capacity:

$$V_s(P_{trial}) := \frac{2 \cdot A_{tbar} \cdot f_{ytbars} \cdot d_v \cdot \left(\cot\left(\theta(P_{trial}) \cdot \frac{\pi}{180}\right)\right)}{s_v(x_{crit})} \qquad V_s(P_{trial}) = 291.264kip$$

Nominal shear capacity:

$$V_{n1}(P_{trial}) := V_c(P_{trial}) + V_s(P_{trial}) + V_p \qquad V_{n1}(P_{trial}) = 410.805kip$$

Apply limit to nominal shear capacity:

$$V_{n2} := 0.25 \cdot f'_c \cdot b_w \cdot d_v = 475.523kip$$

$$V_n(P_{trial}) := \begin{cases} V_{n1}(P_{trial}) & \text{if } V_{n1}(P_{trial}) < V_{n2} \\ V_{n2} & \text{otherwise} \end{cases} \qquad V_n(P_{trial}) = 410.805kip$$

*Values not converged

$V_a(P_{trial}) := P_{trial} + V_{sw}$

$V_n(P_{trial}) = V_a(P_{trial})$

$P_{trial} := \text{Minerr}(P_{trial})$ <- Solve for P_trial

$P_{trial} = 409.033\text{kip}$ ERR = 0

$V_n(P_{trial}) = 417.234\text{kip}$ <- Converged Vn, governed by upper limit of V_n for web crushing

Figure D-3: Tx70-I Nominal Shear Capacity

Per AASHTO 5.8.4.3

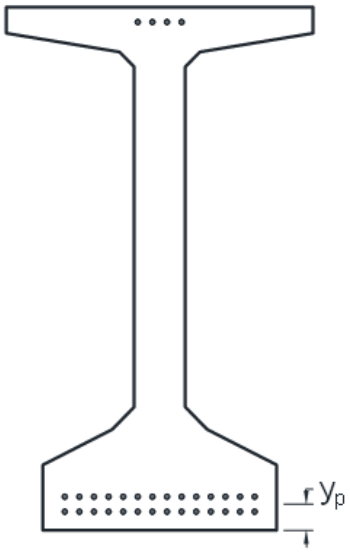

Input Parameters:

Specimen Geometry:

Beam Geometry:

$h_{beam} := 70in$

$b_f := 42in$

$b_w := 7in$

$y_b := 31.91in$

$A_g := 966in^2$

$L := 30ft$

Deck Geometry:

$b_{deck} := 40in$

$h_{deck} := 8in$

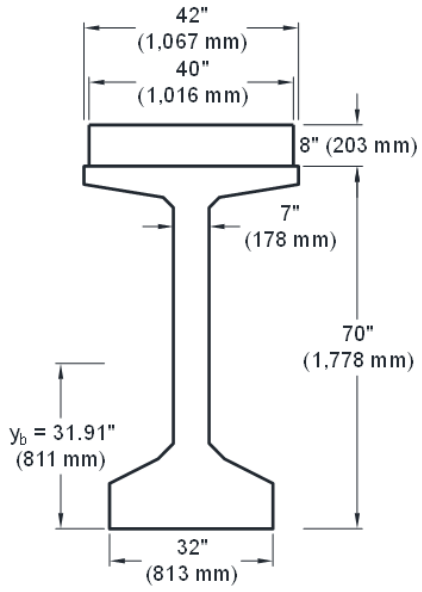

Specimen Self Weight:

$SW := 41.145608kip$ <- Measured

$w_{sw} := \frac{SW}{L} = 0.11429\frac{kip}{in}$

Measured Material Properties:

Beam Concrete:

$f'_c := 10.71ksi$

$E_c := 6096ksi$

Deck Concrete:

$f'_{cdeck} := 7.94ksi$

$E_{cdeck} := 5966ksi$

Transformed Specimen Geometry:

$h_{tot} := h_{beam} + h_{deck} = 78 \cdot in$

Area of concrete on the flexural tension side of the member:

$$A_{ct} := 16.5in \cdot 32in - (4.75in \cdot 9.5in) - (2 \cdot 3in \cdot 9.5in) - 9in^2 + \left(\frac{h_{tot}}{2} - 16.5in\right) \cdot 7in = 574.375in^2$$

Compression Rebar:

$f_{ypbars} := 69.57ksi$

$f_{ytbars} := 72.17ksi$

$A_{tbar} := 0.2in^2$

$A_{pbar} := 0.44in^2$

Tension Rebar:

$A_s := 0in^2$

$E_s := 29000ksi$

Prestressing Strands:

$f_{pu} := 270ksi$

$f_{py} := 0.9 \cdot f_{pu} = 243 \cdot ksi$

$f_{pobot} := 202.5ksi$

$E_p := 29000ksi$

$A_{strand} := 0.294in^2$

$N_{botstrands} := 28$

$N_{topstrands} := 4$

$A_{pbot} := A_{strand} \cdot N_{botstrands} = 8.232in^2$

$A_{ptop} := A_{strand} \cdot N_{topstrands} = 1.176in^2$

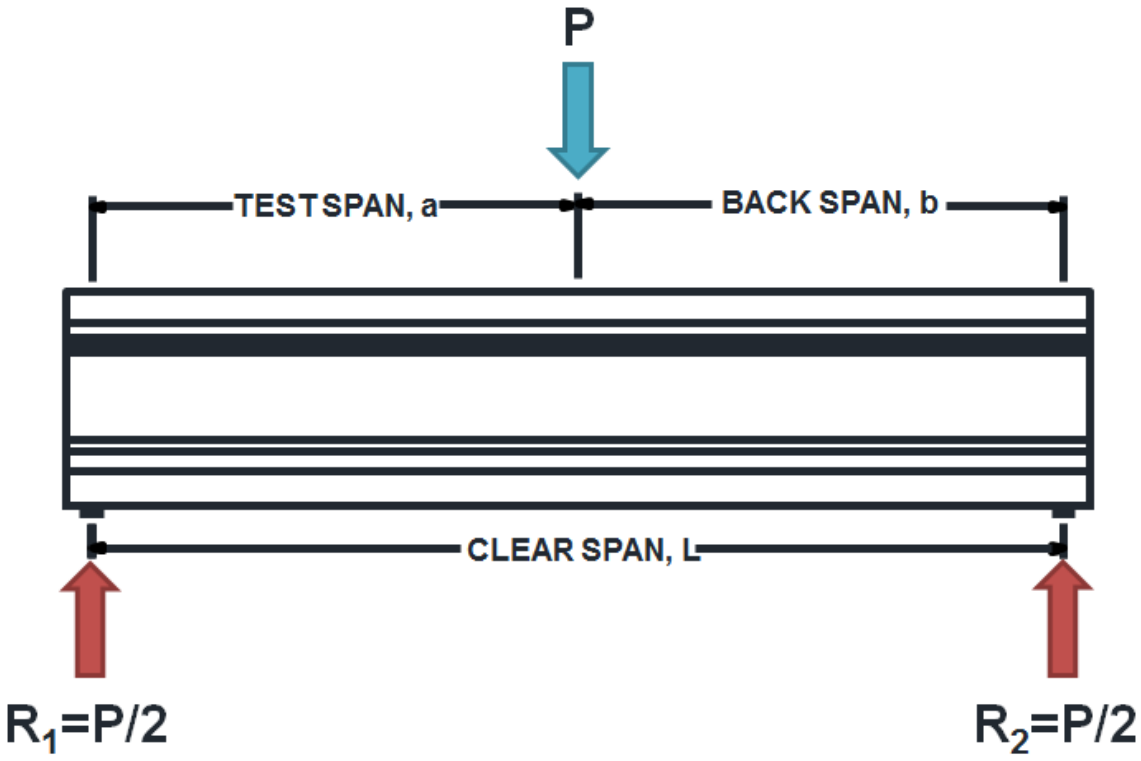

Shear Test Setup:

$L_{span} := 342in$

$a := 171.25in$ <- Measured as built

$P_{trial} := 1500kip$ <- Initial guess for subsequent calcs

$d_v := 67.10366in$ <- Calculated according to AASHTO 5.7.3.1

$L_{bearing} := 9in$

$L_{loadplate} := 12in$

$x_{crit} := a - \frac{L_{loadplate}}{2} - d_v = 98.146in$ <- Location of critical section for shear taken from left support

Solve for Nominal Shear Capacity:

Given <- Solve block for P_trial

Shear at critical section due to applied loads:

$$V_{crit}(P_{trial}) := \frac{P_{trial}}{2}$$

Shear at critical section due to self- weight:

$$V_{sw} := \left(\frac{w_{sw} \cdot L_{span}}{2}\right) - w_{sw} \cdot x_{crit} = 8.327\,kip$$

Total shear at critical section:

$$V_u(P_{trial}) := V_{crit}(P_{trial}) + V_{sw}$$

Shear due to vertical component of prestressing force:

$$V_p := 0ksi$$

Moment at critical section due to applied loads:

$$M_{crit}(P_{trial}) := \frac{P_{trial}}{2} \cdot x_{crit}$$

Moment at critical section due to self- weight:

$$M_{sw} := \frac{w_{sw} \cdot L_{span}}{2} \cdot x_{crit} - \frac{w_{sw} \cdot x_{crit}^{2}}{2} = 1367.711\,kip \cdot in$$

Total moment at critical section:

$$M_{u1}(P_{trial}) := \left|M_{crit}(P_{trial}) + M_{sw}\right|$$

Apply limit to Mu:

$$M_u(P_{trial}) := \begin{cases} M_{u1}(P_{trial}) & \text{if } M_{u1}(P_{trial}) \geq \left|V_u(P_{trial}) - V_p\right| \cdot d_v \\ \left(\left|V_u(P_{trial}) - V_p\right| \cdot d_v\right) & \text{otherwise} \end{cases}$$

Longitudinal Strain:

$$N_u := 0kip$$

$$\varepsilon_{s1}(P_{trial}) := \frac{\left(\frac{\left|M_u(P_{trial})\right|}{d_v} + 0.5N_u + \left|V_u(P_{trial}) - V_p\right| - A_{pbot} \cdot f_{pobot}\right)}{\left(E_s \cdot A_s + E_p \cdot A_{pbot}\right)}$$

$$\varepsilon_{salt}(P_{trial}) := \frac{\left(\frac{\left|M_u(P_{trial})\right|}{d_v} + 0.5N_u + \left|V_u(P_{trial}) - V_p\right| - A_{pbot} \cdot f_{pobot}\right)}{\left(E_s \cdot A_s + E_p \cdot A_{pbot} + E_c \cdot A_{ct}\right)}$$

Apply limits to ε _s:

$$\varepsilon_{s2}(P_{trial}) := \begin{cases} \varepsilon_{s1}(P_{trial}) & \text{if } \varepsilon_{s1}(P_{trial}) \geq 0 \\ \varepsilon_{salt}(P_{trial}) & \text{otherwise} \end{cases}$$

$$\varepsilon_s(P_{trial}) := \begin{cases} -0.0004 \text{ if } \varepsilon_{s2}(P_{trial}) \leq -0.0004 \\ \varepsilon_{s2}(P_{trial}) \text{ if } -0.0004 \leq \varepsilon_{s2}(P_{trial}) \leq 0.00(\\ 0.006 \text{ otherwise} \end{cases}$$

Check for min shear reinforcement:

$$s_v(x_{crit}) := \begin{cases} 3in & \text{if } x_{crit} \leq 36in \\ 8in & \text{otherwise} \end{cases}$$

$$\rho_v := \frac{2A_{tbar} \cdot 100}{s_v(x_{crit}) \cdot b_w} = 0.714 \qquad \rho_{vmin} := 0.0316 \frac{100\sqrt{\left(\frac{f'_c}{ksi}\right)}}{\frac{f_{ytbars}}{ksi}} = 0.143$$

Therefore, minimum shear reinforcement exists, and the size effect is not included

$$\beta(P_{trial}) := \frac{4.8}{(1 + 750 \cdot \varepsilon_s(P_{trial}))} \qquad \beta(P_{trial}) = 2.899$$

$$\theta(P_{trial}) := 29 + 3500\varepsilon_s(P_{trial}) \qquad \theta(P_{trial}) = 32.06$$

Concrete contribution to shear capacity:

$$V_c(P_{trial}) := 0.0316\beta(P_{trial}) \cdot \sqrt{\frac{f'_c}{ksi}} \cdot b_w \cdot d_v \cdot ksi \qquad V_c(P_{trial}) = 140.834kip$$

Reinforcement contribution to shear capacity:

$$V_s(P_{trial}) := \frac{2 \cdot A_{tbar} \cdot f_{ytbars} \cdot d_v \cdot \left(\cot\left(\theta(P_{trial}) \cdot \frac{\pi}{180}\right)\right)}{s_v(x_{crit})} \qquad V_s(P_{trial}) = 386.616kip$$

Nominal shear capacity:

$$V_{n1}(P_{trial}) := V_c(P_{trial}) + V_s(P_{trial}) + V_p \qquad V_{n1}(P_{trial}) = 527.45kip$$

Apply limit to nominal shear capacity:

$$V_{n2} := 0.25 \cdot f'_c \cdot b_w \cdot d_v = 1257.69kip$$

$$V_n(P_{trial}) := \begin{cases} V_{n1}(P_{trial}) & \text{if } V_{n1}(P_{trial}) < V_{n2} \\ V_{n2} & \text{otherwise} \end{cases} \qquad V_n(P_{trial}) = 527.45kip$$

*Values not converged

$$V_a(P_{trial}) := \frac{P_{trial}}{2} + V_{sw}$$

$$V_n(P_{trial}) = V_a(P_{trial})$$

$$P_{trial} := \text{Minerr}(P_{trial})$$ <- Solve for P_trial

$$P_{trial} = 1324.328\text{kip}$$ ERR = 0

$$\boxed{V_n(P_{trial}) = 670.49078\text{kip}}$$ <- Converged Vn

Figure D-4: Tx70-II Nominal Shear Capacity

Per AASHTO 5.8.4.3

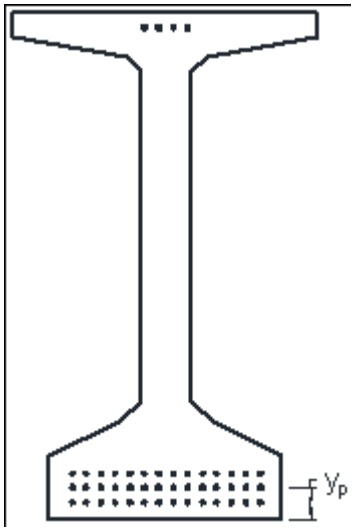

Input Parameters:

Specimen Geometry:

Beam Geometry:

$h_{beam} := 70in$

$b_f := 42in$

$b_w := 7in$

$y_b := 31.91in$

$A_g := 966in^2$

$L := 30ft$

Deck Geometry:

$b_{deck} := 40in$

$h_{deck} := 8in$

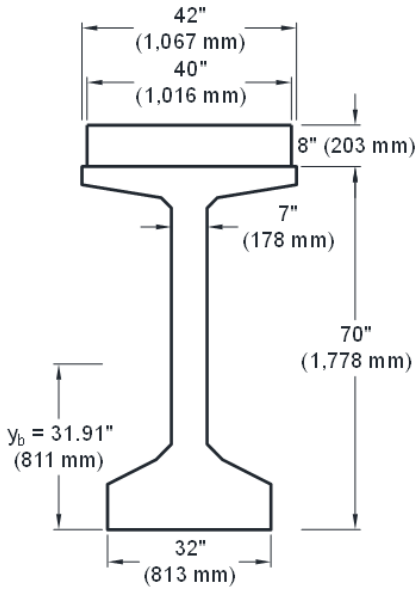

Specimen Self Weight:

$SW := 43.296826kip$ <- Measured

$w_{sw} := \frac{SW}{L} = 0.12027\frac{kip}{in}$

Measured Material Properties:

Beam Concrete:

$f'_c := 12.7ksi$

$E_c := 6015ksi$

Deck Concrete:

$f'_{cdeck} := 9.17ksi$

$E_{cdeck} := 5891ksi$

Transformed Specimen Geometry:

$h_{tot} := h_{beam} + h_{deck} = 78 \cdot in$

Area of concrete on the flexural tension side of the member:

$$A_{ct} := 16.5in \cdot 32in - (4.75in \cdot 9.5in) - (2 \cdot 3in \cdot 9.5in) - 9in^2 + \left(\frac{h_{tot}}{2} - 16.5in \right) \cdot 7in = 574.375in^2$$

Compression Rebar:

$f_{ypbars} := 69.57ksi$

$f_{ytbars} := 72.17ksi$

$A_{tbar} := 0.2in^2$

$A_{pbar} := 0.44in^2$

Tension Rebar:

$A_s := 0in^2$

$E_s := 29000ksi$

Prestressing Strands:

$f_{pu} := 270ksi$

$f_{py} := 0.9 \cdot f_{pu} = 243 \cdot ksi$

$f_{pobot} := 202.5ksi$

$E_p := 29000ksi$

$A_{strand} := 0.294in^2$

$N_{botstrands} := 42$

$N_{topstrands} := 4$

$A_{pbot} := A_{strand} \cdot N_{botstrands} = 12.348in^2$

$A_{ptop} := A_{strand} \cdot N_{topstrands} = 1.176in^2$

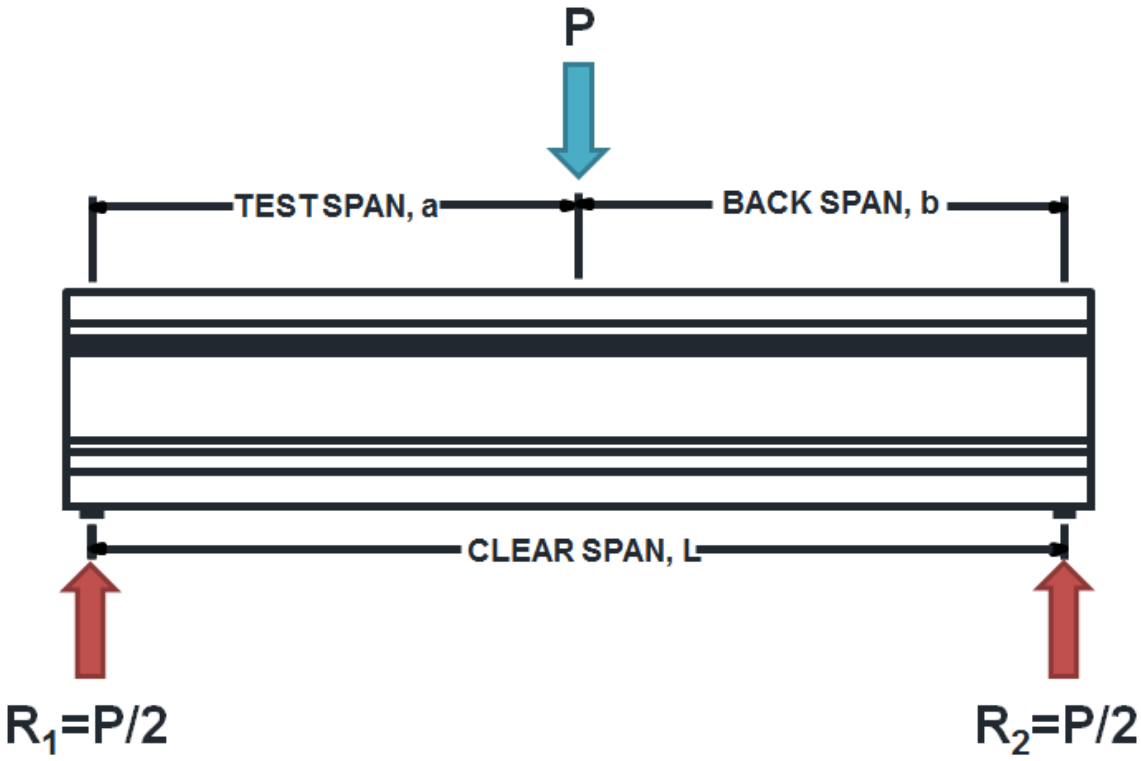

Shear Test Setup:

$L_{span} := 342in$

$a := 171in$ <- Measured as built

$P_{trial} := 1500kip$ <- Initial guess for subsequent calcs

$d_v := 66.15in$ <- Calculated according to AASHTO 5.7.3.1

$L_{bearing} := 9in$

$L_{loadplate} := 12in$

$x_{crit} := a - \frac{L_{loadplate}}{2} - d_v = 98.85in$ <- Location of critical section for shear taken from left support

Solve for Nominal Shear Capacity:

<- Solve block for P_trial

Shear at critical section due to applied loads:

$$V_{crit}(P_{trial}) := \frac{P_{trial}}{2}$$

Shear at critical section due to self -weight:

$$V_{sw} := \left(\frac{w_{sw} \cdot L_{span}}{2}\right) - w_{sw} \cdot x_{crit} = 8.677\,kip$$

Total shear at critical section:

$$V_u(P_{trial}) := V_{crit}(P_{trial}) + V_{sw}$$

Shear due to vertical component of prestressing force:

$$V_p := 0ksi$$

Moment at critical section due to applied loads:

$$M_{crit}(P_{trial}) := \frac{P_{trial}}{2} \cdot x_{crit}$$

Moment at critical section due to self -weight:

$$M_{sw} := \frac{w_{sw} \cdot L_{span}}{2} \cdot x_{crit} - \frac{w_{sw} \cdot x_{crit}^2}{2} = 1445.355\,kip \cdot in$$

Total moment at critical section:

$$M_{u1}(P_{trial}) := \left|M_{crit}(P_{trial}) + M_{sw}\right|$$

Apply limit to Mu:

$$M_u(P_{trial}) := \begin{cases} M_{u1}(P_{trial}) & \text{if } M_{u1}(P_{trial}) \geq \left|V_u(P_{trial}) - V_p\right| \cdot d_v \\ \left(\left|V_u(P_{trial}) - V_p\right| \cdot d_v\right) & \text{otherwise} \end{cases}$$

Longitudinal Strain:

$$N_u := 0kip$$

$$\varepsilon_{s1}(P_{trial}) := \frac{\left(\frac{\left|M_u(P_{trial})\right|}{d_v} + 0.5N_u + \left|V_u(P_{trial}) - V_p\right| - A_{pbot} \cdot f_{pobot}\right)}{\left(E_s \cdot A_s + E_p \cdot A_{pbot}\right)}$$

$$\varepsilon_{salt}(P_{trial}) := \frac{\left(\frac{\left|M_u(P_{trial})\right|}{d_v} + 0.5N_u + \left|V_u(P_{trial}) - V_p\right| - A_{pbot}\cdot f_{pobot}\right)}{\left(E_s\cdot A_s + E_p\cdot A_{pbot} + E_c\cdot A_{ct}\right)}$$

Apply limits to ε_s:

$$\varepsilon_{s2}(P_{trial}) := \begin{cases} \varepsilon_{s1}(P_{trial}) & \text{if } \varepsilon_{s1}(P_{trial}) \geq 0 \\ \varepsilon_{salt}(P_{trial}) & \text{otherwise} \end{cases}$$

$$\varepsilon_s(P_{trial}) := \begin{cases} -0.0004 \text{ if } \varepsilon_{s2}(P_{trial}) \leq -0.0004 \\ \varepsilon_{s2}(P_{trial}) & \text{if } -0.0004 \leq \varepsilon_{s2}(P_{trial}) \leq 0.00 \\ 0.006 \text{ otherwise} \end{cases}$$

Check for min shear reinforcement:

$$s_v(x_{crit}) := \begin{cases} 3in & \text{if } x_{crit} \leq 36in \\ 8in & \text{otherwise} \end{cases}$$

$$\rho_v := \frac{2A_{tbar}\cdot 100}{s_v(x_{crit})\cdot b_w} = 0.714 \qquad \rho_{vmin} := 0.0316\frac{\sqrt{\left(\frac{f'_c}{ksi}\right)}}{\frac{f_{ytbars}}{ksi}} = 0.156$$

Therefore, minimum shear reinforcement exists, and the size effect is not included

$$\beta(P_{trial}) := \frac{4.8}{\left(1 + 750\cdot\varepsilon_s(P_{trial})\right)} \qquad \beta(P_{trial}) = 5.441$$

$$\theta(P_{trial}) := 29 + 3500\,\varepsilon_s(P_{trial}) \qquad \theta(P_{trial}) = 28.45$$

Concrete contribution to shear capacity:

$$V_c(P_{trial}) := 0.0316\beta(P_{trial})\cdot\sqrt{\frac{f'_c}{ksi}}\cdot b_w\cdot d_v\cdot ksi \qquad V_c(P_{trial}) = 283.74kip$$

Reinforcement contribution to shear capacity:

$$V_s(P_{trial}) := \frac{2\cdot A_{tbar}\cdot f_{ytbars}\cdot d_v\cdot\left(\cot\left(\theta(P_{trial})\cdot\frac{\pi}{180}\right)\right)}{s_v(x_{crit})} \qquad V_s(P_{trial}) = 440.552kip$$

Nominal shear capacity:

$$V_{n1}(P_{trial}) := V_c(P_{trial}) + V_s(P_{trial}) + V_p \qquad V_{n1}(P_{trial}) = 724.292kip$$

Apply limit to nominal shear capacity:

$$V_{n2} := 0.25\cdot f'_c\cdot b_w\cdot d_v = 1470.184kip$$

$$V_n(P_{trial}) := \begin{cases} V_{n1}(P_{trial}) & \text{if } V_{n1}(P_{trial}) < V_{n2} \\ V_{n2} & \text{otherwise} \end{cases} \qquad V_n(P_{trial}) = 724.292kip$$

*Values not converged

$$V_a(P_{trial}) := \frac{P_{trial}}{2} + V_{sw}$$

$$V_n(P_{trial}) = V_a(P_{trial})$$

$P_{trial} := \text{Minerr}(P_{trial})$ <- Solve for P_trial

$P_{trial} = 1442.809\,\text{kip}$ ERR = 0

$\boxed{V_n(P_{trial}) = 730.08169\,\text{kip}}$ <- Converged Vn

Figure D-5: Tx46-I Anchorage Calculations

Per AASHTO 5.8.3.5

Input Parameters:

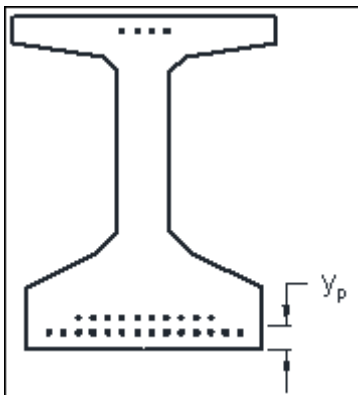

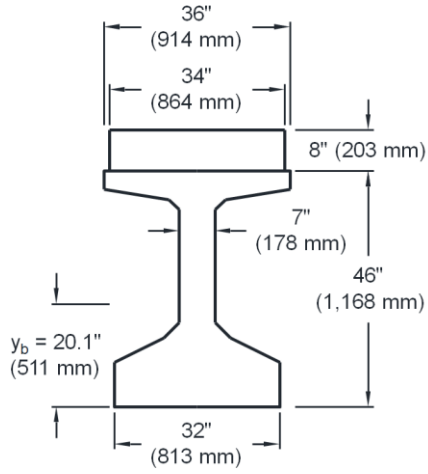

Specimen Geometry:

Beam Geometry:

$L := 30ft$

$h_{tot} := 54in$

Specimen Self Weight:

$SW := 34.830965kip$

$w_{sw} := \frac{SW}{L} = 0.09675\frac{kip}{in}$

Measured Material Properties:

Beam Concrete:

$E_c := 4915ksi$

Transformed Specimen Geometry:

$$A_{ct} := 16.5in \cdot 32in - (4.75in \cdot 9.5in) - (2 \cdot 3in \cdot 9.5in) - 9in^2 + \left(\frac{h_{tot}}{2} - 16.5in\right) \cdot 7in = 490.375in^2$$

Stirrup Rebar:

$f_y := 60.7ksi$

$A_{stirrup} := 0.2in^2 \cdot 2 = 0.4in^2$

Tensile Rebar:

$E_s := 29000ksi$

$A_s := 0in^2$

Test Setup Parameters:

$L_{span} := 28.5ft$

$d_v := 45.603in$

$L_{loadplate} := 12in$

$a := 151.125in$

$x_{crit} := a - \frac{L_{loadplate}}{2} - d_v = 99.522in$

$P_{trial} := 450kip$

Prestressing Strands:

$E_p := 29000\,ksi$ $\quad d_b := 0.7\,in$

$f_{ps} := 244\,ksi$ $\quad f_{pe} := 157.4286\,ksi$

$A_{0.7strand} := 0.294\,in^2$

$N_{botstrands} := 24$

$A_{pbot} := A_{0.7strand} \cdot N_{botstrands} = 7.056\,in^2$

$l_d := 1.6\left(\frac{f_{ps}}{ksi} - \frac{2}{3}\cdot\frac{f_{pe}}{ksi}\right) d_b = 155.733\,in$

$l_t := 60 \cdot d_b = 42 \cdot in$

$f_{pobot} := f_{pe} + \frac{\left(x_{crit} + 9in - l_t\right)}{l_d - l_t}\cdot\left(f_{ps} - f_{pe}\right) = 208.064\,ksi$

Resistance Factors:

$\varphi_f := 1.0$

$\varphi_c := 1.0$

$\varphi_v := 1.0$

Calculations:

Tensile Capacity:

$T_n := A_{pbot}\cdot f_{pobot} + A_s \cdot f_y = 1468.098\,kip$

Anchorage Capacity:

Given <- Solve block for V_n

Shear at critical section due to applied loads:

$V_{crit}\left(P_{trial}\right) := P_{trial}$

Shear at critical section due to self- weight:

$V_{sw} := \left(\frac{w_{sw}\cdot L_{span}}{2}\right) - w_{sw}\cdot x_{crit} = 6.916\,kip$

Total shear at critical section:

$V_u\left(P_{trial}\right) := V_{crit}\left(P_{trial}\right) + V_{sw}$

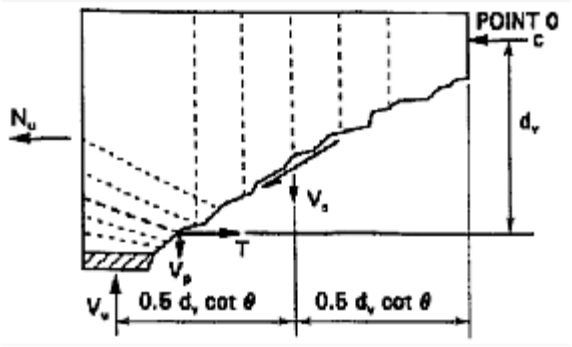

Shear due to vertical component of prestressing force:

$V_p := 0\,ksi$

Moment at critical section due to applied loads:

$$M_{crit}(P_{trial}) := P_{trial} \cdot x_{crit}$$

Moment at critical section due to self- weight:

$$M_{sw} := \frac{w_{sw} \cdot L_{span}}{2} \cdot x_{crit} - \frac{w_{sw} \cdot x_{crit}^{2}}{2} = 1.167 \times 10^{3} \cdot kip \cdot in$$

Total moment at critical section:

$$M_{u1}(P_{trial}) := \left| M_{crit}(P_{trial}) + M_{sw} \right|$$

Apply limit to Mu:

$$M_u(P_{trial}) := \begin{cases} M_{u1}(P_{trial}) & \text{if } M_{u1}(P_{trial}) \geq \left| V_u(P_{trial}) - V_p \right| \cdot d_v \\ \left(\left| V_u(P_{trial}) - V_p \right| \cdot d_v \right) & \text{otherwise} \end{cases}$$

Axial Force:

$$N_u := 0kip$$

Longitudinal Strain:

$$\varepsilon_{s1}(P_{trial}) := \frac{\left(\frac{\left| M_u(P_{trial}) \right|}{d_v} + 0.5 N_u + \left| V_u(P_{trial}) - V_p \right| - A_{pbot} \cdot f_{pobot} \right)}{\left(E_s \cdot A_s + E_p \cdot A_{pbot} \right)}$$

$$\varepsilon_{salt}(P_{trial}) := \frac{\left(\frac{\left| M_u(P_{trial}) \right|}{d_v} + 0.5 N_u + \left| V_u(P_{trial}) - V_p \right| - A_{pbot} \cdot f_{pobot} \right)}{\left(E_s \cdot A_s + E_p \cdot A_{pbot} + E_c \cdot A_{ct} \right)}$$

Apply limits to ε _s:

$$\varepsilon_{s2}(P_{trial}) := \begin{cases} \varepsilon_{s1}(P_{trial}) & \text{if } \varepsilon_{s1}(P_{trial}) \geq 0 \\ \varepsilon_{salt}(P_{trial}) & \text{otherwise} \end{cases}$$

$$\varepsilon_s(P_{trial}) := \begin{cases} -0.0004 \text{ if } \varepsilon_{s2}(P_{trial}) \leq -0.0004 \\ \varepsilon_{s2}(P_{trial}) & \text{if } -0.0004 \leq \varepsilon_{s2}(P_{trial}) \leq 0.00 \\ 0.006 \text{ otherwise} \end{cases}$$

Check for min shear reinforcement:

$$s_v(x_{crit}) := \begin{cases} 3in & \text{if } x_{crit} \leq 36in \\ 6in & \text{otherwise} \end{cases}$$

$$\theta(P_{trial}) := 29 + 3500 \varepsilon_s(P_{trial}) \qquad \theta(P_{trial}) = 28.995$$

Reinforcement contribution to shear capacity:

$$V_s(P_{trial}) := \frac{2 \cdot 0.2\text{in}^2 \cdot f_y \cdot d_v \cdot \left(\cot\left(\theta(P_{trial}) \cdot \frac{\pi}{180} \right) \right)}{s_v(x_{crit})} \qquad V_s(P_{trial}) = 332.984\text{kip}$$

Max Anchorage Demand:

$$T_{max}(P_{trial}) := \frac{\left| M_u(P_{trial}) \right|}{\varphi_f \cdot d_v} + 0.5 \frac{N_u}{\varphi_c} + \left(\left| \frac{V_u(P_{trial})}{\varphi_v} - V_p \right| - 0.5 V_s(P_{trial}) \right) \cdot \cot\left(\theta(P_{trial}) \cdot \frac{\pi}{180} \right)$$

$T_{max}(P_{trial}) = T_n$

$P_{anchorage} := \text{Minerr}(P_{trial}) = 433.909\text{kip}$

$V_{nanchorage}(P_{anchorage}) := V_u(P_{anchorage})$

$$V_{nanchorage}(P_{anchorage}) = 440.825\text{kip}$$

Figure D-6: Tx46-I Anchorage Calculations

Per AASHTO 5.8.3.5

Input Parameters:

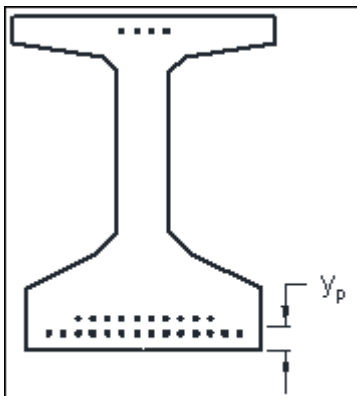

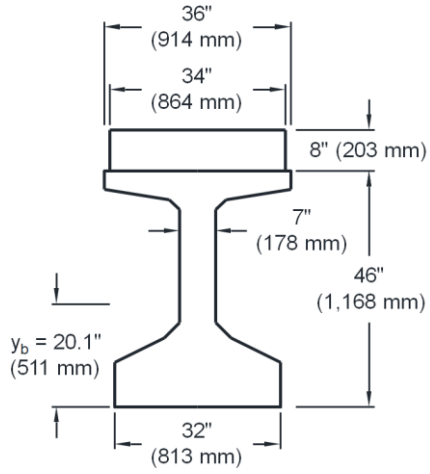

Specimen Geometry:

Beam Geometry:

$L := 30ft$

$h_{tot} := 54in$

Specimen Self Weight:

$SW := 34.830965kip$

$w_{sw} := \frac{SW}{L} = 0.096751\frac{kip}{in}$

Measured Material Properties:

Beam Concrete:

$E_c := 4915ksi$

Transformed Specimen Geometry:

$$A_{ct} := 16.5in \cdot 32in - (4.75in \cdot 9.5in) - (2 \cdot 3in \cdot 9.5in) - 9in^2 + \left(\frac{h_{tot}}{2} - 16.5in\right) \cdot 7in = 490.375in^2$$

Stirrup Rebar:

$f_y := 60.7ksi$

$A_{stirrup} := 0.2in^2 \cdot 2 = 0.4in^2$

Tensile Rebar:

$E_s := 29000ksi$

$A_s := 0in^2$

Test Setup Parameters:

$L_{span} := 28.5ft \qquad d_p := 50.67in$

$d_v := 45.603in$

$L_{bearing} := 8in$

$a := 151.125in$

$P_{trial} := 450kip$

Prestressing Strands:

$E_p := 29000\,ksi$ $\quad d_b := 0.7\,in$ $\quad A_{0.7strand} := 0.294\,in^2$

$f_{ps} := 244\,ksi$ $\quad f_{pe} := 157.4286\,ksi$ $\quad N_{botstrands} := 24$

$A_{pbot} := A_{0.7strand} \cdot N_{botstrands} = 7.056\,in^2$ $\quad f_p := 202.5\,ksi$

$l_t := 60 \cdot d_b = 42\,in$

Resistance Factors:

$\varphi_f := 1.0$

$\varphi_c := 1.0$

$\varphi_v := 1.0$

Calculations:

$\theta(P_{trial}) := 28.5$ <- Initial guess for solve block

Given <- Solve block for V_n

$$x_{crit}(P_{trial}) := \frac{L_{bearing}}{2} + (h_{tot} - d_p) \cdot \cot\left(\theta(P_{trial}) \cdot \frac{\pi}{180}\right)$$

$$f_{pobot}(P_{trial}) := \frac{x_{crit}(P_{trial}) + 9\,in}{l_t} \cdot f_{pe}$$

$$x_{moment} := d_v + \frac{L_{bearing}}{2} = 49.603\,in$$

Tensile Capacity:

$$T_n(P_{trial}) := A_{pbot} \cdot f_{pobot}(P_{trial}) + A_s \cdot f_y$$

Anchorage Capacity:

Shear at critical section due to applied loads:

$V_{crit}(P_{trial}) := P_{trial}$

Shear at critical section due to self- weight:

$$V_{sw} := \left(\frac{w_{sw} \cdot L_{span}}{2}\right) - w_{sw} \cdot x_{momen}$$

Total shear at critical section:

$V_u(P_{trial}) := V_{crit}(P_{trial}) + V_{sw}$

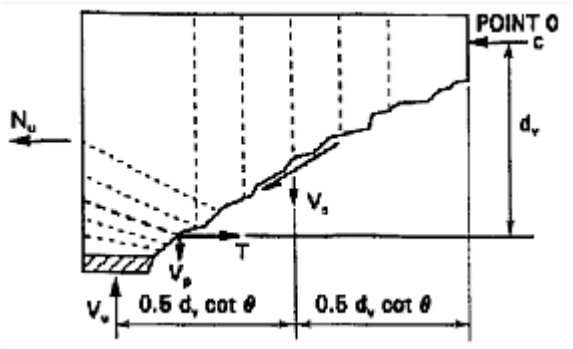

Shear due to vertical component of prestressing force:

$V_p := 0\,ksi$

Moment at critical section due to applied loads:

$$M_{crit}(P_{trial}) := P_{trial} \cdot x_{moment}$$

Moment at critical section due to self -weight:

$$M_{sw} := \frac{w_{sw} \cdot L_{span}}{2} \cdot x_{moment} - \frac{w_{sw} \cdot x_{moment}^{2}}{2}$$

Total moment at critical section:

$$M_{u1}(P_{trial}) := \left| M_{crit}(P_{trial}) + M_{sw} \right|$$

Apply limit to Mu:

$$M_u(P_{trial}) := \begin{cases} M_{u1}(P_{trial}) & \text{if } M_{u1}(P_{trial}) \geq \left| V_u(P_{trial}) - V_p \right| \cdot d_v \\ \left(\left| V_u(P_{trial}) - V_p \right| \cdot d_v \right) & \text{otherwise} \end{cases}$$

Axial Force:

$$N_u := 0kip$$

Longitudinal Strain:

$$\varepsilon_{s1}(P_{trial}) := \frac{\left(\frac{\left| M_u(P_{trial}) \right|}{d_v} + 0.5 N_u + \left| V_u(P_{trial}) - V_p \right| - A_{pbot} \cdot f_p \right)}{\left(E_s \cdot A_s + E_p \cdot A_{pbot} \right)}$$

$$\varepsilon_{salt}(P_{trial}) := \frac{\left(\frac{\left| M_u(P_{trial}) \right|}{d_v} + 0.5 N_u + \left| V_u(P_{trial}) - V_p \right| - A_{pbot} \cdot f_p \right)}{\left(E_s \cdot A_s + E_p \cdot A_{pbot} + E_c \cdot A_{ct} \right)}$$

Apply limits to ε _s:

$$\varepsilon_{s2}(P_{trial}) := \begin{cases} \varepsilon_{s1}(P_{trial}) & \text{if } \varepsilon_{s1}(P_{trial}) \geq 0 \\ \varepsilon_{salt}(P_{trial}) & \text{otherwise} \end{cases}$$

$$\varepsilon_s(P_{trial}) := \begin{cases} -0.0004 \text{ if } \varepsilon_{s2}(P_{trial}) \leq -0.0004 \\ \varepsilon_{s2}(P_{trial}) & \text{if } -0.0004 \leq \varepsilon_{s2}(P_{trial}) \leq 0.00(\\ 0.006 \text{ otherwise} \end{cases}$$

Check for min shear reinforcement:

$$s_v(x_{crit}) := \begin{cases} 3in & \text{if } x_{crit} \leq 36in \\ 6in & \text{otherwise} \end{cases}$$

$$\theta(P_{trial}) := 29 + 3500 \varepsilon_s(P_{trial}) \qquad \theta(P_{trial}) = 28.381$$

Reinforcement contribution to shear capacity:

$$V_s(P_{trial}) := \frac{2 \cdot 0.2\text{in}^2 \cdot f_y \cdot d_v \cdot \left(\cot\left(\theta(P_{trial}) \cdot \frac{\pi}{180}\right)\right)}{s_v(x_{moment})} \qquad V_s(P_{trial}) = 341.566\text{kip}$$

Max Anchorage Demand:

$$T_{max}(P_{trial}) := \left(\frac{V_u(P_{trial})}{\varphi_v} - 0.5 V_s(P_{trial}) - V_p\right) \cdot \cot\left(\theta(P_{trial}) \cdot \frac{\pi}{180}\right)$$

$T_{max}(P_{trial}) = T_n(P_{trial})$

$P_{anchorage} := \text{Minerr}(P_{trial}) = 432.223\text{kip}$ $\qquad ERR = 4.657 \times 10^{-10}$

$V_{nanchorage}(P_{anchorage}) := V_u(P_{anchorage})$ $\qquad T_n(P_{anchorage}) = 506.032\text{kip}$

$T_{max}(P_{anchorage}) = 506.032\text{kip}$

$$V_{nanchorage}(P_{anchorage}) = 443.968\text{kip}$$

$x_{crit}(P_{anchorage}) = 10.133\text{in}$

$f_{pobot}(P_{anchorage}) = 71.717\text{ksi}$

$\theta(P_{anchorage}) = 28.332$

$M_u(P_{anchorage}) = 22141.19\text{kip-in}$

Figure D-7: Tx46-II Anchorage Calculations

Per AASHTO 5.8.3.5

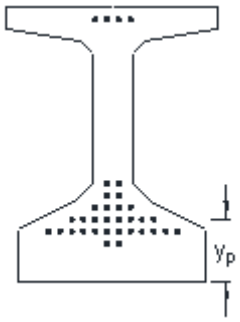

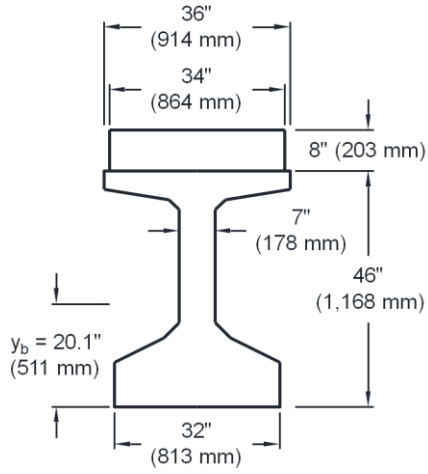

Input Parameters:

Specimen Geometry:

Beam Geometry:

$L := 30ft$

$h_{tot} := 54in$

Specimen Self Weight:

$SW := 34.542858kip$

$w_{sw} := \frac{SW}{L} = 0.095952\frac{kip}{in}$

Measured Material Properties:

Beam Concrete:

$E_c := 5424ksi$

Transformed Specimen Geometry:

$$A_{ct} := 16.5in \cdot 32in - (4.75in \cdot 9.5in) - (2 \cdot 3in \cdot 9.5in) - 9in^2 + \left(\frac{h_{tot}}{2} - 16.5in\right) \cdot 7in = 490.375in^2$$

Stirrup Rebar:

$f_y := 60.7ksi$

$A_{stirrup} := 0.2in^2 \cdot 2 = 0.4in^2$

Tensile Rebar:

$E_s := 29000ksi$

$A_s := 0in^2$

Test Setup Parameters:

$L_{span} := 28.5ft$

$d_v := 39.267in$

$a := 130.8in$

$L_{loadplate} := 9in$

$$x_{crit} := a - \frac{L_{loadplate}}{2} - d_v = 87.033in$$

$P_{trial} := 450kip$

Prestressing Strands:

$E_p := 29000\,ksi$ $d_b := 0.7\,in$

$f_{ps} := 244\,ksi$ $f_{pe} := 166.87\,ksi$

$A_{0.7strand} := 0.294\,in^2$

$N_{botstrands} := 30$

$A_{pbot} := A_{0.7strand} \cdot N_{botstrands} = 8.82\,in^2$

$l_d := 1.6\left(\frac{f_{ps}}{ksi} - \frac{2}{3}\cdot\frac{f_{pe}}{ksi}\right) d_b = 148.684\,in$

$l_t := 60 \cdot d_b = 42\,in$

$f_{pobot} := f_{pe} + \frac{\left(x_{crit} + 9in - l_t\right)}{l_d - l_t}\cdot\left(f_{ps} - f_{pe}\right) = 205.935\,ksi$

Resistance Factors:

$\varphi_f := 1.0$

$\varphi_c := 1.0$

$\varphi_v := 1.0$

Calculations:

Tensile Capacity:

$T_n := A_{pbot}\cdot f_{pobot} + A_s \cdot f_y = 1816.344\,kip$

Anchorage Capacity:

Given <- Solve block for V_n

Shear at critical section due to applied loads:

$V_{crit}(P_{trial}) := P_{trial}$

Shear at critical section due to self- weight:

$V_{sw} := \left(\frac{w_{sw}\cdot L_{span}}{2}\right) - w_{sw}\cdot x_{crit} = 8.057\,kip$

Total shear at critical section:

$V_u(P_{trial}) := V_{crit}(P_{trial}) + V_{sw}$

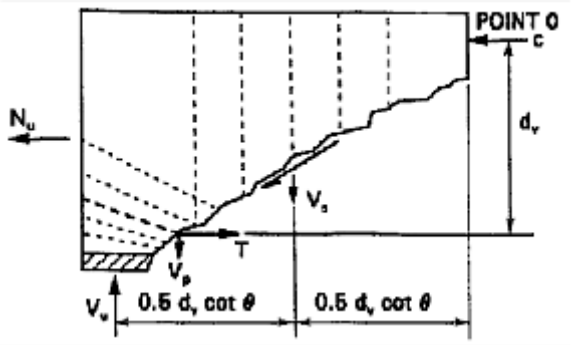

Shear due to vertical component of prestressing force:

$V_p := 0\,ksi$

Moment at critical section due to applied loads:

$$M_{crit}(P_{trial}) := P_{trial} \cdot x_{crit}$$

Moment at critical section due to self- weight:

$$M_{sw} := \frac{w_{sw} \cdot L_{span}}{2} \cdot x_{crit} - \frac{w_{sw} \cdot x_{crit}^{2}}{2} = 1.065 \times 10^{3} \cdot kip \cdot in$$

Total moment at critical section:

$$M_{u1}(P_{trial}) := \left| M_{crit}(P_{trial}) + M_{sw} \right|$$

Apply limit to Mu:

$$M_u(P_{trial}) := \begin{cases} M_{u1}(P_{trial}) & \text{if } M_{u1}(P_{trial}) \geq \left| V_u(P_{trial}) - V_p \right| \cdot d_v \\ \left(\left| V_u(P_{trial}) - V_p \right| \cdot d_v \right) & \text{otherwise} \end{cases}$$

Axial Force:

$$N_u := 0kip$$

Longitudinal Strain:

$$\varepsilon_{s1}(P_{trial}) := \frac{\left(\frac{\left| M_u(P_{trial}) \right|}{d_v} + 0.5 N_u + \left| V_u(P_{trial}) - V_p \right| - A_{pbot} \cdot f_{pobot} \right)}{\left(E_s \cdot A_s + E_p \cdot A_{pbot} \right)}$$

$$\varepsilon_{salt}(P_{trial}) := \frac{\left(\frac{\left| M_u(P_{trial}) \right|}{d_v} + 0.5 N_u + \left| V_u(P_{trial}) - V_p \right| - A_{pbot} \cdot f_{pobot} \right)}{\left(E_s \cdot A_s + E_p \cdot A_{pbot} + E_c \cdot A_{ct} \right)}$$

Apply limits to ε _s:

$$\varepsilon_{s2}(P_{trial}) := \begin{cases} \varepsilon_{s1}(P_{trial}) & \text{if } \varepsilon_{s1}(P_{trial}) \geq 0 \\ \varepsilon_{salt}(P_{trial}) & \text{otherwise} \end{cases}$$

$$\varepsilon_s(P_{trial}) := \begin{cases} -0.0004 \text{ if } \varepsilon_{s2}(P_{trial}) \leq -0.0004 \\ \varepsilon_{s2}(P_{trial}) & \text{if } -0.0004 \leq \varepsilon_{s2}(P_{trial}) \leq 0.00(\\ 0.006 \text{ otherwise} \end{cases}$$

Check for min shear reinforcement:

$$s_v(x_{crit}) := \begin{cases} 3in & \text{if } x_{crit} \leq 36in \\ 6in & \text{otherwise} \end{cases}$$

$$\theta(P_{trial}) := 29 + 3500 \varepsilon_s(P_{trial}) \qquad \theta(P_{trial}) = 28.599$$

Reinforcement contribution to shear capacity:

$$V_s(P_{trial}) := \frac{2 \cdot 0.2\text{in}^2 \cdot f_y \cdot d_v \cdot \left(\cot\left(\theta(P_{trial}) \cdot \frac{\pi}{180}\right)\right)}{s_v(x_{crit})} \qquad V_s(P_{trial}) = 291.452\text{kip}$$

Max Tension Demand:

$$T_{max}(P_{trial}) := \frac{|M_u(P_{trial})|}{\varphi_f \cdot d_v} + 0.5\frac{N_u}{\varphi_c} + \left(\left|\frac{V_u(P_{trial})}{\varphi_v} - V_p\right| - 0.5V_s(P_{trial})\right) \cdot \cot\left(\theta(P_{trial}) \cdot \frac{\pi}{180}\right)$$

$T_{max}(P_{trial}) = T_n$

$P_{anchorage} := \text{Minerr}(P_{trial}) = 504.939\text{kip}$ $\qquad$ $\text{ERR} = 9.313 \times 10^{-10}$

$V_{nanchorage}(P_{anchorage}) := V_u(P_{anchorage})$

$$V_{nanchorage}(P_{anchorage}) = 512.996\text{kip}$$

Figure D-8: Tx46-II Anchorage Calculations

Per AASHTO 5.8.3.5

Input Parameters:

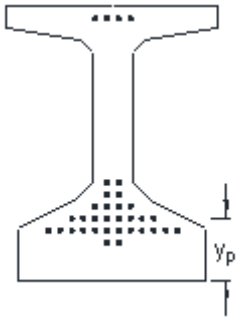

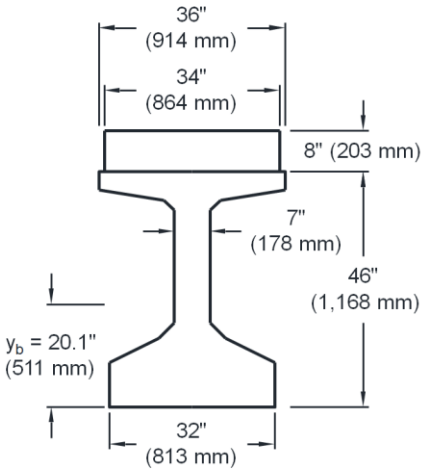

Specimen Geometry:

Beam Geometry:

$L := 30ft$

$h_{tot} := 54in$

Specimen Self Weight:

$SW := 34.542853kip$

$w_{sw} := \frac{SW}{L} = 0.095955\frac{kip}{in}$

Measured Material Properties:

Beam Concrete:

$E_c := 5424ksi$

Transformed Specimen Geometry:

$$A_{ct} := 16.5in \cdot 32in - (4.75in \cdot 9.5in) - (2 \cdot 3in \cdot 9.5in) - 9in^2 + \left(\frac{h_{tot}}{2} - 16.5in\right) \cdot 7in = 490.375in^2$$

Stirrup Rebar:

$f_y := 60.7ksi$

$A_{stirrup} := 0.2in^2 \cdot 2 = 0.4in^2$

Tensile Rebar:

$E_s := 29000ksi$

$A_s := 0in^2$

Test Setup Parameters:

$L_{span} := 28.5ft \qquad d_p := 43.63in$

$d_v := 39.267in$

$L_{bearing} := 8in$

$a := 130.8in$

$P_{trial} := 450kip$

Prestressing Strands:

$E_p := 29000ksi$ $d_b := 0.7in$ $A_{0.7strand} := 0.294in^2$

$f_{ps} := 244ksi$ $f_{pe} := 166.87ksi$ $N_{botstrands} := 30$

$A_{pbot} := A_{0.7strand} \cdot N_{botstrands} = 8.82in^2$ $f_p := 202.5ksi$

$l_t := 60 \cdot d_b = 42in$

Resistance Factors:

$\varphi_f := 1.0$

$\varphi_c := 1.0$

$\varphi_v := 1.0$

Calculations:

$\theta(P_{trial}) := 28.5$ <- Initial guess for solve block

Given <- Solve block for V_n

$$x_{crit}(P_{trial}) := \frac{L_{bearing}}{2} + (h_{tot} - d_p) \cdot \cot\left(\theta(P_{trial}) \cdot \frac{\pi}{180}\right)$$

$$f_{pobot}(P_{trial}) := \frac{x_{crit}(P_{trial}) + 9in}{l_t} \cdot f_{pe}$$

$$x_{moment} := d_v + \frac{L_{bearing}}{2} = 43.267in$$

Tensile Capacity:

$$T_n(P_{trial}) := A_{pbot} \cdot f_{pobot}(P_{trial}) + A_s \cdot f_y$$

Anchorage Capacity:

Shear at critical section due to applied loads:

$V_{crit}(P_{trial}) := P_{trial}$

Shear at critical section due to self-weight:

$$V_{sw} := \left(\frac{w_{sw} \cdot L_{span}}{2}\right) - w_{sw} \cdot x_{momen}$$

Total shear at critical section:

$V_u(P_{trial}) := V_{crit}(P_{trial}) + V_{sw}$

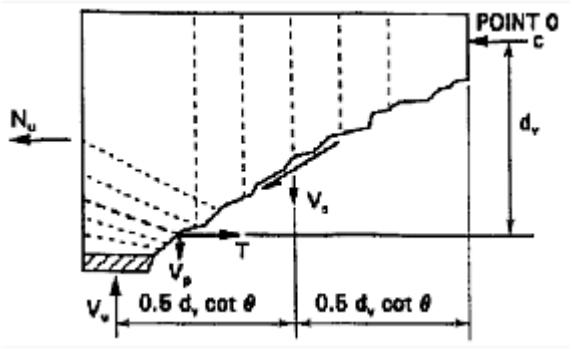

Shear due to vertical component of prestressing force:

$V_p := 0ksi$

Moment at critical section due to applied loads:

$$M_{crit}(P_{trial}) := P_{trial} \cdot x_{moment}$$

Moment at critical section due to self- weight:

$$M_{sw} := \frac{w_{sw} \cdot L_{span}}{2} \cdot x_{moment} - \frac{w_{sw} \cdot x_{moment}^{2}}{2}$$

Total moment at critical section:

$$M_{u1}(P_{trial}) := \left| M_{crit}(P_{trial}) + M_{sw} \right|$$

Apply limit to Mu:

$$M_u(P_{trial}) := \begin{cases} M_{u1}(P_{trial}) & \text{if } M_{u1}(P_{trial}) \geq \left| V_u(P_{trial}) - V_p \right| \cdot d_v \\ \left(\left| V_u(P_{trial}) - V_p \right| \cdot d_v \right) & \text{otherwise} \end{cases}$$

Axial Force:

$$N_u := 0kip$$

Longitudinal Strain:

$$\varepsilon_{s1}(P_{trial}) := \frac{\left(\frac{\left| M_u(P_{trial}) \right|}{d_v} + 0.5 N_u + \left| V_u(P_{trial}) - V_p \right| - A_{pbot} \cdot f_p \right)}{\left(E_s \cdot A_s + E_p \cdot A_{pbot} \right)}$$

$$\varepsilon_{salt}(P_{trial}) := \frac{\left(\frac{\left| M_u(P_{trial}) \right|}{d_v} + 0.5 N_u + \left| V_u(P_{trial}) - V_p \right| - A_{pbot} \cdot f_p \right)}{\left(E_s \cdot A_s + E_p \cdot A_{pbot} + E_c \cdot A_{ct} \right)}$$

Apply limits to ε _s:

$$\varepsilon_{s2}(P_{trial}) := \begin{cases} \varepsilon_{s1}(P_{trial}) & \text{if } \varepsilon_{s1}(P_{trial}) \geq 0 \\ \varepsilon_{salt}(P_{trial}) & \text{otherwise} \end{cases}$$

$$\varepsilon_s(P_{trial}) := \begin{cases} -0.0004 \text{ if } \varepsilon_{s2}(P_{trial}) \leq -0.0004 \\ \varepsilon_{s2}(P_{trial}) & \text{if } -0.0004 \leq \varepsilon_{s2}(P_{trial}) \leq 0.00 \\ 0.006 \text{ otherwise} \end{cases}$$

Check for min shear reinforcement:

$$s_v(x_{crit}) := \begin{cases} 3in & \text{if } x_{crit} \leq 36in \\ 6in & \text{otherwise} \end{cases}$$

$$\theta(P_{trial}) := 29 + 3500 \varepsilon_s(P_{trial}) \qquad \theta(P_{trial}) = 28.025$$

Reinforcement contribution to shear capacity:

$$V_s(P_{trial}) := \frac{2 \cdot 0.2\text{in}^2 \cdot f_y \cdot d_v \cdot \left(\cot\left(\theta(P_{trial}) \cdot \frac{\pi}{180}\right)\right)}{s_v(x_{moment})} \qquad V_s(P_{trial}) = 298.533\text{kip}$$

Max Anchorage Demand:

$$T_{max}(P_{trial}) := \left(\frac{V_u(P_{trial})}{\varphi_v} - 0.5 V_s(P_{trial}) - V_p\right) \cdot \cot\left(\theta(P_{trial}) \cdot \frac{\pi}{180}\right)$$

$T_{max}(P_{trial}) = T_n(P_{trial})$

$P_{anchorage} := \text{Minerr}(P_{trial}) = 750.313\text{kip}$ $\quad ERR = 9.313 \times 10^{-10}$

$V_{nanchorage}(P_{anchorage}) := V_u(P_{anchorage})$ $\quad T_n(P_{anchorage}) = 1.125 \times 10^3 \cdot \text{kip}$

$V_{nanchorage}(P_{anchorage}) = 762.569\text{kip}$ $\quad T_{max}(P_{anchorage}) = 1.125 \times 10^3 \cdot \text{kip}$

$x_{crit}(P_{anchorage}) = 23.099\text{in}$

$f_{pobot}(P_{anchorage}) = 127.533\text{ksi}$

$\theta(P_{anchorage}) = 28.783$

$M_u(P_{anchorage}) = 33083.89\text{kip} \cdot \text{in}$

Figure D-9: Tx70-I Anchorage Calculations

Per AASHTO 5.8.3.5

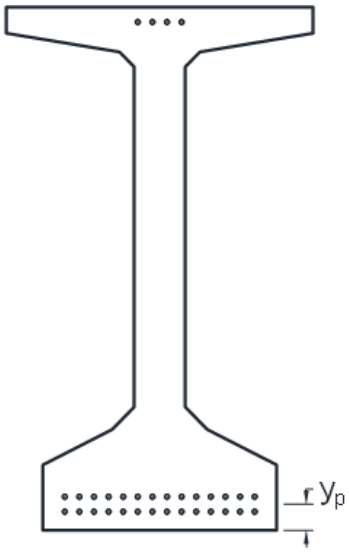

Input Parameters:

Specimen Geometry:

Beam Geometry:

$L := 30ft$

$h_{tot} := 78in$

Specimen Self Weight:

$SW := 41.145608kip$

$w_{sw} := \frac{SW}{L} = 0.114299\frac{kip}{in}$

Measured Material Properties:

Beam Concrete:

$E_c := 6096ksi$

Transformed Specimen Geometry:

$$A_{ct} := 16.5in \cdot 32in - (4.75in \cdot 9.5in) - (2 \cdot 3in \cdot 9.5in) - 9in^2 + \left(\frac{h_{tot}}{2} - 16.5in\right) \cdot 7in = 574.375in^2$$

Stirrup Rebar:

$f_y := 72.17ksi$

$A_{stirrup} := 0.2in^2 \cdot 2 = 0.4in^2$

Tensile Rebar:

$E_s := 29000ksi$

$A_s := 0in^2$

Test Setup Parameters:

$L_{span} := 28.5ft$

$d_v := 67.102666in$

$a := 171.125in$ <- Measured as built

$L_{loadplate} := 12in$

$x_{crit} := a - \frac{L_{loadplate}}{2} - d_v = 98.022in$

$P_{trial} := 1500kip$

Prestressing Strands:

$E_p := 29000ksi$ $d_b := 0.7in$

$f_{ps} := 244ksi$ $f_{pe} := 163.8204ksi$

$A_{0.7strand} := 0.294in^2$

$N_{botstrands} := 28$

$A_{pbot} := A_{0.7strand} \cdot N_{botstrands} = 8.232in^2$

$l_d := 1.6\left(\frac{f_{ps}}{ksi} - \frac{2}{3}\cdot\frac{f_{pe}}{ksi}\right)d_b = 150.961in$

$l_t := 60\cdot d_b = 42\cdot in$

$f_{pobot} := f_{pe} + \frac{\left(x_{crit} + 9in - l_t\right)}{l_d - l_t}\cdot\left(f_{ps} - f_{pe}\right) = 211.668ksi$

Resistance Factors:

$\varphi_f := 1.0$

$\varphi_c := 1.0$

$\varphi_v := 1.0$

Calculations:

Tensile Capacity:

$T_n := A_{pbot}\cdot f_{pobot} + A_s\cdot f_y = 1742.447kip$

Anchorage Capacity:

Given Solve block for V_n

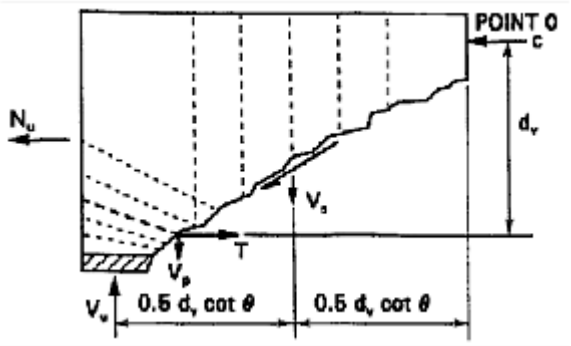

Shear at critical section due to applied loads:

$V_{crit}(P_{trial}) := \frac{P_{trial}}{2}$

Shear at critical section due to self- weight:

$V_{sw} := \left(\frac{w_{sw}\cdot L_{span}}{2}\right) - w_{sw}\cdot x_{crit} = 8.341kip$

Total shear at critical section:

$V_u(P_{trial}) := V_{crit}(P_{trial}) + V_{sw}$

Shear due to vertical component of prestressing force:

$V_p := 0ksi$

Moment at critical section due to applied loads:

$$M_{crit}(P_{trial}) := \frac{P_{trial}}{2} \cdot x_{crit}$$

Moment at critical section due to self- weight:

$$M_{sw} := \frac{w_{sw} \cdot L_{span}}{2} \cdot x_{crit} - \frac{w_{sw} \cdot x_{crit}^{2}}{2} = 1.367 \times 10^{3} \cdot kip \cdot in$$

Total moment at critical section:

$$M_{u1}(P_{trial}) := \left| M_{crit}(P_{trial}) + M_{sw} \right|$$

Apply limit to Mu:

$$M_u(P_{trial}) := \begin{cases} M_{u1}(P_{trial}) & \text{if } M_{u1}(P_{trial}) \geq \left| V_u(P_{trial}) - V_p \right| \cdot d_v \\ \left(\left| V_u(P_{trial}) - V_p \right| \cdot d_v \right) & \text{otherwise} \end{cases}$$

Axial Force:

$N_u := 0kip$

Longitudinal Strain:

$$\varepsilon_{s1}(P_{trial}) := \frac{\left(\frac{\left| M_u(P_{trial}) \right|}{d_v} + 0.5 N_u + \left| V_u(P_{trial}) - V_p \right| - A_{pbot} \cdot f_{pobot} \right)}{\left(E_s \cdot A_s + E_p \cdot A_{pbot} \right)}$$

$$\varepsilon_{salt}(P_{trial}) := \frac{\left(\frac{\left| M_u(P_{trial}) \right|}{d_v} + 0.5 N_u + \left| V_u(P_{trial}) - V_p \right| - A_{pbot} \cdot f_{pobot} \right)}{\left(E_s \cdot A_s + E_p \cdot A_{pbot} + E_c \cdot A_{ct} \right)}$$

Apply limits to ε _s:

$$\varepsilon_{s2}(P_{trial}) := \begin{cases} \varepsilon_{s1}(P_{trial}) & \text{if } \varepsilon_{s1}(P_{trial}) \geq 0 \\ \varepsilon_{salt}(P_{trial}) & \text{otherwise} \end{cases}$$

$$\varepsilon_s(P_{trial}) := \begin{cases} -0.0004 \text{ if } \varepsilon_{s2}(P_{trial}) \leq -0.0004 \\ \varepsilon_{s2}(P_{trial}) & \text{if } -0.0004 \leq \varepsilon_{s2}(P_{trial}) \leq 0.00 \\ 0.006 \text{ otherwise} \end{cases}$$

Check for min shear reinforcement:

$$s_v(x_{crit}) := \begin{cases} 3in & \text{if } x_{crit} \leq 36in \\ 8in & \text{otherwise} \end{cases}$$

$$\theta(P_{trial}) := 29 + 3500 \varepsilon_s(P_{trial}) \qquad \theta(P_{trial}) = 30.933$$

Reinforcement contribution to shear capacity:

$$V_s(P_{trial}) := \frac{A_{stirrup} \cdot f_y \cdot d_v \cdot \left(\cot\left(\theta(P_{trial}) \cdot \frac{\pi}{180}\right)\right)}{s_v(x_{crit})} \qquad V_s(P_{trial}) = 404.058\,kip$$

Max Anchorage Demand:

$$T_{max}(P_{trial}) := \frac{\left|M_u(P_{trial})\right|}{\varphi_f \cdot d_v} + 0.5\frac{N_u}{\varphi_c} + \left(\left|\frac{V_u(P_{trial})}{\varphi_v} - V_p\right| - 0.5V_s(P_{trial})\right) \cdot \cot\left(\theta(P_{trial}) \cdot \frac{\pi}{180}\right)$$

$T_{max}(P_{trial}) = T_n$

$P_{anchorage} := Minerr(P_{trial}) = 1285.891\,kip$ $\qquad ERR = 0$

$V_{nanchorage}(P_{anchorage}) := V_u(P_{anchorage})$

$$V_{nanchorage}(P_{anchorage}) = 651.286\,kip$$

Figure D-10: Tx70-I Anchorage Calculations

Per AASHTO 5.8.3.5

Input Parameters:

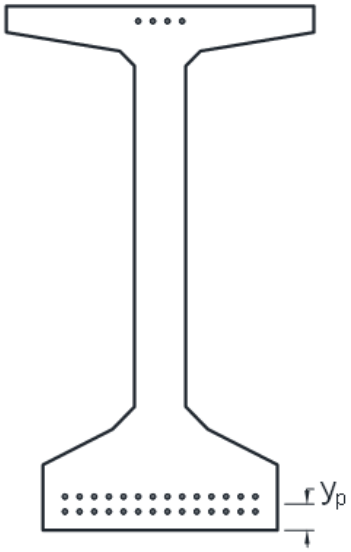

Specimen Geometry:

Beam Geometry:

$L := 30ft$

$h_{tot} := 78in$

Specimen Self Weight:

$SW := 41.145608kip$

$w_{sw} := \frac{SW}{L} = 0.11429\frac{kip}{in}$

Measured Material Properties:

Beam Concrete:

$E_c := 6096ksi$

Transformed Specimen Geometry:

$$A_{ct} := 16.5in \cdot 32in - (4.75in \cdot 9.5in) - (2 \cdot 3in \cdot 9.5in) - 9in^2 + \left(\frac{h_{tot}}{2} - 16.5in\right) \cdot 7in = 574.375in^2$$

Stirrup Rebar:

$f_y := 72.17ksi$

$A_{stirrup} := 0.2in^2 \cdot 2 = 0.4in^2$

Tensile Rebar:

$E_s := 29000ksi$

$A_s := 0in^2$

Test Setup Parameters:

$L_{span} := 28.5ft \qquad d_p := 74.5in$

$d_v := 67.102666in$

$L_{bearing} := 9in$

$a := 171.125in$

$P_{trial} := 1500kip$

Prestressing Strands:

$E_p := 29000ksi$ $d_b := 0.7in$ $A_{0.7strand} := 0.294in^2$

$f_{ps} := 244ksi$ $f_{pe} := 163.8204ksi$ $N_{botstrands} := 28$

$A_{pbot} := A_{0.7strand} \cdot N_{botstrands} = 8.232in^2$ $f_p := 202.5ksi$

$l_t := 60 \cdot d_b = 42 \cdot in$

Resistance Factors:

$\varphi_f := 1.0$

$\varphi_c := 1.0$

$\varphi_v := 1.0$

Calculations:

$\theta(P_{trial}) := 28.5$ <- Initial guess for solve block

Given <- Solve block for V_n

$$x_{crit}(P_{trial}) := \frac{L_{bearing}}{2} + (h_{tot} - d_p) \cdot \cot\left(\theta(P_{trial}) \cdot \frac{\pi}{180}\right)$$

$$f_{pobot}(P_{trial}) := \frac{x_{crit}(P_{trial}) + 9in}{l_t} \cdot f_{pe}$$

$$x_{moment} := d_v + \frac{L_{bearing}}{2} = 71.603in$$

Tensile Capacity:

$$T_n(P_{trial}) := A_{pbot} \cdot f_{pobot}(P_{trial}) + A_s \cdot f_y$$

Anchorage Capacity:

Shear at critical section due to applied loads:

$$V_{crit}(P_{trial}) := \frac{P_{trial}}{2}$$

Shear at critical section due to self -weight:

$$V_{sw} := \left(\frac{w_{sw} \cdot L_{span}}{2}\right) - w_{sw} \cdot x_{momen}$$

Total shear at critical section:

$V_u(P_{trial}) := V_{crit}(P_{trial}) + V_{sw}$

Shear due to vertical component of prestressing force:

$V_p := 0ksi$

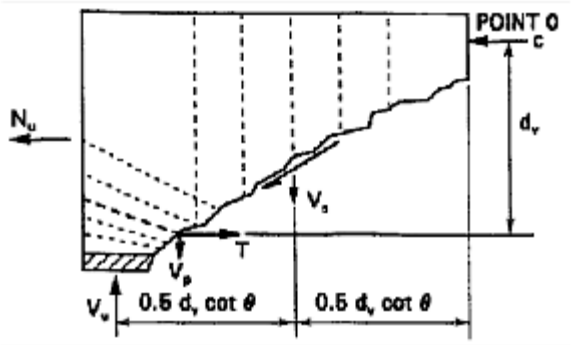

Moment at critical section due to applied loads:

$$M_{crit}(P_{trial}) := \frac{P_{trial}}{2} \cdot x_{momen}$$

Moment at critical section due to self- weight:

$$M_{sw} := \frac{w_{sw} \cdot L_{span}}{2} \cdot x_{moment} - \frac{w_{sw} \cdot x_{moment}^{2}}{2}$$

Total moment at critical section:

$$M_{u1}(P_{trial}) := \left| M_{crit}(P_{trial}) + M_{sw} \right|$$

Apply limit to Mu:

$$M_u(P_{trial}) := \begin{cases} M_{u1}(P_{trial}) & \text{if } M_{u1}(P_{trial}) \geq \left| V_u(P_{trial}) - V_p \right| \cdot d_v \\ \left(\left| V_u(P_{trial}) - V_p \right| \cdot d_v \right) & \text{otherwise} \end{cases}$$

Axial Force:

$N_u := 0kip$

Longitudinal Strain:

$$\varepsilon_{s1}(P_{trial}) := \frac{\left(\frac{\left| M_u(P_{trial}) \right|}{d_v} + 0.5 N_u + \left| V_u(P_{trial}) - V_p \right| - A_{pbot} \cdot f_p \right)}{\left(E_s \cdot A_s + E_p \cdot A_{pbot} \right)}$$

$$\varepsilon_{salt}(P_{trial}) := \frac{\left(\frac{\left| M_u(P_{trial}) \right|}{d_v} + 0.5 N_u + \left| V_u(P_{trial}) - V_p \right| - A_{pbot} \cdot f_p \right)}{\left(E_s \cdot A_s + E_p \cdot A_{pbot} + E_c \cdot A_{ct} \right)}$$

Apply limits to ε _s:

$$\varepsilon_{s2}(P_{trial}) := \begin{cases} \varepsilon_{s1}(P_{trial}) & \text{if } \varepsilon_{s1}(P_{trial}) \geq 0 \\ \varepsilon_{salt}(P_{trial}) & \text{otherwise} \end{cases}$$

$$\varepsilon_s(P_{trial}) := \begin{cases} -0.0004 \text{ if } \varepsilon_{s2}(P_{trial}) \leq -0.0004 \\ \varepsilon_{s2}(P_{trial}) & \text{if } -0.0004 \leq \varepsilon_{s2}(P_{trial}) \leq 0.00 \\ 0.006 \text{ otherwise} \end{cases}$$

Check for min shear reinforcement:

$$s_v(x_{crit}) := \begin{cases} 3in & \text{if } x_{crit} \leq 36in \\ 8in & \text{otherwise} \end{cases}$$

$$\theta(P_{trial}) := 29 + 3500 \varepsilon_s(P_{trial}) \qquad \theta(P_{trial}) = 28.917$$

Reinforcement contribution to shear capacity:

$$V_s(P_{trial}) := \frac{2 \cdot 0.2\,in^2 \cdot f_y \cdot d_v \cdot \left(\cot\left(\theta(P_{trial}) \cdot \frac{\pi}{180}\right)\right)}{s_v(x_{moment})} \qquad V_s(P_{trial}) = 438.331\,kip$$

Max Anchorage Demand:

$$T_{max}(P_{trial}) := \left(\frac{V_u(P_{trial})}{\varphi_v} - 0.5\,V_s(P_{trial}) - V_p\right) \cdot \cot\left(\theta(P_{trial}) \cdot \frac{\pi}{180}\right)$$

$T_{max}(P_{trial}) = T_n(P_{trial})$

$P_{anchorage} := Minerr(P_{trial}) = 1119.222\,kip$ $\quad ERR = 4.657 \times 10^{-10}$

$T_n(P_{anchorage}) = 640.448\,kip$

$V_{nanchorage}(P_{anchorage}) := V_u(P_{anchorage})$ $\quad T_{max}(P_{anchorage}) = 640.448\,kip$

$V_{nanchorage}(P_{anchorage}) = 570.972\,kip$

$x_{crit}(P_{anchorage}) = 10.946\,in$

$f_{pobot}(P_{anchorage}) = 77.8\,ksi$

$\theta(P_{anchorage}) = 28.549$

$M_u(P_{anchorage}) = 41176.074\,kip \cdot in$

Figure D-11: Tx70-II Anchorage Calculations

Per AASHTO 5.8.3.5

Input Parameters:

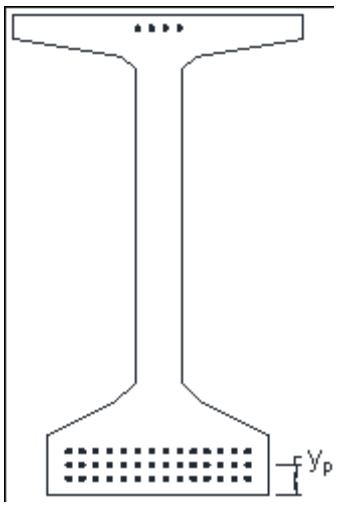

Specimen Geometry:

Beam Geometry:

$L := 30ft$

$h_{tot} := 78in$

Specimen Self Weight:

$SW := 43.296826kip$

$w_{sw} := \frac{SW}{L} = 0.12027\frac{kip}{in}$

Measured Material Properties:

Beam Concrete:

$E_c := 6015ksi$

Transformed Specimen Geometry:

$$A_{ct} := 16.5in \cdot 32in - (4.75in \cdot 9.5in) - (2 \cdot 3in \cdot 9.5in) - 9in^2 + \left(\frac{h_{tot}}{2} - 16.5in\right) \cdot 7in = 574.375in^2$$

Stirrup Rebar:

$f_y := 72.17ksi$

$A_{stirrup} := 0.2in^2 \cdot 2 = 0.4in^2$

Tensile Rebar:

$E_s := 29000ksi$

$A_s := 0in^2$

Test Setup Parameters:

$L_{span} := 28.5ft$

$d_v := 66.15in$

$a := 171in$ <- Measured as built

$L_{loadplate} := 12in$

$$x_{crit} := a - \frac{L_{loadplate}}{2} - d_v = 98.85in$$

$P_{trial} := 1500kip$

Prestressing Strands:

$E_p := 29000\,ksi$ $\quad d_b := 0.7\,in$

$f_{ps} := 244\,ksi$ $\quad f_{pe} := 156.5795\,ksi$

$A_{0.7strand} := 0.294\,in^2$

$N_{botstrands} := 42$

$A_{pbot} := A_{0.7strand} \cdot N_{botstrands} = 12.348\,in^2$

$l_d := 1.6\left(\frac{f_{ps}}{ksi} - \frac{2}{3}\cdot\frac{f_{pe}}{ksi}\right) d_b = 156.367\,in$

$l_t := 60 \cdot d_b = 42 \cdot in$

$f_{pobot} := f_{pe} + \frac{\left(x_{crit} + 9in - l_t\right)}{l_d - l_t}\cdot\left(f_{ps} - f_{pe}\right) = 206.914\,ksi$

Resistance Factors:

$\varphi_f := 1.0$

$\varphi_c := 1.0$

$\varphi_v := 1.0$

Calculations:

Tensile Capacity:

$T_n := A_{pbot}\cdot f_{pobot} + A_s \cdot f_y = 2554.976\,kip$

Anchorage Capacity:

Given $\quad$ Solve block for V_n

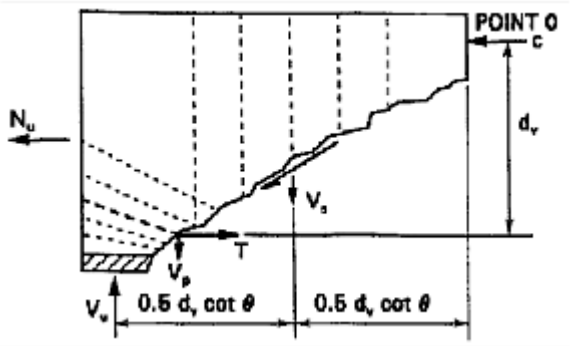

Shear at critical section due to applied loads:

$V_{crit}(P_{trial}) := \frac{P_{trial}}{2}$

Shear at critical section due to self- weight:

$V_{sw} := \left(\frac{w_{sw}\cdot L_{span}}{2}\right) - w_{sw}\cdot x_{crit} = 8.677\,kip$

Total shear at critical section:

$V_u(P_{trial}) := V_{crit}(P_{trial}) + V_{sw}$

Shear due to vertical component of prestressing force:

$V_p := 0\,ksi$

Moment at critical section due to applied loads:

$$M_{crit}(P_{trial}) := \frac{P_{trial}}{2} \cdot x_{crit}$$

Moment at critical section due to self -weight:

$$M_{sw} := \frac{w_{sw} \cdot L_{span}}{2} \cdot x_{crit} - \frac{w_{sw} \cdot x_{crit}^{2}}{2} = 1.445 \times 10^{3} \cdot kip \cdot in$$

Total moment at critical section:

$$M_{u1}(P_{trial}) := \left| M_{crit}(P_{trial}) + M_{sw} \right|$$

Apply limit to Mu:

$$M_u(P_{trial}) := \begin{cases} M_{u1}(P_{trial}) & \text{if } M_{u1}(P_{trial}) \geq \left| V_u(P_{trial}) - V_p \right| \cdot d_v \\ \left(\left| V_u(P_{trial}) - V_p \right| \cdot d_v \right) & \text{otherwise} \end{cases}$$

Axial Force:

$N_u := 0kip$

Longitudinal Strain:

$$\varepsilon_{s1}(P_{trial}) := \frac{\left(\frac{\left| M_u(P_{trial}) \right|}{d_v} + 0.5 N_u + \left| V_u(P_{trial}) - V_p \right| - A_{pbot} \cdot f_{pobot} \right)}{\left(E_s \cdot A_s + E_p \cdot A_{pbot} \right)}$$

$$\varepsilon_{salt}(P_{trial}) := \frac{\left(\frac{\left| M_u(P_{trial}) \right|}{d_v} + 0.5 N_u + \left| V_u(P_{trial}) - V_p \right| - A_{pbot} \cdot f_{pobot} \right)}{\left(E_s \cdot A_s + E_p \cdot A_{pbot} + E_c \cdot A_{ct} \right)}$$

Apply limits to ε _s:

$$\varepsilon_{s2}(P_{trial}) := \begin{cases} \varepsilon_{s1}(P_{trial}) & \text{if } \varepsilon_{s1}(P_{trial}) \geq 0 \\ \varepsilon_{salt}(P_{trial}) & \text{otherwise} \end{cases}$$

$$\varepsilon_s(P_{trial}) := \begin{cases} -0.0004 \text{ if } \varepsilon_{s2}(P_{trial}) \leq -0.0004 \\ \varepsilon_{s2}(P_{trial}) \text{ if } -0.0004 \leq \varepsilon_{s2}(P_{trial}) \leq 0.00 \\ 0.006 \text{ otherwise} \end{cases}$$

Check for min shear reinforcement:

$$s_v(x_{crit}) := \begin{cases} 3in & \text{if } x_{crit} \leq 36in \\ 8in & \text{otherwise} \end{cases}$$

$\theta(P_{trial}) := 29 + 3500 \varepsilon_s(P_{trial})$ $\theta(P_{trial}) = 28.4$

Reinforcement contribution to shear capacity:

$$V_s(P_{trial}) := \frac{A_{stirrup} \cdot f_y \cdot d_v \cdot \left(\cot\left(\theta(P_{trial}) \cdot \frac{\pi}{180}\right)\right)}{s_v(x_{crit})} \qquad V_s(P_{trial}) = 441.471\,kip$$

Max Anchorage Demand:

$$T_{max}(P_{trial}) := \frac{\left|M_u(P_{trial})\right|}{\varphi_f \cdot d_v} + 0.5\frac{N_u}{\varphi_c} + \left(\left|\frac{V_u(P_{trial})}{\varphi_v} - V_p\right| - 0.5V_s(P_{trial})\right) \cdot \cot\left(\theta(P_{trial}) \cdot \frac{\pi}{180}\right)$$

$T_{max}(P_{trial}) = T_n$

$P_{anchorage} := Minerr(P_{trial}) = 1755.692\,kip$ $\qquad ERR = 1.863 \times 10^{-9}$

$V_{nanchorage}(P_{anchorage}) := V_u(P_{anchorage})$

$$V_{nanchorage}(P_{anchorage}) = 886.523\,kip$$

Figure D-12: Tx70-II Anchorage Calculations

Per AASHTO 5.8.3.5

Input Parameters:

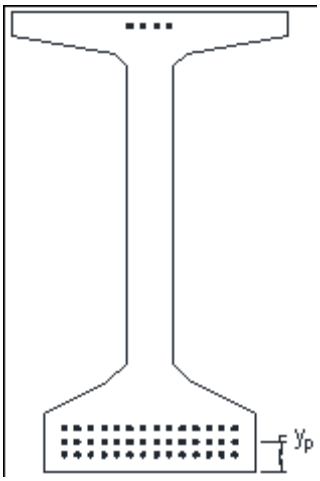

Specimen Geometry:

Beam Geometry:

$L := 30ft$

$h_{tot} := 78in$

Specimen Self Weight:

$SW := 43.296826kip$

$w_{sw} := \frac{SW}{L} = 0.12027\frac{kip}{in}$

Measured Material Properties:

Beam Concrete:

$E_c := 6015ksi$

Transformed Specimen Geometry:

$$A_{ct} := 16.5in \cdot 32in - (4.75in \cdot 9.5in) - (2 \cdot 3in \cdot 9.5in) - 9in^2 + \left(\frac{h_{tot}}{2} - 16.5in\right) \cdot 7in = 574.375in^2$$

Stirrup Rebar:

$f_y := 72.17ksi$

$A_{stirrup} := 0.2in^2 \cdot 2 = 0.4in^2$

Tensile Rebar:

$E_s := 29000ksi$

$A_s := 0in^2$

Test Setup Parameters:

$L_{span} := 28.5ft \qquad d_p := 73.5in$

$d_v := 66.15in$

$L_{bearing} := 9in$

$a := 17in$

$P_{trial} := 1500kip$

Prestressing Strands:

$E_p := 29000ksi$ $d_b := 0.7in$ $A_{0.7strand} := 0.294in^2$

$f_{ps} := 244ksi$ $f_{pe} := 156.5795ksi$ $N_{botstrands} := 42$

$A_{pbot} := A_{0.7strand} \cdot N_{botstrands} = 12.348in^2$ $f_p := 202.5ksi$

$l_t := 60 \cdot d_b = 42 \cdot in$

Resistance Factors:

$\varphi_f := 1.0$

$\varphi_c := 1.0$

$\varphi_v := 1.0$

Calculations:

$\theta(P_{trial}) := 28.5$ <- Initial guess for solve block

Given <- Solve block for V_n

$$x_{crit}(P_{trial}) := \frac{L_{bearing}}{2} + (h_{tot} - d_p) \cdot \cot\left(\theta(P_{trial}) \cdot \frac{\pi}{180}\right)$$

$$f_{pobot}(P_{trial}) := \frac{x_{crit}(P_{trial}) + 9in}{l_t} \cdot f_{pe}$$

$$x_{moment} := d_v + \frac{L_{bearing}}{2} = 70.65in$$

Tensile Capacity:

$$T_n(P_{trial}) := A_{pbot} \cdot f_{pobot}(P_{trial}) + A_s \cdot f_y$$

Anchorage Capacity:

Shear at critical section due to applied loads:

$$V_{crit}(P_{trial}) := \frac{P_{trial}}{2}$$

Shear at critical section due to self -weight:

$$V_{sw} := \left(\frac{w_{sw} \cdot L_{span}}{2}\right) - w_{sw} \cdot x_{momen}$$

Total shear at critical section:

$$V_u(P_{trial}) := V_{crit}(P_{trial}) + V_{sw}$$

Shear due to vertical component of prestressing force:

$V_p := 0ksi$

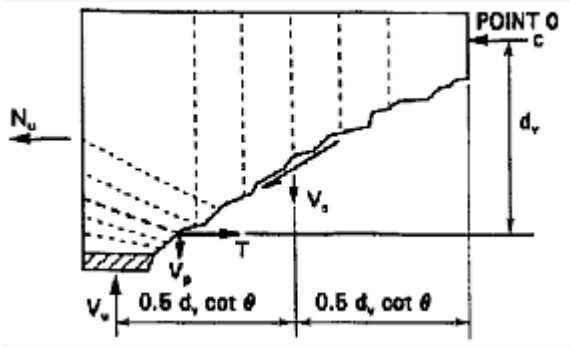

Moment at critical section due to applied loads:

$$M_{crit}(P_{trial}) := \frac{P_{trial}}{2} \cdot x_{moment}$$

Moment at critical section due to self- weight:

$$M_{sw} := \frac{w_{sw} \cdot L_{span}}{2} \cdot x_{moment} - \frac{w_{sw} \cdot x_{moment}^{2}}{2}$$

Total moment at critical section:

$$M_{u1}(P_{trial}) := \left| M_{crit}(P_{trial}) + M_{sw} \right|$$

Apply limit to Mu:

$$M_u(P_{trial}) := \begin{cases} M_{u1}(P_{trial}) & \text{if } M_{u1}(P_{trial}) \geq \left| V_u(P_{trial}) - V_p \right| \cdot d_v \\ \left(\left| V_u(P_{trial}) - V_p \right| \cdot d_v \right) & \text{otherwise} \end{cases}$$

Axial Force:

$N_u := 0kip$

Longitudinal Strain:

$$\varepsilon_{s1}(P_{trial}) := \frac{\left(\frac{\left| M_u(P_{trial}) \right|}{d_v} + 0.5 N_u + \left| V_u(P_{trial}) - V_p \right| - A_{pbot} \cdot f_p \right)}{\left(E_s \cdot A_s + E_p \cdot A_{pbot} \right)}$$

$$\varepsilon_{salt}(P_{trial}) := \frac{\left(\frac{\left| M_u(P_{trial}) \right|}{d_v} + 0.5 N_u + \left| V_u(P_{trial}) - V_p \right| - A_{pbot} \cdot f_p \right)}{\left(E_s \cdot A_s + E_p \cdot A_{pbot} + E_c \cdot A_{ct} \right)}$$

Apply limits to ε _s:

$$\varepsilon_{s2}(P_{trial}) := \begin{cases} \varepsilon_{s1}(P_{trial}) & \text{if } \varepsilon_{s1}(P_{trial}) \geq 0 \\ \varepsilon_{salt}(P_{trial}) & \text{otherwise} \end{cases}$$

$$\varepsilon_s(P_{trial}) := \begin{cases} -0.0004 \text{ if } \varepsilon_{s2}(P_{trial}) \leq -0.0004 \\ \varepsilon_{s2}(P_{trial}) & \text{if } -0.0004 \leq \varepsilon_{s2}(P_{trial}) \leq 0.00 \\ 0.006 \text{ otherwise} \end{cases}$$

Check for min shear reinforcement:

$$s_v(x_{crit}) := \begin{cases} 3in & \text{if } x_{crit} \leq 36in \\ 8in & \text{otherwise} \end{cases}$$

$$\theta(P_{trial}) := 29 + 3500 \varepsilon_s(P_{trial}) \qquad \theta(P_{trial}) = 28.156$$

Reinforcement contribution to shear capacity:

$$V_s(P_{trial}) := \frac{2 \cdot 0.2\,in^2 \cdot f_y \cdot d_v \cdot \left(\cot\left(\theta(P_{trial}) \cdot \frac{\pi}{180}\right)\right)}{s_v(x_{moment})} \qquad V_s(P_{trial}) = 446.008\,kip$$

Max Anchorage Demand:

$$T_{max}(P_{trial}) := \left(\frac{V_u(P_{trial})}{\varphi_v} - 0.5\,V_s(P_{trial}) - V_p\right) \cdot \cot\left(\theta(P_{trial}) \cdot \frac{\pi}{180}\right)$$

$T_{max}(P_{trial}) = T_n(P_{trial})$

$P_{anchorage} := Minerr(P_{trial}) = 1495.355\,kip$ $\qquad ERR = 0$

$V_{nanchorage}(P_{anchorage}) := V_u(P_{anchorage})$ $\qquad T_n(P_{anchorage}) = 1002.995\,kip$

$V_{nanchorage}(P_{anchorage}) = 759.746\,kip$ $\qquad T_{max}(P_{anchorage}) = 1002.995\,kip$

$x_{crit}(P_{anchorage}) = 12.788\,in$

$f_{pobot}(P_{anchorage}) = 81.227\,ksi$

$\theta(P_{anchorage}) = 28.151$

$M_u(P_{anchorage}) = 53976.229\,kip \cdot in$

Figure D-13: Tx46-I Nominal Shear Capacity

Per ACI 318-14 11.5

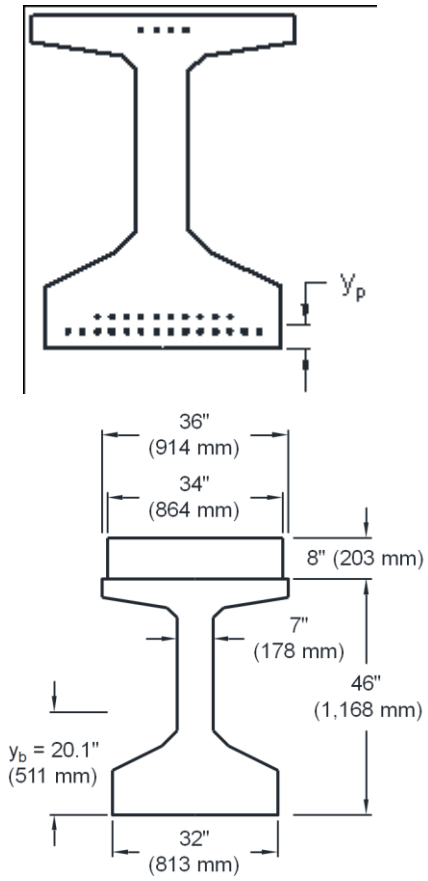

Input Parameters:

Specimen Geometry:

Beam Geometry:

$h_{beam} := 46in$

$b_f := 36in$

$b_w := 7in$

$y_b := 20.1in$

$A_g := 761in^2$

$L := 30ft$

$I_x := 198089in^4$

Deck Geometry:

$t_{deck} := 8in$

$b_{deck} := 34in$

$h_{deck} := 8in$

$A_{deck} := t_{deck} \cdot b_{deck} = 272 \cdot in^2$

Specimen Self Weight:

$SW := 34.830965kip$

$w_{sw} := \frac{SW}{L} = 0.096755\frac{kip}{in}$

Measured Material Properties:

Beam Concrete:

$f'_c := 7.6 \times 1000psi = 7600psi$

$E_c := 4915ksi$

Beam Concrete:

$f'_{cdeck} := 10.71 \times 1000psi = 10710psi$

$E_{cdeck} := 6934ksi$

Transformed Specimen Geometry:

$$n := \frac{E_{cdeck}}{E_c} = 1.411$$

$$h_{tot} := h_{beam} + h_{deck} = 54\,in$$

$$A_{tr} := A_g + A_{deck} \cdot n = 1144.733\,in^2$$

$$y_{tr} := \frac{A_g \cdot y_b + n \cdot A_{deck} \cdot \left(h_{tot} - \frac{t_{deck}}{2} \right)}{A_{tr}} = 30.123\,in$$

$$I_{tr} := I_x + \frac{n \cdot b_{deck} \cdot t_{deck}^{3}}{12} + n \cdot A_{deck} \cdot \left(h_{tot} - \frac{t_{deck}}{2} - y_{tr} \right)^2 = 351747.185\,in^4$$

Stirrups:

$f_y := 60.7\,ksi$

$A_{stirrup} := 2 \cdot 0.2\,in^2 = 0.4\,in^2$

$E_s := 29000\,ksi$

$s := 6\,in$

Prestressing Strands:

$d_b := 0.7\,in$

$f_{po} := 157.4286089 \times 1000\,psi = 157428.609\,psi$

$E_p := 29000\,ksi$

$A_{strand} := 0.294\,in^2$

$N_{botstrands} := 24$

$A_{pbot} := A_{strand} \cdot N_{botstrands} = 7.056\,in^2$

$L_{transfer} := 50 \cdot d_b = 35\,in$

$P_{ps} := f_{po} \cdot A_{pbot} = 1110.816\,kip$

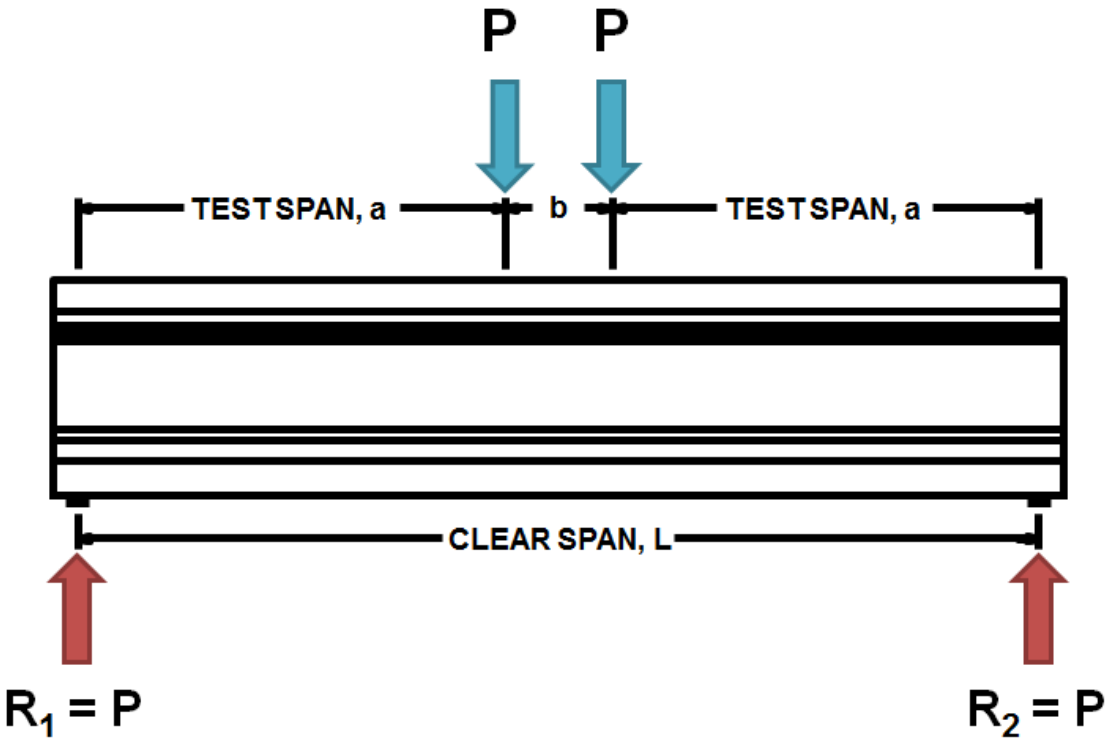

Shear Test Setup:

$L_{span} := 342in$

$a := 151.125in$ <- Measured as built

$P_{trial} := 515kip$ <- Initial guess for subsequent calcs

$y_p := 3.33in$

$d_p := max\left(0.8 \cdot h_{tot}, h_{tot} - y_p\right) = 50.67in$

$L_{bearing} := 8in$

$L_{loadplate} := 12in$

$L_{oh} := 9in$

$x_{crit} := a + L_{oh} - \frac{L_{loadplate}}{2} - \frac{h_{tot}}{2} = 127.125in$ <- Location of critical section for shear taken from left end face

$W_{loadframe} := 22.586385kip$

$W_{beam} := 34.830965kip$

$e_p := y_b - y_p = 16.77in$ <- Eccentricity of strand centroid

Solve for Nominal Shear Capacity:

Given <- Solve block for P_trial

$$V_u(P_{trial}) := P_{trial} + \frac{W_{loadframe}}{2} + \frac{W_{beam}}{2} - w_{sw}\cdot x_{crit}$$

$$V_d := \frac{W_{beam} + W_{loadframe}}{2} - w_{sw}\cdot x_{crit} = 16.409\,kip$$

$$V_i(P_{trial}) := V_u(P_{trial}) - V_d$$

$$M_u(P_{trial}) := -w_{sw}\cdot\frac{x_{crit}^2}{2} + \left(\frac{W_{beam} + W_{loadframe}}{2}\right)\cdot\left(x_{crit} - L_{oh}\right) + P_{trial}\cdot x_{crit}$$

$$M_{sw} := -w_{sw}\cdot\frac{x_{crit}^2}{2} + \frac{W_{beam}}{2}\cdot\left(x_{crit} - L_{oh}\right) = 1.275\times 10^3\cdot kip\cdot in$$

$$M_d := \frac{W_{loadframe}}{2}\cdot\left(x_{crit} - L_{oh}\right) = 1.334\times 10^3\cdot kip\cdot in$$

$$M_{dtot} := M_{sw} + M_d = 2.609\times 10^3\cdot kip\cdot in$$

$$M_{max}(P_{trial}) := M_u(P_{trial}) - M_{dtot}$$

$$f_d := \frac{M_{sw}\cdot y_b}{I_x} + \frac{M_d\cdot y_{tr}}{I_{tr}} = 243.657\,psi$$

$$f_{pe} := \frac{P_{ps}}{A_g} + P_{ps}\cdot e_p\cdot\frac{y_b}{I_x} = 3349.894\,psi$$

$$f_{pc} := \frac{P_{ps}}{A_g} - \left[P_{ps}\cdot e_p\cdot\frac{\left(y_{tr} - y_b\right)}{I_x}\right] + M_{sw}\cdot\frac{\left(y_{tr} - y_b\right)}{I_x} = 581.648\,psi$$

$$M_{cr} := \left(\frac{I_{tr}}{y_{tr}}\right)\cdot\left(6\cdot\sqrt{f'_c\cdot psi} + f_{pe} - f_d\right) = 42379.554\,kip\cdot in$$

$$V_{ci}(P_{trial}) := 0.6\sqrt{f'_c\cdot psi}\cdot b_w\cdot d_p + \frac{V_i(P_{trial})\cdot M_{cr}}{M_{max}(P_{trial})} + V_d$$

$$V_{cilimit} := 1.7\sqrt{f'_c\cdot psi}\cdot b_w\cdot d_p$$

$$V_{ci}(P_{trial}) := \max\left(V_{ci}(P_{trial}), V_{cilimit}\right)$$

$$V_{cw} := b_w\cdot d_p\cdot\left(3.5\sqrt{f'_c\cdot psi} + 0.3 f_{pc}\right) = 170.116\,kip$$

$$V_c(P_{trial}) := \min\left(V_{ci}(P_{trial}), V_{cw}\right)$$

$$V_s := \frac{A_{stirrup}\cdot f_y\cdot d_p}{s} = 205.045\,kip$$

$V_n(P_{trial}) := V_c(P_{trial}) + V_s$

$V_{nlimit}(P_{trial}) := V_c(P_{trial}) + 8 \cdot \sqrt{f'_c \cdot psi} \cdot b_w \cdot d_p$

$V_n(P_{trial}) := \min(V_n(P_{trial}), V_{nlimit}(P_{trial}))$

$V_n(P_{trial}) = V_u(P_{trial})$ <- Convergence criteria

$P_{final} := \text{Minerr}(P_{trial})$

$P_{final} = 358.751\,kip$ <- Converge on applied load

Calculated ACI Shear Capacity:

$\boxed{V_n(P_{final}) = 375.16\,kip}$

Converged Values:

$V_i(P_{final}) = 358.751\,kip$

$M_u(P_{final}) = 48215.651\,kip \cdot in$

$M_{max}(P_{final}) = 45606.237\,kip \cdot in$

$V_{ci}(P_{final}) = 368.331\,kip$

$V_{cw} = 170.116\,kip$

$V_c(P_{final}) = 170.116\,kip$

$V_s = 205.045\,kip$

Figure D-14: Tx46-I Nominal Shear Capacity

Per ACI 318-14 11.5

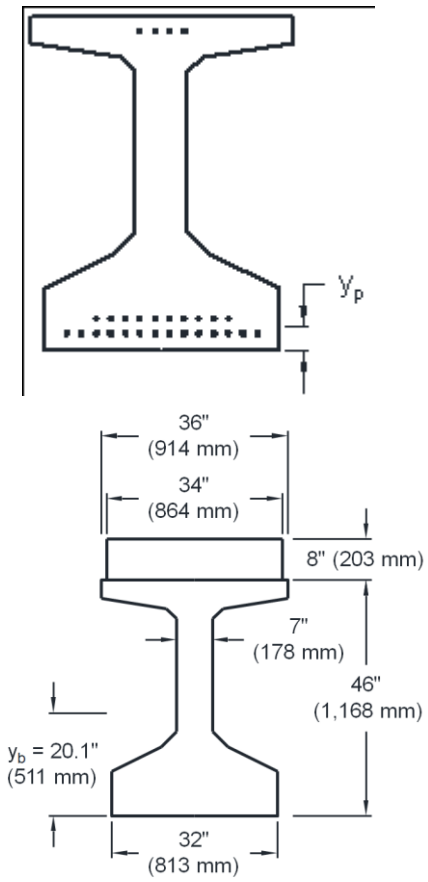

Input Parameters:

Specimen Geometry:

Beam Geometry:

$h_{beam} := 46in$

$b_f := 36in$

$b_w := 7in$

$y_b := 20.1in$

$A_g := 761in^2$

$L := 30ft$

$I_x := 198089in^4$

Deck Geometry:

$t_{deck} := 8in$

$b_{deck} := 34in$

$h_{deck} := 8in$

$A_{deck} := t_{deck} \cdot b_{deck} = 272 \cdot in^2$

Specimen Self Weight:

$SW := 34.830965kip$

$w_{sw} := \frac{SW}{L} = 0.09675\frac{kip}{in}$

Measured Material Properties:

Beam Concrete:

$f'_c := 7.6 \times 1000psi = 7600psi$

$E_c := 4915ksi$

Beam Concrete:

$f'_{cdeck} := 10.71 \times 1000psi = 10710psi$

$E_{cdeck} := 6934ksi$

Transformed Specimen Geometry:

$$n := \frac{E_{cdeck}}{E_c} = 1.411$$

$$h_{tot} := h_{beam} + h_{deck} = 54\,in$$

$$A_{tr} := A_g + A_{deck} \cdot n = 1144.733\,in^2$$

$$y_{tr} := \frac{A_g \cdot y_b + n \cdot A_{deck} \cdot \left(h_{tot} - \frac{t_{deck}}{2} \right)}{A_{tr}} = 30.123\,in$$

$$I_{tr} := I_x + \frac{n \cdot b_{deck} \cdot t_{deck}^{3}}{12} + n \cdot A_{deck} \cdot \left(h_{tot} - \frac{t_{deck}}{2} - y_{tr} \right)^2 = 351747.185\,in^4$$

Stirrups:

$$f_y := 60.7\,ksi$$

$$A_{stirrup} := 2 \cdot 0.2\,in^2 = 0.4\,in^2$$

$$E_s := 29000\,ksi$$

$$s := 6\,in$$

Prestressing Strands:

$$d_b := 0.7\,in$$

$$f_{po} := 157.4286089 \times 1000\,psi = 157428.609\,psi$$

$$E_p := 29000\,ksi$$

$$A_{strand} := 0.294\,in^2$$

$$N_{botstrands} := 24$$

$$A_{pbot} := A_{strand} \cdot N_{botstrands} = 7.056\,in^2$$

$$L_{transfer} := 50 \cdot d_b = 35\,in$$

$$P_{ps} := f_{po} \cdot A_{pbot} = 1110.816\,kip$$

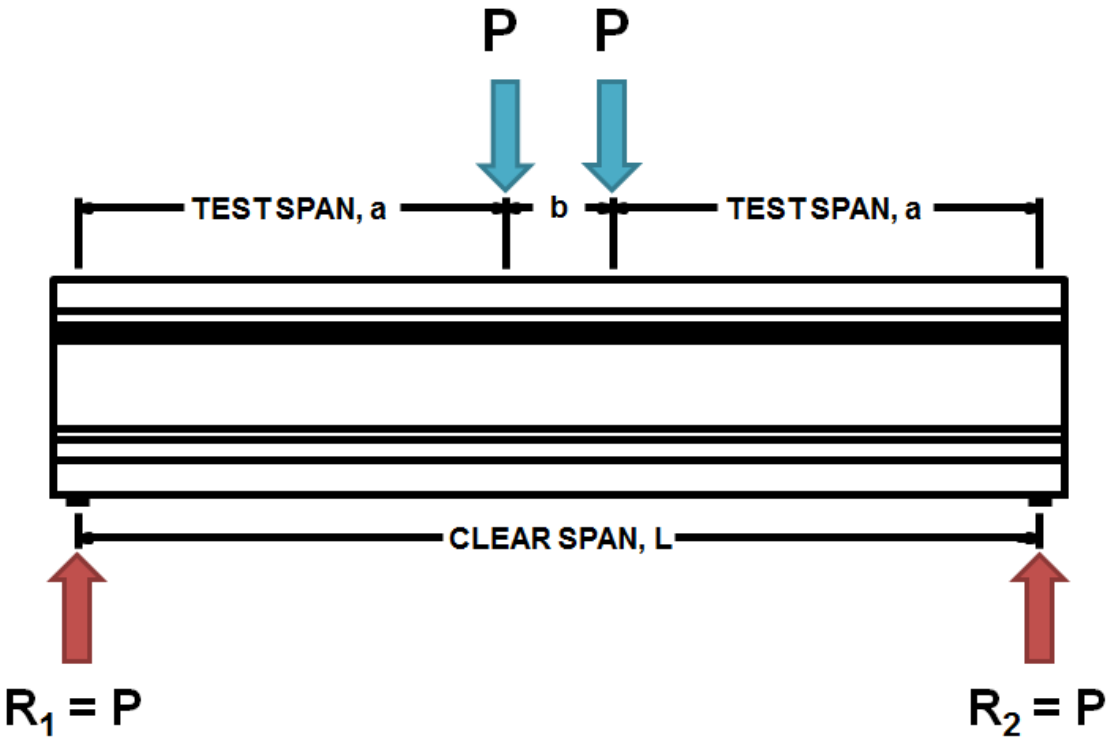

Shear Test Setup:

$L_{span} := 342in$

$a := 151.125in$ <- Measured as built

$P_{trial} := 515kip$ <- Initial guess for subsequent calcs

$y_p := 3.33in$

$d_p := max\left(0.8 \cdot h_{tot}, h_{tot} - y_p\right) = 50.67in$

$L_{bearing} := 8in$

$L_{loadplate} := 12in$

$L_{oh} := 9in$

$x_{crit} := \frac{h_{tot}}{2} + L_{oh} + \frac{L_{bearing}}{2} = 40in$ <- Location of critical section for shear taken from left end face

$W_{loadframe} := 22.586385kip$

$W_{beam} := 34.830965kip$

$e_p := y_b - y_p = 16.77in$ <- Eccentricity of strand centroid

Solve for Nominal Shear Capacity:

Given <- Solve block for P_trial

$$V_u(P_{trial}) := P_{trial} + \frac{W_{loadframe}}{2} + \frac{W_{beam}}{2} - w_{sw} \cdot x_{crit}$$

$$V_d := \frac{W_{beam} + W_{loadframe}}{2} - w_{sw} \cdot x_{crit} = 24.839\,kip$$

$$V_i(P_{trial}) := V_u(P_{trial}) - V_d$$

$$M_u(P_{trial}) := -w_{sw} \cdot \frac{x_{crit}^2}{2} + \left(\frac{W_{beam} + W_{loadframe}}{2}\right) \cdot (x_{crit} - L_{oh}) + P_{trial} \cdot x_{crit}$$

$$M_{sw} := -w_{sw} \cdot \frac{x_{crit}^2}{2} + \frac{W_{beam}}{2} \cdot (x_{crit} - L_{oh}) = 462.478\,kip \cdot in$$

$$M_d := \frac{W_{loadframe}}{2} \cdot (x_{crit} - L_{oh}) = 350.089\,kip \cdot in$$

$$M_{dtot} := M_{sw} + M_d = 812.567\,kip \cdot in$$

$$M_{max}(P_{trial}) := M_u(P_{trial}) - M_{dtot}$$

$$f_d := \frac{M_{sw} \cdot y_b}{I_x} + \frac{M_d \cdot y_{tr}}{I_{tr}} = 76.908\,psi$$

$$f_{pe} := \frac{P_{ps}}{A_g} + P_{ps} \cdot e_p \cdot \frac{y_b}{I_x} = 3349.894\,psi$$

$$f_{pc} := \frac{P_{ps}}{A_g} - \left[P_{ps} \cdot e_p \cdot \frac{(y_{tr} - y_b)}{I_x}\right] + M_{sw} \cdot \frac{(y_{tr} - y_b)}{I_x} = 540.516\,psi$$

$$M_{cr} := \left(\frac{I_{tr}}{y_{tr}}\right) \cdot \left(6 \cdot \sqrt{f'_c \cdot psi} + f_{pe} - f_d\right) = 44326.682\,kip \cdot in$$

$$V_{ci}(P_{trial}) := 0.6\sqrt{f'_c \cdot psi} \cdot b_w \cdot d_p + \frac{V_i(P_{trial}) \cdot M_{cr}}{M_{max}(P_{trial})} + V_d$$

$$V_{cilimit} := 1.7\sqrt{f'_c \cdot psi} \cdot b_w \cdot d_p$$

$$V_{ci}(P_{trial}) := \max(V_{ci}(P_{trial}), V_{cilimit})$$

$$V_{cw} := b_w \cdot d_p \cdot \left(3.5\sqrt{f'_c \cdot psi} + 0.3 f_{pc}\right) = 165.739\,kip$$

$$V_c(P_{trial}) := \min(V_{ci}(P_{trial}), V_{cw})$$

$$V_s := \frac{A_{stirrup} \cdot f_y \cdot d_p}{s} = 205.045\,kip$$

$V_n(P_{trial}) := V_c(P_{trial}) + V_s$

$V_{nlimit}(P_{trial}) := V_c(P_{trial}) + 8 \cdot \sqrt{f'_c \cdot psi} \cdot b_w \cdot d_p$

$V_n(P_{trial}) := \min(V_n(P_{trial}), V_{nlimit}(P_{trial}))$

$V_n(P_{trial}) = V_u(P_{trial})$ <- Convergence criteria

$P_{final} := \text{Minerr}(P_{trial})$

$P_{final} = 345.945kip$ <- Converge on applied load

Calculated ACI Shear Capacity:

$$V_n(P_{final}) = 370.783kip$$

Converged Values:

$V_i(P_{final}) = 345.945kip$

$M_u(P_{final}) = 14650.356kip \cdot in$

$M_{max}(P_{final}) = 13837.79kip \cdot in$

$V_{ci}(P_{final}) = 1151.558kip$

$V_{cw} = 165.739kip$

$V_c(P_{final}) = 165.739kip$

$V_s = 205.045kip$

Figure D-15: Tx46-II Nominal Shear Capacity

Per ACI 318-14 11.5

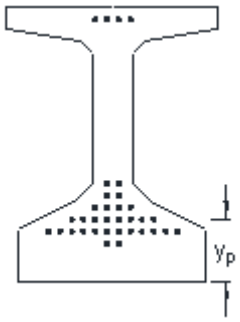

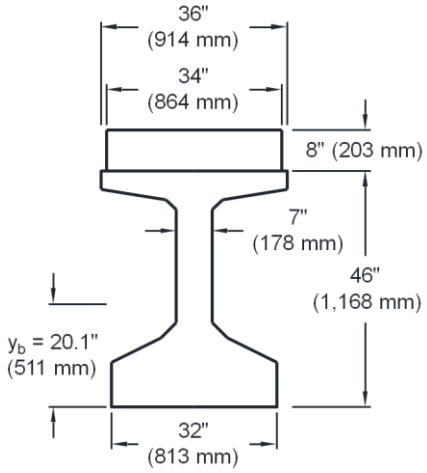

Input Parameters:

Specimen Geometry:

Beam Geometry:

$h_{beam} := 46in$

$b_f := 36in$

$b_w := 7in$

$y_b := 20.1in$

$A_g := 761in^2$

$L := 30ft$

$I_x := 198089in^4$

Deck Geometry:

$t_{deck} := 8in$

$b_{deck} := 34in$

$h_{deck} := 8in$

$A_{deck} := t_{deck} \cdot b_{deck} = 272 \cdot in^2$

Specimen Self Weight:

$SW := 34.542858kip$

$w_{sw} := \frac{SW}{L} = 0.095952\frac{kip}{in}$

Measured Material Properties:

Beam Concrete:

$f'_c := 6.92 \times 1000psi = 6920psi$

$E_c := 5424ksi$

Beam Concrete:

$f'_{cdeck} := 7.93 \times 1000psi = 7930psi$

$E_{cdeck} := 5906ksi$

Transformed Specimen Geometry:

$$n := \frac{E_{cdeck}}{E_c} = 1.089$$

$$h_{tot} := h_{beam} + h_{deck} = 54\,in$$

$$A_{tr} := A_g + A_{deck} \cdot n = 1057.171\,in^2$$

$$y_{tr} := \frac{A_g \cdot y_b + n \cdot A_{deck} \cdot \left(h_{tot} - \frac{t_{deck}}{2} \right)}{A_{tr}} = 28.477\,in$$

$$I_{tr} := I_x + \frac{n \cdot b_{deck} \cdot t_{deck}^{3}}{12} + n \cdot A_{deck} \cdot \left(h_{tot} - \frac{t_{deck}}{2} - y_{tr} \right)^2 = 336871.639\,in^4$$

Stirrups:

$f_y := 60.7\,ksi$

$A_{stirrup} := 2 \cdot 0.2\,in^2 = 0.4\,in^2$

$E_s := 29000\,ksi$

$s := 6\,in$

Prestressing Strands:

$d_b := 0.7\,in$

$f_{po} := 166.87384 \times 1000\,psi = 166873.84\,psi$

$E_p := 29000\,ksi$

$A_{strand} := 0.294\,in^2$

$N_{botstrands} := 30$

$A_{pbot} := A_{strand} \cdot N_{botstrands} = 8.82\,in^2$

$L_{transfer} := 50 \cdot d_b = 35\,in$

$P_{ps} := f_{po} \cdot A_{pbot} = 1471.827\,kip$

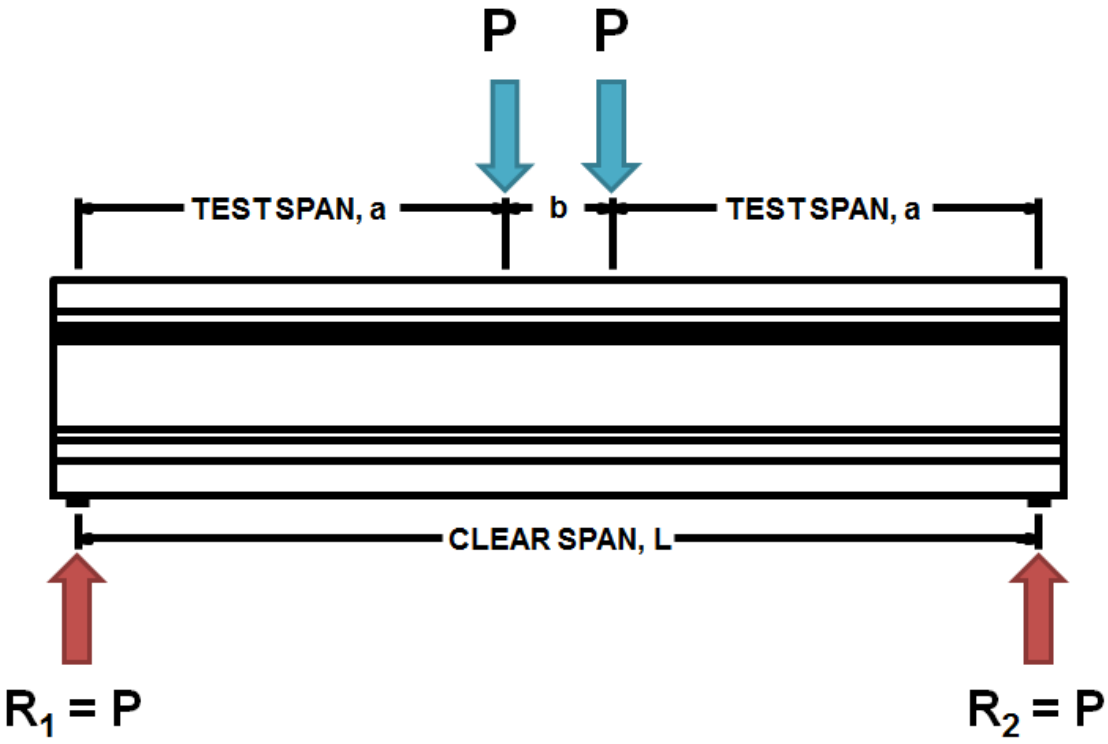

Shear Test Setup:

$L_{span} := 342in$

$a := 130.8in$ <- Measured as built

$P_{trial} := 515kip$ <- Initial guess for subsequent calcs

$y_p := 10.37in$

$d_p := max\left(0.8 \cdot h_{tot}, h_{tot} - y_p\right) = 43.63in$

$L_{bearing} := 8in$

$L_{loadplate} := 12in$

$L_{oh} := 9in$

$x_{crit} := a + L_{oh} - \frac{L_{loadplate}}{2} - \frac{h_{tot}}{2} = 106.8in$ <- Location of critical section for shear taken from left end face

$W_{loadframe} := 22.586385kip$

$W_{beam} := 34.542853kip$

$e_p := y_b - y_p = 9.73in$ <- Eccentricity of strand centroid

Solve for Nominal Shear Capacity:

Given <- Solve block for P_trial

$$V_u(P_{trial}) := P_{trial} + \frac{W_{loadframe}}{2} + \frac{W_{beam}}{2} - w_{sw} \cdot x_{crit}$$

$$V_d := \frac{W_{beam} + W_{loadframe}}{2} - w_{sw} \cdot x_{crit} = 18.317\,kip$$

$$V_i(P_{trial}) := V_u(P_{trial}) - V_d$$

$$M_u(P_{trial}) := -w_{sw} \cdot \frac{x_{crit}^2}{2} + \left(\frac{W_{beam} + W_{loadframe}}{2}\right) \cdot (x_{crit} - L_{oh}) + P_{trial} \cdot x_{crit}$$

$$M_{sw} := -w_{sw} \cdot \frac{x_{crit}^2}{2} + \frac{W_{beam}}{2} \cdot (x_{crit} - L_{oh}) = 1.142 \times 10^3 \cdot kip \cdot in$$

$$M_d := \frac{W_{loadframe}}{2} \cdot (x_{crit} - L_{oh}) = 1.104 \times 10^3 \cdot kip \cdot in$$

$$M_{dtot} := M_{sw} + M_d = 2.246 \times 10^3 \cdot kip \cdot in$$

$$M_{max}(P_{trial}) := M_u(P_{trial}) - M_{dtot}$$

$$f_d := \frac{M_{sw} \cdot y_b}{I_x} + \frac{M_d \cdot y_{tr}}{I_{tr}} = 209.234\,psi$$

$$f_{pe} := \frac{P_{ps}}{A_g} + P_{ps} \cdot e_p \cdot \frac{y_b}{I_x} = 3387.203\,psi$$

$$f_{pc} := \frac{P_{ps}}{A_g} - \left[P_{ps} \cdot e_p \cdot \frac{(y_{tr} - y_b)}{I_x}\right] + M_{sw} \cdot \frac{(y_{tr} - y_b)}{I_x} = 1.377 \times 10^3\,psi$$

$$M_{cr} := \left(\frac{I_{tr}}{y_{tr}}\right) \cdot \left(6 \cdot \sqrt{f'_c \cdot psi} + f_{pe} - f_d\right) = 43499.088\,kip \cdot in$$

$$V_{ci}(P_{trial}) := 0.6\sqrt{f'_c \cdot psi} \cdot b_w \cdot d_p + \frac{V_i(P_{trial}) \cdot M_{cr}}{M_{max}(P_{trial})} + V_d$$

$$V_{cilimit} := 1.7\sqrt{f'_c \cdot psi} \cdot b_w \cdot d_p$$

$$V_{ci}(P_{trial}) := \max(V_{ci}(P_{trial}), V_{cilimit})$$

$$V_{cw} := b_w \cdot d_p \cdot \left(3.5\sqrt{f'_c \cdot psi} + 0.3 f_{pc}\right) = 215.065\,kip$$

$$V_c(P_{trial}) := \min(V_{ci}(P_{trial}), V_{cw})$$

$$V_s := \frac{A_{stirrup} \cdot f_y \cdot d_p}{s} = 176.556\,kip$$

$V_n(P_{trial}) := V_c(P_{trial}) + V_s$

$V_{nlimit}(P_{trial}) := V_c(P_{trial}) + 8 \cdot \sqrt{f'_c \cdot psi} \cdot b_w \cdot d_p$

$V_n(P_{trial}) := \min(V_n(P_{trial}), V_{nlimit}(P_{trial}))$

$V_n(P_{trial}) = V_u(P_{trial})$ <- Convergence criteria

$P_{final} := \text{Minerr}(P_{trial})$

$P_{final} = 373.304 kip$ <- Converge on applied load

Calculated ACI Shear Capacity:

$$V_n(P_{final}) = 391.621 kip$$

Converged Values:

$V_i(P_{final}) = 373.304 kip$

$M_u(P_{final}) = 42115.25 kip \cdot in$

$M_{max}(P_{final}) = 39868.858 kip \cdot in$

$V_{ci}(P_{final}) = 440.855 kip$

$V_{cw} = 215.065 kip$

$V_c(P_{final}) = 215.065 kip$

$V_s = 176.556 kip$

Figure D-16: Tx46-II Nominal Shear Capacity

Per ACI 318-14 11.5

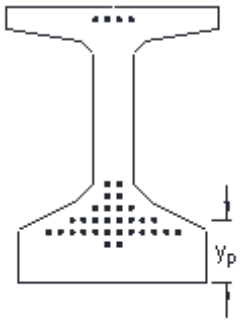

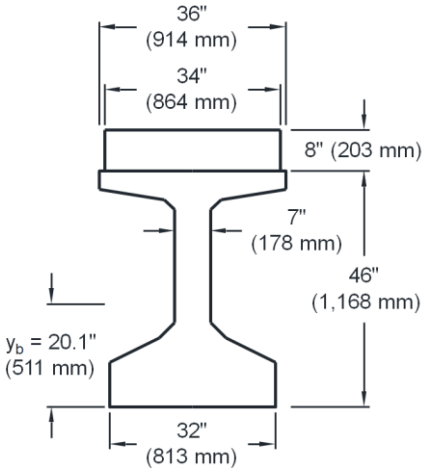

Input Parameters:

Specimen Geometry:

Beam Geometry:

$h_{beam} := 46in$

$b_f := 36in$

$b_w := 7in$

$y_b := 20.1in$

$A_g := 761in^2$

$L := 30ft$

$I_x := 198089in^4$

Deck Geometry:

$t_{deck} := 8in$

$b_{deck} := 34in$

$h_{deck} := 8in$

$A_{deck} := t_{deck} \cdot b_{deck} = 272 \cdot in^2$

Specimen Self Weight:

$SW := 34.542853kip$

$w_{sw} := \frac{SW}{L} = 0.095952\frac{kip}{in}$

Measured Material Properties:

Beam Concrete:

$f'_c := 6.92 \times 1000psi = 6920psi$

$E_c := 5424ksi$

Beam Concrete:

$f'_{cdeck} := 7.93 \times 1000psi = 7930psi$

$E_{cdeck} := 5906ksi$

Transformed Specimen Geometry:

$$n := \frac{E_{cdeck}}{E_c} = 1.089$$

$$h_{tot} := h_{beam} + h_{deck} = 54\,in$$

$$A_{tr} := A_g + A_{deck} \cdot n = 1057.171\,in^2$$

$$y_{tr} := \frac{A_g \cdot y_b + n \cdot A_{deck} \cdot \left(h_{tot} - \frac{t_{deck}}{2} \right)}{A_{tr}} = 28.477\,in$$

$$I_{tr} := I_x + \frac{n \cdot b_{deck} \cdot t_{deck}^{3}}{12} + n \cdot A_{deck} \cdot \left(h_{tot} - \frac{t_{deck}}{2} - y_{tr} \right)^2 = 336871.639\,in^4$$

Stirrups:

$f_y := 60.7\,ksi$

$A_{stirrup} := 2 \cdot 0.2\,in^2 = 0.4\,in^2$

$E_s := 29000\,ksi$

$s := 6\,in$

Prestressing Strands:

$d_b := 0.7\,in$

$f_{po} := 166.87384 \times 1000\,psi = 166873.84\,psi$

$E_p := 29000\,ksi$

$A_{strand} := 0.294\,in^2$

$N_{botstrands} := 30$

$A_{pbot} := A_{strand} \cdot N_{botstrands} = 8.82\,in^2$

$L_{transfer} := 50 \cdot d_b = 35\,in$

$P_{ps} := f_{po} \cdot A_{pbot} = 1471.827\,kip$

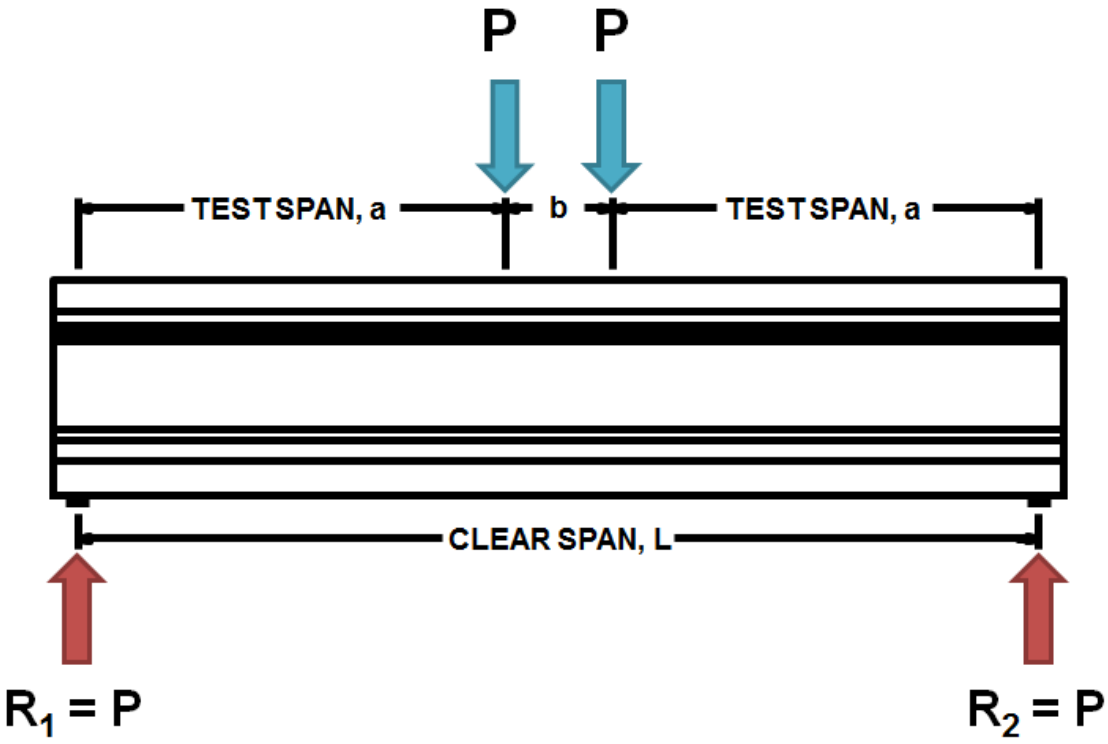

Shear Test Setup:

$L_{span} := 342in$

$a := 130.8in$ <- Measured as built

$P_{trial} := 515kip$ <- Initial guess for subsequent calcs

$y_p := 10.37in$

$d_p := max\left(0.8 \cdot h_{tot}, h_{tot} - y_p\right) = 43.63\,in$

$L_{bearing} := 8in$

$L_{loadplate} := 12in$

$L_{oh} := 9in$

$x_{crit} := \frac{h_{tot}}{2} + L_{oh} + \frac{L_{bearing}}{2} = 40 \cdot in$ <- Location of critical section for shear taken from left end face

$W_{loadframe} := 22.586385kip$

$W_{beam} := 34.542853kip$

$e_p := y_b - y_p = 9.73 \cdot in$ <- Eccentricity of strand centroid

Solve for Nominal Shear Capacity:

Given <- Solve block for P_trial

$$V_u(P_{trial}) := P_{trial} + \frac{W_{loadframe}}{2} + \frac{W_{beam}}{2} - w_{sw} \cdot x_{crit}$$

$$V_d := \frac{W_{beam} + W_{loadframe}}{2} - w_{sw} \cdot x_{crit} = 24.727\,kip$$

$$V_i(P_{trial}) := V_u(P_{trial}) - V_d$$

$$M_u(P_{trial}) := -w_{sw} \cdot \frac{x_{crit}^2}{2} + \left(\frac{W_{beam} + W_{loadframe}}{2}\right) \cdot (x_{crit} - L_{oh}) + P_{trial} \cdot x_{crit}$$

$$M_{sw} := -w_{sw} \cdot \frac{x_{crit}^2}{2} + \frac{W_{beam}}{2} \cdot (x_{crit} - L_{oh}) = 458.652\,kip \cdot in$$

$$M_d := \frac{W_{loadframe}}{2} \cdot (x_{crit} - L_{oh}) = 350.089\,kip \cdot in$$

$$M_{dtot} := M_{sw} + M_d = 808.741\,kip \cdot in$$

$$M_{max}(P_{trial}) := M_u(P_{trial}) - M_{dtot}$$

$$f_d := \frac{M_{sw} \cdot y_b}{I_x} + \frac{M_d \cdot y_{tr}}{I_{tr}} = 76.133\,psi$$

$$f_{pe} := \frac{P_{ps}}{A_g} + P_{ps} \cdot e_p \cdot \frac{y_b}{I_x} = 3387.203\,psi$$

$$f_{pc} := \frac{P_{ps}}{A_g} - \left[P_{ps} \cdot e_p \cdot \frac{(y_{tr} - y_b)}{I_x}\right] + M_{sw} \cdot \frac{(y_{tr} - y_b)}{I_x} = 1.348 \times 10^3\,psi$$

$$M_{cr} := \left(\frac{I_{tr}}{y_{tr}}\right) \cdot \left(6 \cdot \sqrt{f'_c \cdot psi} + f_{pe} - f_d\right) = 45073.638\,kip \cdot in$$

$$V_{ci}(P_{trial}) := 0.6\sqrt{f'_c \cdot psi} \cdot b_w \cdot d_p + \frac{V_i(P_{trial}) \cdot M_{cr}}{M_{max}(P_{trial})} + V_d$$

$$V_{cilimit} := 1.7\sqrt{f'_c \cdot psi} \cdot b_w \cdot d_p$$

$$V_{ci}(P_{trial}) := \max(V_{ci}(P_{trial}), V_{cilimit})$$

$$V_{cw} := b_w \cdot d_p \cdot \left(3.5\sqrt{f'_c \cdot psi} + 0.3 f_{pc}\right) = 212.417\,kip$$

$$V_c(P_{trial}) := \min(V_{ci}(P_{trial}), V_{cw})$$

$$V_s := \frac{A_{stirrup} \cdot f_y \cdot d_p}{s} = 176.556\,kip$$

$V_n(P_{trial}) := V_c(P_{trial}) + V_s$

$V_{nlimit}(P_{trial}) := V_c(P_{trial}) + 8 \cdot \sqrt{f'_c \cdot psi} \cdot b_w \cdot d_p$

$V_n(P_{trial}) := \min(V_n(P_{trial}), V_{nlimit}(P_{trial}))$

$V_n(P_{trial}) = V_u(P_{trial})$ <- Convergence criteria

$P_{final} := \text{Minerr}(P_{trial})$

$P_{final} = 364.247 kip$ <- Converge on applied load

Calculated ACI Shear Capacity:

$V_n(P_{final}) = 388.974 kip$

Converged Values:

$V_i(P_{final}) = 364.247 kip$

$M_u(P_{final}) = 15378.621 kip \cdot in$

$M_{max}(P_{final}) = 14569.88 kip \cdot in$

$V_{ci}(P_{final}) = 1166.811 kip$

$V_{cw} = 212.417 kip$

$V_c(P_{final}) = 212.417 kip$

$V_s = 176.556 kip$

Figure D-17: Tx70-I Nominal Shear Capacity

Per ACI 318-14 11.5

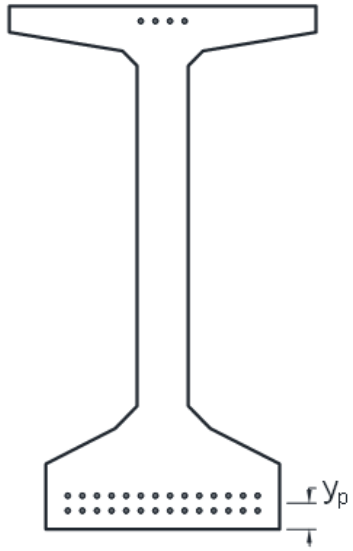

Input Parameters:

Specimen Geometry:

Beam Geometry:

$h_{beam} := 70in$

$b_f := 42in$

$b_w := 7in$

$y_b := 31.91in$

$A_g := 966in^2$

$L := 30ft$

$I_x := 628747in^4$

Deck Geometry:

$t_{deck} := 8in$

$b_{deck} := 40in$

$h_{deck} := 8in$

$A_{deck} := t_{deck} \cdot b_{deck} = 320in^2$

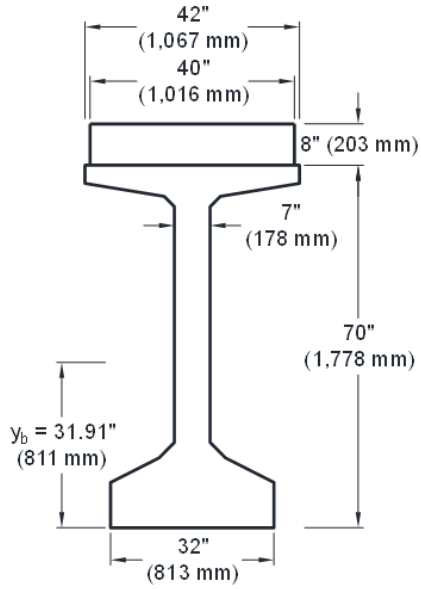

Specimen Self Weight:

$SW := 41.145608kip$

$w_{sw} := \frac{SW}{L} = 0.11429\frac{kip}{in}$

Measured Material Properties:

Beam Concrete:

$f'_c := 10.71 \times 1000psi = 10710psi$

$E_c := 6096ksi$

Beam Concrete:

$f'_{cdeck} := 7.94 \times 1000psi = 7940psi$

$E_{cdeck} := 5966ksi$

Transformed Specimen Geometry:

$$n := \frac{E_{cdeck}}{E_c} = 0.979$$

$$h_{tot} := h_{beam} + h_{deck} = 78\,in$$

$$A_{tr} := A_g + A_{deck} \cdot n = 1279.176\,in^2$$

$$y_{tr} := \frac{A_g \cdot y_b + n \cdot A_{deck} \cdot \left(h_{tot} - \frac{t_{deck}}{2} \right)}{A_{tr}} = 42.215\,in$$

$$I_{tr} := I_x + \frac{n \cdot b_{deck} \cdot t_{deck}^{3}}{12} + n \cdot A_{deck} \cdot \left(h_{tot} - \frac{t_{deck}}{2} - y_{tr} \right)^2 = 946819.743\,in^4$$

Stirrups:

$$f_y := 72.2\,ksi$$

$$A_{stirrup} := 2 \cdot 0.2\,in^2 = 0.4\,in^2$$

$$E_s := 29000\,ksi$$

$$s := 8\,in$$

Prestressing Strands:

$$d_b := 0.7\,in$$

$$f_{po} := 163.8204 \times 1000\,psi = 163820.4\,psi$$

$$E_p := 29000\,ksi$$

$$A_{strand} := 0.294\,in^2$$

$$N_{botstrands} := 28$$

$$A_{pbot} := A_{strand} \cdot N_{botstrands} = 8.232\,in^2$$

$$L_{transfer} := 50 \cdot d_b = 35\,in$$

$$P_{ps} := f_{po} \cdot A_{pbot} = 1348.57\,kip$$

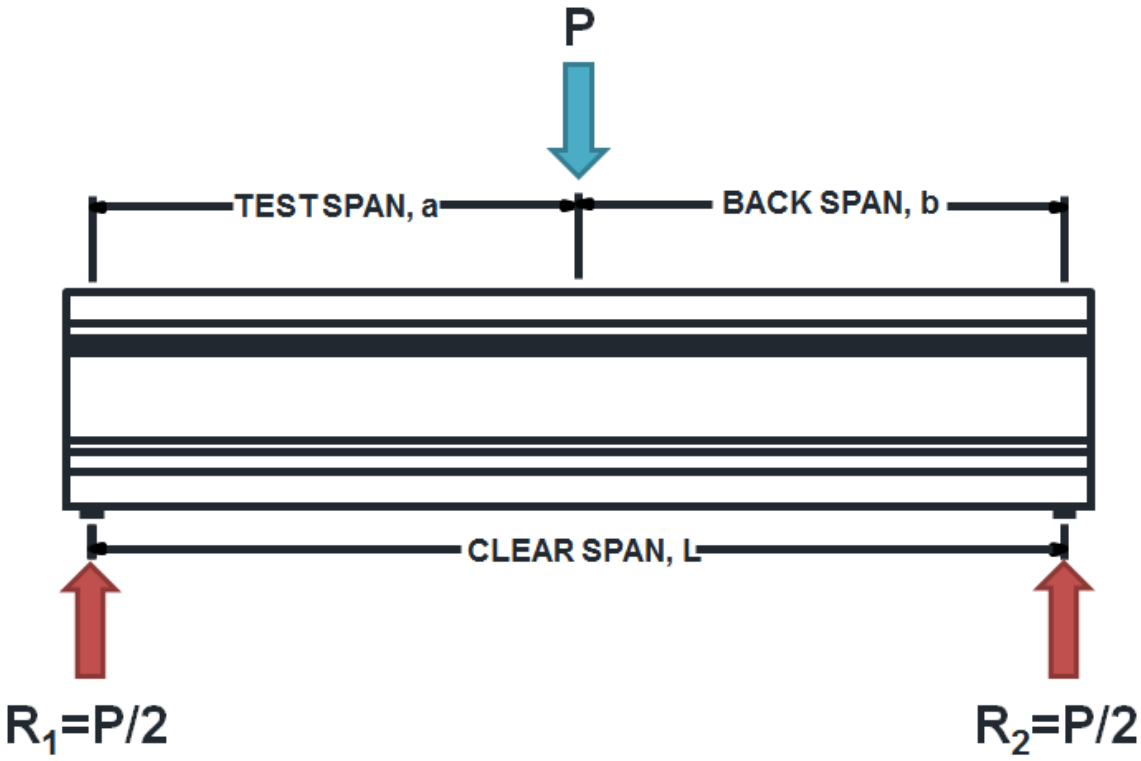

Shear Test Setup:

$L_{span} := 342in$

$a := 171.125in$ <- Measured as built

$P_{trial} := 515kip$ <- Initial guess for subsequent calcs

$y_p := 3.5in$

$d_p := max\left(0.8 \cdot h_{tot}, h_{tot} - y_p\right) = 74.5 \cdot in$

$L_{bearing} := 9in$

$L_{loadplate} := 12in$

$L_{oh} := 9in$

$x_{crit} := a + L_{oh} - \frac{L_{loadplate}}{2} - \frac{h_{tot}}{2} = 135.125in$ <- Location of critical section for shear taken from left end face

$W_{loadframe} := 17.352164kip$

$W_{beam} := 41.145608kip$

$e_p := y_b - y_p = 28.41 \cdot in$ <- Eccentricity of strand centroid

Solve for Nominal Shear Capacity:

Given <- Solve block for P_trial

$$V_u(P_{trial}) := P_{trial} + \frac{W_{loadframe}}{2} + \frac{W_{beam}}{2} - w_{sw}\cdot x_{crit}$$

$$V_d := \frac{W_{beam} + W_{loadframe}}{2} - w_{sw}\cdot x_{crit} = 13.805\,kip$$

$$V_i(P_{trial}) := V_u(P_{trial}) - V_d$$

$$M_u(P_{trial}) := -w_{sw}\cdot\frac{x_{crit}^2}{2} + \left(\frac{W_{beam} + W_{loadframe}}{2}\right)\cdot\left(x_{crit} - L_{oh}\right) + P_{trial}\cdot x_{crit}$$

$$M_{sw} := -w_{sw}\cdot\frac{x_{crit}^2}{2} + \frac{W_{beam}}{2}\cdot\left(x_{crit} - L_{oh}\right) = 1.551\times 10^3\cdot kip\cdot in$$

$$M_d := \frac{W_{loadframe}}{2}\cdot\left(x_{crit} - L_{oh}\right) = 1.094\times 10^3\cdot kip\cdot in$$

$$M_{dtot} := M_{sw} + M_d = 2645.588\,kip\cdot in$$

$$M_{max}(P_{trial}) := M_u(P_{trial}) - M_{dtot}$$

$$f_d := \frac{M_{sw}\cdot y_b}{I_x} + \frac{M_d\cdot y_{tr}}{I_{tr}} = 127.521\,psi$$

$$f_{pe} := \frac{P_{ps}}{A_g} + P_{ps}\cdot e_p\cdot\frac{y_b}{I_x} = 3340.479\,psi$$

$$f_{pc} := \frac{P_{ps}}{A_g} - \left[P_{ps}\cdot e_p\cdot\frac{\left(y_{tr} - y_b\right)}{I_x}\right] + M_{sw}\cdot\frac{\left(y_{tr} - y_b\right)}{I_x} = 793.538\,psi$$

$$M_{cr} := \left(\frac{I_{tr}}{y_{tr}}\right)\cdot\left(6\cdot\sqrt{f'_c\cdot psi} + f_{pe} - f_d\right) = 85989.05\,kip\cdot in$$

$$V_{ci}(P_{trial}) := 0.6\sqrt{f'_c\cdot psi}\cdot b_w\cdot d_p + \frac{V_i(P_{trial})\cdot M_{cr}}{M_{max}(P_{trial})} + V_d$$

$$V_{cilimit} := 1.7\sqrt{f'_c\cdot psi}\cdot b_w\cdot d_p$$

$$V_{ci}(P_{trial}) := \max\left(V_{ci}(P_{trial}), V_{cilimit}\right)$$

$$V_{cw} := b_w\cdot d_p\cdot\left(3.5\sqrt{f'_c\cdot psi} + 0.3 f_{pc}\right) = 313.043\,kip$$

$$V_c(P_{trial}) := \min\left(V_{ci}(P_{trial}), V_{cw}\right)$$

$$V_s := \frac{A_{stirrup}\cdot f_y\cdot d_p}{s} = 268.945\,kip$$

$V_n(P_{trial}) := V_c(P_{trial}) + V_s$

$V_{nlimit}(P_{trial}) := V_c(P_{trial}) + 8 \cdot \sqrt{f_c \cdot psi} \cdot b_w \cdot d_p$

$V_n(P_{trial}) := \min(V_n(P_{trial}), V_{nlimit}(P_{trial}))$

$V_n(P_{trial}) = V_u(P_{trial})$ <- Convergence criteria

$P_{final} := \text{Minerr}(P_{trial})$

$P_{final} = 568.183kip$ <- Converge on applied load

Calculated ACI Shear Capacity:

$V_n(P_{final}) = 581.988kip$

Converged Values:

$V_i(P_{final}) = 568.183kip$

$M_u(P_{final}) = 79421.254kip \cdot in$

$M_{max}(P_{final}) = 76775.666kip \cdot in$

$V_{ci}(P_{final}) = 682.553kip$

$V_{cw} = 313.043kip$

$V_c(P_{final}) = 313.043kip$

$V_s = 268.945kip$

Figure D-18: Tx70-I Nominal Shear Capacity

Per ACI 318-14 11.5

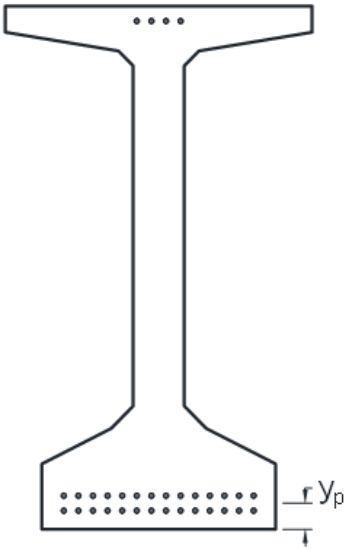

Input Parameters:

Specimen Geometry:

Beam Geometry:

$h_{beam} := 70in$

$b_f := 42in$

$b_w := 7in$

$y_b := 31.91in$

$A_g := 966in^2$

$L := 30ft$

$I_x := 628747in^4$

Deck Geometry:

$t_{deck} := 8in$

$b_{deck} := 40in$

$h_{deck} := 8in$

$A_{deck} := t_{deck} \cdot b_{deck} = 320in^2$

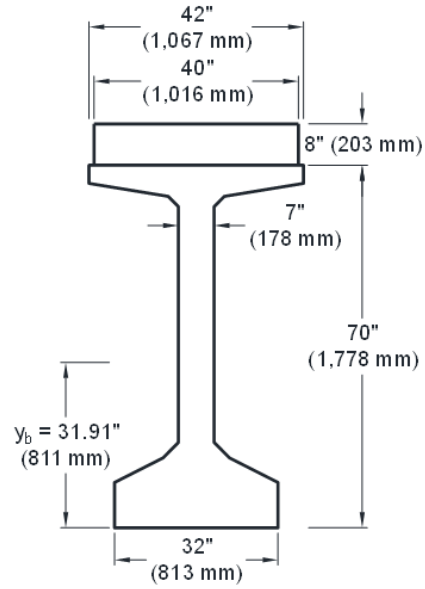

Specimen Self Weight:

$SW := 41.145608kip$

$w_{sw} := \frac{SW}{L} = 0.11429\frac{kip}{in}$

Measured Material Properties:

Beam Concrete:

$f'_c := 10.71 \times 1000psi = 10710psi$

$E_c := 6096ksi$

Beam Concrete:

$f'_{cdeck} := 7.94 \times 1000psi = 7940psi$

$E_{cdeck} := 5966ksi$

Transformed Specimen Geometry:

$$n := \frac{E_{cdeck}}{E_c} = 0.979$$

$$h_{tot} := h_{beam} + h_{deck} = 78\cdot in$$

$$A_{tr} := A_g + A_{deck}\cdot n = 1279.176\,in^2$$

$$y_{tr} := \frac{A_g\cdot y_b + n\cdot A_{deck}\cdot\left(h_{tot} - \frac{t_{deck}}{2}\right)}{A_{tr}} = 42.215\,in$$

$$I_{tr} := I_x + \frac{n\cdot b_{deck}\cdot t_{deck}^{3}}{12} + n\cdot A_{deck}\cdot\left(h_{tot} - \frac{t_{deck}}{2} - y_{tr}\right)^2 = 946819.743\,in^4$$

Stirrups:

$$f_y := 72.2ksi$$

$$A_{stirrup} := 2\cdot 0.2in^2 = 0.4\,in^2$$

$$E_s := 29000ksi$$

$$s := 8in$$

Prestressing Strands:

$$d_b := 0.7in$$

$$f_{po} := 163.8204\times 1000psi = 163820.4\,psi$$

$$E_p := 29000ksi$$

$$A_{strand} := 0.294in^2$$

$$N_{botstrands} := 28$$

$$A_{pbot} := A_{strand}\cdot N_{botstrands} = 8.232\,in^2$$

$$L_{transfer} := 50\cdot d_b = 35\cdot in$$

$$P_{ps} := f_{po}\cdot A_{pbot} = 1348.57kip$$

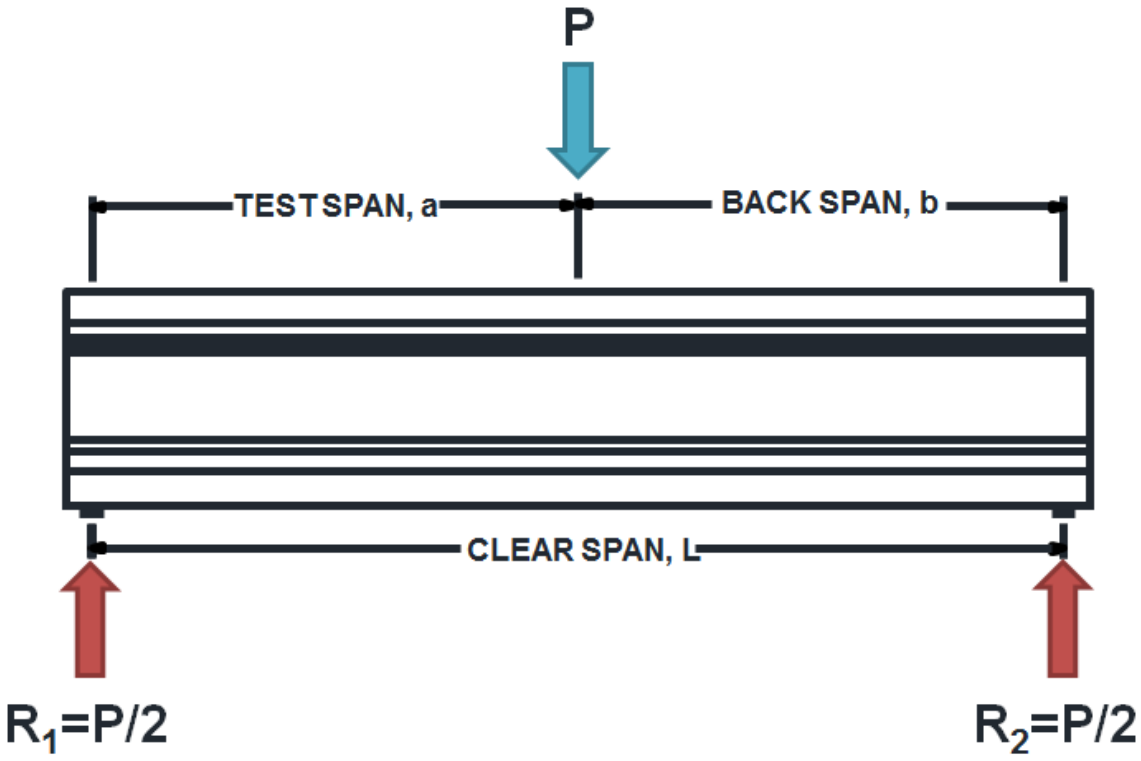

Shear Test Setup:

$L_{span} := 342in$

$a := 171.125in$ <- Measured as built

$P_{trial} := 515kip$ <- Initial guess for subsequent calcs

$y_p := 3.5in$

$d_p := max\left(0.8 \cdot h_{tot}, h_{tot} - y_p\right) = 74.5 in$

$L_{bearing} := 9in$

$L_{loadplate} := 12in$

$L_{oh} := 9in$

$x_{crit} := \frac{h_{tot}}{2} + L_{oh} + \frac{L_{bearing}}{2} = 52.5 in$ <- Location of critical section for shear taken from left end face

$W_{loadframe} := 17.352164kip$

$W_{beam} := 41.145608kip$

$e_p := y_b - y_p = 28.41 in$ <- Eccentricity of strand centroid

Solve for Nominal Shear Capacity:

Given <- Solve block for P_trial

$$V_u(P_{trial}) := P_{trial} + \frac{W_{loadframe}}{2} + \frac{W_{beam}}{2} - w_{sw} \cdot x_{crit}$$

$$V_d := \frac{W_{beam} + W_{loadframe}}{2} - w_{sw} \cdot x_{crit} = 23.248\,kip$$

$$V_i(P_{trial}) := V_u(P_{trial}) - V_d$$

$$M_u(P_{trial}) := -w_{sw} \cdot \frac{x_{crit}^2}{2} + \left(\frac{W_{beam} + W_{loadframe}}{2}\right) \cdot (x_{crit} - L_{oh}) + P_{trial} \cdot x_{crit}$$

$$M_{sw} := -w_{sw} \cdot \frac{x_{crit}^2}{2} + \frac{W_{beam}}{2} \cdot (x_{crit} - L_{oh}) = 737.406\,kip \cdot in$$

$$M_d := \frac{W_{loadframe}}{2} \cdot (x_{crit} - L_{oh}) = 377.41\,kip \cdot in$$

$$M_{dtot} := M_{sw} + M_d = 1114.816\,kip \cdot in$$

$$M_{max}(P_{trial}) := M_u(P_{trial}) - M_{dtot}$$

$$f_d := \frac{M_{sw} \cdot y_b}{I_x} + \frac{M_d \cdot y_{tr}}{I_{tr}} = 54.252\,psi$$

$$f_{pe} := \frac{P_{ps}}{A_g} + P_{ps} \cdot e_p \cdot \frac{y_b}{I_x} = 3340.479\,psi$$

$$f_{pc} := \frac{P_{ps}}{A_g} - \left[P_{ps} \cdot e_p \cdot \frac{(y_{tr} - y_b)}{I_x}\right] + M_{sw} \cdot \frac{(y_{tr} - y_b)}{I_x} = 780.198\,psi$$

$$M_{cr} := \left(\frac{I_{tr}}{y_{tr}}\right) \cdot \left(6 \cdot \sqrt{f'_c \cdot psi} + f_{pe} - f_d\right) = 87632.38\,kip \cdot in$$

$$V_{ci}(P_{trial}) := 0.6\sqrt{f'_c \cdot psi} \cdot b_w \cdot d_p + \frac{V_i(P_{trial}) \cdot M_{cr}}{M_{max}(P_{trial})} + V_d$$

$$V_{cilimit} := 1.7\sqrt{f'_c \cdot psi} \cdot b_w \cdot d_p$$

$$V_{ci}(P_{trial}) := \max(V_{ci}(P_{trial}), V_{cilimit})$$

$$V_{cw} := b_w \cdot d_p \cdot \left(3.5\sqrt{f'_c \cdot psi} + 0.3 f_{pc}\right) = 310.956\,kip$$

$$V_c(P_{trial}) := \min(V_{ci}(P_{trial}), V_{cw})$$

$$V_s := \frac{A_{stirrup} \cdot f_y \cdot d_p}{s} = 268.945\,kip$$

$V_n(P_{trial}) := V_c(P_{trial}) + V_s$

$V_{nlimit}(P_{trial}) := V_c(P_{trial}) + 8 \cdot \sqrt{f'_c \cdot psi} \cdot b_w \cdot d_p$

$V_n(P_{trial}) := \min(V_n(P_{trial}), V_{nlimit}(P_{trial}))$

$V_n(P_{trial}) = V_u(P_{trial})$ <- Convergence criteria

$P_{final} := \text{Minerr}(P_{trial})$

$P_{final} = 556.652\,kip$ <- Converge on applied load

Calculated ACI Shear Capacity:

$\boxed{V_n(P_{final}) = 579.901\,kip}$

Converged Values:

$V_i(P_{final}) = 556.652\,kip$

$M_u(P_{final}) = 30339.051\,kip \cdot in$

$M_{max}(P_{final}) = 29224.235\,kip \cdot in$

$V_{ci}(P_{final}) = 1724.818\,kip$

$V_{cw} = 310.956\,kip$

$V_c(P_{final}) = 310.956\,kip$

$V_s = 268.945\,kip$

Figure D-19: Tx70-II Nominal Shear Capacity

Per ACI 318-14 11.5

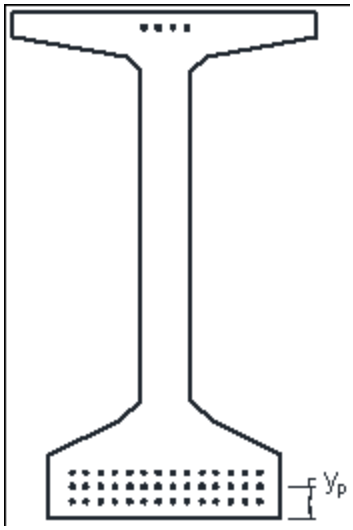

Input Parameters:

Specimen Geometry:

Beam Geometry:

$h_{beam} := 70in$

$b_f := 42in$

$b_w := 7in$

$y_b := 31.91in$

$A_g := 966in^2$

$L := 30ft$

$I_x := 628747in^4$

Deck Geometry:

$t_{deck} := 8in$

$b_{deck} := 40in$

$h_{deck} := 8in$

$A_{deck} := t_{deck} \cdot b_{deck} = 320in^2$

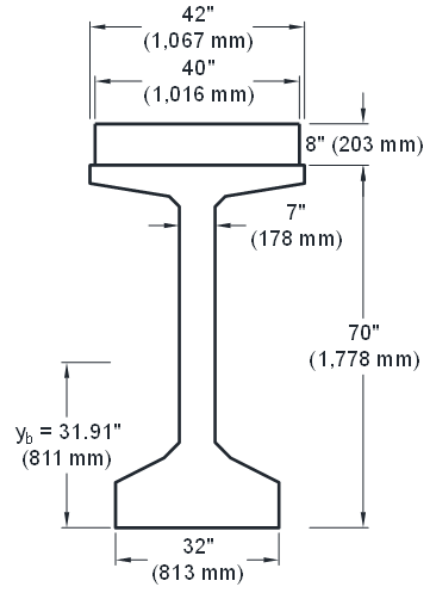

Specimen Self Weight:

$SW := 43.296826kip$

$w_{sw} := \frac{SW}{L} = 0.12027\frac{kip}{in}$

Measured Material Properties:

Beam Concrete:

$f'_c := 12.7 \times 1000psi = 12700psi$

$E_c := 6015ksi$

Beam Concrete:

$f'_{cdeck} := 9.17 \times 1000psi = 9170psi$

$E_{cdeck} := 5891ksi$

Transformed Specimen Geometry:

$$n := \frac{E_{cdeck}}{E_c} = 0.979$$

$$h_{tot} := h_{beam} + h_{deck} = 78\cdot in$$

$$A_{tr} := A_g + A_{deck}\cdot n = 1279.403\,in^2$$

$$y_{tr} := \frac{A_g\cdot y_b + n\cdot A_{deck}\cdot\left(h_{tot} - \frac{t_{deck}}{2}\right)}{A_{tr}} = 42.22\,in$$

$$I_{tr} := I_x + \frac{n\cdot b_{deck}\cdot t_{deck}^{3}}{12} + n\cdot A_{deck}\cdot\left(h_{tot} - \frac{t_{deck}}{2} - y_{tr}\right)^2 = 946938.104\,in^4$$

Stirrups:

$$f_y := 72.2ksi$$

$$A_{stirrup} := 2\cdot 0.2in^2 = 0.4\,in^2$$

$$E_s := 29000ksi$$

$$s := 8in$$

Prestressing Strands:

$$d_b := 0.7in$$

$$f_{po} := 156.5795\times 1000psi = 156579.5\,psi$$

$$E_p := 29000ksi$$

$$A_{strand} := 0.294in^2$$

$$N_{botstrands} := 42$$

$$A_{pbot} := A_{strand}\cdot N_{botstrands} = 12.348\,in^2$$

$$L_{transfer} := 50\cdot d_b = 35\cdot in$$

$$P_{ps} := f_{po}\cdot A_{pbot} = 1933.444\,kip$$

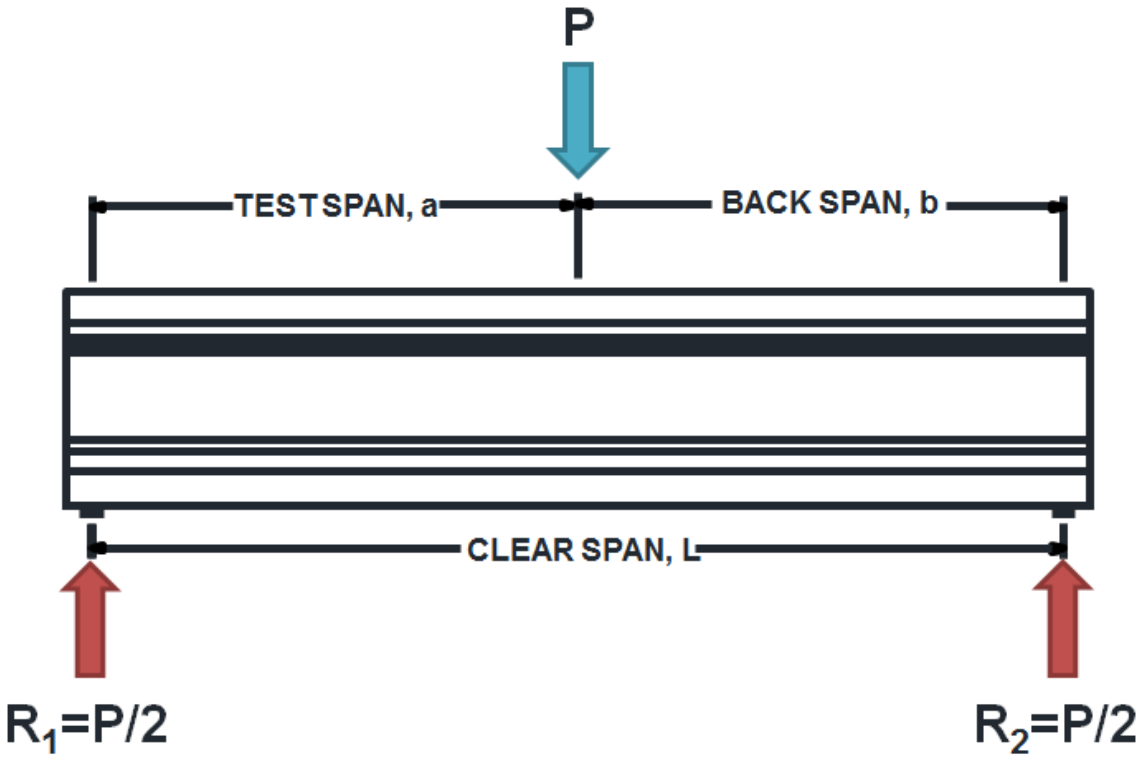

Shear Test Setup:

$L_{span} := 342in$

$a := 171in$ <- Measured as built

$P_{trial} := 515kip$ <- Initial guess for subsequent calcs

$y_p := 4.5in$

$d_p := \max\left(0.8 \cdot h_{tot}, h_{tot} - y_p\right) = 73.5 \cdot in$

$L_{bearing} := 9in$

$L_{loadplate} := 12in$

$L_{oh} := 9in$

$x_{crit} := a + L_{oh} - \frac{L_{loadplate}}{2} - \frac{h_{tot}}{2} = 135 \cdot in$ <- Location of critical section for shear taken from left end face

$W_{loadframe} := 20.942371kip$

$W_{beam} := 43.296826kip$

$e_p := y_b - y_p = 27.41 \cdot in$ <- Eccentricity of strand centroid

Solve for Nominal Shear Capacity:

Given <- Solve block for P_trial

$$V_u(P_{trial}) := P_{trial} + \frac{W_{loadframe}}{2} + \frac{W_{beam}}{2} - w_{sw}\cdot x_{crit}$$

$$V_d := \frac{W_{beam} + W_{loadframe}}{2} - w_{sw}\cdot x_{crit} = 15.883\,kip$$

$$V_i(P_{trial}) := V_u(P_{trial}) - V_d$$

$$M_u(P_{trial}) := -w_{sw}\cdot\frac{x_{crit}^2}{2} + \left(\frac{W_{beam} + W_{loadframe}}{2}\right)\cdot\left(x_{crit} - L_{oh}\right) + P_{trial}\cdot x_{crit}$$

$$M_{sw} := -w_{sw}\cdot\frac{x_{crit}^2}{2} + \frac{W_{beam}}{2}\cdot\left(x_{crit} - L_{oh}\right) = 1.632\times 10^3\cdot kip\cdot in$$

$$M_d := \frac{W_{loadframe}}{2}\cdot\left(x_{crit} - L_{oh}\right) = 1.319\times 10^3\cdot kip\cdot in$$

$$M_{dtot} := M_{sw} + M_d = 2951.119\,kip\cdot in$$

$$M_{max}(P_{trial}) := M_u(P_{trial}) - M_{dtot}$$

$$f_d := \frac{M_{sw}\cdot y_b}{I_x} + \frac{M_d\cdot y_{tr}}{I_{tr}} = 141.64\,psi$$

$$f_{pe} := \frac{P_{ps}}{A_g} + P_{ps}\cdot e_p\cdot\frac{y_b}{I_x} = 4691.118\,psi$$

$$f_{pc} := \frac{P_{ps}}{A_g} - \left[P_{ps}\cdot e_p\cdot\frac{\left(y_{tr} - y_b\right)}{I_x}\right] + M_{sw}\cdot\frac{\left(y_{tr} - y_b\right)}{I_x} = 1.159\times 10^3\,psi$$

$$M_{cr} := \left(\frac{I_{tr}}{y_{tr}}\right)\cdot\left(6\cdot\sqrt{f'_c\cdot psi} + f_{pe} - f_d\right) = 1.172\times 10^5\cdot kip\cdot in$$

$$V_{ci}(P_{trial}) := 0.6\sqrt{f'_c\cdot psi}\cdot b_w\cdot d_p + \frac{V_i(P_{trial})\cdot M_{cr}}{M_{max}(P_{trial})} + V_d$$

$$V_{cilimit} := 1.7\sqrt{f'_c\cdot psi}\cdot b_w\cdot d_p$$

$$V_{ci}(P_{trial}) := \max\left(V_{ci}(P_{trial}), V_{cilimit}\right)$$

$$V_{cw} := b_w\cdot d_p\cdot\left(3.5\sqrt{f'_c\cdot psi} + 0.3 f_{pc}\right) = 381.859\,kip$$

$$V_c(P_{trial}) := \min\left(V_{ci}(P_{trial}), V_{cw}\right)$$

$$V_s := \frac{A_{stirrup}\cdot f_y\cdot d_p}{s} = 265.335\,kip$$

$V_n(P_{trial}) := V_c(P_{trial}) + V_s$

$V_{nlimit}(P_{trial}) := V_c(P_{trial}) + 8 \cdot \sqrt{f'_c \cdot psi} \cdot b_w \cdot d_p$

$V_n(P_{trial}) := \min(V_n(P_{trial}), V_{nlimit}(P_{trial}))$

$V_n(P_{trial}) = V_u(P_{trial})$ <- Convergence criteria

$P_{final} := \text{Minerr}(P_{trial})$

$P_{final} = 631.31 \cdot kip$ <- Converge on applied load

Calculated ACI Shear Capacity:

$V_n(P_{final}) = 647.194kip$

Converged Values:

$V_i(P_{final}) = 631.31 \cdot kip$

$M_u(P_{final}) = 88178.028kip \cdot in$

$M_{max}(P_{final}) = 85226.91kip \cdot in$

$V_{ci}(P_{final}) = 918.843kip$

$V_{cw} = 381.859kip$

$V_c(P_{final}) = 381.859kip$

$V_s = 265.335kip$

Figure D-20: Tx70-II Nominal Shear Capacity

Per ACI 318-14 11.5

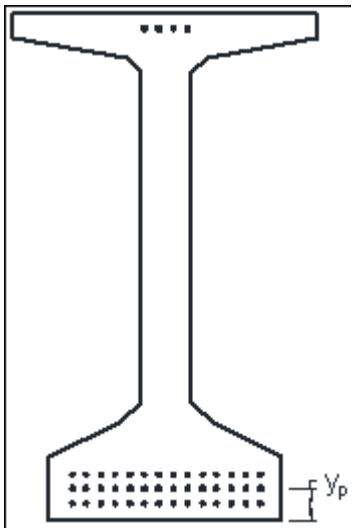

Input Parameters:

Specimen Geometry:

Beam Geometry:

$h_{beam} := 70in$

$b_f := 42in$

$b_w := 7in$

$y_b := 31.91in$

$A_g := 966in^2$

$L := 30ft$

$I_x := 628747in^4$

Deck Geometry:

$t_{deck} := 8in$

$b_{deck} := 40in$

$h_{deck} := 8in$

$A_{deck} := t_{deck} \cdot b_{deck} = 320 \cdot in^2$

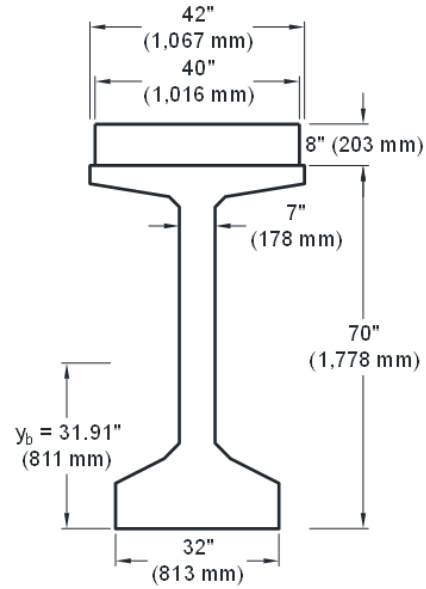

Specimen Self Weight:

$SW := 43.296826kip$

$w_{sw} := \frac{SW}{L} = 0.12027\frac{kip}{in}$

Measured Material Properties:

Beam Concrete:

$f'_c := 12.7 \times 1000psi = 12700psi$

$E_c := 6015ksi$

Beam Concrete:

$f'_{cdeck} := 9.17 \times 1000psi = 9170psi$

$E_{cdeck} := 5891ksi$

Transformed Specimen Geometry:

$$n := \frac{E_{cdeck}}{E_c} = 0.979$$

$$h_{tot} := h_{beam} + h_{deck} = 78\,in$$

$$A_{tr} := A_g + A_{deck} \cdot n = 1279.403\,in^2$$

$$y_{tr} := \frac{A_g \cdot y_b + n \cdot A_{deck} \cdot \left(h_{tot} - \frac{t_{deck}}{2} \right)}{A_{tr}} = 42.22\,in$$

$$I_{tr} := I_x + \frac{n \cdot b_{deck} \cdot t_{deck}^{3}}{12} + n \cdot A_{deck} \cdot \left(h_{tot} - \frac{t_{deck}}{2} - y_{tr} \right)^2 = 946938.104\,in^4$$

Stirrups:

$$f_y := 72.2\,ksi$$

$$A_{stirrup} := 2 \cdot 0.2\,in^2 = 0.4\,in^2$$

$$E_s := 29000\,ksi$$

$$s := 8\,in$$

Prestressing Strands:

$$d_b := 0.7\,in$$

$$f_{po} := 156.5795 \times 1000\,psi = 156579.5\,psi$$

$$E_p := 29000\,ksi$$

$$A_{strand} := 0.294\,in^2$$

$$N_{botstrands} := 42$$

$$A_{pbot} := A_{strand} \cdot N_{botstrands} = 12.348\,in^2$$

$$L_{transfer} := 50 \cdot d_b = 35\,in$$

$$P_{ps} := f_{po} \cdot A_{pbot} = 1933.444\,kip$$

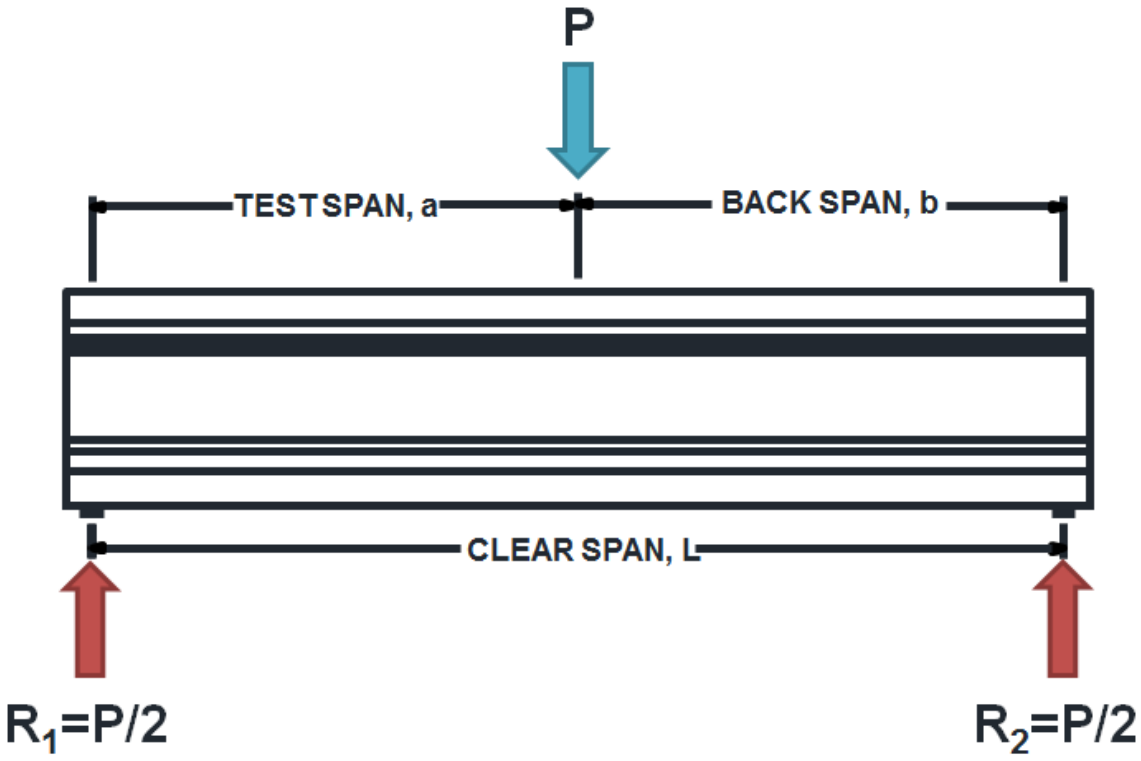

Shear Test Setup:

$L_{span} := 342in$

$a := 171in$ <- Measured as built

$P_{trial} := 515kip$ <- Initial guess for subsequent calcs

$y_p := 4.5in$

$d_p := \max\left(0.8 \cdot h_{tot}, h_{tot} - y_p\right) = 73.5 \cdot in$

$L_{bearing} := 9in$

$L_{loadplate} := 12in$

$L_{oh} := 9in$

$x_{crit} := \frac{h_{tot}}{2} + L_{oh} + \frac{L_{bearing}}{2} = 52.5\,in$ <- Location of critical section for shear taken from left end face

$W_{loadframe} := 20.942371kip$

$W_{beam} := 43.296826kip$

$e_p := y_b - y_p = 27.41 \cdot in$ <- Eccentricity of strand centroid

Solve for Nominal Shear Capacity:

Given <- Solve block for P_trial

$$V_u(P_{trial}) := P_{trial} + \frac{W_{loadframe}}{2} + \frac{W_{beam}}{2} - w_{sw} \cdot x_{crit}$$

$$V_d := \frac{W_{beam} + W_{loadframe}}{2} - w_{sw} \cdot x_{crit} = 25.805\,kip$$

$$V_i(P_{trial}) := V_u(P_{trial}) - V_d$$

$$M_u(P_{trial}) := -w_{sw} \cdot \frac{x_{crit}^2}{2} + \left(\frac{W_{beam} + W_{loadframe}}{2}\right) \cdot (x_{crit} - L_{oh}) + P_{trial} \cdot x_{crit}$$

$$M_{sw} := -w_{sw} \cdot \frac{x_{crit}^2}{2} + \frac{W_{beam}}{2} \cdot (x_{crit} - L_{oh}) = 775.96\,kip \cdot in$$

$$M_d := \frac{W_{loadframe}}{2} \cdot (x_{crit} - L_{oh}) = 455.497\,kip \cdot in$$

$$M_{dtot} := M_{sw} + M_d = 1231.457\,kip \cdot in$$

$$M_{max}(P_{trial}) := M_u(P_{trial}) - M_{dtot}$$

$$f_d := \frac{M_{sw} \cdot y_b}{I_x} + \frac{M_d \cdot y_{tr}}{I_{tr}} = 59.69\,psi$$

$$f_{pe} := \frac{P_{ps}}{A_g} + P_{ps} \cdot e_p \cdot \frac{y_b}{I_x} = 4691.118\,psi$$

$$f_{pc} := \frac{P_{ps}}{A_g} - \left[P_{ps} \cdot e_p \cdot \frac{(y_{tr} - y_b)}{I_x}\right] + M_{sw} \cdot \frac{(y_{tr} - y_b)}{I_x} = 1.145 \times 10^3\,psi$$

$$M_{cr} := \left(\frac{I_{tr}}{y_{tr}}\right) \cdot \left(6 \cdot \sqrt{f'_c \cdot psi} + f_{pe} - f_d\right) = 1.19 \times 10^5 \cdot kip \cdot in$$

$$V_{ci}(P_{trial}) := 0.6\sqrt{f'_c \cdot psi} \cdot b_w \cdot d_p + \frac{V_i(P_{trial}) \cdot M_{cr}}{M_{max}(P_{trial})} + V_d$$

$$V_{cilimit} := 1.7\sqrt{f'_c \cdot psi} \cdot b_w \cdot d_p$$

$$V_{ci}(P_{trial}) := \max(V_{ci}(P_{trial}), V_{cilimit})$$

$$V_{cw} := b_w \cdot d_p \cdot \left(3.5\sqrt{f'_c \cdot psi} + 0.3 f_{pc}\right) = 379.693\,kip$$

$$V_c(P_{trial}) := \min(V_{ci}(P_{trial}), V_{cw})$$

$$V_s := \frac{A_{stirrup} \cdot f_y \cdot d_p}{s} = 265.335\,kip$$

$V_n(P_{trial}) := V_c(P_{trial}) + V_s$

$V_{nlimit}(P_{trial}) := V_c(P_{trial}) + 8 \cdot \sqrt{f'_c \cdot psi} \cdot b_w \cdot d_p$

$V_n(P_{trial}) := \min(V_n(P_{trial}), V_{nlimit}(P_{trial}))$

$V_n(P_{trial}) = V_u(P_{trial})$ <- Convergence criteria

$P_{final} := \text{Minerr}(P_{trial})$

$P_{final} = 619.222kip$ <- Converge on applied load

Calculated ACI Shear Capacity:

$V_n(P_{final}) = 645.028kip$

Converged Values:

$V_i(P_{final}) = 619.222kip$

$M_u(P_{final}) = 33740.622kip \cdot in$

$M_{max}(P_{final}) = 32509.165kip \cdot in$

$V_{ci}(P_{final}) = 2328.044kip$

$V_{cw} = 379.693kip$

$V_c(P_{final}) = 379.693kip$

$V_s = 265.335kip$

Figure D-21: Tx46-I Horizontal Shear Calculations
Per Hovell (2011)

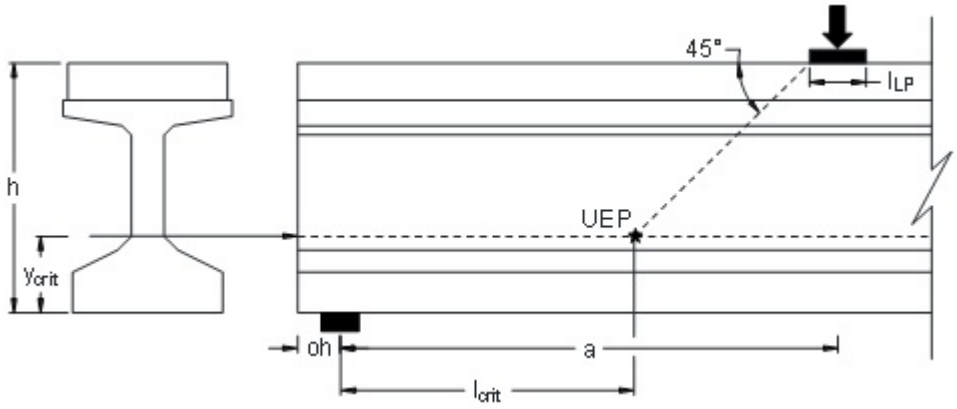

Horizontal Shear Demand:

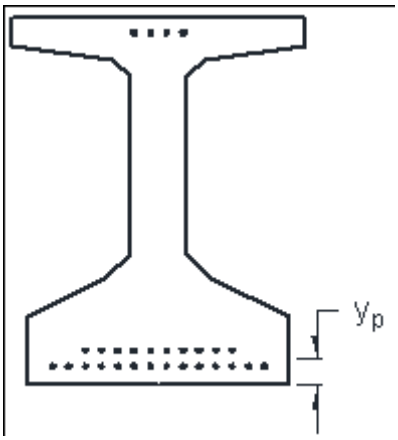

Input Parameters:

Test Setup Geometry:

$l_{LP} := 12in$ <- Load plate width

$a := 151.125in$ <- Shear span

$oh := 9in$ <- Overhang length

$y_{crit} := 16.5in$ <- Vert distance to web-flange interface

$h := 54in$ <- Total specimen height

$b_w := 7in$ <- Web width

$d_v := 45.603in$ <- Distance between tens & comp resultants

Tested Capacity:

$V_{applied} := 510.4613kip$ <- V_test, measured

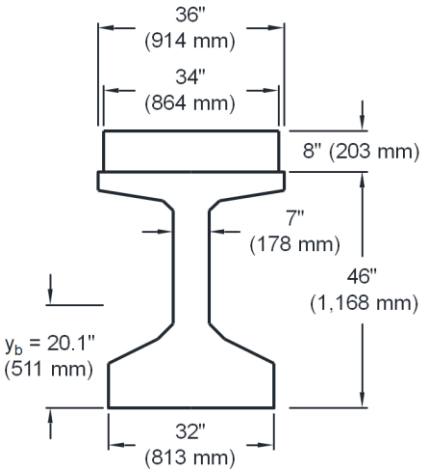

Calculations:

$$v_{hs} := \frac{V_{applied}}{b_w \cdot d_v} = 1.599ksi$$

$$l_{UEP} := a + oh - \frac{l_{LP}}{2} - h + y_{crit} = 116.625in$$

$$l_{crit} := l_{UEP} - oh = 107.625in$$

$$\boxed{V_{uhs} := v_{hs} \cdot b_w \cdot l_{crit} = 1204.71kip}$$

Horizontal Shear Capacity:

Input Parameters:

$k_d := 1.0$ <- Given for beams with symmetric shear reinf

$c := 0.4ksi$ <- Cohesion coefficient, given for monolithically placed normal-weight concrete

$\mu := 1.4$ <- Friction coefficient, given

$f_y := 60.7ksi$ <- Measured, as built

$l_t := 60 \cdot 0.7in = 42 \cdot in$ <- Transfer length for 0.7" strand

$l_1 := 38.5in$ <- Length of evaluation region 1

$l_2 := l_{UEP} - l_1 = 78.125\,in$ <- Length of evaluation region 2

$A_{rbars} := 0.2in^2 \cdot 2 = 0.4\,in^2$

$f_{pobot} := 157.4286089ksi$

$N_{botstrands} := 24$

$A_{0.7strand} := 0.294in^2$

$f'_c := 7.6ksi$

$K_1 := 0.25$ <- Limit factor, given for monolithically placed normal-weight concrete

$K_2 := 1.5ksi$ <- Limit factor, given for monolithically placed normal-weight concrete

Calculations:

Region 1:

Concrete area engaged in interface shear:

$A_{cv} := b_w \cdot l_1 = 269.5\,in^2$

Area of shear reinforcement crossing the shear plane within Acv:

$A_{vf} := 13 \cdot \left(A_{rbars}\right) = 5.2\,in^2$

Prestressing force transferred to beam within region of interest:

$P_{PS} := N_{botstrands} \cdot A_{0.7strand} \cdot f_{pobot} = 1110.816kip$

Region 1 HS Capacity:

$V_{n11} := k_d \cdot \left[c \cdot A_{cv} + \mu \cdot \left(A_{vf} \cdot f_y - 0.04 \cdot P_{PS}\right)\right] = 487.49\,kip$

Limits:

$V_{n12} := K_1 \cdot f'_c \cdot A_{cv} = 512.05\,kip$

$V_{n13} := K_2 \cdot A_{cv} = 404.25\,kip$

$V_{n1} := \min\left(V_{n11}, V_{n12}, V_{n13}\right) = 404.25\,kip$

Region 2:

Concrete area engaged in interface shear:

$A_{cv} := b_w \cdot l_2 = 546.875 in^2$

Area of shear reinforcement crossing the shear plane within Acv:

$A_{vf} := 13 \cdot \left(A_{rbars}\right) = 5.2 in^2$

Region 2 HS Capacity:

$V_{n21} := k_d \cdot \left[c \cdot A_{cv} + \mu \cdot \left(A_{vf} \cdot f_y\right)\right] = 660.646 kip$

Limits:

$V_{n22} := K_1 \cdot f'_c \cdot A_{cv} = 1.039 \times 10^3 \cdot kip$

$V_{n23} := K_2 \cdot A_{cv} = 820.312 kip$

$V_{n2} := \min\left(V_{n21}, V_{n22}, V_{n23}\right) = 660.646 kip$

Total HS Capacity:

$V_{nhs} := V_{n1} + V_{n2} = 1064.896 kip$

Total Vertical Shear Capacity:

$$V_n := \frac{V_{nhs} \cdot d_v}{l_{crit}} = 451.219 kip$$

Figure D-22: Tx46-II Horizontal Shear Calculations
Per Hovell (2011)

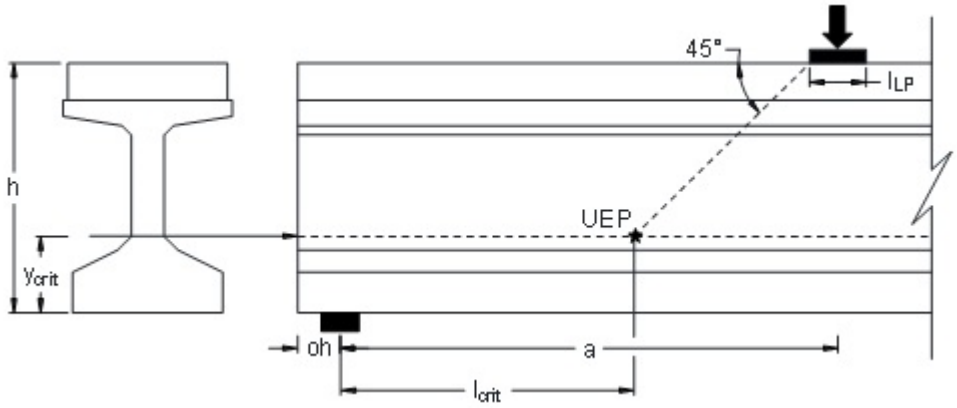

Horizontal Shear Demand:

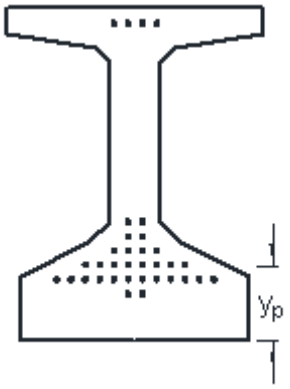

Input Parameters:

Test Setup Geometry:

$l_{LP} := 12in$ <- Load plate width

$a := 1308in$ <- Shear span

$oh := 9in$ <- Overhang length

$y_{crit} := 16.5in$ <- Vert distance to web-flange interface

$h := 54in$ <- Total specimen height

$b_w := 7in$ <- Web width

$d_v := 39.267in$ <- Distance between tens & comp resultants

Tested Capacity:

$V_{applied} := 433.789kip$ <- V_test, measured

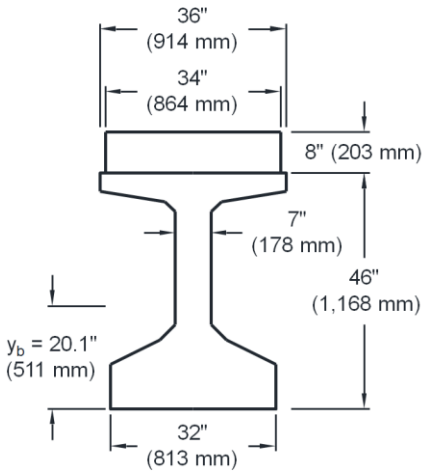

Calculations:

$$v_{hs} := \frac{V_{applied}}{b_w \cdot d_v} = 1.578ksi$$

$$l_{UEP} := a + oh - \frac{l_{LP}}{2} - h + y_{crit} = 96.3in$$

$$l_{crit} := l_{UEP} - oh = 87.3in$$

$$V_{uhs} := v_{hs} \cdot b_w \cdot l_{crit} = 964.417kip$$

Horizontal Shear Capacity:

Input Parameters:

$k_d := 1.0$ <- Given for beams with symmetric shear reinf

$c := 0.4ksi$ <- Cohesion coefficient, given for monolithically placed normal-weight concrete

$\mu := 1.4$ <- Friction coefficient, given

$f_y := 60.7ksi$ <- Measured, as built

$l_t := 60 \cdot 0.7in = 42 \cdot in$ <- Transfer length for 0.7" strand

$l_1 := 38.5in$ <- Length of evaluation region 1

$l_2 := l_{UEP} - l_1 = 57.8 \cdot in$ <- Length of evaluation region 2

$A_{rbars} := 0.2in^2 \cdot 2 = 0.4in^2$

$f_{pobot} := 166.87384ksi$

$N_{botstrands} := 30$

$A_{0.7strand} := 0.294in^2$

$f'_c := 6.92ksi$

$K_1 := 0.25$ <- Limit factor, given for monolithically placed normal-weight concrete

$K_2 := 1.5ksi$ <- Limit factor, given for monolithically placed normal-weight concrete

Calculations:

Region 1:

Concrete area engaged in interface shear:

$A_{cv} := b_w \cdot l_1 = 269.5in^2$

Area of shear reinforcement crossing the shear plane within Acv:

$A_{vf} := 13 \cdot \left(A_{rbars}\right) = 5.2in^2$

Prestressing force transferred to beam within region of interest:

$P_{PS} := N_{botstrands} \cdot A_{0.7strand} \cdot f_{pobot} = 1471.827kip$

Region 1 HS Capacity:

$V_{n11} := k_d \cdot \left[c \cdot A_{cv} + \mu \cdot \left(A_{vf} \cdot f_y - 0.04 \cdot P_{PS}\right)\right] = 467.274kip$

Limits:

$V_{n12} := K_1 \cdot f'_c \cdot A_{cv} = 466.235kip$

$V_{n13} := K_2 \cdot A_{cv} = 404.25kip$

$V_{n1} := \min\left(V_{n11}, V_{n12}, V_{n13}\right) = 404.25kip$

Region 2:

Concrete area engaged in interface shear:

$A_{cv} := b_w \cdot l_2 = 404.6 in^2$

Area of shear reinforcement crossing the shear plane within Acv:

$A_{vf} := 9 \cdot \left(A_{rbars}\right) = 3.6 in^2$

Region 2 HS Capacity:

$V_{n21} := k_d \cdot \left[c \cdot A_{cv} + \mu \cdot \left(A_{vf} \cdot f_y\right)\right] = 467.768 kip$

Limits:

$V_{n22} := K_1 \cdot f'_c \cdot A_{cv} = 699.958 kip$

$V_{n23} := K_2 \cdot A_{cv} = 606.9 kip$

$V_{n2} := \min\left(V_{n21}, V_{n22}, V_{n23}\right) = 467.768 kip$

Total HS Capacity:

$V_{nhs} := V_{n1} + V_{n2} = 872.018 kip$

Total Vertical Shear Capacity:

$$V_n := \frac{V_{nhs} \cdot d_v}{l_{crit}} = 392.228 kip$$

Figure D-23: Tx70-I Horizontal Shear Calculations
Per Hovell (2011)

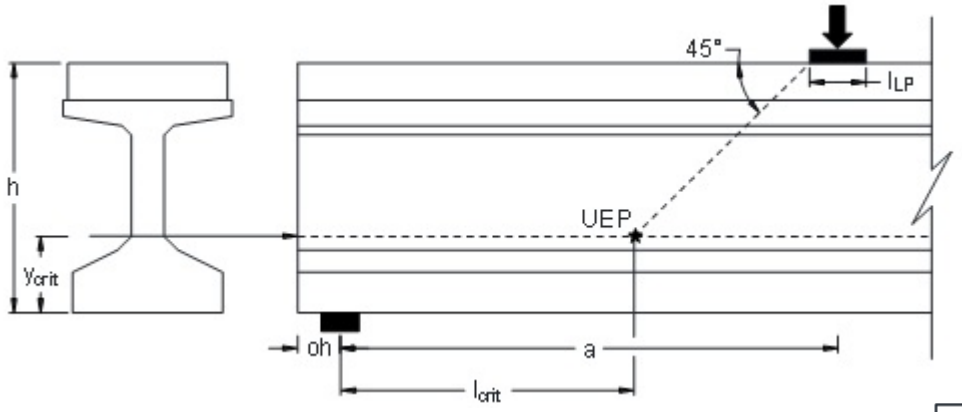

Horizontal Shear Demand:

Input Parameters:

Test Setup Geometry:

$l_{LP} := 12in$ <- Load plate width

$a := 171.25in$ <- Shear span

$oh := 9in$ <- Overhang length

$y_{crit} := 16.5in$ <- Vert distance to web-flange interface

$h := 78in$ <- Total specimen height

$b_w := 7in$ <- Web width

$d_v := 67.10366in$ <- Distance between tens & comp resultants

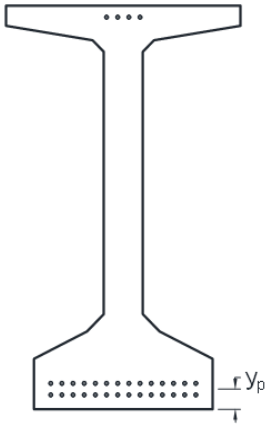

Tested Capacity:

$V_{applied} := 713.0527kip$ <- V_test, measured

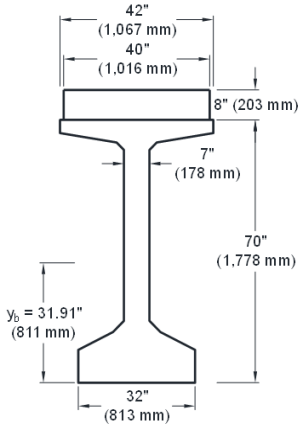

Calculations:

$$v_{hs} := \frac{V_{applied}}{b_w \cdot d_v} = 1.518ksi$$

$$l_{UEP} := a + oh - \frac{l_{LP}}{2} - h + y_{crit} = 112.75in$$

$$l_{crit} := l_{UEP} - oh = 103.75in$$

$$\boxed{V_{uhs} := v_{hs} \cdot b_w \cdot l_{crit} = 1102.462kip}$$

Horizontal Shear Capacity:

Input Parameters:

$k_d := 1.0$ <- Given for beams with symmetric shear reinf

$c := 0.4ksi$ <- Cohesion coefficient, given for monolithically placed normal-weight concrete

$\mu := 1.4$ <- Friction coefficient, given

$f_y := 72.2ksi$ <- Measured, as built

$l_t := 60 \cdot 0.7in = 42 \cdot in$ <- Transfer length for 0.7" strand

$l_1 := 38.5in$ <- Length of evaluation region 1

$l_2 := l_{UEP} - l_1 = 74.25in$ <- Length of evaluation region 2

$A_{rbars} := 0.2in^2 \cdot 2 = 0.4in^2$

$f_{pobot} := 163.8204ksi$

$N_{botstrands} := 28$

$A_{0.7strand} := 0.294in^2$

$f'_c := 10.71ksi$

$K_1 := 0.25$ <- Limit factor, given for monolithically placed normal-weight concrete

$K_2 := 1.5ksi$ <- Limit factor, given for monolithically placed normal-weight concrete

Calculations:

Region 1:

Concrete area engaged in interface shear:

$A_{cv} := b_w \cdot l_1 = 269.5in^2$

Area of shear reinforcement crossing the shear plane within Acv:

$A_{vf} := 13 \cdot \left(A_{rbars}\right) = 5.2in^2$

Prestressing force transferred to beam within region of interest:

$P_{PS} := N_{botstrands} \cdot A_{0.7strand} \cdot f_{pobot} = 1348.57kip$

Region 1 HS Capacity:

$V_{n11} := k_d \cdot \left[c \cdot A_{cv} + \mu \cdot \left(A_{vf} \cdot f_y - 0.04 \cdot P_{PS}\right)\right] = 557.896kip$

Limits:

$V_{n12} := K_1 \cdot f'_c \cdot A_{cv} = 721.586kip$

$V_{n13} := K_2 \cdot A_{cv} = 404.25kip$

$V_{n1} := \min\left(V_{n11}, V_{n12}, V_{n13}\right) = 404.25kip$

Region 2:

Concrete area engaged in interface shear:

$A_{cv} := b_w \cdot l_2 = 519.75 in^2$

Area of shear reinforcement crossing the shear plane within Acv:

$A_{vf} := 9 \cdot (A_{rbars}) = 3.6 in^2$

Region 2 HS Capacity:

$V_{n21} := k_d \cdot [c \cdot A_{cv} + \mu \cdot (A_{vf} \cdot f_y)] = 571.788 kip$

Limits:

$V_{n22} := K_1 \cdot f'_c \cdot A_{cv} = 1.392 \times 10^3 \cdot kip$

$V_{n23} := K_2 \cdot A_{cv} = 779.625 kip$

$V_{n2} := \min(V_{n21}, V_{n22}, V_{n23}) = 571.788 kip$

Total HS Capacity:

$V_{nhs} := V_{n1} + V_{n2} = 976.038 kip$

Total Vertical Shear Capacity:

$$V_n := \frac{V_{nhs} \cdot d_v}{l_{crit}} = 631.284 kip$$

Figure D-24: Tx70-II Horizontal Shear Calculations
Per Hovell (2011)

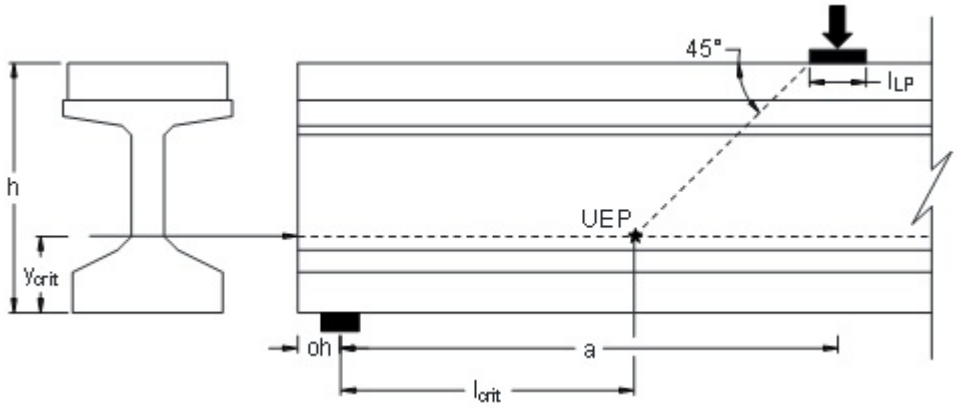

Horizontal Shear Demand:

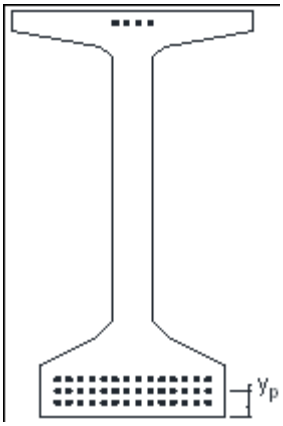

Input Parameters:

Test Setup Geometry:

$l_{LP} := 12in$ <- Load plate width

$a := 171in$ <- Shear span

$oh := 9in$ <- Overhang length

$y_{crit} := 16.5in$ <- Vert distance to web-flange interface

$h := 78in$ <- Total specimen height

$b_w := 7in$ <- Web width

$d_v := 66.15in$ <- Distance between tens & comp resultants

Tested Capacity:

$V_{applied} := 831.8169kip$ <- V_test, measured

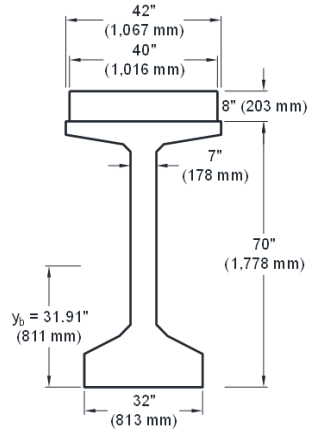

Calculations:

$$v_{hs} := \frac{V_{applied}}{b_w \cdot d_v} = 1.796ksi$$

$$l_{UEP} := a + oh - \frac{l_{LP}}{2} - h + y_{crit} = 112.5in$$

$$l_{crit} := l_{UEP} - oh = 103.5in$$

$$\boxed{V_{uhs} := v_{hs} \cdot b_w \cdot l_{crit} = 1301.482kip}$$

Horizontal Shear Capacity:

Input Parameters:

$k_d := 1.0$ <- Given for beams with symmetric shear reinf

$c := 0.4ksi$ <- Cohesion coefficient, given for monolithically placed normal-weight concrete

$\mu := 1.4$ <- Friction coefficient, given

$f_y := 72.2ksi$ <- Measured, as built

$l_t := 60 \cdot 0.7in = 42 \cdot in$ <- Transfer length for 0.7" strand

$l_1 := 38.5in$ <- Length of evaluation region 1

$l_2 := l_{UEP} - l_1 = 74 \cdot in$ <- Length of evaluation region 2

$A_{rbars} := 0.2in^2 \cdot 2 = 0.4in^2$

$f_{pobot} := 156.579ksi$

$N_{botstrands} := 42$

$A_{0.7strand} := 0.294in^2$

$f'_c := 12.7ksi$

$K_1 := 0.25$ <- Limit factor, given for monolithically placed normal-weight concrete

$K_2 := 1.5ksi$ <- Limit factor, given for monolithically placed normal-weight concrete

Calculations:

Region 1:

Concrete area engaged in interface shear:

$A_{cv} := b_w \cdot l_1 = 269.5in^2$

Area of shear reinforcement crossing the shear plane within Acv:

$A_{vf} := 13 \cdot \left(A_{rbars}\right) = 5.2in^2$

Prestressing force transferred to beam within region of interest:

$P_{PS} := N_{botstrands} \cdot A_{0.7strand} \cdot f_{pobot} = 1933.444kip$

Region 1 HS Capacity:

$V_{n11} := k_d \cdot \left[c \cdot A_{cv} + \mu \cdot \left(A_{vf} \cdot f_y - 0.04 \cdot P_{PS}\right)\right] = 525.143kip$

Limits:

$V_{n12} := K_1 \cdot f'_c \cdot A_{cv} = 855.663kip$

$V_{n13} := K_2 \cdot A_{cv} = 404.25kip$

$V_{n1} := \min\left(V_{n11}, V_{n12}, V_{n13}\right) = 404.25kip$

Region 2:

Concrete area engaged in interface shear:

$A_{cv} := b_w \cdot l_2 = 518 \cdot in^2$

Area of shear reinforcement crossing the shear plane within Acv:

$A_{vf} := 9 \cdot \left(A_{rbars}\right) = 3.6 in^2$

Region 2 HS Capacity:

$V_{n21} := k_d \cdot \left[c \cdot A_{cv} + \mu \cdot \left(A_{vf} \cdot f_y\right)\right] = 571.088 kip$

Limits:

$V_{n22} := K_1 \cdot f'_c \cdot A_{cv} = 1.645 \times 10^3 \cdot kip$

$V_{n23} := K_2 \cdot A_{cv} = 777 \cdot kip$

$V_{n2} := \min\left(V_{n21}, V_{n22}, V_{n23}\right) = 571.088 kip$

Total HS Capacity:

$V_{nhs} := V_{n1} + V_{n2} = 975.338 kip$

Total Vertical Shear Capacity:

$$V_n := \frac{V_{nhs} \cdot d_v}{l_{crit}} = 623.368 kip$$

Table D-1: AASHTO LRFD-MCFT shear capacity calculation summary

Specimen ID	P, kips	V_s, kips	V_c, kips	V_n, kips
Tx46-I	445	328	124	452
Tx46-II	409	293	124	417
Tx70-I	1,324	437	234	670
Tx70-II	1,443	442	288	730

Table D-2: AASHTO LRFD-anchorage shear capacity calculation summary

Specimen ID	Section under investigation	P, kips	V_s, kips	M_u, kip-in	T_{max}, kips	V_n, kips
Tx46-I	d_v from load plate	434	334	44,351	1,468	441
	edge of bearing pad	432	342	22,141	506	444
Tx46-II	d_v from load plate	505	289	45,011	1,816	513
	edge of bearing pad	750	289	33,089	1,125	763
Tx70-I	d_v from load plate	1,286	439	64,390	1,742	651
	edge of bearing pad	1,119	445	41,176	640	571
Tx70-II	d_v from load plate	1,756	436	88,220	2,555	887
	edge of bearing pad	1,495	446	53,976	1,003	750

Table D-3: ACI shear capacity calculation summary

Specimen ID	Section under investigation	V_{ci}, kips	V_{cw}, kips	V_s, kips	V_n, kips
Tx46-I	h/2 from load plate	359	170	205	375
	h/2 from bearing pad	1,152	166		371
Tx46-II	h/2 from load plate	441	215	177	392
	h/2 from bearing pad	1,167	212		389
Tx70-I	h/2 from load plate	683	313	269	582
	h/2 from bearing pad	1,725	311		580
Tx70-II	h/2 from load plate	919	382	265	647
	h/2 from bearing pad	2,328	380		645

Table D-4: Horizontal shear capacity calculation summary

Specimen ID	V_{n1}, kips	V_{n2}, kips	V_{nhs}, kips	V_n, kips
Tx46-I	404	661	1,065	451
Tx46-II	404	468	872	392
Tx70-I	404	572	976	631
Tx70-II	404	571	975	623

REFERENCES

AASHTO. (2014). *AASHTO LRFD Bridge Design Specifications, U.S. Customary Units 7th edition.* Washington, D.C.

Abyaneh, R. A. (2016). *Computational Modeling of Prestress Transfer, End-Region Cracks and Shear Behavior in Prestressed Concrete I-Girders Employing Large-Diameter Strands.* Austin, TX: The University of Texas at Austin.

ACI (American Concrete Institute). (2014). *Building Code Requirements for Structural Concrete (ACI 318-14), and Commentary.* Farmington Hills, MI: ACI.

ASTM. (2014). *ASTM C39/C39M Standard Test Method for Compressive Strength of Cylindrical Concrete Specimens.* West Conshohocken, PA: ASTM.

ASTM. (2014). *ASTM C469/C469M Standard Test Method for Static Modulusof Elasticity and Poisson's Ratio of Concrete in Compression.* West Conshohocken, PA: ASTM.

ASTM. (2015). *ASTM C78/C78M Standard Test Method for Flexural Strength of Concrete (Using Simple Beam with Third-Point Loading).* West Conshohocken, PA: ASTM.

ASTM. (2016). *ASTM A1061/A1061M Standard Test Methods for Testing Multi-Wire Steel Prestressing Strand.* West Conshohocken, PA: ASTM.

ASTM. (2016). *ASTM A370 Standard Test Methods and Definitions for Mechanical Testing of Steel Products.* West Conshohocken, PA: ASTM.

Garber, D. B., Gallardo, J. M., Deschenes, D. J., & Bayrak, M. ASCE, O. (2016). Nontraditional Shear Failures in Bulb-T Prestressed Concrete Bridge Girders. *Journal of Bridge Engineering (ASCE)*.

Hovell, C., Avendano, A., Moore, A., Dunkman, D., Bayrak, O., & Jirsa, J. (2012). *Structural Performance of Texas U-Beams at Prestress Transfer and Under Shear-Critical Loads.* Austin, TX: Center for Transportation Research at The University of Texas at Austin.

Langefeld, D. P. (2012). *Anchorage-Controlled Shear Capacity of Prestressed Bridge Girders.* Austin, TX: The University of Texas at Austin.

Nakamura, E., Avendano, A. R., & Bayrak, O. (2013). Shear Database for Prestressed Concrete Members. *ACI Structural Journal*, 909-918.

Ross, M.ASCE, B. E., Hamilton, H. R., & Consolazio, G. R. (2014). Experimental Study of End Region Detailing and Shear Behavior of Concrete I-Girders. *Journal of Bridge Engineering (ASCE)*.

Salazar, J. L. (2016). *End-Region Behavior of Precast, Prestressed I-Girders Employing 0.7-inch Prestressing Strands.* Austin, TX: The University of Texas at Austin.

Tadros, M. K., & Morcous, G. (2011). *Impact of 0.7 Inch Diameter Strands on NU I-Girders.* Lincoln, NE: Nebraska Department of Roads (NDOR).

Texas Department of Transportation (TxDOT). (2015). Concrete I-Girder Details. Austin, TX.